DRAFT REPORT

TWO TEST LEVEL 2 BRIDGE RAILING AND TRANSITION SYSTEMS FOR TRANSVERSE GLUE-LAMINATED TIMBER DECKS

Submitted by

Karla A. Polivka, M.S.M.E., E.I.T. [1]
Research Associate Engineer

Ronald K. Faller, Ph.D., P.E. [1]
Research Assistant Professor

Michael A. Ritter, P.E. [2]
Project Leader

Barry T. Rosson, Ph.D., P.E. [1]
Associate Professor

John R. Rohde, Ph.D., P.E. [1]
Associate Professor

Eric A. Keller, B.S.M.E., E.I.T. [1]
Former Research Associate Engineer

MIDWEST ROADSIDE SAFETY FACILITY [1]
University of Nebraska-Lincoln
527 Nebraska Hall
Lincoln, Nebraska 68588-0529
(402) 472-6864

U.S. DEPARTMENT OF AGRICULTURE [2]
Forest Service
Forest Products Laboratory
Engineered Wood Products and Structures
One Gifford Pichot Dr.
Madison, Wisconsin 53705
(608) 231-9229

MwRSF Research Report No. TRP-03-125-03

March 11, 2003

Technical Report Documentation Page

1. Report No.	2.	3. Recipient's Accession No.
4. Title and Subtitle Two Test Level 2 Bridge Railing and Transition Systems for Transverse Glue-Laminated Timber Decks		5. Report Date March 11, 2003 6.
7. Author(s) Polivka, K.A., Faller, R.K., Rosson, B.T., Ritter, M.A., Rohde, J.R., and Keller, E.A.		8. Performing Organization Report No. TRP-03-125-03
9. Performing Organization Name and Address Midwest Roadside Safety Facility (MwRSF) University of Nebraska-Lincoln 527 Nebraska Hall Lincoln, NE 68588-0529		10. Project/Task/Work Unit No. 11. Contract © or Grant (G) No. FP-95-RJVA-2630
12. Sponsoring Organization Name and Address U.S. Department of Agriculture Forest Service Forest Products Laboratory One Gifford Pinchot Drive Madison, Wisconsin 53705		13. Type of Report and Period Covered Draft Report 1995-2003 14. Sponsoring Agency Code

15. Supplementary Notes

Prepared in cooperation with U.S. Department of Transportation, Federal Highway Administration

16. Abstract (Limit: 200 words)

Two bridge railing and approach guardrail transition systems for use on bridges with transverse glue-laminated timber decks were developed and crash tested for use on medium-service-level roadways. The bridge railing and transition systems were subjected to full-scale crash tests in accordance with the Test Level 2 (TL-2) safety performance criteria presented in NCHRP Report No. 350, *Recommended Procedures for the Safety Performance Evaluation of Highway Features*. The first railing system was constructed with steel hardware, whereas the second railing system was configured with glulam timber components. Four full-scale crash tests were performed, and the bridge railing and transition systems were acceptable according to current safety standards.

17. Document Analysis/Descriptors	18. Availability Statement
Highway Safety, Longitudinal Barrier, Bridge Railings, Approach Guardrail Transition, Roadside Appurtenances, Crash Test, Compliance Test, Timber Bridge	No restrictions. Document available from: National Technical Information Services, Springfield, Virginia 22161

19. Security Class (this report)	20. Security Class (this page)	21. No. of Pages	22. Price
Unclassified	Unclassified	351	

DISCLAIMER STATEMENT

The contents of this report reflect the views of the authors who are responsible for the facts and the accuracy of the data presented herein. The contents do not necessarily reflect the official views or policies of the Federal Highway Administration nor the United States Department of Agriculture, Forest Service, Forest Products Laboratory. This report does not constitute a standard, specification, or regulation.

ACKNOWLEDGMENTS

The authors wish to acknowledge several sources that made a contribution to the success of this research project: (1) John Foreman, Alamo Wood Products, Inc., Albert Lea, Minnesota, for all your cooperation and supplying the glulam materials at a very competitive price; (2) Matthew Smith, Laminated Concepts Inc., Elmira, New York, for completing the bridge deck design and preparing standard plans; (3) MwRSF personnel for constructing the bridge structure and barrier systems as well as conducting the crash tests; (4) Daniel Mushett, Highway Timber Products Co. - a division of Cox Industries for donating wood guardrail posts and blockouts; and (5) the Office of Sponsored Programs and the Center for Infrastructure Research, University of Nebraska-Lincoln, Lincoln, NE for matching support.

A special thanks is also given to the following individuals who made a contribution to the completion of this research project.

Federal Highway Administration

Sheila R. Duwadi, P.E., Turner-Fairbank Highway Research Center

Midwest Roadside Safety Facility

D.L. Sicking, Ph.D., P.E., Professor and MwRSF Director
B.G. Pfeifer, Ph.D., P.E., Former Research Associate Engineer
J.C. Holloway, M.S.C.E., E.I.T., Research Associate Engineer
K.L. Krenk, B.S.M.A., Shop Manager
M.L. Hanau, Laboratory Mechanic I
Undergraduate and Graduate Assistants

Dunlap Photography

James Dunlap, President and Owner

TABLE OF CONTENTS

Page

List of Figures

Page

List of Tables

Page

1 INTRODUCTION

1.1 Problem Statement

For more than 30 years, numerous bridge railing systems have been developed and evaluated according to established vehicular crash testing standards. Most bridge railings previously crash tested have consisted of concrete, steel, and aluminum railings attached to concrete bridge decks. It is well known that a growing number of timber bridges with transverse and longitudinal timber bridge decks are being constructed throughout the United States. Therefore, the demand for crashworthy railing systems has become more evident with the increasing use of timber deck bridges located on secondary highways, county roads, and local roads. During the last fourteen years, several crashworthy bridge railing systems have been developed for use on longitudinal timber deck bridges. In addition, these railing systems were developed for multiple service levels, ranging from low-speed, low-volume roads to higher-service level roadways. More recently, researchers developed two higher-performance-level railing systems for use on transverse timber deck bridges (1-2). However, little research has been conducted to develop crashworthy bridge railing systems for use on transverse timber deck bridges located on low-to-medium service roadways. For timber to be a viable and economical alternative in the construction of transverse timber decks, additional vehicular bridge railing systems must be developed and crash tested for timber deck bridges located on these roadways.

In recognition of the need to develop bridge railing systems for this medium-service level, the United States Department of agriculture (USDA) Forest Service, Forest Products Laboratory (FPL), in cooperation with the Midwest Roadside Safety Facility (MwRSF) and the Federal

Highway Administration (FHWA), undertook the task of developing two medium-service-level bridge railings and approach guardrail transitions.

1.2 Objective

The primary objective of this research project was to develop and evaluate two new bridge railings and approach guardrail transitions for use with transverse glue-laminated (glulam) timber deck bridges located on medium-service-level roadways. The bridge railing and transition systems were developed to meet the Test Level 2 (TL-2) evaluation criteria described in the National Cooperative Highway Research Program (NCHRP) Report No. 350, *Recommended Procedures for the Safety Performance Evaluation of Highway Features* (3). The first bridge railing was a steel system constructed using a thrie beam rail, an upper structural channel rail, and wide-flange posts and blockouts. The second bridge railing was a wood system constructed using a rectangular rail, posts, and blockouts, all manufactured from glulam timber.

The secondary objective of the research project was to determine the actual forces imparted to key components of the bridge railing systems during impact of the test vehicles. A knowledge of these force levels would allow bridge researchers and designers to make minor modifications to the crash tested designs without additional full-scale crash testing, and it provides insight into the development of future systems.

1.3 Scope

The research objectives were accomplished with the successful completion of several tasks. First, a literature review was performed on previously developed low-to-medium-performance level bridge railing systems, as well as bridge railings developed for timber deck bridges. This review was deemed necessary because it was envisioned that the two new bridge railing designs would

likely use technologies and design details from existing crashworthy railing systems. Second, bridge railing concepts were prepared so that an analysis and design phase could be performed on all structural members and connections. Third, computer simulation modeling was conducted using BARRIER VII to aid in the analysis and design of the bridge railing and approach guardrail transition systems. Fourth, strain gauge instrumentation was placed on selected structural components to help determine the actual dynamic loads imparted into the bridge railing and deck systems. The researchers deemed that the dynamic load information was necessary because additional economy could be provided with the downsizing of specific structural components. Fifth, a total of four full-scale vehicle crash tests were performed by using ¾-ton pickup trucks, two crash tests on each bridge railing and transition. Finally, the test results were analyzed, evaluated, and documented. Conclusions and recommendations were then made that pertain to the safety performance of each bridge railing and transition system.

2 LITERATURE REVIEW

2.1 Bridge Railings for Timber Deck Bridges

Over the past fourteen years, MwRSF and FPL engineers have designed and developed several bridge railings and transitions for use on longitudinal glulam timber deck bridges and transverse timber deck bridges. Eleven bridge railings have been developed for several design impact conditions, including American Association of State Highway and Transportation Officials (AASHTO) Performance Levels 1 and 2 (PL-1 and PL-2) (4) and NCHRP Report No. 350 TL-1 and TL-4 (3), as well as for very low-speed, low-volume roadways (5-19). The bridge railing systems developed for longitudinal timber decks include: (1) an AASHTO PL-1 Glulam Rail with Curb bridge railing (5-9); (2) an AASHTO PL-1 Glulam Rail without Curb bridge railing (5-9); (3) an AASHTO PL-1 Steel Thrie-Beam Rail bridge railing (5-9); (4) an AASHTO PL-2 Steel Thrie-Beam with top-mounted Channel Rail bridge railing (6-10); (5) a NCHRP Report No. 350 TL-4 Glulam Rail with Curb bridge railing (6-10); (6) a Low-Height Curb-Type Sawn Timber bridge railing for low-speed, low-volume roads (11-12); (7) a NCHRP Report No. 350 TL-1 low-cost Breakaway W-Beam bridge railing (11,13); (8) a NCHRP Report No. 350 TL-1 Curb-Type Glulam Rail bridge railing (11,14); and (9) a NCHRP Report No. 350 TL-1 Top-Mounted W-Beam bridge railing (11,15). The bridge railing systems developed for transverse timber decks include: (1) a NCHRP Report No. 350 TL-4 Glulam Rail bridge railing and approach guardrail transition (1-2, 17-18); and (2) a NCHRP Report No. 350 TL-4 Steel Thrie-Beam Rail bridge railing and approach guardrail transition (1-2, 17-18). Subsequently, standard plans were developed for adapting several of these wood systems to concrete deck bridges (19).

Two other research programs conducted in the United States provide information on the

crashworthiness of bridge railings for use on timber deck bridges. The first program was performed at Southwest Research Institute (SwRI) in the late 1980's in which crash tests were conducted according to AASHTO PL-1 conditions on a glulam rail with a curb bridge railing system attached to a spike-laminated longitudinal timber bridge deck (20). In 1993, a second research project was conducted by the Constructed Facilities Center (CFC) at West Virginia University with crash testing performed by the Texas Transportation Institute (TTI). Crash tests were performed according to AASHTO PL-1 conditions on three bridge railing systems and one transition system attached to a transverse glulam timber deck (21-24).

3 TEST REQUIREMENTS AND EVALUATION CRITERIA

3.1 Test Requirements

Longitudinal barriers, such as bridge railings and approach guardrail transitions, must satisfy the requirements provided in NCHRP Report No. 350 to be accepted for use on new construction projects or as a replacement for existing barrier designs not meeting current safety standards. The recently published NCHRP Report No. 350 provides for six test levels for evaluating longitudinal barriers, as shown in Table 1. Although this document does not contain objective criteria for the conditions under which each test level is to be used, safety hardware developed to meet the lower test levels are generally intended for use on lower service level roadways while higher test level hardware is intended for use on higher service level roadways.

According to the TL-2 criteria of NCHRP Report No. 350, longitudinal barriers must be subjected to two full-scale vehicle crash tests: (1) an 820-kg small car impacting at a speed of 70.0 km/hr and at an angle of 20 degrees; and (2) a 2,000-kg pickup truck impacting at a speed of 70.0 km/hr and at an angle of 25 degrees. For this research project, the two bridge railing and approach guardrail transition systems were crash tested using only the pickup truck impact conditions. Although the small car test is used to evaluate the overall performance of the length-of-need section and to assess occupant risk problems that arise from snagging or overturning of the vehicle, it was deemed unnecessary for several reasons.

First, during the design and development phase of both barrier systems, special attention was given to prevent geometric incompatibilities that would cause the small car tests to fail due to excessive snagging or overturning. Second, the structural adequacy of the medium service level barrier systems is not a concern for the small car test due to the relatively minor impact severity

when compared to the impact severity for the pickup truck impact conditions. The impact severity of the pickup truck test is approximately 270 percent greater than that provided by the small car test. Third, a small car crash test was successfully conducted on a similar wood bridge railing system previously developed by MwRSF (5). Finally, thrie beam barriers struck by small cars have been shown to meet safety performance standards and to be essentially rigid (25-27), with no significant potential for occupant risk problems that arise from snagging or overturning. For these reasons, the 820-kg small car crash test was considered unnecessary for each bridge railing and approach guardrail transition system developed under this research project. The test conditions for the required test matrices are shown in Table 1.

3.2 Evaluation Criteria

Evaluation criteria for full-scale crash testing are based on three appraisal areas: (1) structural adequacy; (2) occupant risk; and (3) vehicle trajectory after collision. Criteria for structural adequacy are intended to evaluate the ability of the railing to contain, redirect, or allow controlled vehicle penetration in a predictable manner. Occupant risk evaluates the degree of hazard to occupants of the impacting vehicle. Vehicle trajectory after collision is a measure of the potential for the post-impact trajectory of the vehicle to cause subsequent multi-vehicle accidents. It is also an indicator of the potential safety hazard for the occupants of the other vehicles or the occupants of the impacting vehicle when subjected to secondary collisions with other fixed objects. These three evaluation criteria are defined in Table 2. The full-scale vehicle crash tests were conducted and reported in accordance with the procedures provided in NCHRP Report No. 350.

Table 1. NCHRP Report No. 350 Test Levels, Crash Test Conditions, and Evaluation Criteria for Longitudinal Barriers and Transitions

Test Level	Test Designation	Test Vehicle	Impact Conditions		Evaluation Criteria
			Speed (km/hr)	Angle (degrees)	
TL-1	1-10	Small Car	50	20	A,D,F,H,I,K,M
	1-11	Pickup Truck	50	25	A,D,F,K,L,M
TL-2	2-10	Small Car	70	20	A,D,F,H,I,K,M
	2-11	Pickup Truck	70	25	A,D,F,K,L,M
TL-3	3-10	Small Car	100	20	A,D,F,H,I,K,M
	3-11	Pickup Truck	100	25	A,D,F,K,L,M
TL-4	4-10	Small Car	100	20	A,D,F,H,I,K,M
	4-11	Pickup Truck	100	25	A,D,F,K,L,M
	4-12	Single-Unit Truck	80	15	A,D,G,K,M
TL-5	5-10	Small Car	100	20	A,D,F,H,I,K,M
	5-11	Pickup Truck	100	25	A,D,F,K,L,M
	5-12	Tractor/Van Trailer	80	15	A,D,G,K,M
TL-6	6-10	Small Car	100	20	A,D,F,H,I,K,M
	6-11	Pickup Truck	100	25	A,D,F,K,L,M
	6-12	Tractor/Tank Trailer	80	15	A,D,G,K,M

Table 2. Relevant NCHRP Report No. 350 Evaluation Criteria (3)

Structural Adequacy	A. Test article should contain and redirect the vehicle; the vehicle should not penetrate, underride, or override the installation although controlled lateral deflection of the test article is acceptable.
Occupant Risk	D. Detached elements, fragments or other debris from the test article should not penetrate or show potential for penetrating the occupant compartment, or present and undue hazard to other traffic, pedestrians, or personnel in a work zone. Deformations of, or intrusions into, the occupant compartment that could cause serious injuries should not be permitted.
	F. The vehicle should remain upright during and after collision although moderate roll, pitching and yawing are acceptable.
	G. It is preferable, although not essential, that the vehicle remain upright during and after collision.
	H. Longitudinal and lateral occupant impact velocities should fall below the preferred value of 9 m/s, or at least below the maximum allowable value of 12 m/s.
	I. Longitudinal and lateral occupant ridedown accelerations should fall below the preferred value of 15 G's, or at least below the maximum allowable value of 20 G's.
Vehicle Trajectory	K. After collision it is preferable that the vehicle's trajectory not intrude into adjacent traffic lanes.
	L. The occupant impact velocity in the longitudinal direction should not exceed 12 m/s and the occupant ridedown acceleration in the longitudinal direction should not exceed 20 G's.
	M. The exit angle from the test article preferably should be less than 60 percent of test impact angle, measured at time of vehicle loss of contact with test device.

4 TEST SITE PREPARATION

4.1 Bridge Construction

A full-size simulated timber bridge deck system was constructed at the MwRSF outdoor test site for use in the development of the two new bridge railing and approach guardrail transition systems. The full-size system was selected to ensure that the research results were representative of actual bridge site conditions. In the following sections, site details are provided that pertain to the construction of the test pit, bridge substructure, and bridge superstructure. It is noted that the bridge system described below was used for both the wood and steel bridge railing systems.

4.1.1 Test Pit

A test pit was constructed in the existing concrete tarmac by cutting out a rectangular shape slab of concrete, measuring 60.96-m long by 6.10-m wide. The 60.96-mm length was required to accommodate the 36.58-m long bridge and a 22.86-m long bridge approach section and attached guardrail. The pit was then excavated to a depth of approximately 2.13 m to provide clearance for constructing the bridge substructure and to provide the necessary clearance to allow personnel to stand upright and work below the bridge deck. Following the soil excavation, retaining walls were constructed on three sides of the test pit to prevent erosion of the subgrade soils located below the concrete tarmac.

4.1.2 Bridge Substructure

After the soil was excavated from the test pit, four reinforced concrete bridge supports were constructed on the bottom of the test pit. Design details are shown in Figures 1 through 4. Photographs of the concrete support construction as well as the completed supports and retaining wall are shown in Figure 5. The supports were founded at the necessary elevations with respect to

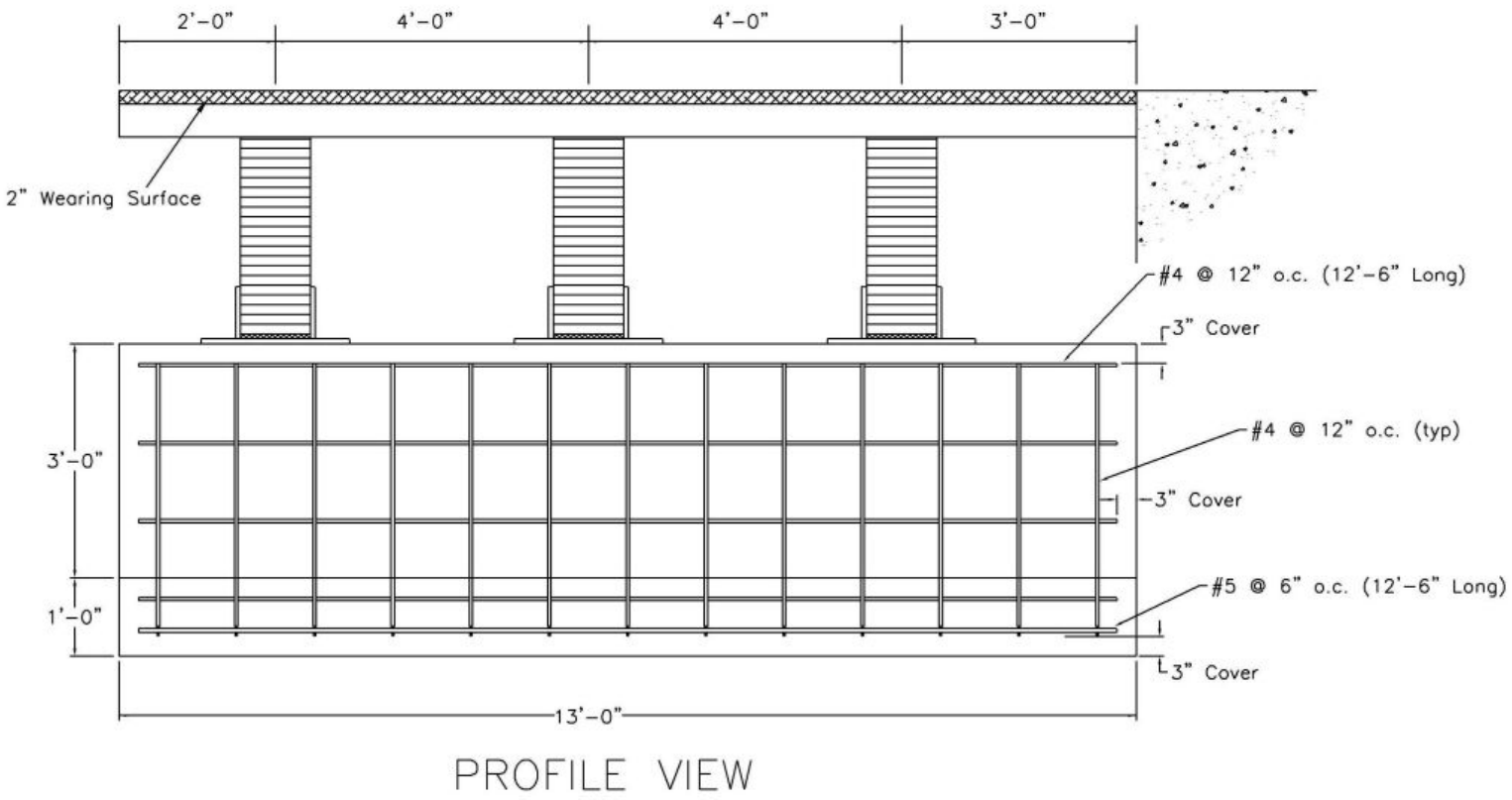

Figure 1. Bridge Substructure Details - Profile View

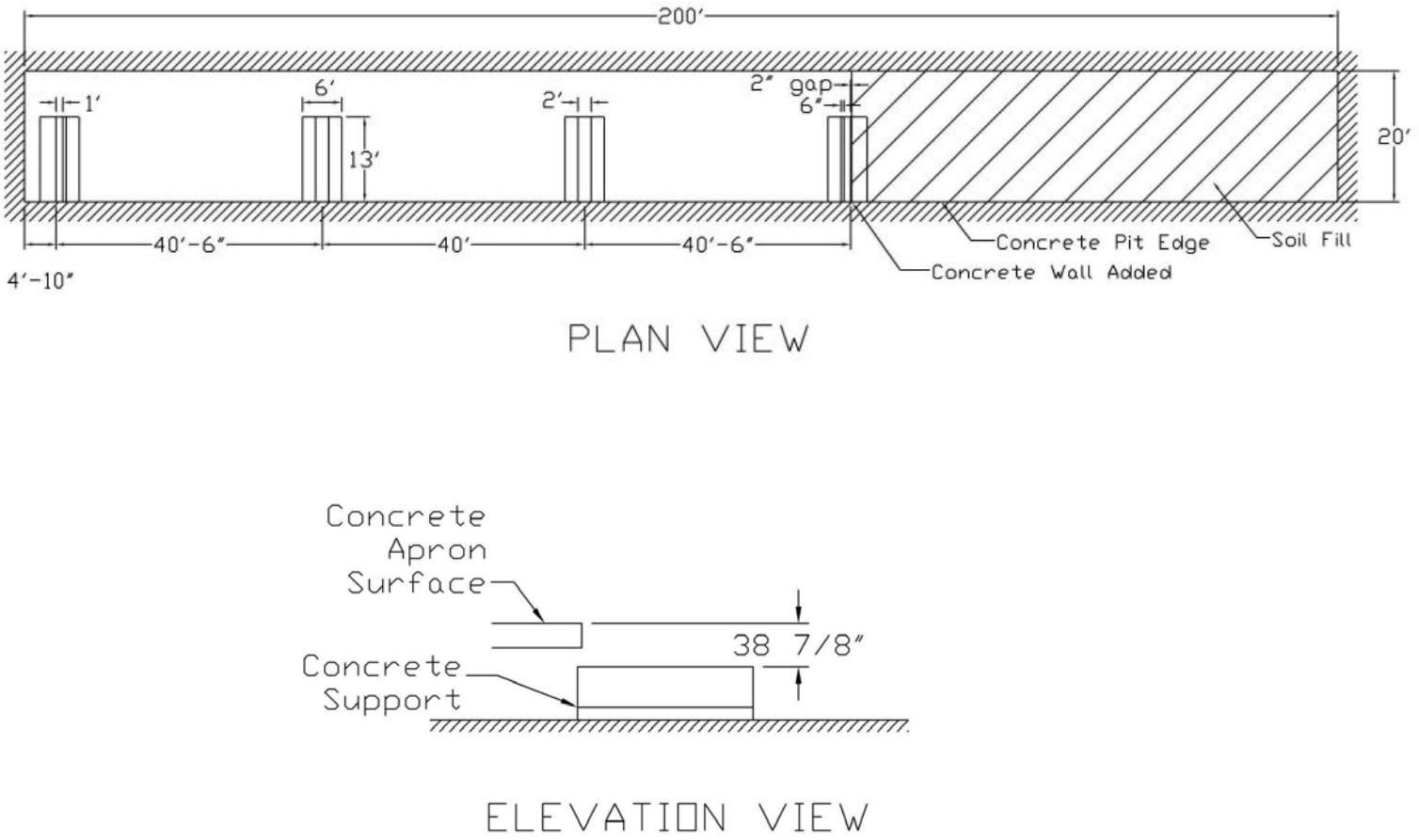

Figure 2. Bridge Substructure Details - Plan and Elevation Views

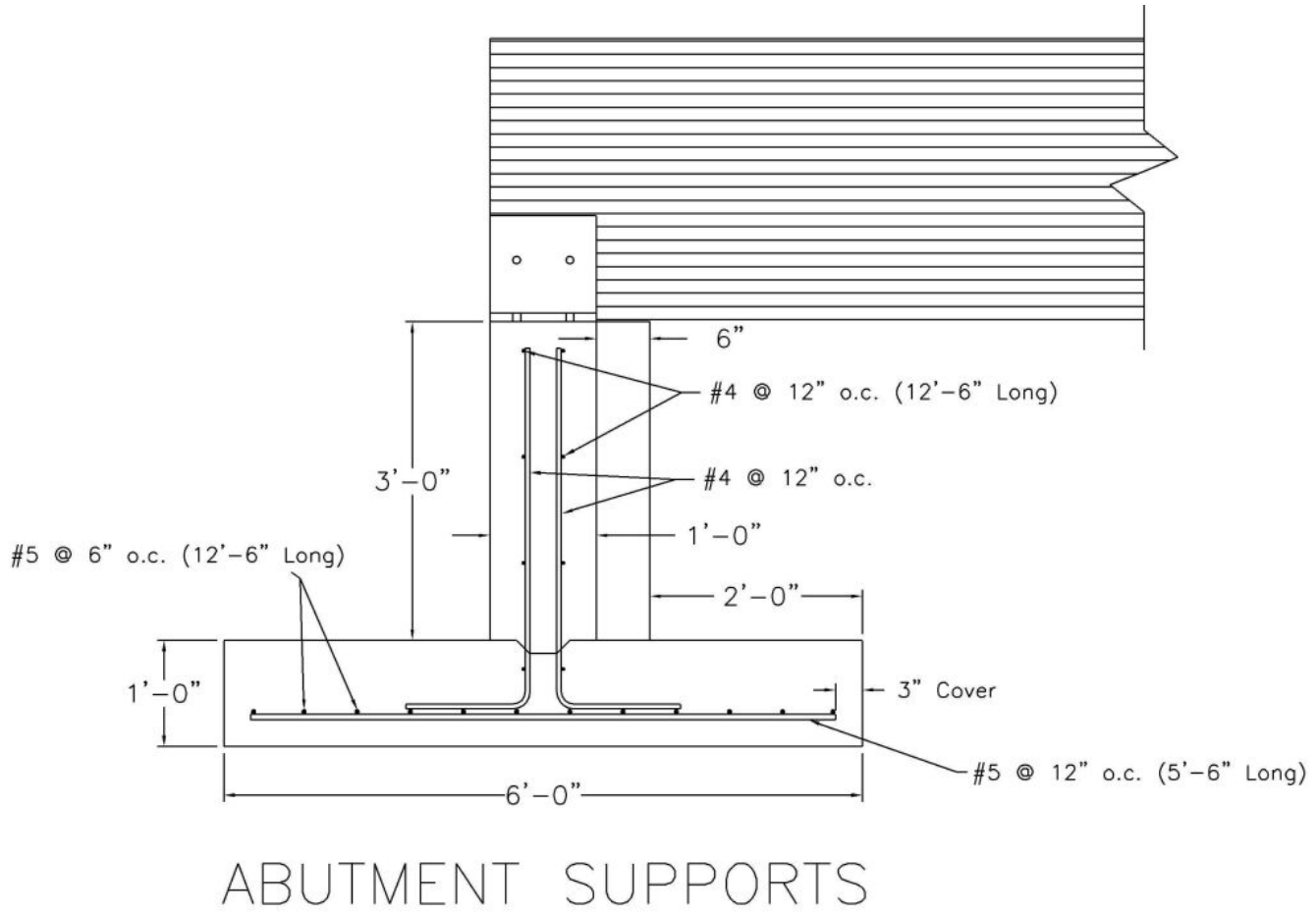

Figure 3. Bridge Substructure Details - Abutment Supports

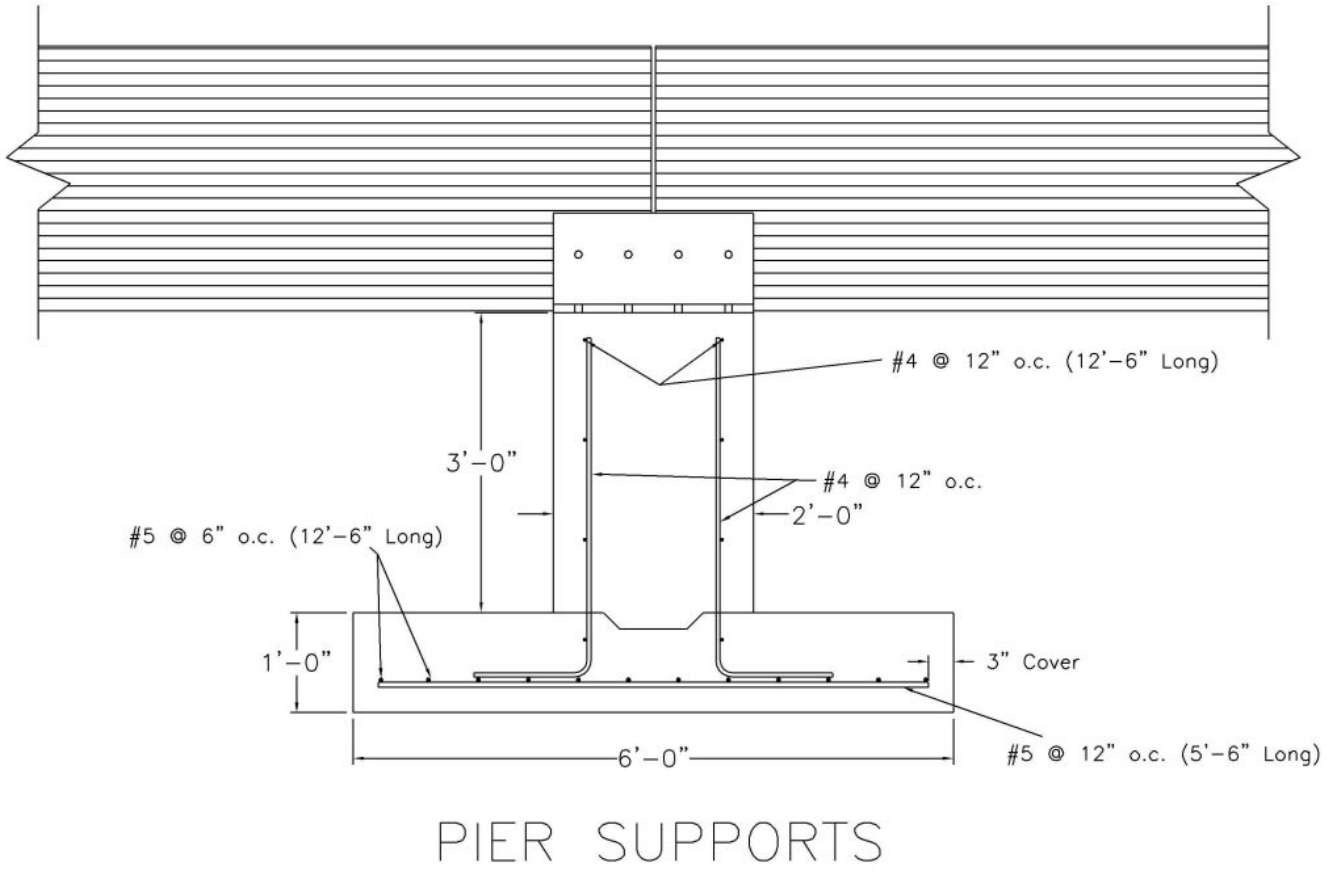

Figure 4. Bridge Substructure Details - Pier Supports

Figure 5. Bridge Substructure Construction

the concrete tarmac such that the surface of the bridge deck would be at an elevation approximately 51 mm below the grade of the concrete tarmac. This allowed for a wearing surface to be placed on the top of the bridge deck that would have a final grade at the same elevation as the concrete tarmac.

The inner two concrete bridge supports had a center-to-center spacing of 12.19 m whereas the outer two spacings were 12.12-m on center. The concrete bridge supports were constructed perpendicular to the roadway, providing a simple span between the concrete bridge supports, as shown in Figure 6. The top of the two exterior concrete bridge supports measured 457-mm wide by 3.96-m long by 914-mm high. The top of the two interior concrete bridge supports measured 610-mm wide by 3.96-m long by 914-mm high. The concrete bridge supports were attached to rectangular concrete spread footings measuring 305-mm thick by 1.83-m wide by 3.96-m long.

Three welded steel bearing assemblies were mounted to the top of each concrete bridge support to allow for the rigid attachment between the supports and bridge girders, as shown in Figure 6. The bearing assemblies were fabricated with 19-mm steel plate, as shown in Figures 1 through 4. Stainless steel threaded rods, measuring 19-mm diameter by 381-mm long, were embedded and epoxied into the top surface of the concrete bridge supports and used for the rigid attachment. Neoprene bearing pads, measuring 19-mm thick, were placed in the bearing assemblies to soften the contact interface between the assemblies and the girders. Originally, the bearing assemblies were fabricated to fit 273-mm wide girders. However, the bridge design was modified after the bearing assemblies were fabricated, including a reduction in the girder width to 222-mm wide. Therefore, shims were used to adapt the bearing assemblies to fit 222-mm wide girders.

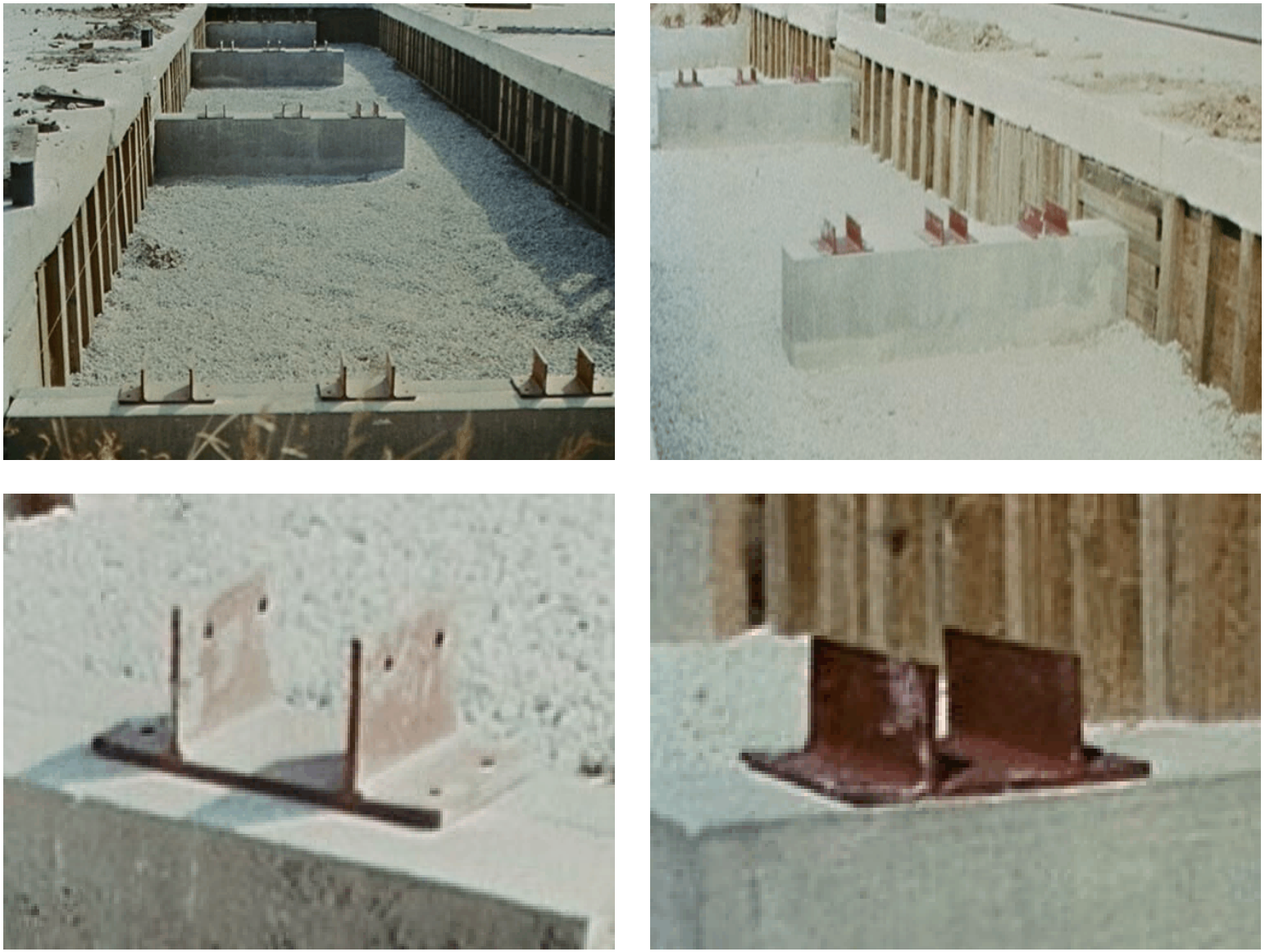

Figure 6. Bridge Substructure and Retaining Walls

4.1.3 Bridge Superstructure

Following the completion of the bridge substructure, the bridge superstructure was constructed. The superstructure consisted of nine glulam girders, twenty-four glulam diaphragms, and thirty transverse glulam deck panels. The bridge superstructure was constructed with three girders spanning between any two concrete bridge supports. For any two girders in a span, four glulam diaphragms were bolted between the girders to provided lateral stiffness to the bridge structure. Each glulam girder measured 222-mm wide by 768-mm deep by 12.17-m long, while the glulam diaphragms measured 130-mm wide by 629-mm deep by 997-mm long. The glulam panels were attached to the girders using standard aluminum deck brackets. Each glulam panel measured 130-mm thick by 1,216-mm wide by 3.96-m long. All glulam superstructure components were fabricated with Southern Yellow Pine (SYP) and treated with pentachlorophenol in heavy oil to a minimum net retention of 9.61 kg/m^3 as specified in American Wood-Preservers' Association (AWPA) Standard C14 (28). The girders were fabricated to meet Grade 24F-V3 while the deck panels, and diaphragms were fabricated from Combination No. 47 material.

One of the advantages of timber bridges is the ease of construction and the fact that a bridge can be erected in seasonal conditions that would not be conducive to poured concrete construction. These advantages became evident in this project as it took less than three days in sub-freezing temperatures with minimal equipment and a relatively small labor force to erect the bridge superstructure. The sequence of the superstructure construction is shown in Figures 7 through 9.

Figure 7. Bridge Superstructure Construction

Figure 8. Bridge Superstructure Construction

Figure 9. Bridge Superstructure Construction

5 TEST CONDITIONS

5.1 Test Facility

The testing facility is located at the Lincoln Air-Park on the northwest (NW) side of the Lincoln Municipal Airport and is approximately 8.0 km NW of the University of Nebraska-Lincoln.

5.2 Vehicle Tow and Guidance System

A reverse cable tow system with a 1:2 mechanical advantage was used to propel the test vehicle. The distance traveled and the speed of the tow vehicle were one-half that of the test vehicle. The test vehicle was released from the tow cable before impact with the barrier. A digital speedometer in the tow vehicle was utilized to increase the accuracy of the test vehicle impact speed.

A vehicle guidance system developed by Hinch (29) was used to steer the test vehicle. A guide-flag, attached to the left-front wheel and the guide cable, was sheared off before impact. The 9.5-mm diameter guide cable was tensioned to approximately 13.3 kN, and supported laterally and vertically every 30.48 m by hinged stanchions. The hinged stanchions stood upright while holding up the guide cable, but as the vehicle was towed down the line, the guide-flag struck and knocked each stanchion to the ground. For the pickup truck test, the vehicle guidance system was approximately 305-m long.

5.3 Test Vehicle

5.3.1 Steel System

Two full-scale vehicle crash tests were performed during the development of the steel bridge railing and approach guardrail transition system. Test STCR-1 was performed on the bridge railing, while test STCR-2 was conducted on the approach guardrail transition.

For test STCR-1, a 1990 Chevrolet 2500 ¾-ton pickup truck was used as the test vehicle.

The test inertial and gross static weights were 1,966 kg. The test vehicle is shown in Figure 10, and vehicle dimensions are shown in Figure 11.

For test STCR-2, a 1990 Chevrolet 2500 ¾-ton pickup truck was used as the test vehicle. The test inertial and gross static weights were 2,035 kg. The test vehicle is shown in Figure 12, and vehicle dimensions are shown in Figure 13.

5.3.2 Wood System

Two full-scale vehicle crash tests were performed during the development of the wood bridge railing and approach guardrail transition system. Test WRBP-1 was performed on the bridge railing, while test WRBP-2 was conducted on the approach guardrail transition.

For test WRBP-1, a 1994 Ford F-250 ¾-ton pickup truck was used as the test vehicle. The test inertial and gross static weights were 2,031 kg. The test vehicle is shown in Figure 14, and vehicle dimensions are shown in Figure 15.

For test WRBP-2, a 1993 Ford F-250 ¾-ton pickup truck was used as the test vehicle. The test inertial and gross static weights were 2,011 kg. The test vehicle is shown in Figure 16, and vehicle dimensions are shown in Figure 17.

5.3.3 Center-of-Mass Determination, Vehicle Targets, and Alignment

The Suspension Method (30) was used to determine the vertical component of the center of gravity for the pickup truck test vehicles. This method is based on the principle that the center of gravity of any freely suspended body is in the vertical plane through the point of suspension. The vehicle was suspended successively in three positions, and the respective planes containing the center of gravity were established. The intersection of these planes pinpointed the location of the center of gravity. The locations of the final centers of gravity are shown in Figures 10 through 17.

Figure 10. Test Vehicle, Test STCR-1

Date: 9/29/98 Test Number: STCR-1 Model: 2500

Make: Chevrolet Vehicle I.D.#: 1GCFC24Z8LZ193682

Tire Size: 275/45R16 Year: 1990 Odometer: 39,759

*(All Measurements Refer to Impacting Side)

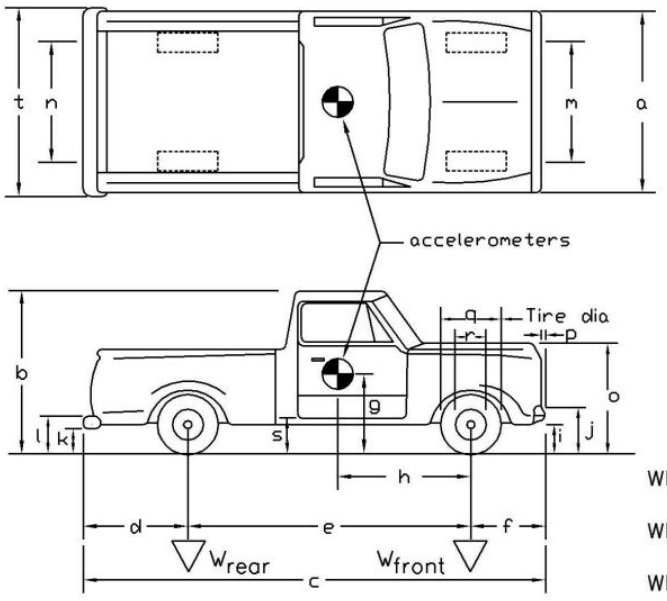

Vehicle Geometry – mm

a	1873	b	1791
c	5537	d	1315
e	3327	f	851
g	737	h	1499
i	394	j	610
k	533	l	730
m	1584	n	1616
o	975	p	89
q	762	r	445
s	435	t	1867

Wheel Center Height Front 375

Wheel Center Height Rear 368

Wheel Well Clearance (FR) 857

Wheel Well Clearance (RR) 927

Engine Type V6

Engine Size 4.3L 262 ci

Transmission Type:

(Automatic) or Manual

FWD or (RWD) or 4WD

Weights – kg	Curb	Test Inertial	Gross Static
W_{front}	1065	1080	1080
W_{rear}	851	886	886
W_{total}	1916	1966	1966

Note any damage prior to test: dents in right & left doors, tail gate beat up

Figure 11. Vehicle Dimensions, Test STCR-1

Figure 12. Test Vehicle, Test STCR-2

Date: 9/30/98 Test Number: STCR-2 Model: 2500

Make: Chevy Vehicle I.D.#: 1GBGC24K9ME174319

Tire Size: 245/75R16 Year: 1990 Odometer: 141265

*(All Measurements Refer to Impacting Side)

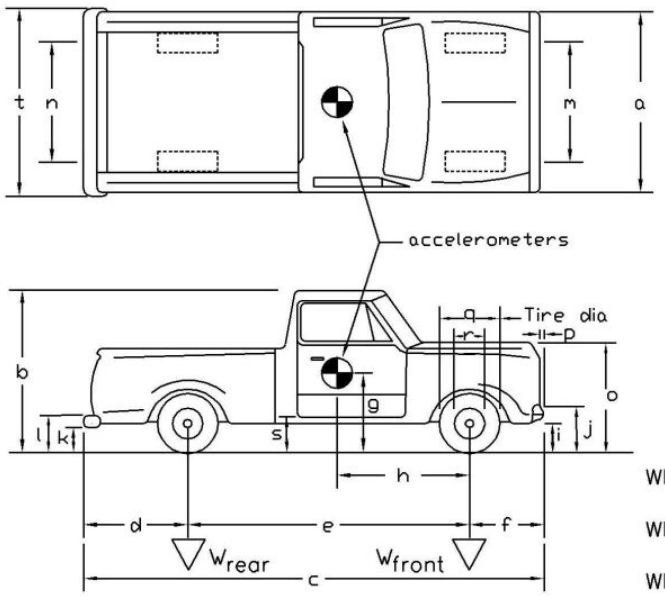

Vehicle Geometry – mm

a	1892	b	1842
c	5537	d	1295
e	3327	f	864
g	737	h	1359
i	464	j	679
k	635	l	838
m	1613	n	1613
o	1092	p	102
q	749	r	445
s	495	t	1829

Wheel Center Height Front 368

Wheel Center Height Rear 381

Wheel Well Clearance (FR) 908

Wheel Well Clearance (RR) 984

Engine Type Gas–V8

Engine Size 5.7L 350 ci

Transmission Type:

(Automatic) or Manual

FWD or (RWD) or 4WD

Weights – kg	Curb	Test Inertial	Gross Static
W_{front}	1173	1172	1172
W_{rear}	855	863	863
W_{total}	2028	2035	2035

Note any damage prior to test: Passenger side box dent/Driver side door scratch

Figure 13. Vehicle Dimensions, Test STCR-2

Figure 14. Test Vehicle, Test WRBP-1

Date: 12/15/99 Test Number: WRBP-1 Model: 2000P / F-250

Make: FORD Vehicle I.D.#: 1FTHF25YXNNA70501

Tire Size: LT 235/85 R16 Year: 1992 Odometer: 115,829

*(All Measurements Refer to Impacting Side)

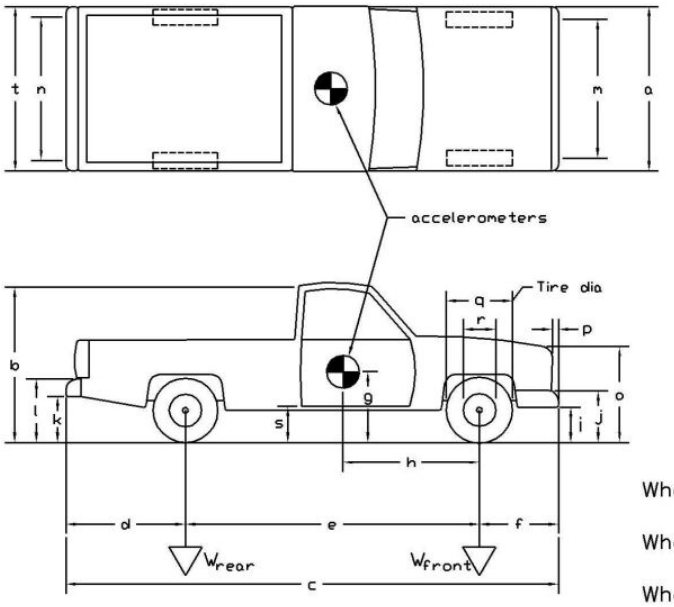

Vehicle Geometry – mm

a	1943	b	1880
c	5512	d	1295
e	3378	f	838
g	737	h	1464
i	508	j	724
k	546	l	711
m	1664	n	1638
o	1130	p	114
q	800	r	445
s	533	t	1930

Wheel Center Height Front 381

Wheel Center Height Rear 381

Wheel Well Clearance (FR) 899

Wheel Well Clearance (RR) 949

Engine Type 6 CYL. GAS

Engine Size 300 CID 4.9 L

Transmission Type:

Automatic or (Manual)

FWD or (RWD) or 4WD

Weights – kg	Curb	Test Inertial	Gross Static
W_{front}	1144	1138	1138
W_{rear}	900	894	894
W_{total}	2045	2031	2031

Note any damage prior to test: FRONT BOX DAMAGE (CARGO DAMAGE)
DRIVERS SIDE BOX REAR RAIL DENT
SMALL DENT PASS. SIDE BOX LOWER

Figure 15. Vehicle Dimensions, Test WRBP-1

Figure 16. Test Vehicle, Test WRBP-2

Date: 2/3/00 Test Number: WRBP-2 Model: F 250-2000P

Make: Ford Vehicle I.D.#: 1FTHF25Y3PNB35921

Tire Size: LT 238/85 R-16 Year: 1993 Odometer: 133300

*(All Measurements Refer to Impacting Side)

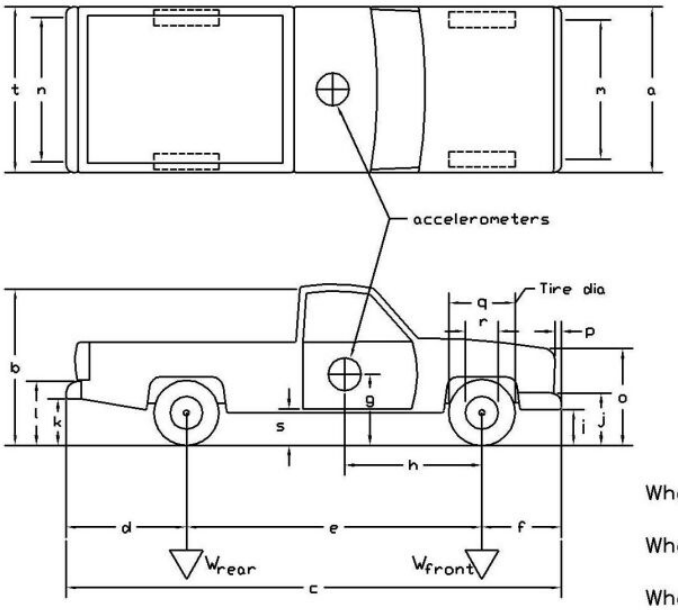

Vehicle Geometry – mm

a	1956	b	1873
c	5512	d	1327
e	3378	f	864
g	738	h	1375
i	476	j	654
k	591	l	800
m	1670	n	1622
o	1156	p	86
q	794	r	445
s	562	t	1854

Wheel Center Height Front 384

Wheel Center Height Rear 387

Wheel Well Clearance (FR) 889

Wheel Well Clearance (RR) 972

Engine Type 6 CYL. GAS

Engine Size 300 CID

Transmission Type:

(Automatic) or Manual

FWD or (RWD) or 4WD

Weights – kg	Curb	Test Inertial	Gross Static
W_{front}	1138	1143	1143
W_{rear}	954	841	868
W_{total}	2092	2032	2011

Note any damage prior to test: NONE

Figure 17. Vehicle Dimensions, Test WRBP-2

Vehicle ballast, consisting of steel plates and/or sand bags, was used to obtain the desired test weight.

Square, black and white-checkered targets were placed on the vehicle to aid in the analysis of the high-speed film, as shown in Figures 10, 12, 14, 16, and 18 through 21. Targets were placed on the center of gravity which were viewable on both the left and right sides of the vehicle and on the top of the vehicle. The remaining targets were located for reference so that they could be viewed from the high-speed cameras for film analysis.

The front wheels of the test vehicles were aligned for camber, caster, and toe-in values of zero so that the vehicles would track properly along the guide cable. Two 5B flash bulbs were mounted on both the hood and roof of the vehicles to pinpoint the time of impact with the barrier on the high-speed film. The flash bulbs were fired by a pressure tape switch mounted on the front face of the bumper. A remote controlled brake system was installed in the test vehicles so the vehicles could be brought safely to a stop after the test.

5.4 Data Acquisition Systems

5.4.1 Accelerometers

One triaxial piezoresistive accelerometer system with a range of ±200 G's was used to measure the acceleration in the longitudinal, lateral, and vertical directions at a sample rate of 10,000 Hz. The environmental shock and vibration sensor/recorder system, Model EDR-4M6, was developed by Instrumented Sensor Technology (IST) of Okemos, Michigan and includes three differential channels as well as three single-ended channels. The EDR-4 was configured with 6 Mb of RAM memory and a 1,500 Hz lowpass filter. Computer software, "DynaMax 1 (DM-1)" and "DADiSP" were used to digitize, analyze, and plot the accelerometer data.

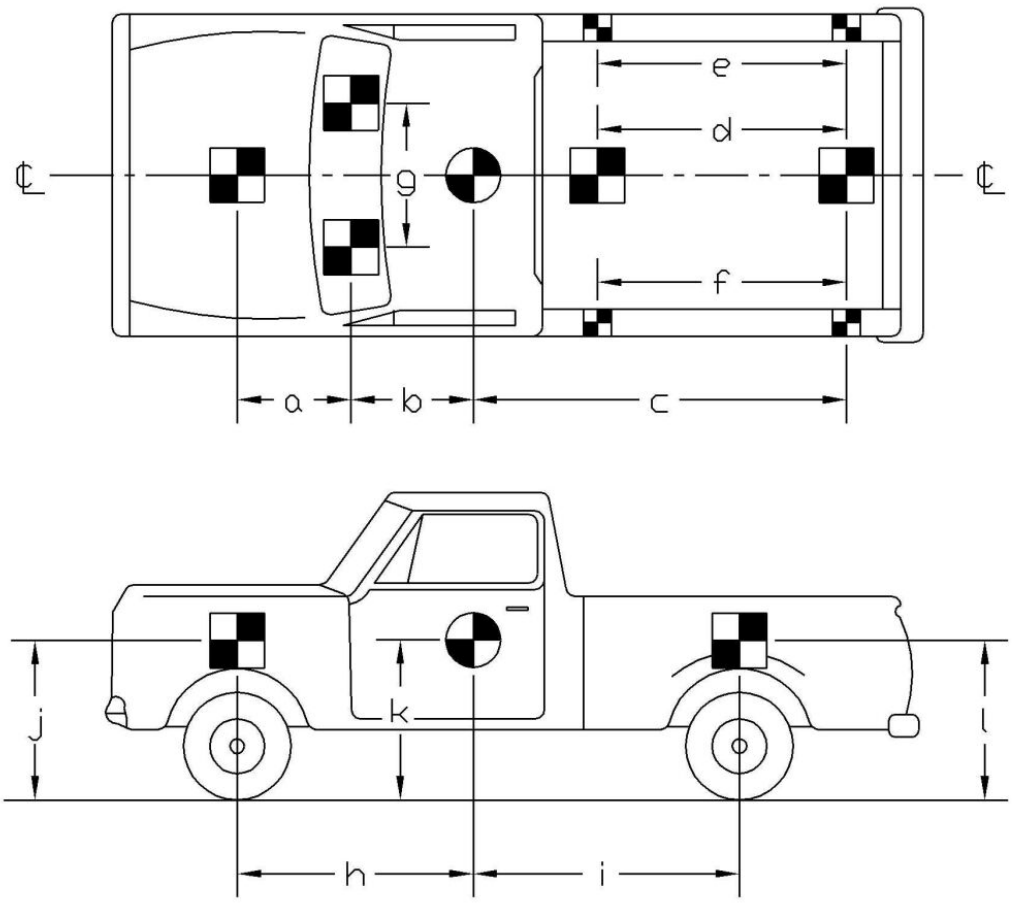

TEST #: STCR-1

TARGET GEOMETRY (mm)

a	1283	b	724	c	2311	d	1454
e	2076	f	2089	g	978	h	1499
i	1848	j	911	k	737	l	984

Figure 18. Vehicle Target Locations, Test STCR-1

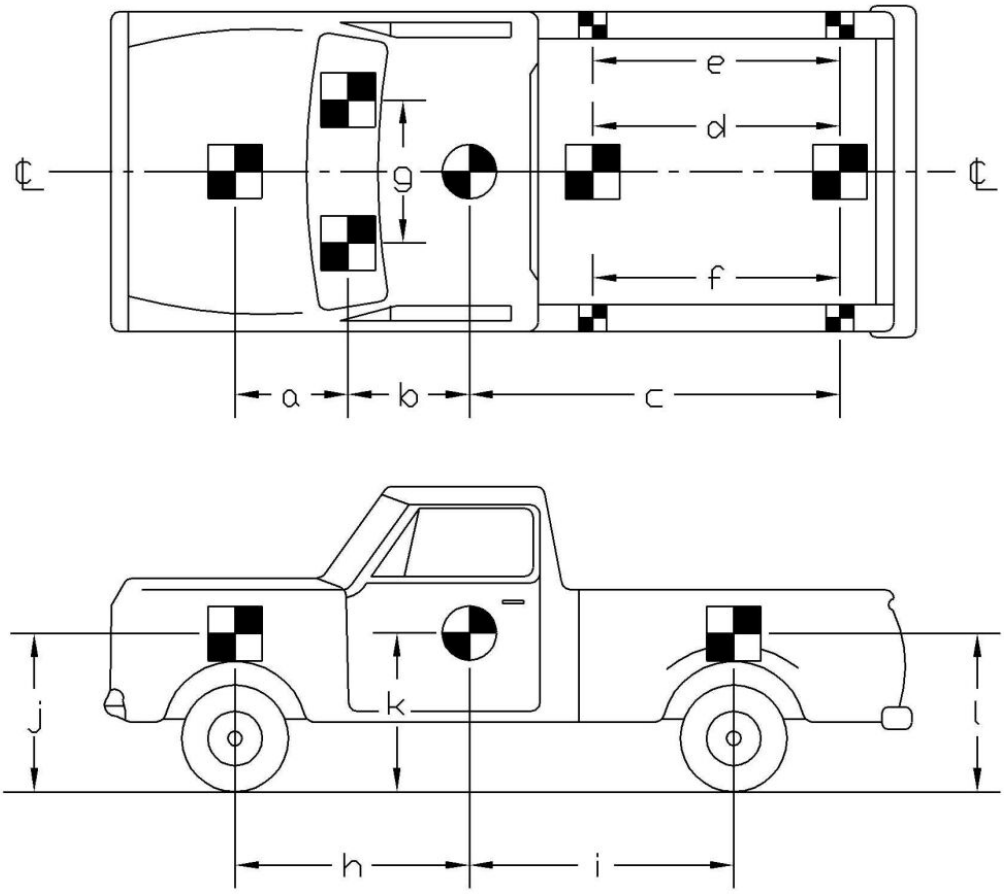

TEST #: STCR-2

TARGET GEOMETRY (mm)

a	953	b	711	c	1715	d	1832
e	2143	f	2146	g	1041	h	1359
i	1969	j	1019	k	737	l	1095

Figure 19. Vehicle Target Locations, Test STCR-2

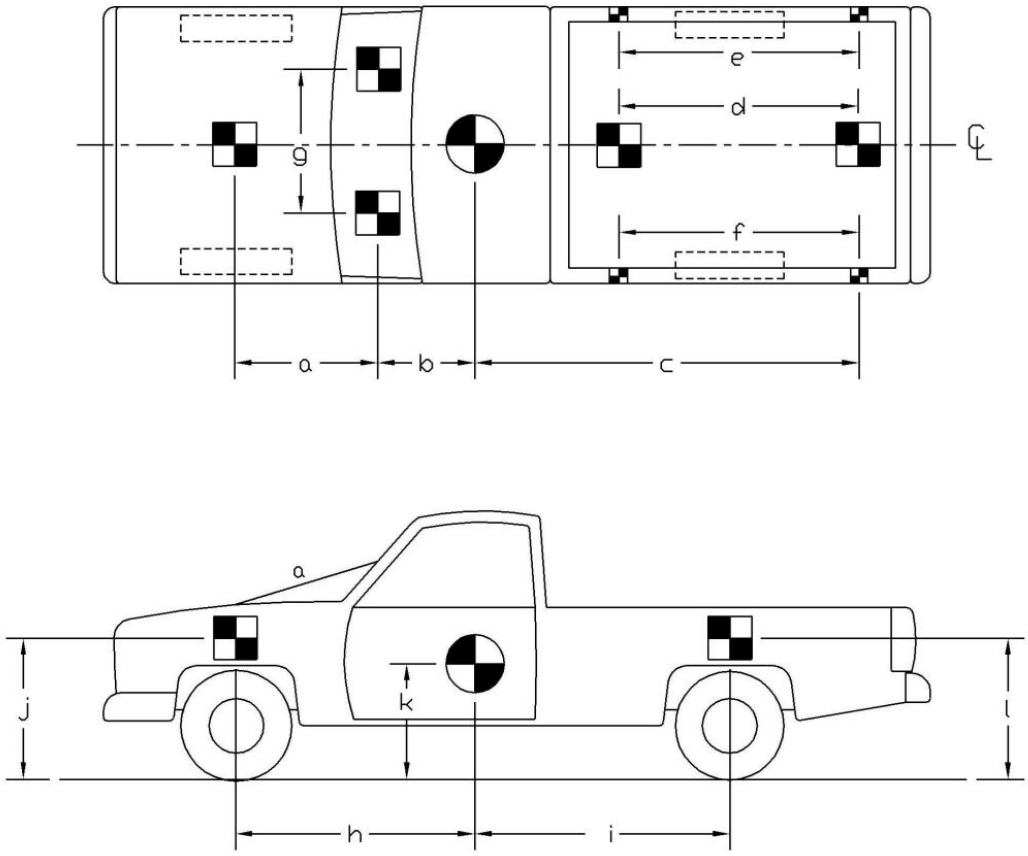

TEST #: WRBP-1

TARGET GEOMETRY (mm)

a	1080	d	1746	g	1041	j	997
b	711	e	2197	h	1486	k	738
c	2616	f	2197	i	1892	l	1054

Figure 20. Vehicle Target Locations, Test WRBP-1

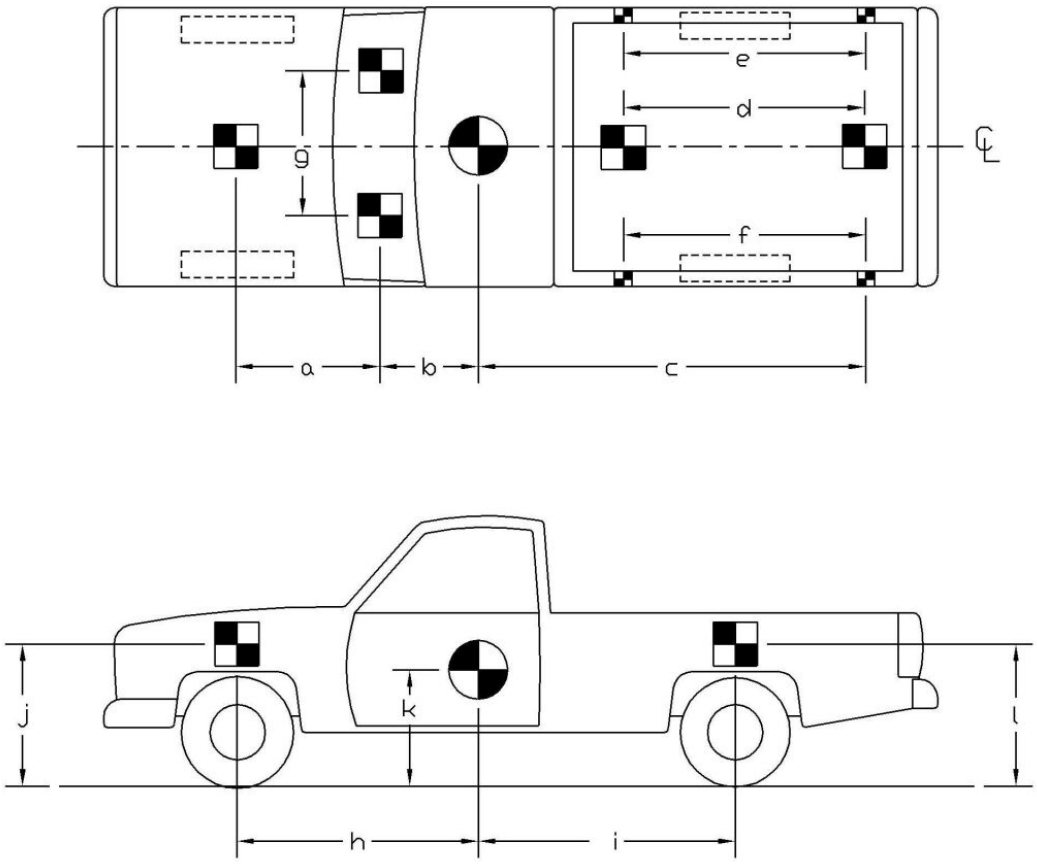

TEST #: WRBP-2

TARGET GEOMETRY (mm)

a	940	d	1899	g	1029	j	991
b	718	e	2197	h	1458	k	738
c	2743	f	2197	i	1918	l	1073

Figure 21. Vehicle Target Locations, Test WRBP-2

A backup triaxial piezoresistive accelerometer system with a range of ±200 G's was also used to measure the acceleration in the longitudinal, lateral, and vertical directions at a sample rate of 3,200 Hz. The environmental shock and vibration sensor/recorder system, Model EDR-3, was developed by Instrumented Sensor Technology (IST) of Okemos, Michigan. The EDR-3 was configured with 256 Kb of RAM memory and a 1,120 Hz lowpass filter. Computer software, "DynaMax 1 (DM-1)" and "DADiSP", were used to digitize, analyze, and plot the accelerometer data.

5.4.2 Rate Transducer

For tests STCR-1 and STCR-2, a Humphrey 3-axis rate transducer with a range of 250 deg/sec in each of the three directions (pitch, roll, and yaw) was used to measure the angular velocity of the test vehicles. For tests WRBP-1 and WRBP-2, a Humphrey 3-axis rate transducer with a range of 360 deg/sec in each of the three directions (pitch, roll, and yaw) was used to measure the angular velocity of the test vehicles. The rate transducer was rigidly attached to the vehicles near the center of gravity of the test vehicle. Rate transducer signals, excited by a 28 volt DC power source, were received through the three single-ended channels located externally on the EDR-4M6 and stored in the internal memory. The raw data measurements were then downloaded for analysis and plotting. Computer software, "DynaMax 1 (DM-1)," "Test Point," and"DADiSP", were used to digitize, analyze, and plot the rate transducer data.

5.4.3 High-Speed Photography

For tests STCR-1 and STCR-2, five high-speed 16-mm Red Lake Locam cameras, with operating speed of approximately 500 frames/sec, were used to film the crash tests. A Locam, with a wide-angle 12.5-mm lens, was placed above the test installation to provide a field of view

perpendicular to the ground. A Locam, a SVHS video camera, and a 35-mm still camera were placed downstream from the impact point and had a field of view parallel to the barrier. A Locam and a SVHS video camera were placed on the traffic side of the barrier and had a field of view perpendicular to the barrier. Another Locam was placed upstream and behind the barrier. A Locam and a SVHS video camera were placed downstream and behind the barrier. A schematic of all nine camera locations for tests STCR-1 and STCR-2 are shown in Figures 22 and 23, respectively.

For test WRBP-1, five high-speed, 16-mm Red Lake Locam cameras, with operating speed of approximately 500 frames/sec, were used to film the crash tests. A Locam, with a wide-angle 12.5-mm lens, was placed above the test installation to provide a field of view perpendicular to the ground. A Locam, a SVHS video camera, and a 35-mm still camera were placed downstream from the impact point and had a field of view parallel to the barrier. A Locam and a SVHS video camera were placed on the traffic side of the barrier and had a field of view perpendicular to the barrier. A Canon digital video camera was placed upstream and behind the barrier. A Locam was placed downstream and behind the barrier. Another Locam and a SVHS video camera were placed further downstream and behind the barrier. A schematic of all ten camera locations for test WRBP-1 is shown in Figure 24.

For test WRBP-2, five high-speed,16-mm Red Lake Locam cameras, with operating speed of approximately 500 frames/sec, were used to film the crash tests. A Locam, with a wide-angle 12.5-mm lens, was placed above the test installation to provide a field of view perpendicular to the ground. A Locam, a SVHS video camera, and a 35-mm still camera were placed downstream from the impact point and had a field of view parallel to the barrier. A Locam and a SVHS video camera were placed on the traffic side of the barrier and had a field of view perpendicular to the barrier. An

E/cam high-speed video camera was placed upstream and behind the barrier. A Locam was placed behind the barrier and had a field of view perpendicular to the point of impact. A Canon digital video camera was placed downstream and behind the barrier. A Locam and a SVHS video camera were placed further downstream and behind the barrier. A schematic of all eleven camera locations for test WRBP-2 is shown in Figure 25. The film was analyzed using the Vanguard Motion Analyzer. Actual camera speed and camera divergence factors were considered in the analysis of the high-speed film.

5.4.4 Pressure Tape Switches

For each test, five pressure-activated tape switches, equally spaced, were used to determine the speed of the vehicle before impact. Each tape switch fired a strobe light which sent an electronic timing signal to the data acquisition system as the right-front tire of the test vehicle passed over it. Test vehicle speeds were determined from electronic timing mark data recorded on "EGAA" software. Strobe lights and high-speed film analysis are used only as a backup in the event that vehicle speeds cannot be determined from the electronic data.

5.4.5 Bridge Railing Instrumentation

For tests STCR-1 and WRBP-1, electronic sensors were placed on selected regions and components of the bridge railing systems. The types of sensors used for the crash tests were strain gauges and are described below.

5.4.5.1 Strain Gauges

For test STCR-1, twenty strain gauges were installed on several of the bridge railing components of bridge post nos. 6 through 8, consisting of thirteen gauges located on the top deck mounting plates, five gauges located on the bottom deck mounting plates, and two gauges located

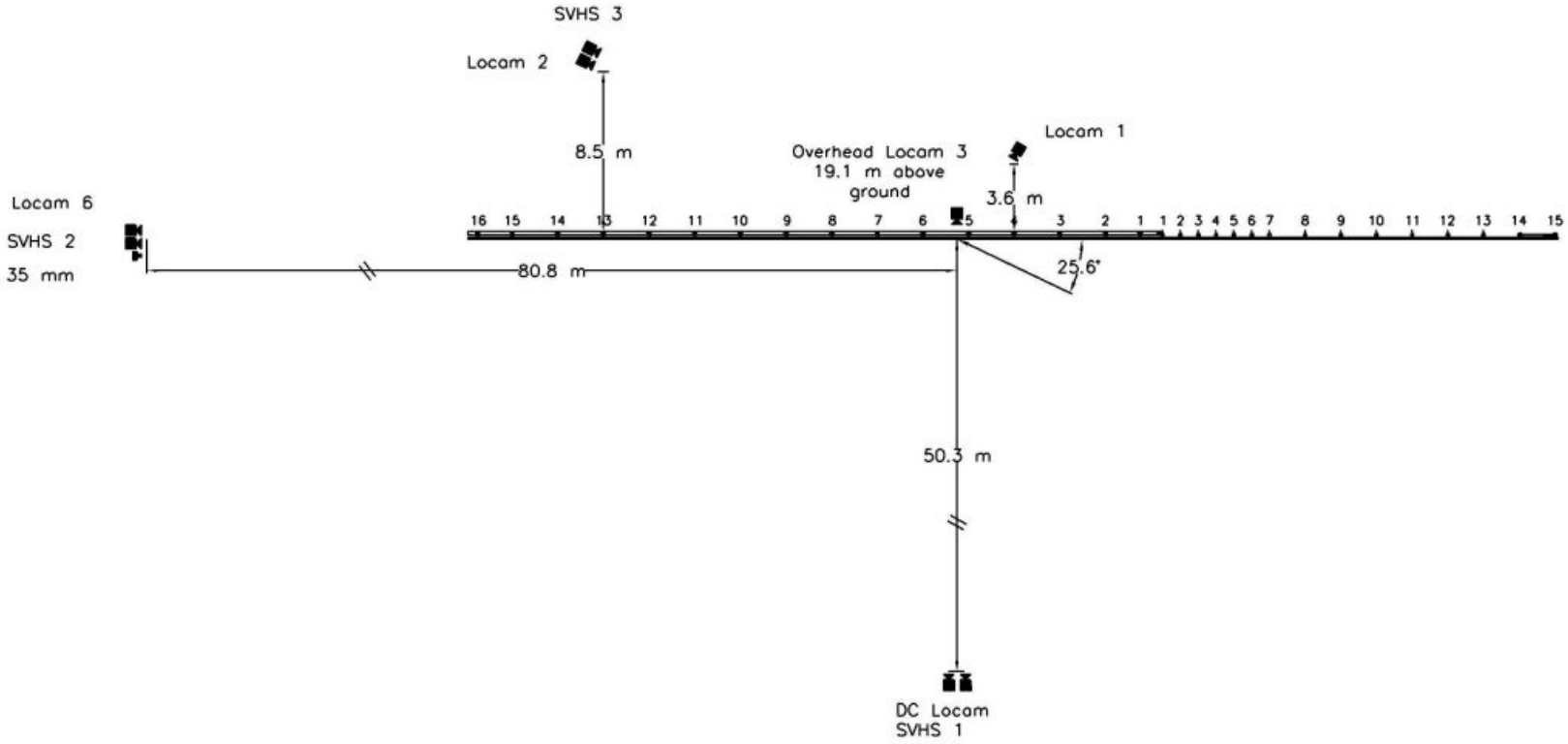

Figure 22. Location of High-Speed Cameras, Test STCR-1

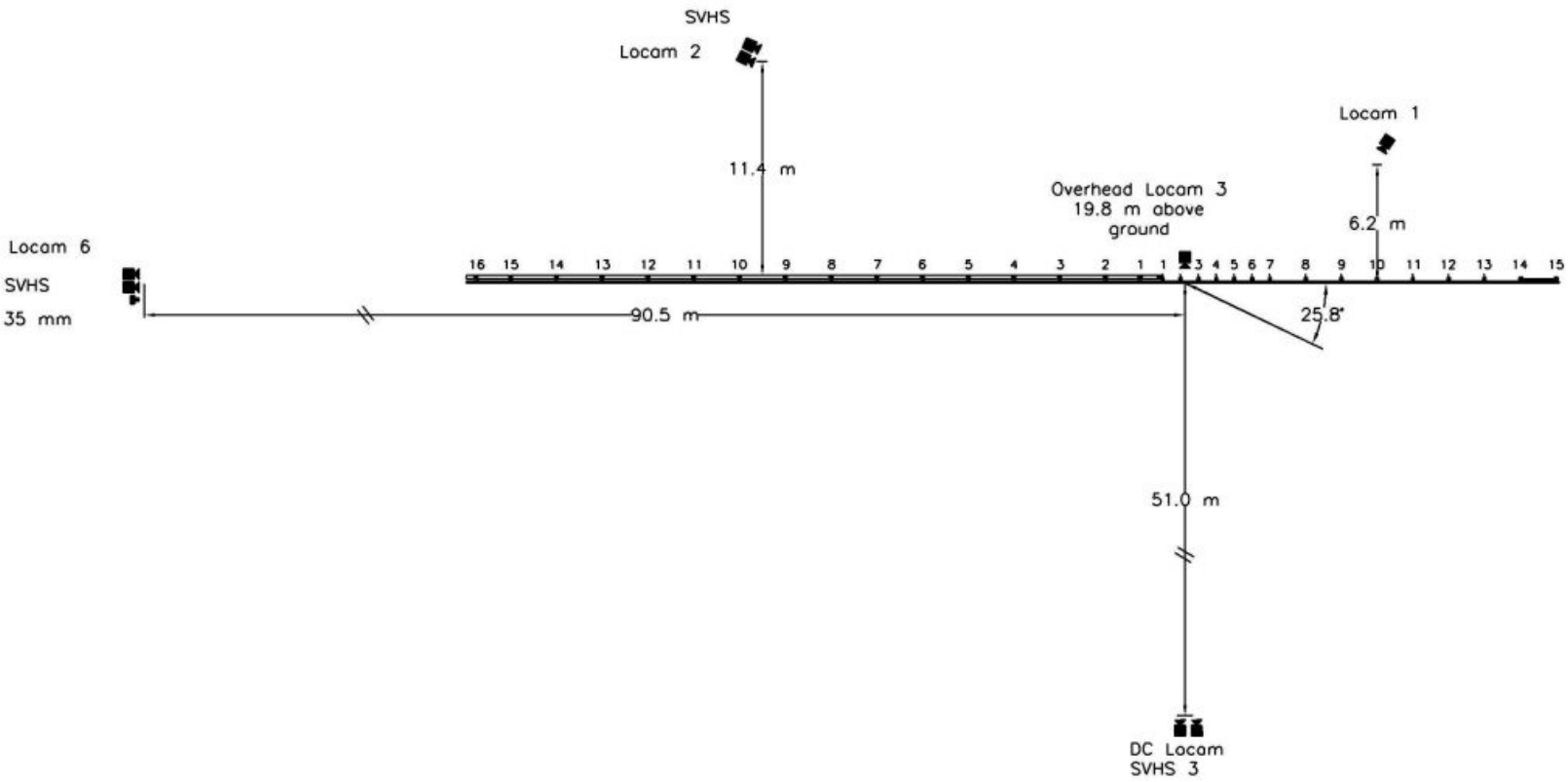

Figure 23. Location of High-Speed Cameras, Test STCR-2

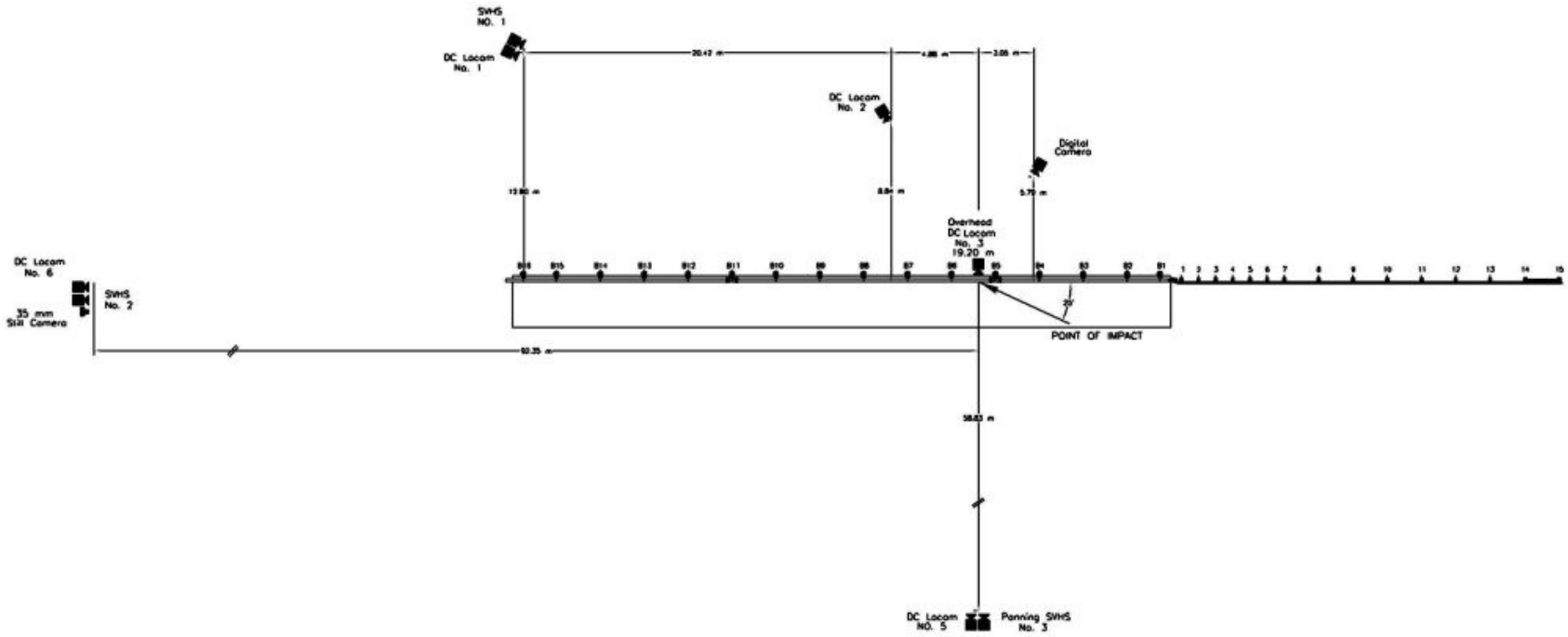

Figure 24. Location of High-Speed Cameras, Test WRBP-1

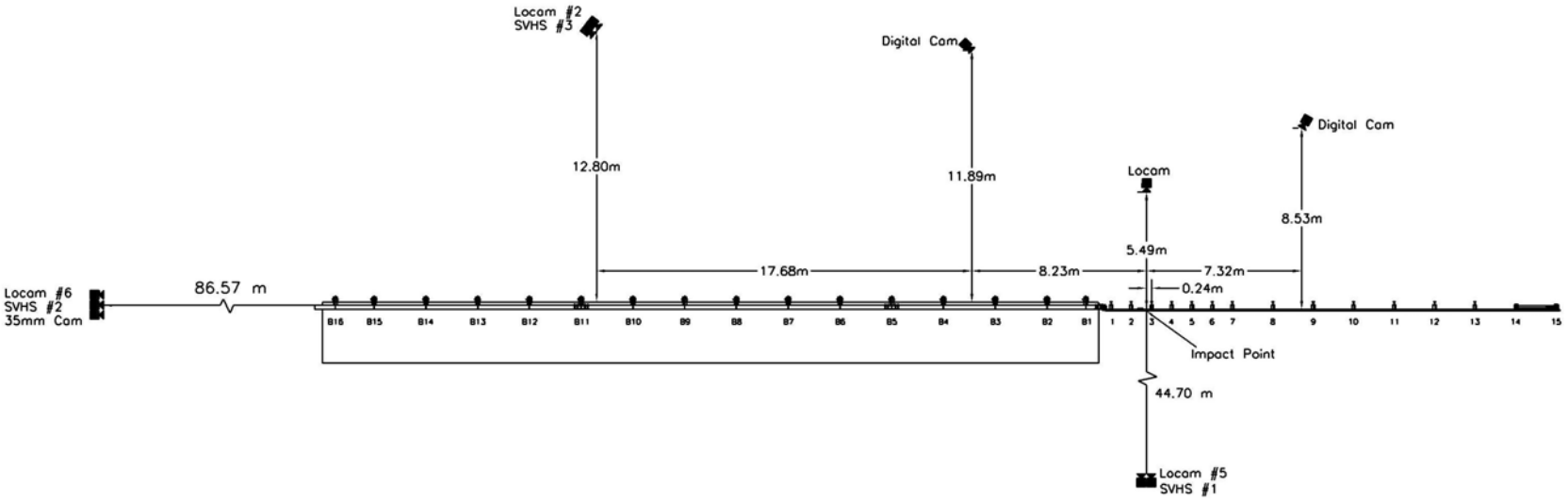

Figure 25. Location of High-Speed Cameras, Test WRBP-2

on the front and back flanges of a bridge post. The typical strain gauge positions are shown in Figure 26. Actual strain gauge locations are shown in Appendix A.

For test WRBP-1, twenty-three strain gauges were installed on several of the bridge railing components of bridge post nos. 5 through 7, consisting of twenty-one gauges located on the top deck mounting plates and two gauges located on the front and back sides of the bent post plate of a bridge post. The typical strain gauge positions are shown in Figure 27. Actual strain gauge locations are shown in Appendix B.

For tests STCR-1 and WRBP-1, the components were instrumented with weldable strain gauges, consisting of gauge type LWK-06-W250B-350. The nominal resistance of the gauges was 350.0 ± 1.4 ohms with a gauge factor equal to 2.02. The operating temperature limits of the gauges was -195 to +260 degrees Celsius. The strain limits of the gauges were 0.5% in tension or compression (5000 $\mu\epsilon$). The strain gauges were manufactured by the Micro-Measurements Division of Measurements Group, Inc. of Raleigh, North Carolina. The installation procedure required that the metal surface be clean and free from debris and oxidation. Once the surface had been prepared, the gauges were spot welded to the test surface.

A Measurements Group Vishay Model 2310 signal conditioning amplifier was used to condition and amplify the low-level signals to high-level outputs for multichannel, simultaneous dynamic recording on "Test Point" software. After each signal was amplified, it was sent to a Keithly Metrabyte DAS-1802HC data acquisition board, and then stored permanently on the portable computer. The sample rate for all gauges was 10,000 samples per second (10,000 Hz), and the duration of sampling was 6 seconds for test STCR-1 and 10 seconds for test WRBP-1.

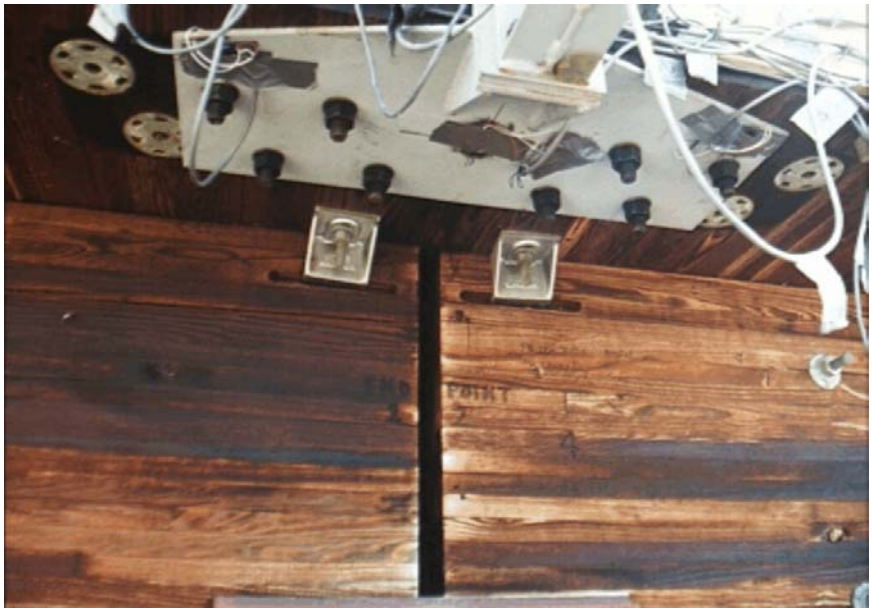

Figure 26. Typical Strain Gauge Locations, Test STCR-1

Figure 27. Typical Strain Gauge Locations, Test WRBP-1

6 STEEL SYSTEM DEVELOPMENT

Prior to this research, there have been no NCHRP Report No. 350 TL-2 bridge railing systems developed for use on transverse glulam timber deck bridges. However, in 1998, a TL-4 steel thrie beam and structural tube bridge railing system was developed for use on a transverse deck bridge and successfully full-scale crash tested by MwRSF (1-2,17). Thus, it was determined that concepts from this railing system could be successfully implemented into the design of the TL-2 steel bridge railing system.

As a result, the TL-2 steel bridge railing system was configured similarly to the TL-4 steel bridge railing system previously developed for transverse decks (1-2,17). However, several design modifications were deemed necessary since the TL-2 impact condition provided a reduced impact severity from the TL-4 impact condition. As a result, the upper structural tube rail on the TL-4 system was replaced with a channel rail section. This modification not only provided reduced weight but improved constructability. Other design modifications included a reduction in the size of the deck mounting plates and a decrease in the number of vertical bolts used to attach the mounting plates to the timber deck panels.

A 2,428-mm post spacing, also used with the TL-4 railings for transverse decks, was selected instead of the usual 1,905-mm post spacing. The increased post spacing was selected to optimize the design and to significantly improve the constructability of the railing system, which was based on 1,219-mm wide deck panels. The researchers believed these changes in the bridge railing design were necessary to provide additional economy over the TL-4 bridge railing system.

During the railing development, the researchers considered whether to design the bridge railing with or without the upper channel rail section. If an upper channel rail was not used,

dynamic deflections likely would be excessive, thus potentially resulting in vehicle pocketing between bridge posts or vehicle rollover on redirection. If an upper channel rail was used, then greater load distribution would occur between the bridge posts, thus resulting in the reduced pocketing and improved stability of the pickup truck on redirection. For the final system, a more-conservative design approach was chosen, and the upper channel rail was retained.

7 STEEL SYSTEM DESIGN DETAILS

7.1 Steel Bridge Railing

The bridge railing system consisted of five major components: (1) wide-flange bridge posts; (2) rail blockouts; (3) a thrie beam rail; (4) an upper structural channel rail; and (5) deck-mounting plates. Photographs of the bridge railing system are shown in Figures 28 through 30. The overall layout of the bridge railing system is shown in Figure 31. Design details of the bridge railing system are shown in Figures 32 through 40.

Sixteen galvanized ASTM A36 W152x17.9 structural wide-flange steel posts, measuring 1086-mm long, were used to support the steel railing, as shown in Figures 30, 33, and 39. The bridge posts were spaced 2,438 mm on center. The lower end of each post was bolted to two ASTM A36 steel plates that were connected to the top and bottom surfaces of the bridge deck with vertical bolts, as shown in Figure 37. The top and bottom plate assemblies were attached to each post with four ASTM A325 hex head bolts, sized 22-mm diameter x 73-mm long for the top two plate bolts and 16-mm diameter x 64-mm long for the bottom two plate bolts. The plate assemblies were attached to the deck with eight ASTM A307 22-mm diameter x 197-mm long bolts with 102-mm diameter shear plates located between both the upper and lower deck mounting plates an the glulam deck, as shown in Figure 37. The bolt location and spacing are shown in Figure 37 and 38.

As shown in Figures 31 and 32, the steel rail consisted of 3.42-mm thick thrie beam mounted 804 mm above the timber deck surface, as measured from the ground to the top of the rail. The thrie beam rail was offset 152 mm away from the posts with galvanized, ASTM A36 W152x17.9 structural wide-flange steel spacer blocks measuring 397-mm long, as shown in Figures 33 and 39.

The upper cap rail consisted of galvanized, ASTM A36 C200x17 structural steel channel

sections attached to the top of the steel spacer blocks, as shown in Figures 33 and 34. The distance from the bridge deck to the top of the channel rail was 813 mm. Design details of the channel railing sections are shown in Figure 35. The channel rail sections were attached to the spacer blocks with ASTM A36 structural steel angles measuring 89 mm x 89 mm x 8 mm, as shown in Figure 36. Each channel rail section was spliced together with ASTM A36 structural steel splice plates, as shown in Figure 36. The layout of the channel rail sections is shown in Figure 31.

The steel thrie beam rail was anchored at the downstream end of the bridge railing system with a rigid assembly consisting of welded steel plates and structural steel tubes that were bolted to the thrie beam rail and anchored to the concrete tarmac located at the MwRSF's outdoor test site, as shown in Figures 28 and 29. The downstream anchor assembly was necessary to develop the tensile capacity of the rail at the downstream end of the bridge railing system.

A 51-mm thick, concrete wearing surface was placed on top of the transverse glulam deck panels. This deck surface treatment was added in order to represent actual field conditions where an asphalt surface would likely be overlaid on the bridge for resistance to both wear and moisture. For the overlay, a 20.7 MPa concrete mix was used with Type III Portland cement, 9.5-mm minus aggregate, and fiber mesh additive.

Figure 28. Steel Bridge Railing System

Figure 29. Steel Bridge Railing System

Figure 30. Steel Bridge Railing System - Bridge Posts

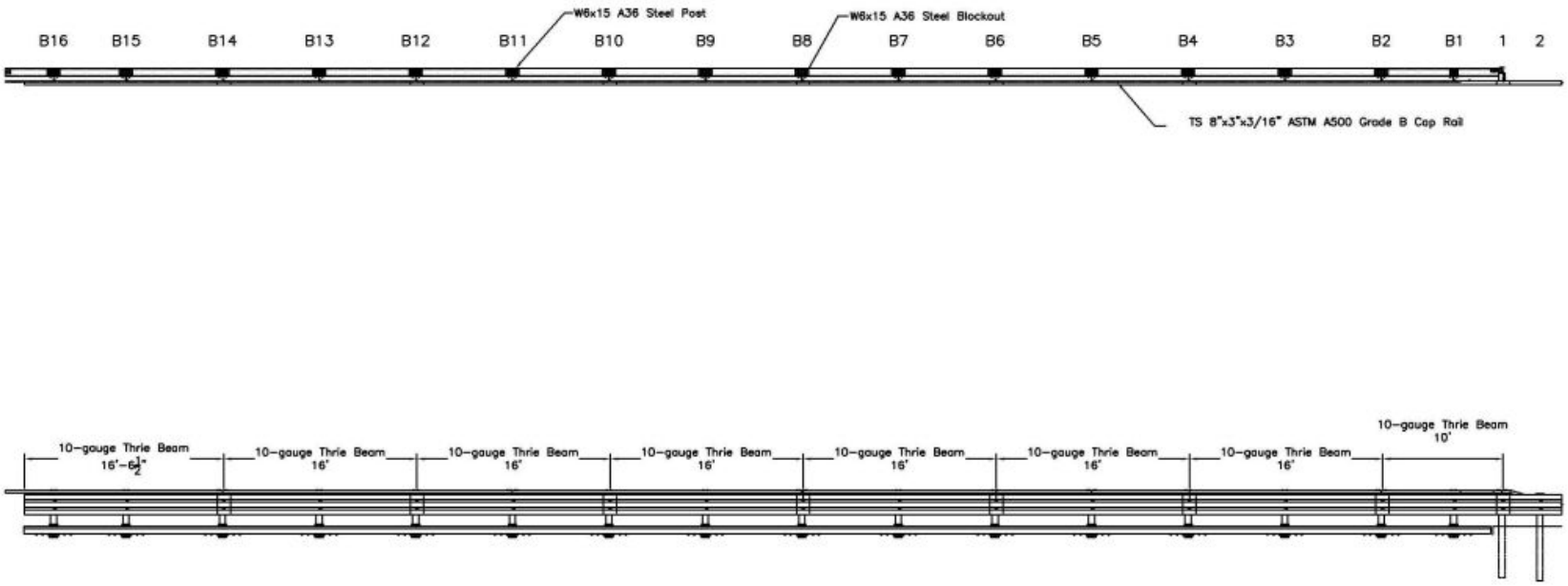

Figure 31. Overall Layout of Steel Bridge Railing System

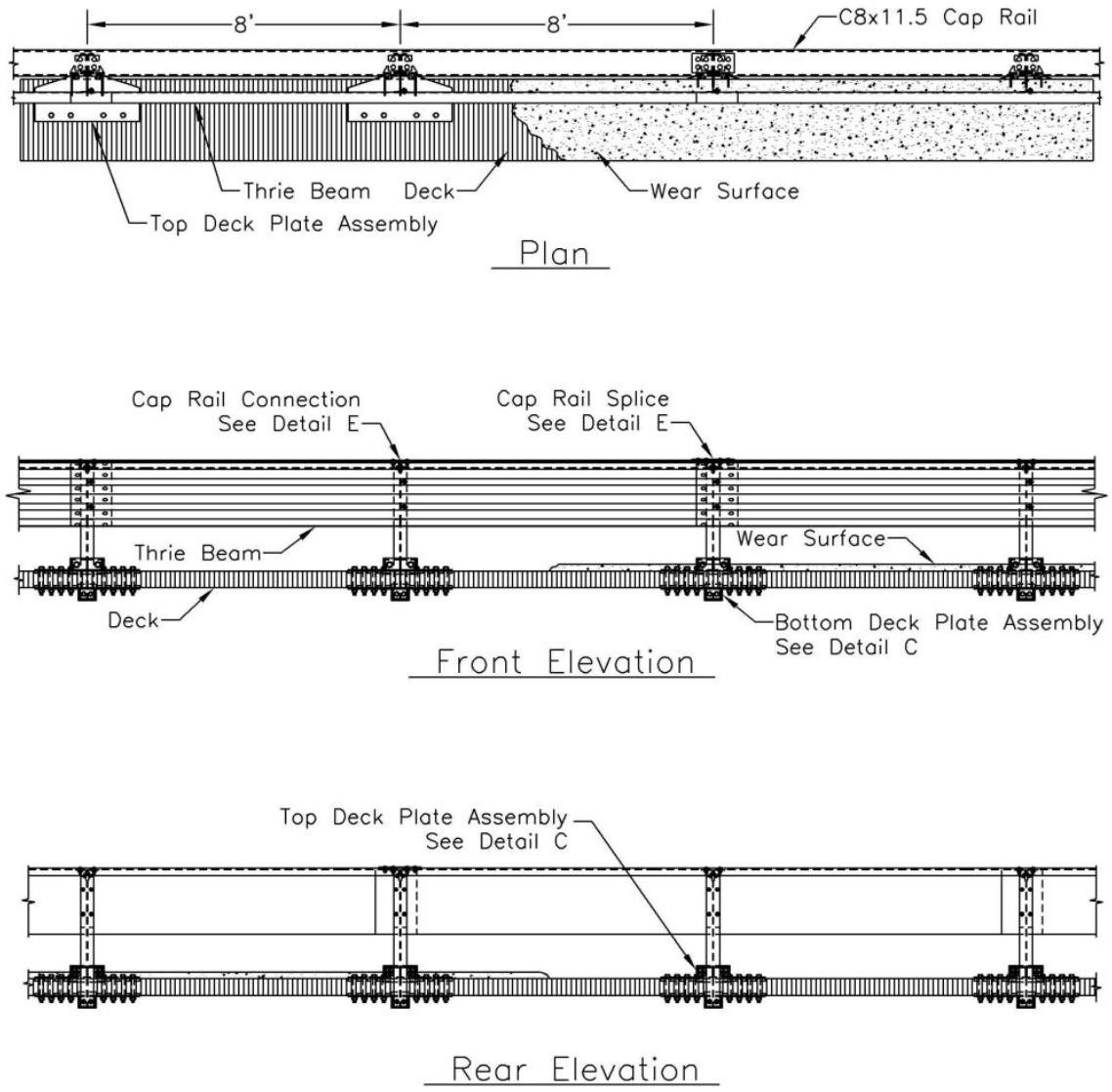

Figure 32. General Configuration of Steel Bridge Railing System

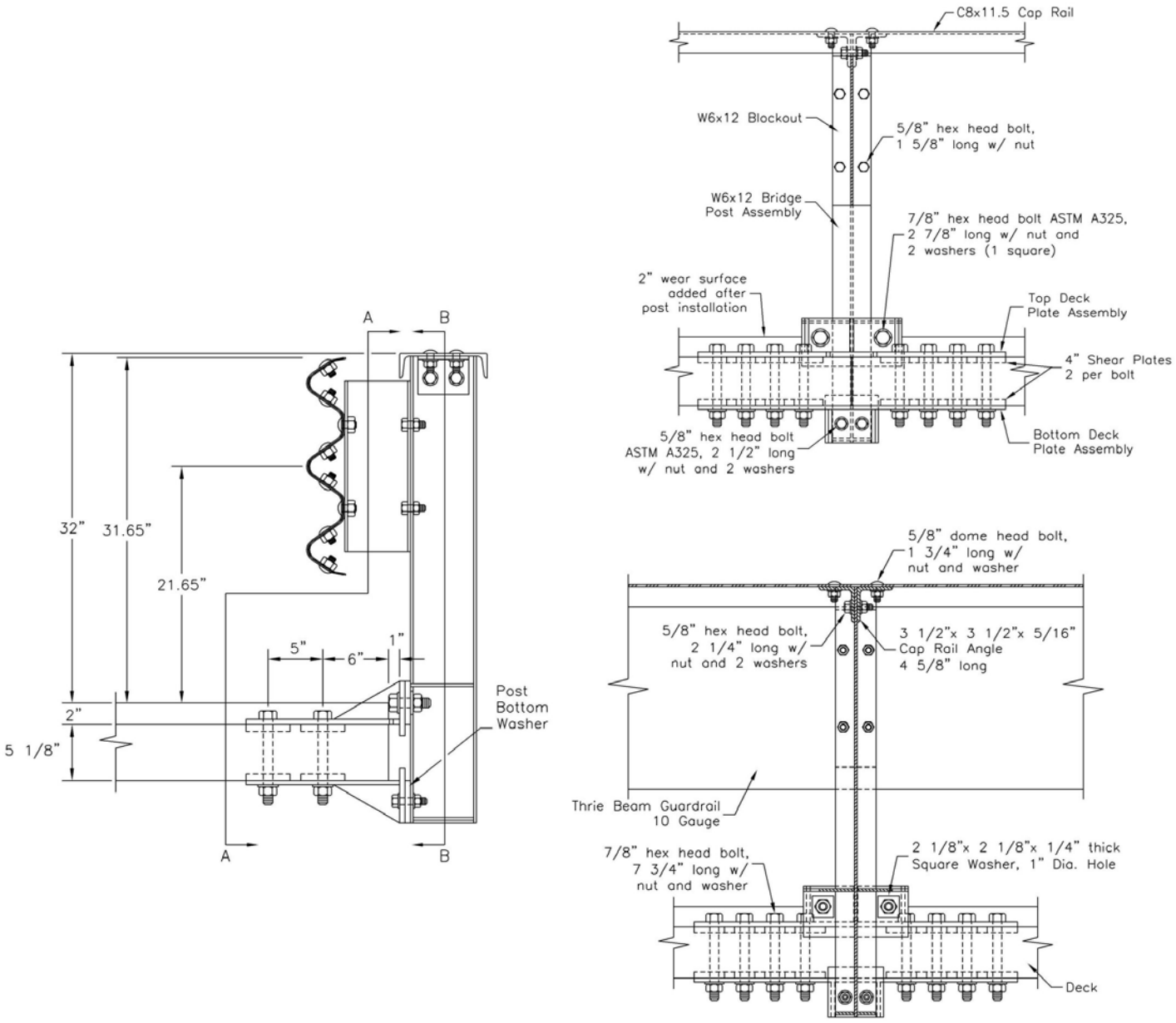

Figure 33. Bridge Railing Design Details - Steel System

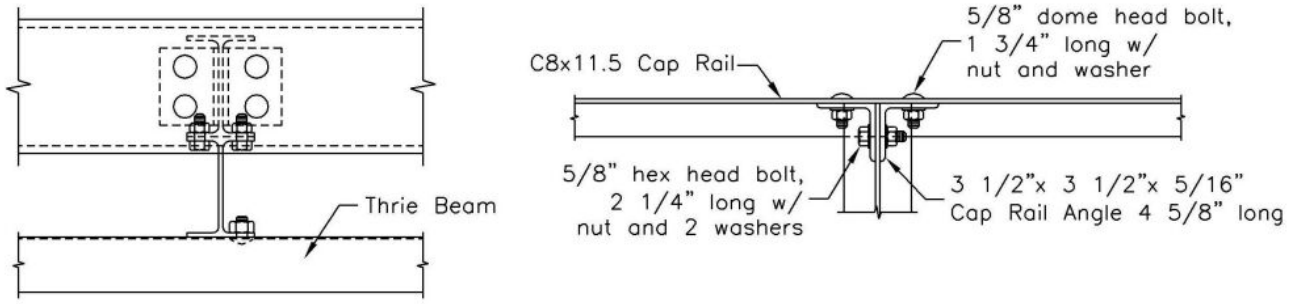

Cap Rail Connection

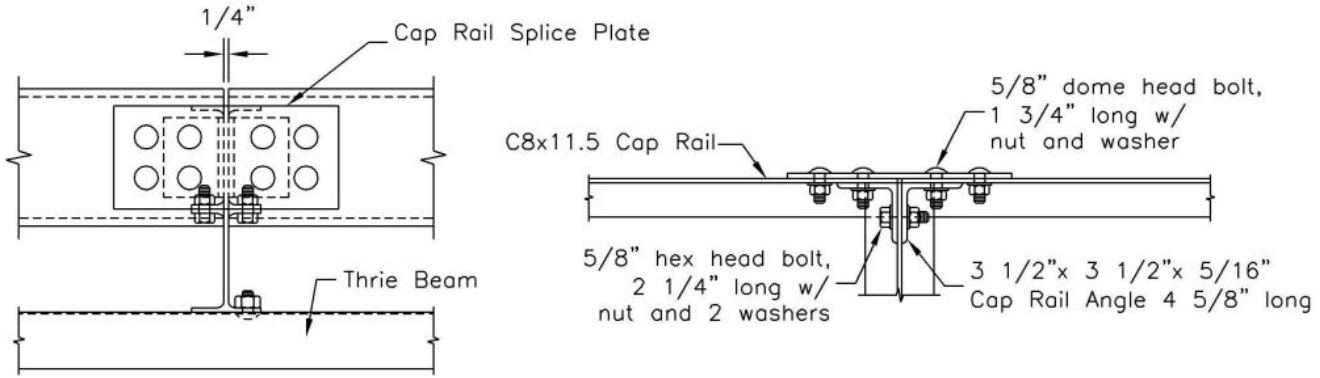

Cap Rail Splice

Figure 34. Cap Rail Connection and Cap Rail Splice Design Details

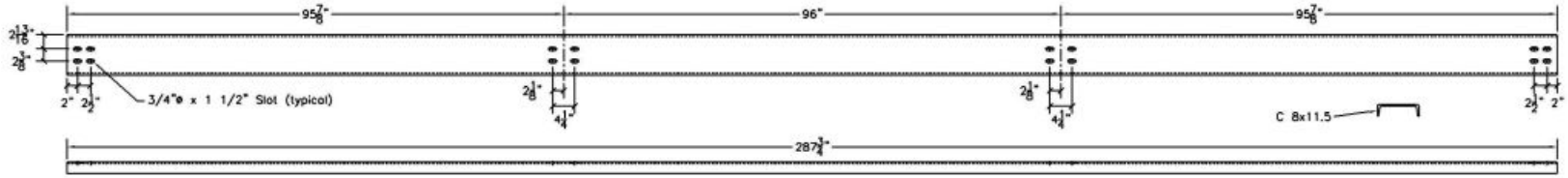

Cap Rail, Type 1

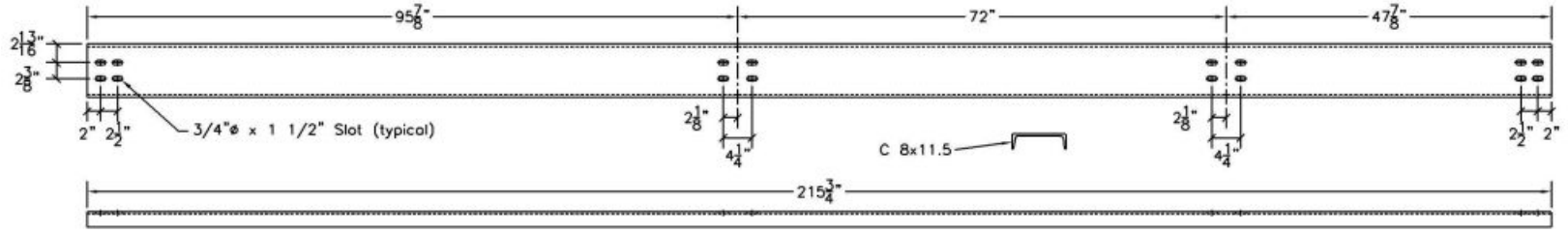

Cap Rail, Type 2

Figure 35. Cap Rails

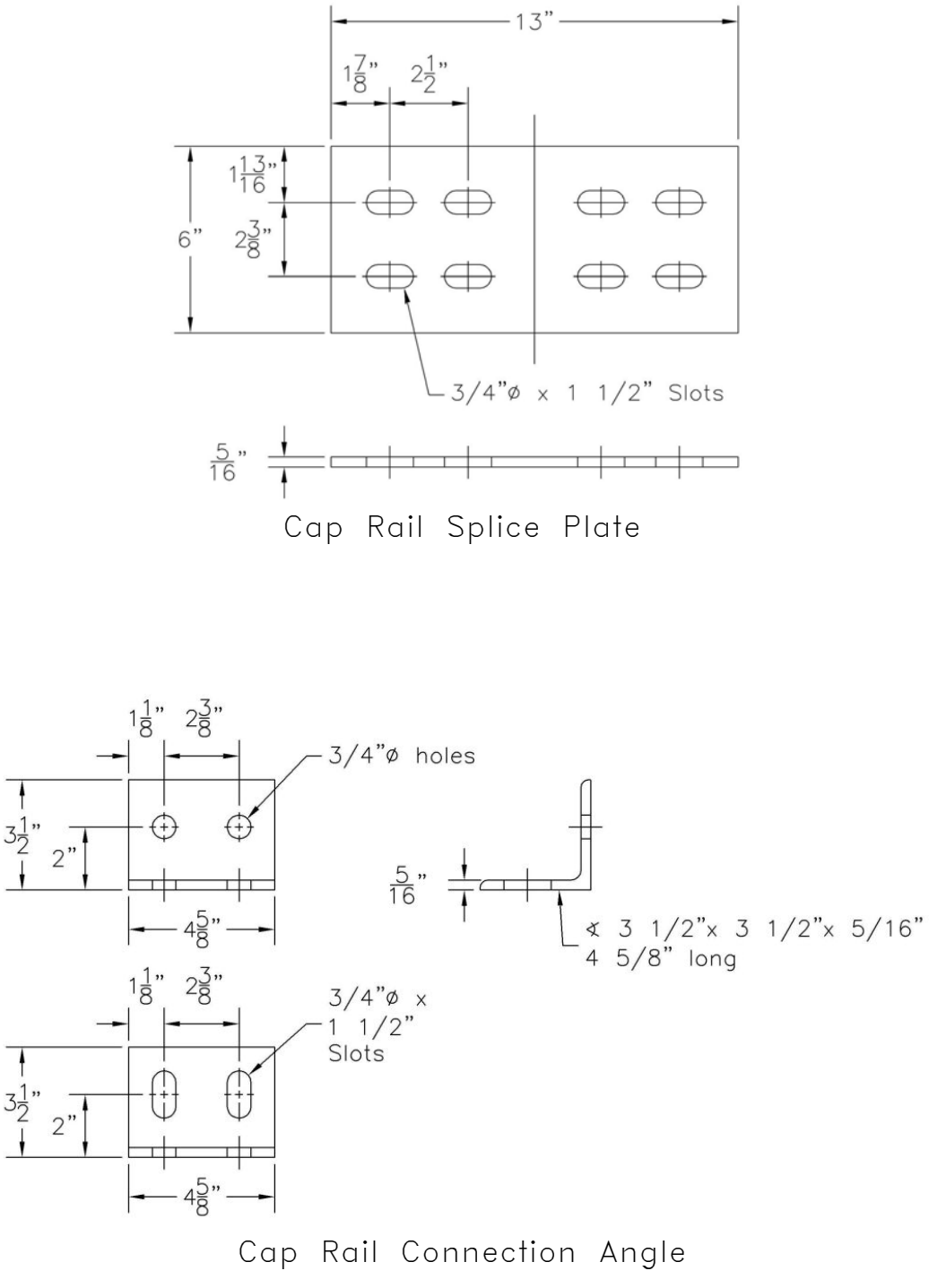

Figure 36. Cap Rail Splice Plate and Connection Angle Details

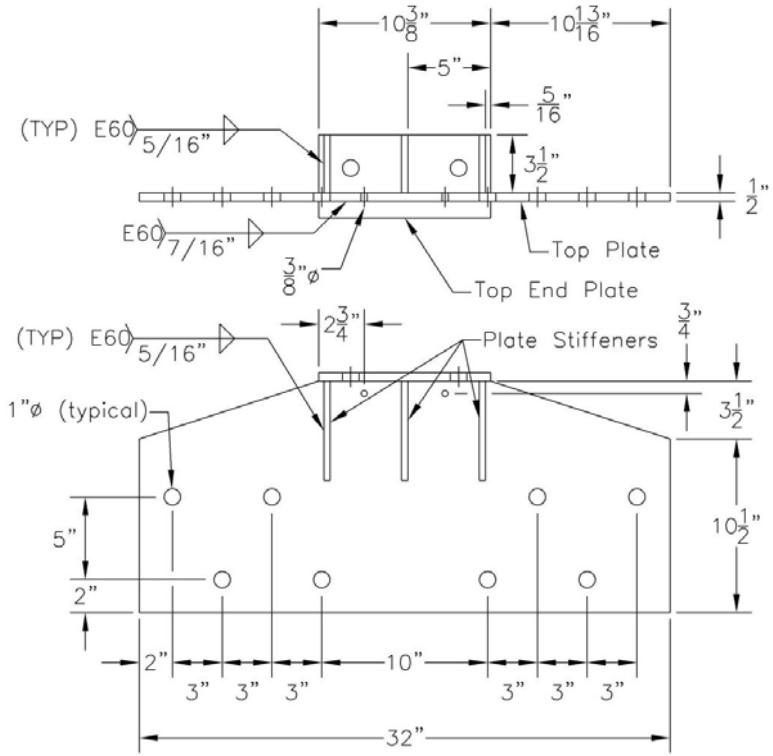

Top Deck Plate Assembly

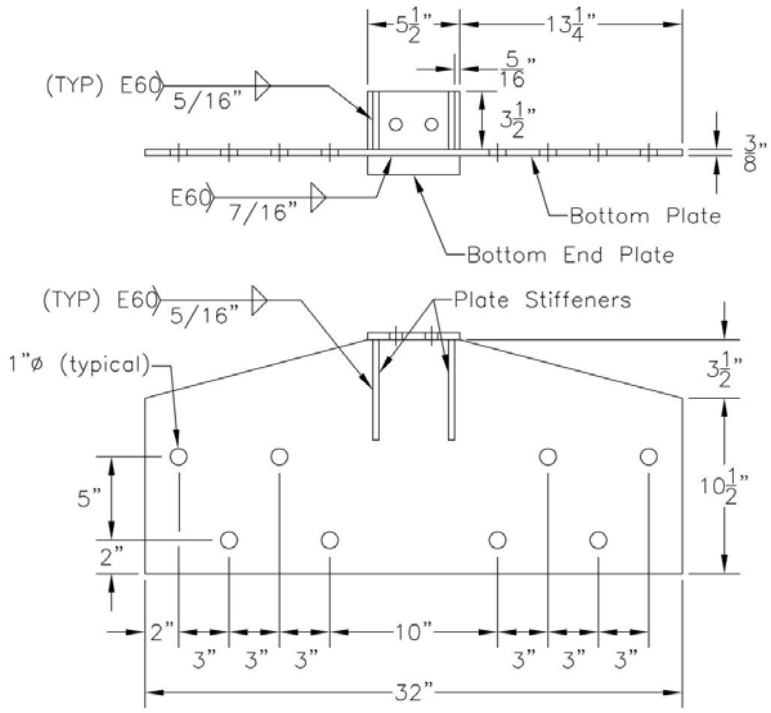

Bottom Deck Plate Assembly

Figure 37. Top and Bottom Deck Plate Assemblies

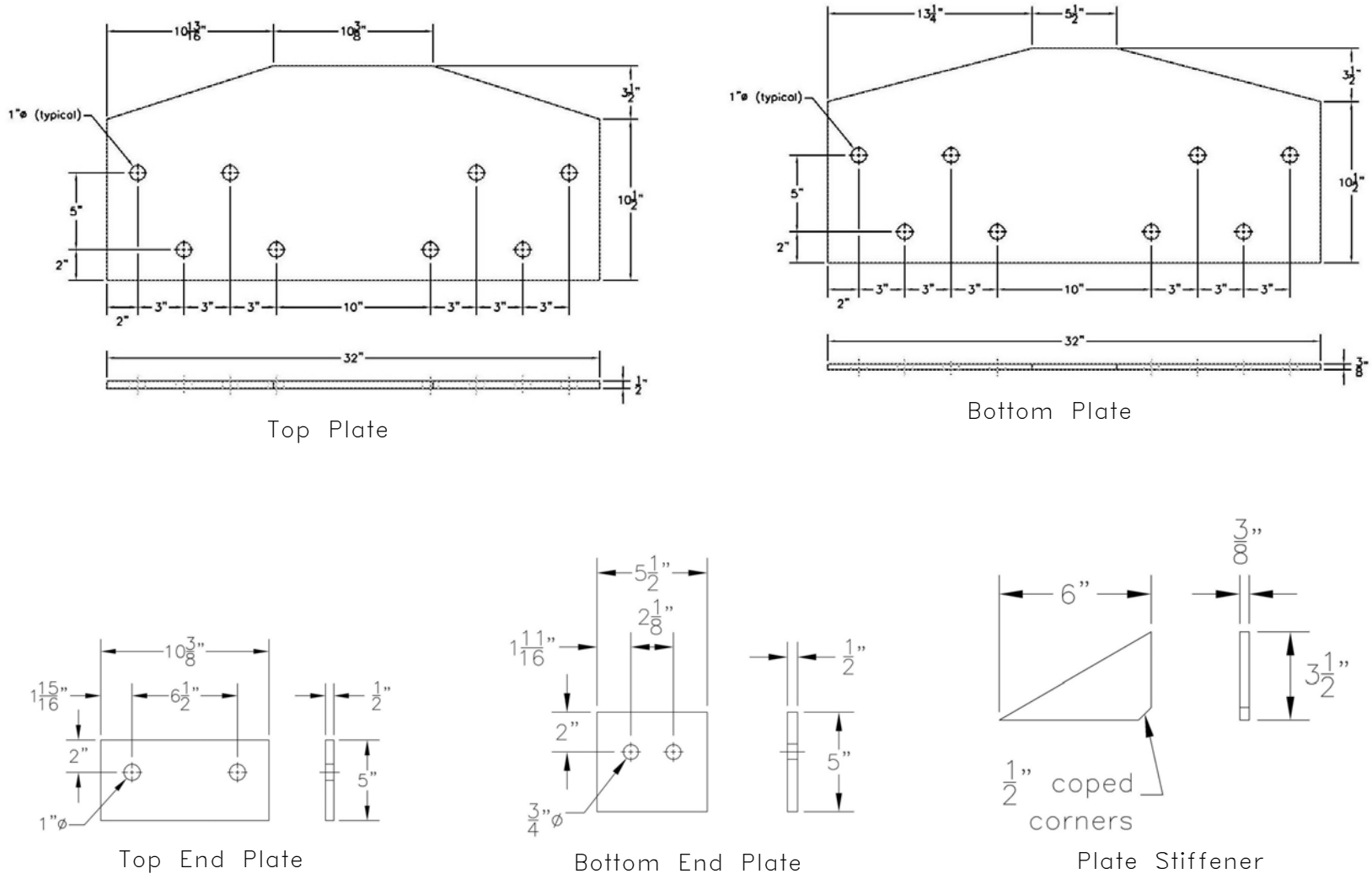

Figure 38. Top and Bottom Deck Plate Assembly Component Details

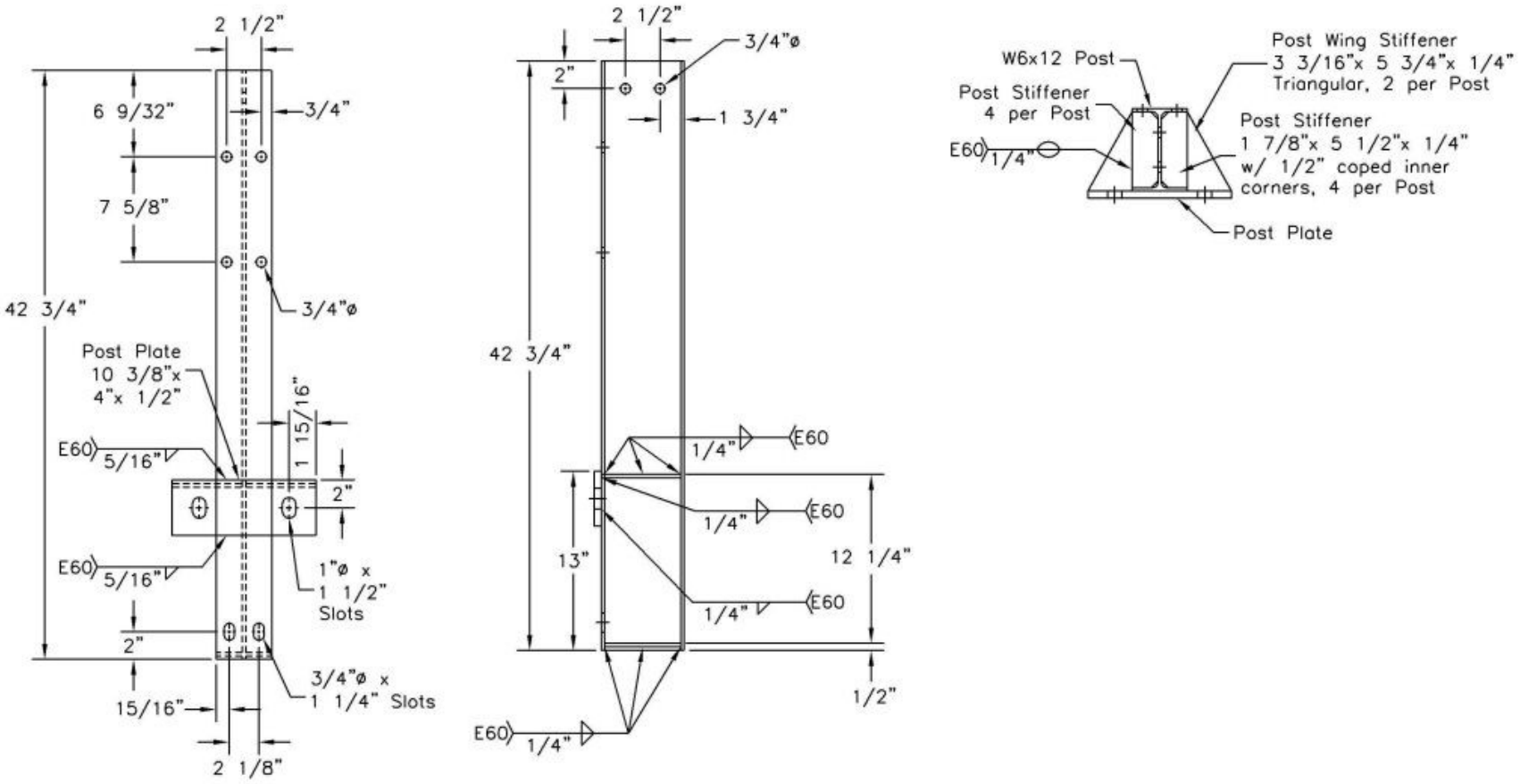

Figure 39. Bridge Post Assembly Details

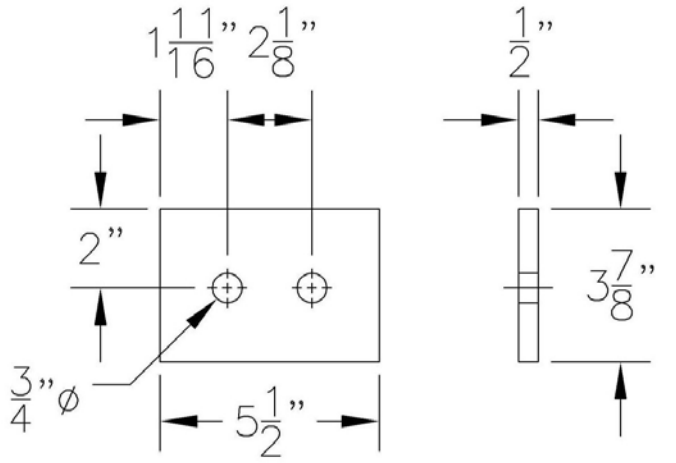

Post Plate Washer

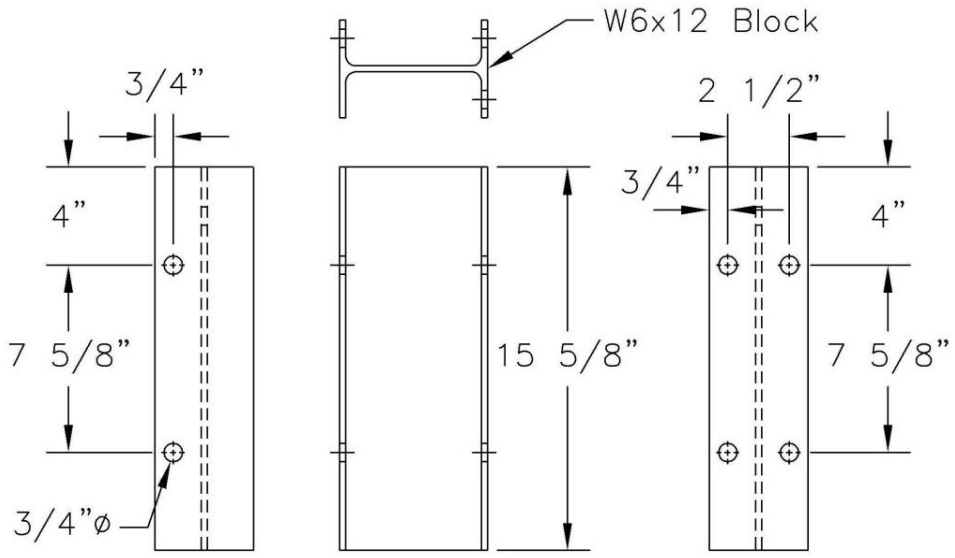

Spacer Block

Figure 40. Post Plate Washer and Spacer Block Details

7.2 Approach Guardrail Transition

An approach guardrail transition system was attached to the upstream end of the bridge railing system and was used to connect the standard guardrail to the bridge rail. The approach guardrail transition system consisted of nine major components: (1) a thrie beam rail section; (2) a W-beam to thrie beam transition section; (3) standard W-beam guardrail; (5) steel guardrail posts; (6) timber blockouts; (7) sloped structural steel channel rail transition and terminator; and (8) a simulated end anchorage system. Photographs of the approach guardrail transition system are shown in Figures 41 through 45. The overall layout of the approach guardrail transition system is shown in Figure 46. Design details of the approach guardrail transition system are provided in Figures 47 through 52.

The thrie beam rail was fabricated from 3.42-mm thick steel and measured 3,810-mm long. A 2.66-mm thick W-beam to thrie beam transition section, measuring 1,905-mm long, was used to connect the thrie beam guardrail to 15,240 mm of standard 2.66-mm thick W-beam guardrail. The thrie beam and W-beam rails had a top mounting height of 804 mm and 706 mm, respectively, as measured from the roadway surface to the top of the rails. Lap-splice connections between the steel rail sections were configured to reduce vehicle snagging at the splice during the crash tests.

Transition cap rail was fabricated from galvanized, ASTM A36 C200x17 structural steel channel, which was notched, bent, and welded together as shown in Figure 48. Transition cap rail was attached to the top of the steel spacer blocks at bridge post nos. 1 and 2 and the cap rail terminator, as shown in Figure 48. Design details of the transition cap rail section and cap rail terminator are shown in Figures 48 through 50. The layout of the transition cap rail and the cap rail terminator is shown in Figure 48.

The system was constructed with fifteen guardrail posts, as shown in Figures 46, 51, and 52. Post nos. 1 through 5 consisted of galvanized, ASTM A36 steel W152x13.4 sections measuring 2,134-mm long. Post nos. 6 and 7 were W152x13.4 steel sections measuring 1,981-mm long. Post nos. 8 through 13 were also W152x13.4 sections but measuring 1,829-mm long. Post nos. 14 and 15 were timber posts measuring 140-mm wide x 190-mm deep x 1,080-mm long and were placed in steel foundation tubes. The timber posts and foundation tubes were part of an anchorage system used to develop the required tensile capacity of the guardrail at the upstream end of the system.

For post nos. 1 through 13, treated timber blockouts were used to space the thrie beam and W-beam guardrails away from the traffic-side face of each guardrail post. The blockouts were fabricated from SYP, Grade No. 1 material and treated with CCA. For post nos. 1 through 5, a wood blockout, measuring 152-mm wide x 203-mm deep x 483-mm long, was used with thrie beam guardrail. At post no. 6, a wood blockout, measuring 152-mm wide x 203-mm deep x 483-mm long, was used at the midspan of the W-beam to thrie beam transition section. For post nos. 7 through 13, a wood blockout, measuring 152-mm wide x 203-mm deep x 368-mm long, was used with W-beam guardrail.

The soil embedment depths for post nos. 1 through 5, 6, 7, and 8 through 13 were 1,372 mm, 1,191 mm, 1,247 mm, and 1,095 mm, respectively, as shown in Figures 51 and 52. The steel posts were placed in a compacted coarse, crushed limestone material that met Grading B of AASHTO M147-65 (1990) as found in NCHRP Report No. 350.

Figure 41. Approach Guardrail Transition - Front View

Figure 42. Approach Guardrail Transition - Back View

Figure 43. Approach Guardrail Transition - Parallel View

Figure 44. Connection to Steel Bridge Railing System

Figure 45. Approach Guardrail Transition Posts

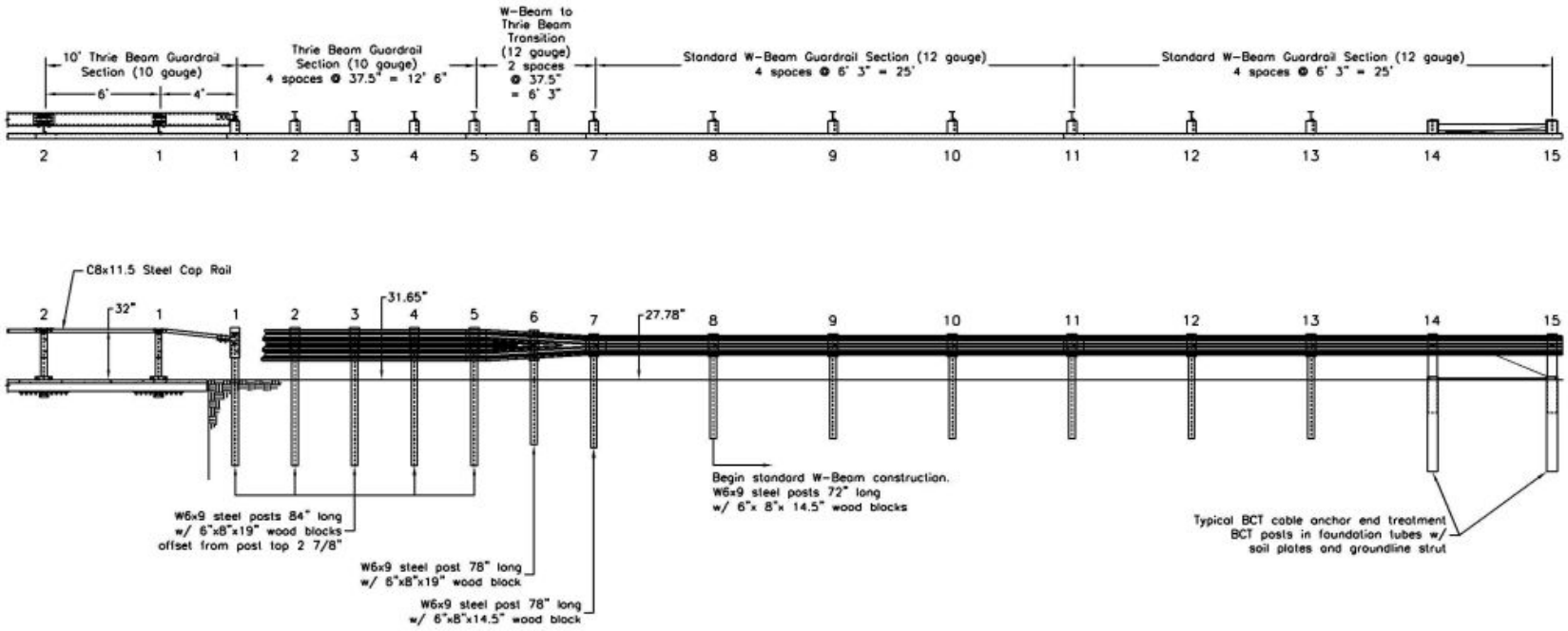

Figure 46. Overall Layout of Approach Guardrail Transition System - Steel System

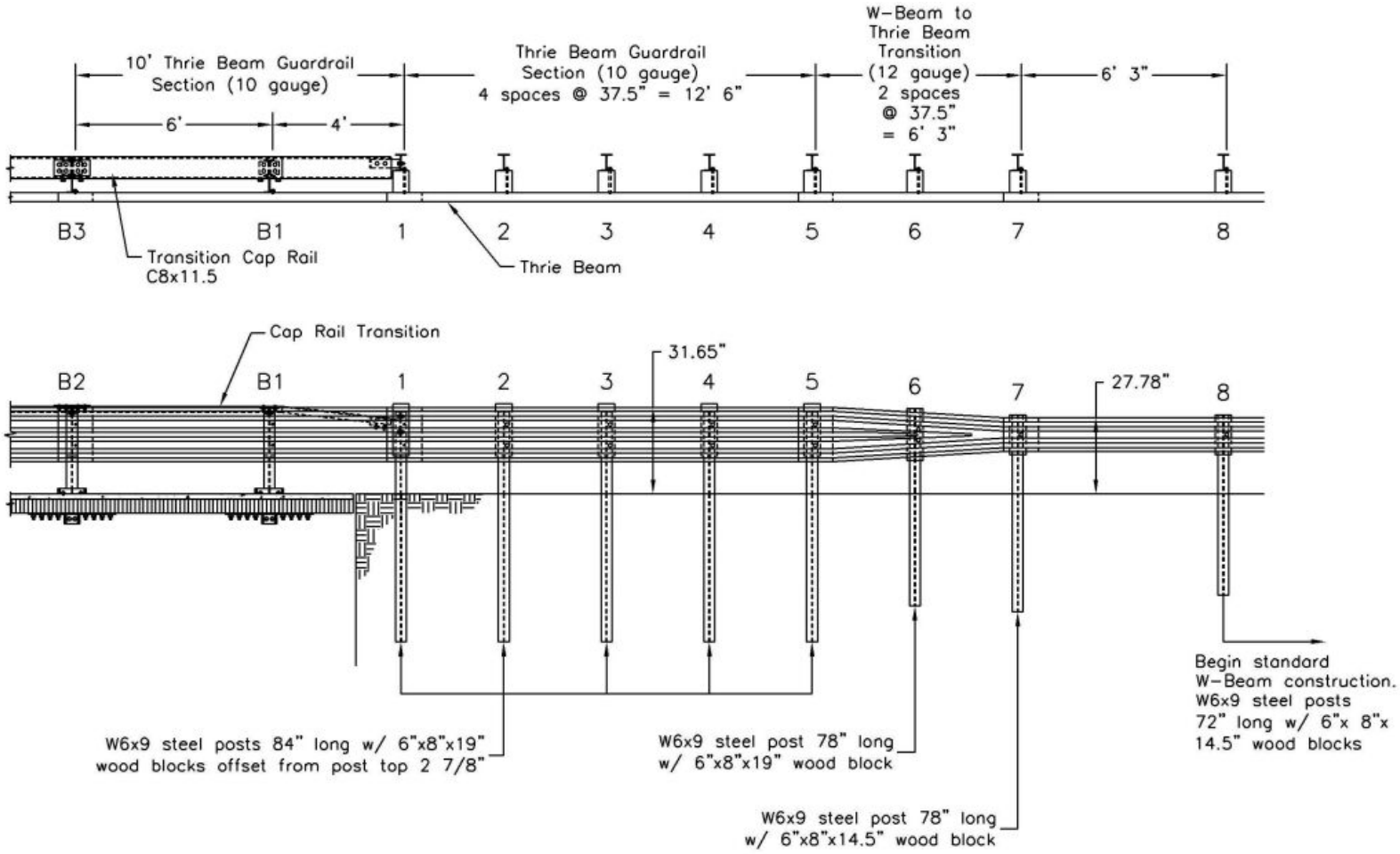

Figure 47. General Configuration of Approach Guardrail Transition System - Steel System

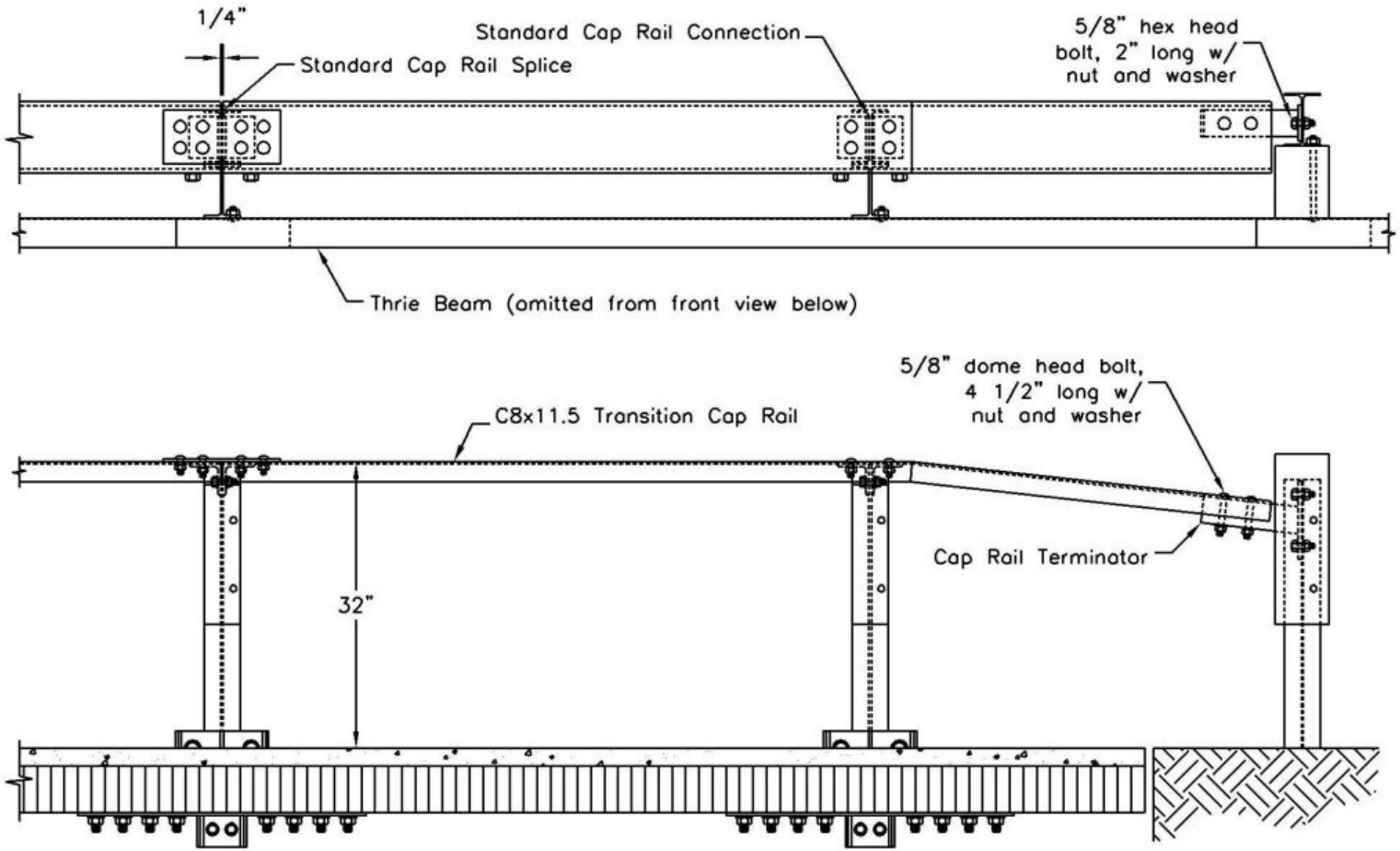

Figure 48. Cap Rail Transition Details - Steel System

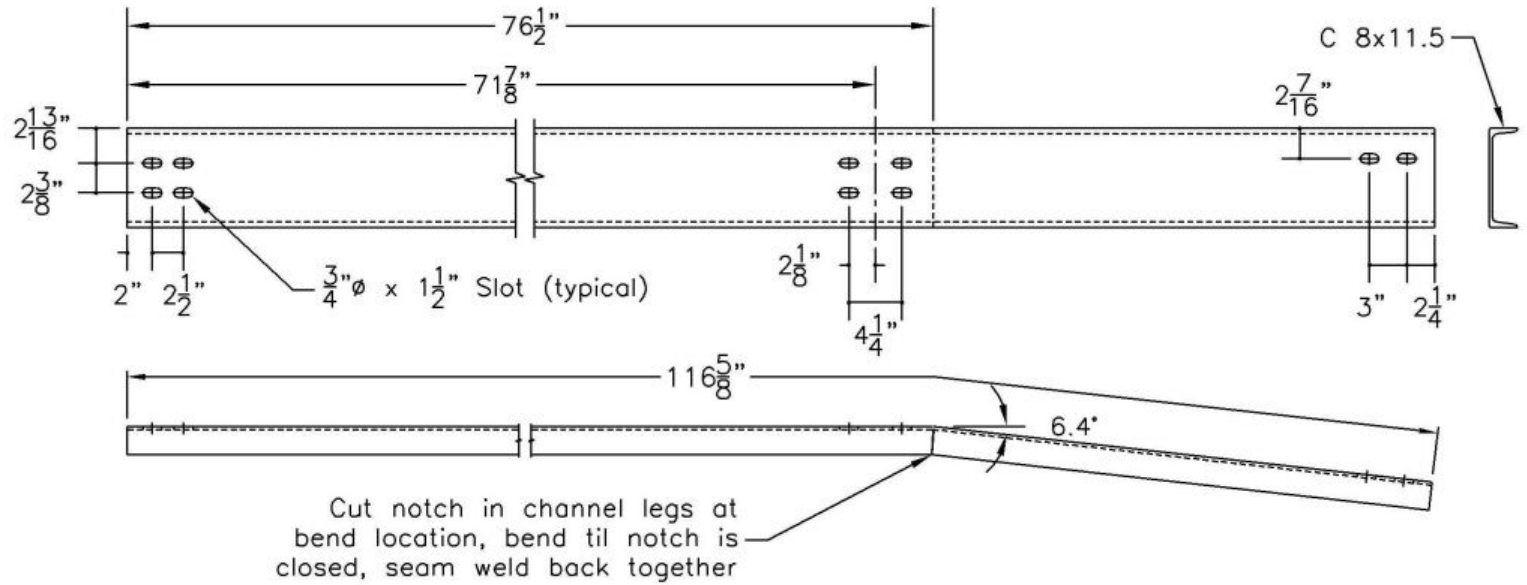

Figure 49. Cap Transition Rail Details

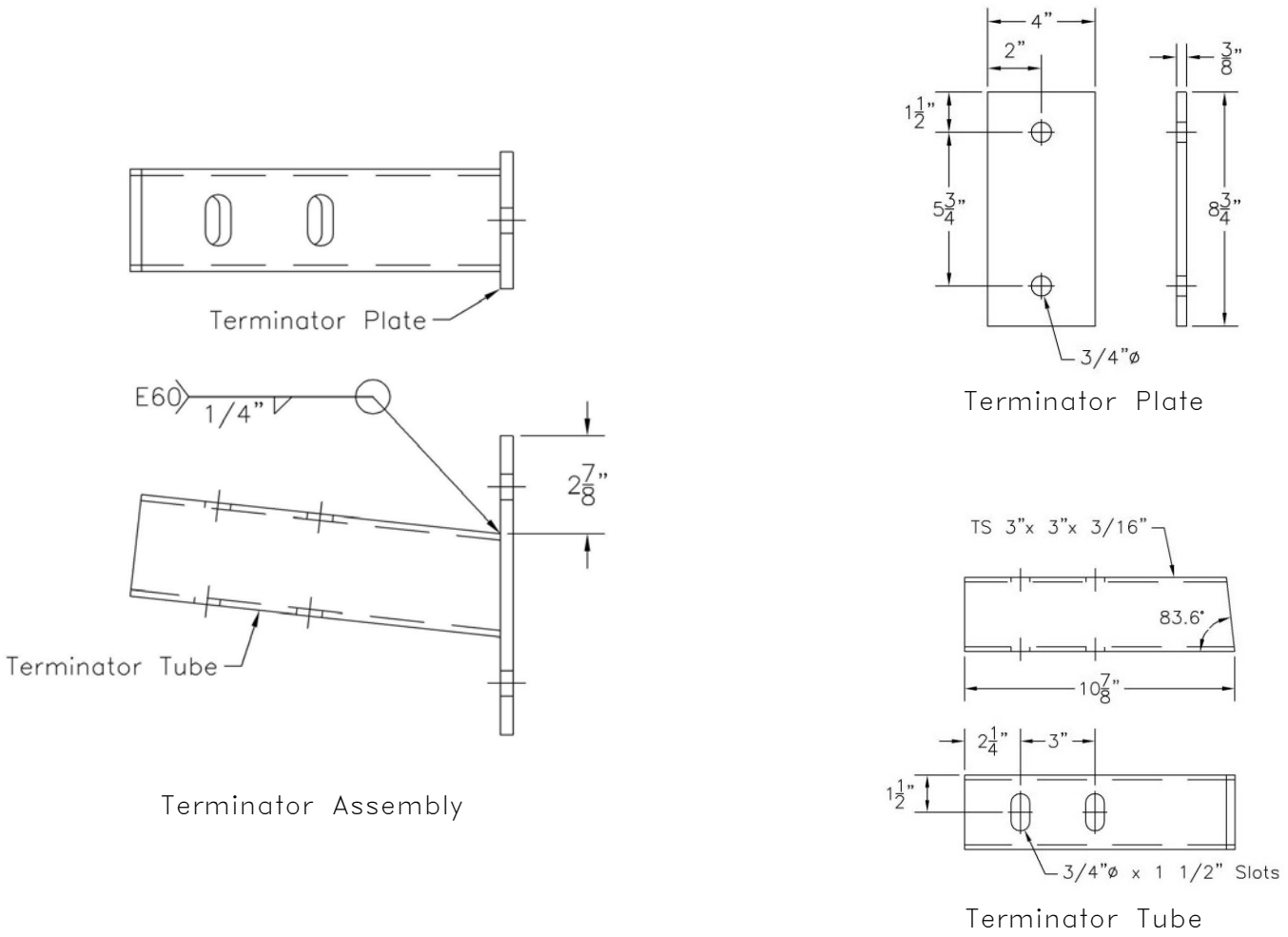

Figure 50. Tube Rail Terminator Details

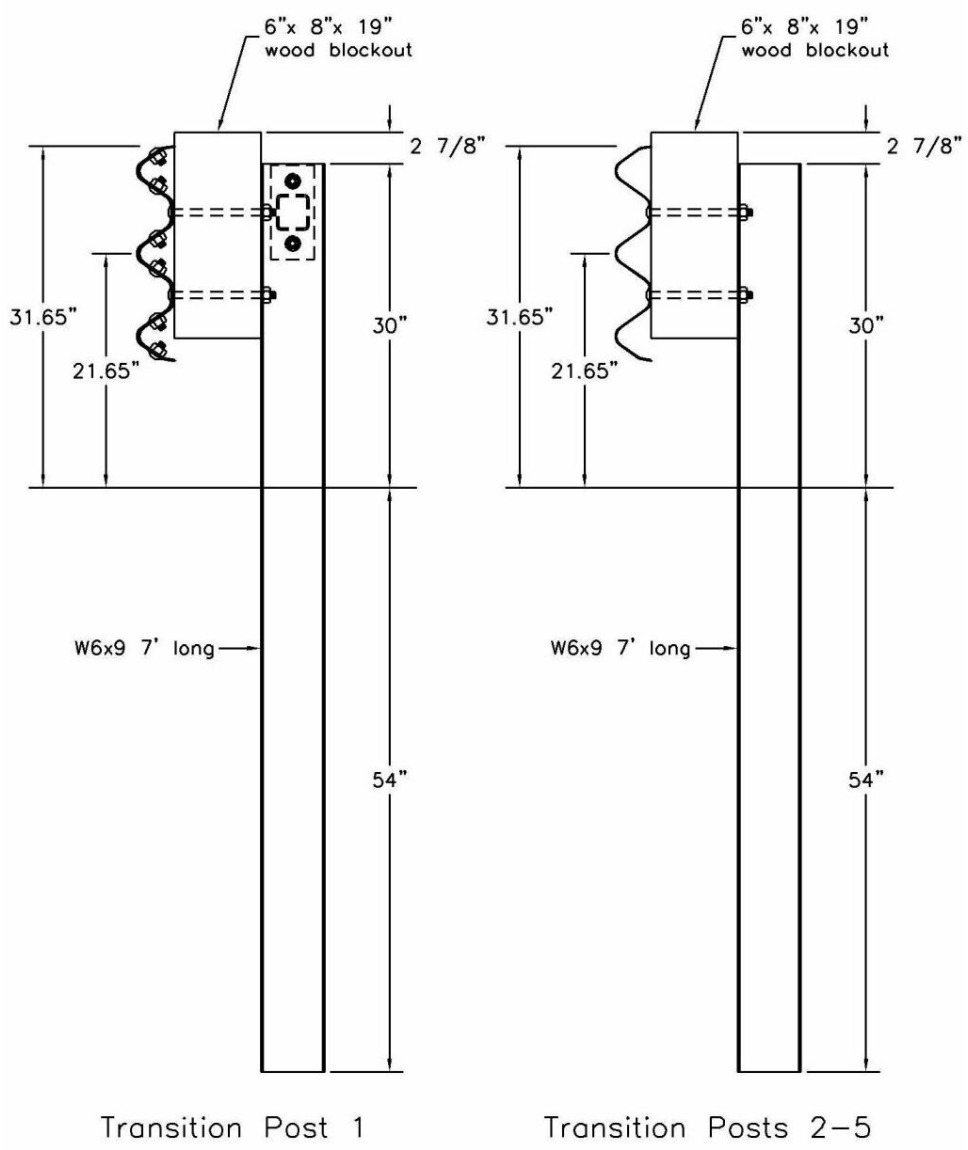

Figure 51. Transition Post Nos. 1 through 5 Configurations

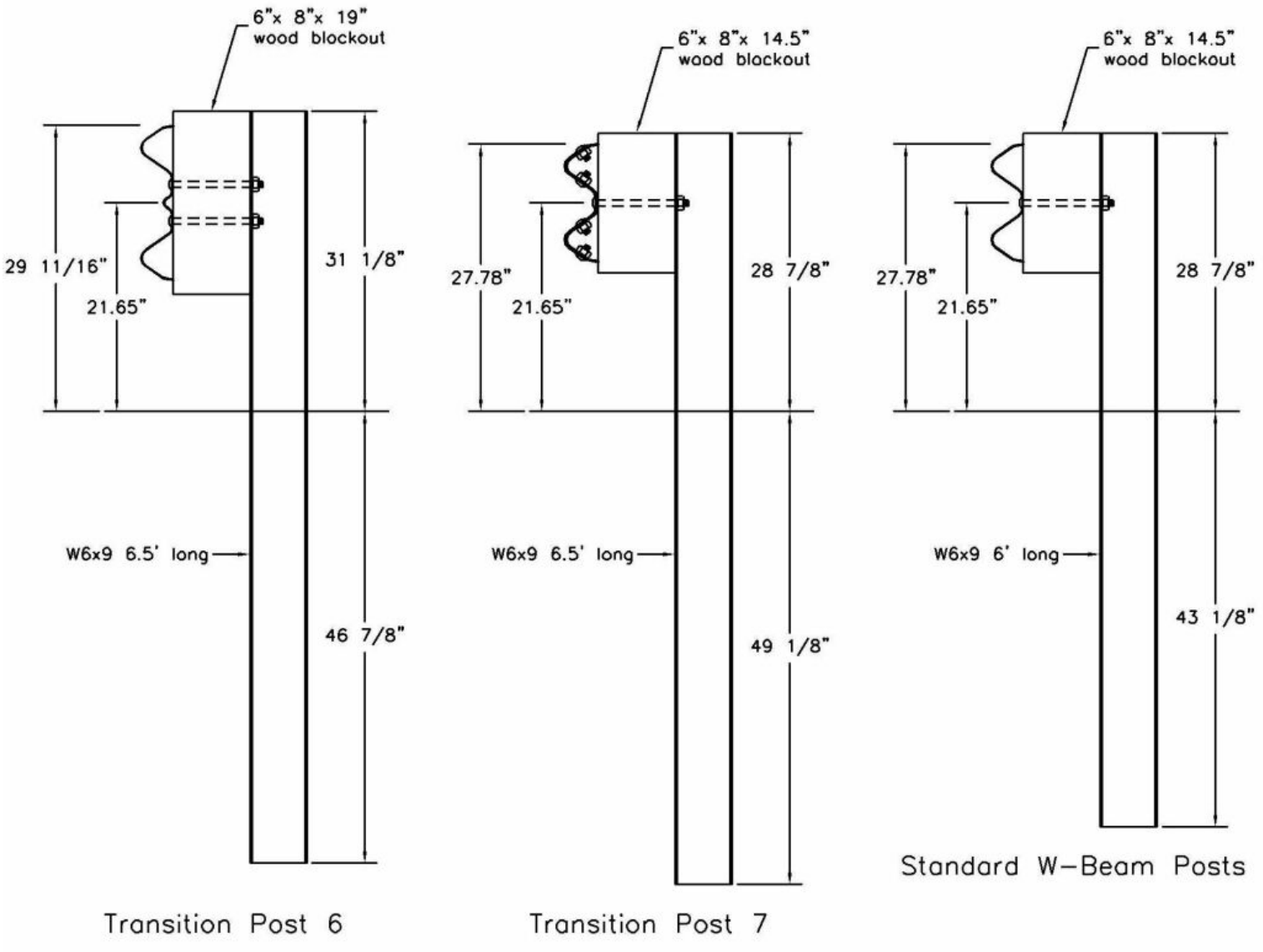

Figure 52. Transition Post Nos. 6 through 13 Configurations

8 COMPUTER SIMULATION

8.1 Introduction

Computer simulation modeling with BARRIER VII (31) was performed to analyze and predict the dynamic performance of the steel bridge railing and approach guardrail transition systems prior to full-scale vehicle crash testing. The simulations were conducted modeling a 2,000-kg pickup truck impacting at a speed of 70.0 km/hr and at an angle of 25 degrees. The BARRIER VII finite element models of the bridge railing and approach guardrail transition systems as well as the idealized finite element, 2-dimensional vehicle model for the pickup truck are shown in Appendix C. Typical computer simulation input data files for each system are shown in Appendix D. Computer simulation was also used to determine the critical impact point (CIP) for the steel bridge railing and approach guardrail transition systems.

8.2 BARRIER VII Results

8.2.1 Bridge Railing Results

The simulation results indicated that the steel bridge railing system described in Section No. 7 would satisfactorily redirect the 2,000-kg pickup truck. In addition, all structural hardware would remain functional during the vehicle impact with the bridge railing system.

For the 2,000-kg pickup truck impact simulation, the CIP was determined to occur with an impact between bridge post nos. 5 and 6 or 610-mm downstream from the centerline of post no. 5. The maximum dynamic and permanent set deflections of the steel thrie beam rail, as measured from the roadway surface to the center of the thrie beam rail, were 231 mm and 169 mm, respectively. The maximum dynamic and permanent set deflections of the steel channel rail, as measured from the roadway surface to the center of the channel rail, were 210 mm and 163 mm, respectively. The

pickup truck became parallel to the bridge railing at 0.224 sec with a velocity of 51.5 km/hr. At 0.350 sec after impact, the pickup truck exited the bridge railing with a velocity of 49.3 km/hr and at an angle of 11.8 degrees.

8.2.2 Approach Guardrail Transition Results

The simulation results indicated that the approach guardrail transition system would satisfactorily redirect the 2,000-kg pickup truck. In addition, all structural hardware would remain functional during the vehicle impact with the approach guardrail transition system.

For the 2,000-kg pickup truck impact simulation, the CIP was determined to occur with an impact at the midspan between transition post no. 2 and 3 or 238-mm upstream of post no. 2. The maximum dynamic and permanent set deflections of the thrie beam rail, as measured from the roadway surface to the center of the thrie beam rail, were 99 mm and 49 mm, respectively. The maximum dynamic and permanent set deflections of the channel rail, as measured from the roadway surface to the center of the channel rail, were 131 mm and 65 mm, respectively. The pickup truck became parallel to the bridge railing at 0.255 sec with a velocity of 53.6 km/hr. At 0.352 sec after impact, the pickup truck exited the bridge railing with a velocity of 51.1 km/hr and at an angle of 6.1 degrees.

9 CRASH TEST NO. 1 (STEEL SYSTEM - BRIDGE RAILING)

9.1 Test STCR-1

The 1,966-kg pickup truck impacted the bridge railing at a speed of 66.6 km/hr and at an angle of 25.6 degrees. A summary of the test results and the sequential photographs are shown in Figure 53. Additional sequential photographs are shown in Figures 54 and 55. Documentary photographs of the crash test are shown in Figures 56 and 57.

9.2 Test Description

Initial impact occurred between bridge post nos. 5 and 6 or 610 mm downstream from bridge post no. 5, as shown in Figure 58. At 0.012 sec after initial impact with the rail, post nos. 5 and 6 rotated backward. At this same time, the vehicle's front bumper was deformed under the rail. At 0.018 sec, the right-front corner of the hood was positioned at post no. 6. At 0.031 sec, the right-front fender deformed inward as the right-front tire contacted the rail. At 0.058 sec, the hood extended over the midspan of the rail between post nos. 6 and 7, and the right-front tire protruded under the rail. At 0.078 sec, the right-front corner of the hood reached post no. 7 as the truck began to redirect. At 0.104 sec, the vehicle rolled counter-clockwise (CCW) toward the rail as the top of the right-side door was ajar. At 0.115 sec, the right-front corner of the hood extended over the rail with the front of the vehicle positioned at the midspan between post nos. 7 and 8. At 0.129 sec, the front of the truck continued to slide along the rail with a piece of the grill becoming detached. At 0.145, the left-front wheel left the ground, and the truck continued to roll CCW toward the rail. At this same time, the right-front corner of the hood was positioned at post no. 8. At 0.177 sec, the left-rear wheel left became airborne as the right-front corner of the hood was positioned at the midspan between post nos. 8 and 9. At 0.213 sec, the right-front corner of the hood was positioned at post

no. 9. At 0.229 sec after impact, the truck became parallel to the bridge rail with a velocity of 46.1 km/hr. At 0.247 sec, the rear of the truck contacted the rail with both left wheels airborne. At 0.254 sec, the right-rear wheel came off the ground. At 0.278 sec, the rear bumper was on top of the rail at the initial impact point. At 0.312 sec, the rear of the truck extend over the rail at post no. 6 as it pitched upward. At 0.323 sec, the right-rear wheel well was positioned on the rail. At 0.349 sec, the right-front wheel assembly deformed under the truck as the right-rear tire contacted the ground. At 0.386 sec, the rear of the vehicle was positioned at post no. 7. At 0.402 sec, the rear of the truck reached its highest point in the air. At 0.436 sec, the left-front tire contacted the ground. At 0.462 sec, the vehicle rolled clockwise (CW) away from the rail. At 0.519 sec after impact, the truck exited the bridge rail at an angle of 14.7 degrees and a speed of 45.2 km/hr. At 0.596 sec, the left-rear tire contacted the ground as the truck continued away from the rail. The vehicle's post-impact trajectory is shown in Figure 53. The vehicle came to rest behind the system, approximately 59.1-m downstream from the impact point and 27.5-m laterally behind a line projected parallel to the traffic-side face of the bridge railing, as shown in Figure 59.

9.3 Bridge Rail Damage

Damage to the bridge rail was minimal, as shown in Figures 60 through 64. Bridge railing damage consisted mostly of a deformed thrie beam section, contact marks on a bridge rail section, deformed steel posts, and damaged spacer blocks. The physical damage to the thrie beam rail revealed that approximately 3.8 m of rail was damaged between bridge post nos. 5 and 7. The thrie beam rail damage consisted of scrape and contact marks along all corrugations in the impact area. The top channel rail remained undamaged.

Minor permanent set of the guardrail and posts is shown in Figure 64. Contact marks were

found on the front face of post no. 6 about 152-mm up from the overlay surface. At post nos. 5 and 6, the Portland cement concrete overlay cracked, and a small separation between the post and deck plate occurred. At post no. 6, contact marks were also found on the exposed gussets of the deck plate. No significant post or guardrail damage occurred upstream of post no. 4 nor downstream of post no. 8.

The maximum lateral permanent set deflections for midspan rail, post, and channel rail locations, as determined from field measurements in the impact region, were approximately 102 mm at 1,219-mm upstream from the centerline of bridge post no. 6, 35 mm at bridge post no. 6, and 36 mm at bridge post no. 6, respectively. The maximum dynamic lateral deflections for midspan rail, post, and channel rail locations, as determined from high-speed film analysis, were 157 mm at 1,219-mm upstream from the centerline of bridge post no. 6, 110 mm at bridge post no. 6, and 78 mm at midspan between bridge post nos. 5 and 6, respectively. The effective coefficient of friction was determined to be approximately 0.49.

9.4 Vehicle Damage

Exterior vehicle damage was moderate and occurred at several vehicle body locations, as shown in Figures 65 through 67. Most of the vehicle damage occurred near the right-front corner of the vehicle, consisting primarily of damage to the fender, hood, bumper, door, and front wheel assembly. The right-front ball joint disengaged and the upper A-frame arm was bent back toward the firewall. The right-front lower control arm, tie-rod end, and sway bar were bent inward. The right corner of the front bumper was deformed around the frame horn. The right-front fender was deformed inward toward the engine compartment. Contact marks were found along the right-side door of the truck due to contact with the thrie beam rail. The top of the right-side door jarred open.

The right-rear steel rim was deformed, but the tire remained inflated. The right-rear box fender was deformed inward. The right corner of the rear bumper was scraped and deformed. Interior vehicle deformations to the right-side floorboard, as shown in Figure 67, were judged insufficient to cause serious injury to the vehicle occupants. No deformations occurred to the left side nor the roof, and all window glass remained undamaged.

9.5 Occupant Risk Values

The longitudinal and lateral occupant impact velocities were determined to be 5.34 m/sec and 6.58 m/sec, respectively. The maximum 0.010-sec average occupant ridedown decelerations in the longitudinal and lateral directions were 5.76 g's and 6.01 g's, respectively. It is noted that the occupant impact velocities and occupant ridedown decelerations were within the suggested limits provided in NCHRP Report No. 350. The results of the occupant risk, determined from accelerometer data, are summarized in Figure 53. Results are shown graphically in Appendix E. Due to technical difficulties, the rate transducer did not collect the roll, pitch, and yaw data. However, roll, pitch, and yaw data were collected from film analysis and are shown graphically in Appendix F.

9.6 Discussion

The analysis of the test results for test STCR-1 showed that the steel bridge railing adequately contained and redirected the vehicle with controlled lateral displacements of the bridge rail. There were no detached elements nor fragments which showed potential for penetrating the occupant compartment or presented undue hazard to other traffic. Minor deformations to the occupant compartment were evident but not considered excessive enough to cause serious injuries to the occupants. The test vehicle did not penetrate nor ride over the bridge rail and remained

upright during and after the collision. Vehicle roll, pitch, and yaw angular displacements were noted, but they were deemed acceptable because they did not adversely influence the occupant risk safety criteria nor cause rollover. After collision, the vehicle's trajectory revealed minimum intrusion into adjacent traffic lanes. In addition, the vehicle's exit angle was less than 60 percent of the impact angle. Therefore, test STCR-1 conducted on the steel bridge rail system was determined to be acceptable according to the TL-2 safety performance criteria provided in NCHRP Report No. 350.

9.7 Barrier Instrumentation Results

For test STCR-1, strain gauges were located on selected components of the steel bridge railing system. The results of the strain gauge analysis are summarized in Table 3. Results of the strain gauge analysis are also shown graphically in Appendix G.

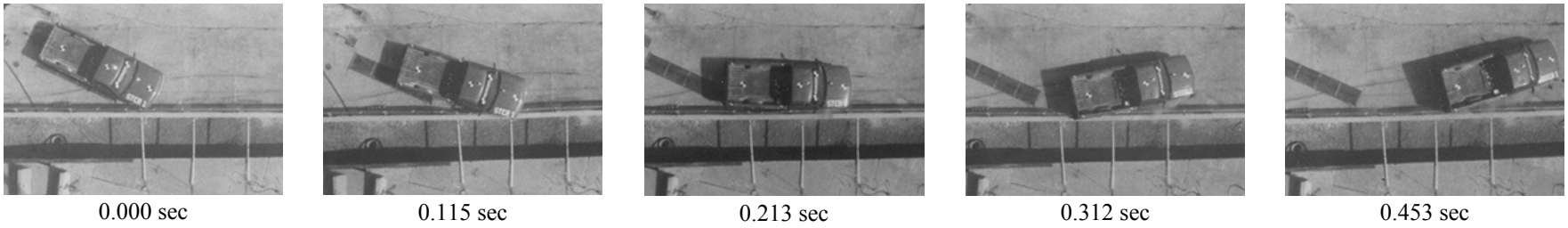

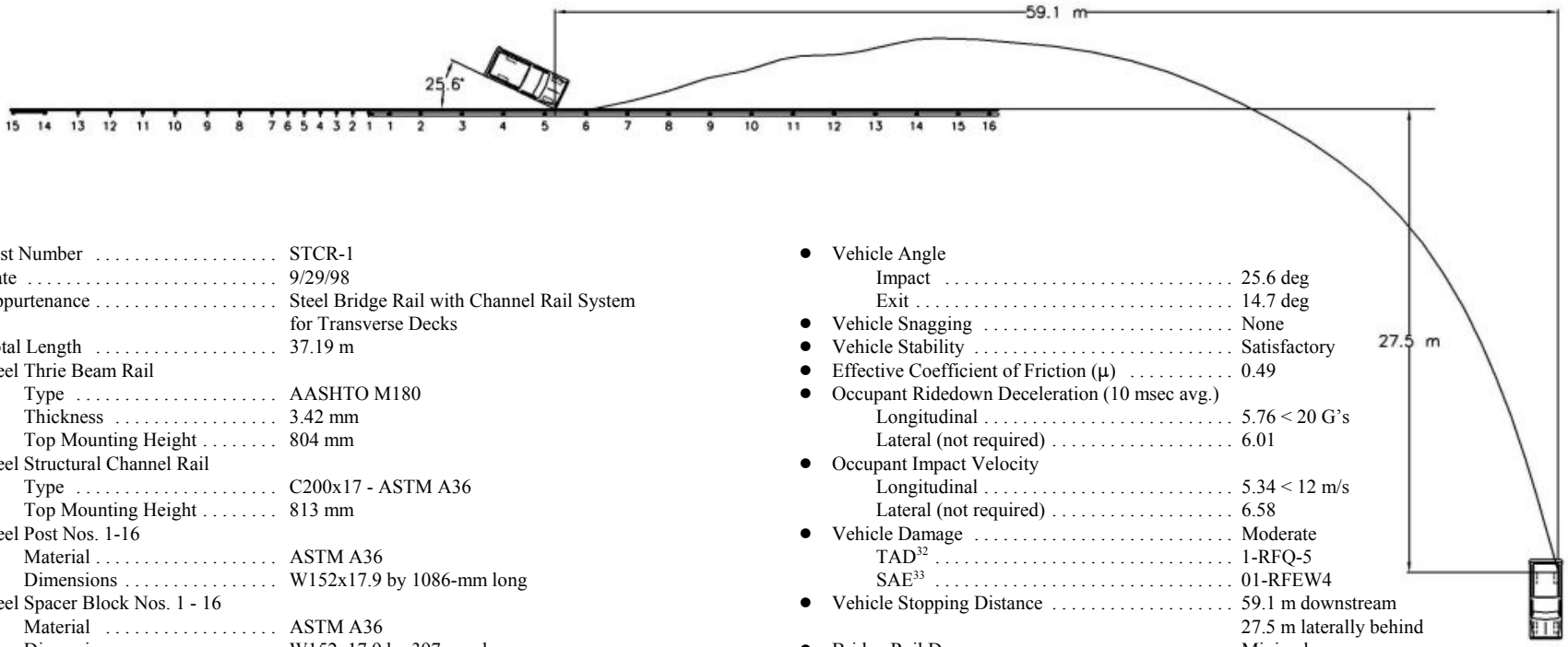

- Test Number STCR-1
- Date 9/29/98
- Appurtenance . . . . . Steel Bridge Rail with Channel Rail System for Transverse Decks
- Total Length . . . . . 37.19 m
- Steel Thrie Beam Rail
  - Type . . . . . AASHTO M180
  - Thickness . . . . . 3.42 mm
  - Top Mounting Height . . . . . 804 mm
- Steel Structural Channel Rail
  - Type . . . . . C200x17 - ASTM A36
  - Top Mounting Height . . . . . 813 mm
- Steel Post Nos. 1-16
  - Material . . . . . ASTM A36
  - Dimensions . . . . . W152x17.9 by 1086-mm long
- Steel Spacer Block Nos. 1 - 16
  - Material . . . . . ASTM A36
  - Dimensions . . . . . W152x17.9 by 397-mm long
- Vehicle Model . . . . . 1990 Chevy 2500 ¾-Ton Pickup Truck
  - Curb . . . . . 1,916 kg
  - Test Inertial . . . . . 1,966 kg
  - Gross Static . . . . . 1,966 kg
- Vehicle Speed
  - Impact . . . . . 66.6 km/hr
  - Exit . . . . . 45.2 km/hr
- Vehicle Angle
  - Impact . . . . . 25.6 deg
  - Exit . . . . . 14.7 deg
- Vehicle Snagging . . . . . None
- Vehicle Stability . . . . . Satisfactory
- Effective Coefficient of Friction (μ) 0.49
- Occupant Ridedown Deceleration (10 msec avg.)
  - Longitudinal . . . . . 5.76 < 20 G's
  - Lateral (not required) 6.01
- Occupant Impact Velocity
  - Longitudinal . . . . . 5.34 < 12 m/s
  - Lateral (not required) 6.58
- Vehicle Damage . . . . . Moderate
  - TAD[32] 1-RFQ-5
  - SAE[33] 01-RFEW4
- Vehicle Stopping Distance . . . . . 59.1 m downstream 27.5 m laterally behind
- Bridge Rail Damage . . . . . Minimal
- Maximum Deflection – Thrie Beam
  - Permanent Set . . . . . 102 mm
  - Dynamic . . . . . 157 mm
- Maximum Deflections – Channel
  - Permanent Set . . . . . 36 mm
  - Dynamic . . . . . 78 mm

Figure 53. Summary of Test Results and Sequential Photographs, Test STCR-1

0.000 sec

0.349 sec

0.104 sec

0.606 sec

0.177 sec

0.761 sec

0.297 sec

Figure 54. Additional Sequential Photographs, Test STCR-1

0.000 sec

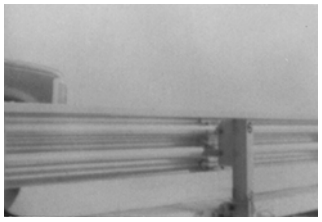

0.000 sec

0.085 sec

0.057 sec

0.127 sec

0.117 sec

0.286 sec

0.252 sec

0.355 sec

0.323 sec

Figure 55. Additional Sequential Photographs, Test STCR-1

Figure 56. Documentary Photographs, Test STCR-1

Figure 57. Documentary Photographs, Test STCR-1

Figure 58. Impact Locations, Test STCR-1

Figure 59. Final Vehicle Position and Trajectory Marks, Test STCR-1

Figure 60. Barrier Damage, Test STCR-1

Figure 61. Post No. 5 Damage, Test STCR-1

Figure 62. Post No. 6 Damage, Test STCR-1

Figure 63. Cracking in Portland Cement Concrete Overlay, Test STCR-1

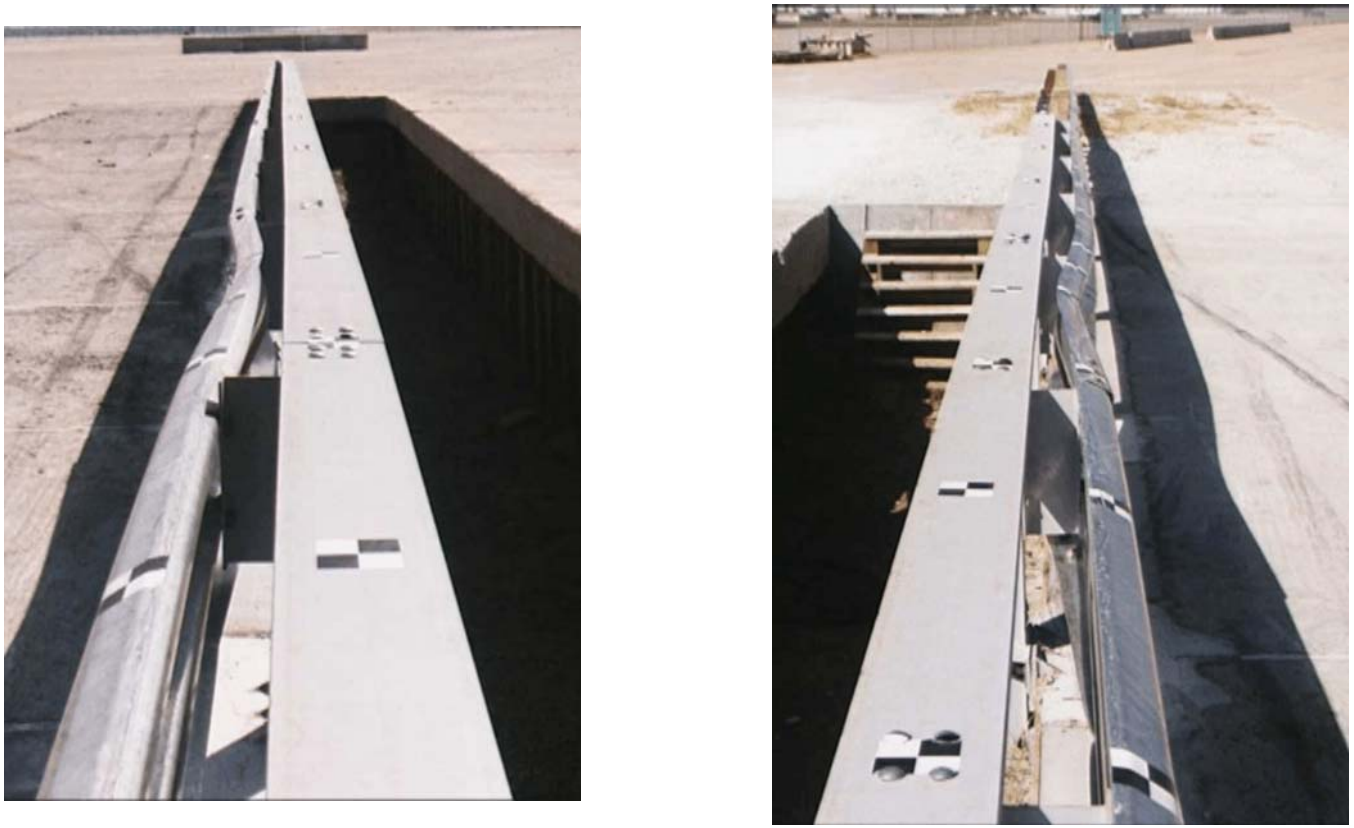

Figure 64. Permanent Set Deformations, Test STCR-1

Figure 65. Vehicle Damage, Test STCR-1

Figure 66. Vehicle Damage, Test STCR-1

Figure 67. Occupant Compartment Deformations, Test STCR-1

Table 3. Strain Gauge Results, Test STCR-1

Strain Gauge No.	Gauge Location	Maximum μ Strain[1] (mm/mm)	Maximum Plate Stress[2] (MPa)	Comments
1	Top Plate No. 5	182	32.1	Most upstream bolt in row closest to post - perpendicular to rail
2	Top Plate No. 5	628	130.0	Bolt on upstream side near middle of plate in row closest to post - perpendicular to rail
3	Top Plate No. 5	397	82.2	Middle - perpendicular to rail
4	Top Plate No. 5	588	121.6	Bolt on downstream side near middle of plate in row closest to post - perpendicular to rail
5	Top Plate No. 5	116	24.0	Most downstream bolt in row closest to post - perpendicular to rail
6	Bottom Plate No. 5	544	112.5	Middle - perpendicular to rail
7	Top Plate No. 6	265	54.7	Most upstream bolt in row closest to post - perpendicular to rail
8	Top Plate No. 6	1853	Plate Yield	Bolt on upstream side near middle of plate in row closest to post - perpendicular to rail
9	Top Plate No. 6	NA	NA	Middle - perpendicular to rail
10	Top Plate No. 6	1708	Plate Yield	Bolt on downstream side near middle of plate in row closest to post - perpendicular to rail
11	Top Plate No. 6	238	49.2	Most downstream bolt in row closest to post - perpendicular to rail
12	Bottom Plate No. 6	238	49.2	Most upstream bolt in row closest to post - perpendicular to rail
13	Bottom Plate No. 6	923	191.0	Middle - perpendicular to rail
14	Bottom Plate No. 6	167	34.5	Most downstream bolt in row closest to post - perpendicular to rail
15	Flange Post No. 6	2234	Plate Yield	Traffic-side face
16	Flange Post No. 6	1345	278.1	Back-side face
17	Top Plate No. 7	97	20.0	Most upstream bolt in row closest to post - perpendicular to rail
18	Top Plate No. 7	253	52.4	Middle - perpendicular to rail
19	Top Plate No. 7	174	35.9	Most downstream bolt in row closest to post - perpendicular to rail
20	Bottom Plate No. 7	233	48.1	Middle - perpendicular to rail

[1] - All strain values are shown as the absolute value only.

[2] - For ASTM A36 steel plates, elastic stress values are shown as the absolute value only and calculated by multiplying the strain by the modulus of elasticity equal to 207,000 MPa (30,000 ksi). Minimum yield stress for the plates is 248 MPa (36 ksi).

NA - Not available or not applicable.

10 CRASH TEST NO. 2 (STEEL SYSTEM - APPROACH GUARDRAIL TRANSITION)

10.1 Test STCR-2

The 2,035-kg pickup truck impacted the approach guardrail transition at a speed of 69.9 km/hr and at an angle of 25.8 degrees. A summary of the test results and the sequential photographs are shown in Figure 68. Additional sequential photographs are shown in Figures 69 and 70. Documentary photographs of the crash test are shown in Figures 71 through 73.

10.2 Test Description

Initial impact occurred between transition post nos. 2 and 3 or 238 mm upstream from transition post no. 2, as shown in Figure 74. At 0.006 sec after impact, the right-front corner of the hood was positioned at transition post no. 2. At 0.022 sec, the right-front wheel impacted the rail. At 0.030 sec, the front bumper and grill deformed. At 0.040 sec, transition post no. 2 rotated backward. At 0.048 sec, transition post no. 1 rotated backward as the hood extended over the rail. At 0.058 sec, the right-front corner of the hood was positioned at transition post no. 1. At 0.067 sec, the right-front fender was hanging over the rail at transition post no.1. At 0.074 sec, the left-front wheel became airborne. At 0.088 sec, the right-front corner of the vehicle was positioned at the midspan between transition post no. 1 and bridge post no. 1. At 0.120 sec, the right-front corner of the vehicle was positioned at bridge post no. 1 as the vehicle slid along the rail with the rear end yawing toward the rail. At 0.130 sec, the right-rear fender was extending over the rail while the rear of the truck was rolling towards the rail. At 0.138 sec, the left-front tire became airborne. At 0.154 sec, the left-rear tire became airborne. At 0.174 sec, the right-front corner of the vehicle was positioned at the midspan between bridge post nos. 1 and 2. At 0.188 sec, the vehicle continued to yaw away from the rail. At 0.238 sec, the right-front corner of the hood was at post no. 2. At 0.272

sec after impact, the truck became parallel to the bridge rail with a velocity of 50.0 km/hr. At 0.300 sec, the rear of the truck contacted the rail. At this same time, the left side of the truck was airborne as the truck rolled CCW toward the rail. At 0.346 sec, the lower right rear of the box slid up the rail. At 0.366 sec, the rear end of the vehicle was positioned at transition post no. 1. At 0.380 sec, the right-rear corner of the truck box lost contact with the rail as the rear of the truck ascended higher into the air. At 0.426 sec, the right-rear tire became airborne. At 0.453 sec, the rear end of the vehicle was positioned at bridge post no. 1. At 0.460 sec, the rear corner of the box was contacting the rail and sliding along it. At 0.500 sec after impact, the truck exited the bridge rail at an angle of 17.6 degrees and a speed of 45.5 km/hr. At 0.644 sec, the left-front tire contacted the ground. At 0.684 sec, the truck rolled CW away from the rail. At 0.756 sec, the rear of the truck reached its maximum pitch angle. At 0.856 sec, the left-rear tire contacted the ground as the truck continued away from the rail. At 0.958 sec, the right-rear tire contacted the ground. The vehicle's post-impact trajectory is shown in Figure 68. The vehicle came to rest 21.0-m downstream from impact and 3.7-m laterally away from the traffic-side face of the bridge rail, as shown in Figure 75.

10.3 Bridge Rail and Approach Guardrail Terminal Damage

Damage to the approach guardrail transition and bridge railing was minimal, as shown in Figures 76 through 80. The damage consisted mostly of deformed thrie beam, contact marks on a thrie beam section and the top tube rail, deformed bridge posts, and displaced guardrail posts. The physical damage to the thrie beam rail was found between transition post no. 3 and bridge post no. 1, as shown in Figure 76. The thrie beam damage consisted of moderate deformation and flattening of the impacted section of rail between transition post no. 3 and bridge post no. 1. Contact marks

were found on the guardrail from 241-mm upstream of transition post no. 2 through transition post no. 2.

No contact marks nor damage was observed on the transition posts, but movement of the posts was evident by the 32-mm, 13-mm, and 2-mm soil gaps at the front faces of transition post nos. 2, 3, and 4, respectively. Transition post no. 1 did not move due to reinforcement of the upper channel rail. Bridge post no. 1 was permanently deformed during the test, as shown in Figure 77. The concrete deck cracked around the deck-to-post connection at bridge post no. 1. No significant guardrail damage occurred upstream of transition post no. 4 nor downstream of bridge post no. 1. All blockouts remained undamaged.

The maximum lateral permanent set deflections for midspan rail, post, and channel rail locations, as determined from field measurements in the impact region, were approximately 117 mm at 476-mm downstream from the centerline of transition post no. 1, 98 mm at transition post no. 1, and 98 mm at transition post no. 1, respectively. The maximum dynamic lateral deflections for midspan rail, post, and channel rail locations, as determined from high-speed film analysis, were 183 mm at the centerline of transition post no. 1, 202 mm at transition post no. 1, and 167 mm at midspan between transition post no. 1 and bridge post no. 1, respectively. The effective coefficient of friction was determined to be approximately 0.42.

10.4 Vehicle Damage

Exterior vehicle damage was minimal, as shown in Figures 81 through 83. The right corner of the front bumper and the right-side quarter panel were crushed inward, as shown in Figures 81 and 82. The right-front upper A-frame assembly was bent downward and a small crack occurred where the assembly attached to the truck frame. The right-front steel rim was slightly deformed, and

the tire was deflated. A minor crease was found at the joint between the right-side door and quarter panel, but the door remained undamaged. The rear of the box's right-side was bent slightly inward. Contact marks were found on the right side of the rear bumper. The right-rear steel rim was damaged, but the tire remained inflated. All window glass remained undamaged. No occupant compartment damage occurred, as shown in Figure 83.

10.5 Occupant Risk Values

The longitudinal and lateral occupant impact velocities were determined to be 5.15 m/sec and 5.41 m/sec, respectively. The maximum 0.010-sec average occupant ridedown decelerations in the longitudinal and lateral directions were 4.22 g's and 6.06 g's, respectively. It is noted that the occupant impact velocities and occupant ridedown decelerations were within the suggested limits provided in NCHRP Report No. 350. The results of the occupant risk, determined from accelerometer data, are summarized in Figure 68. Results are shown graphically in Appendix H. Due to technical difficulties, the rate transducer did not collect the roll, pitch, and yaw data. However, roll, pitch, and yaw data was collected from film analysis and are shown graphically in Appendix I.

10.6 Discussion

The analysis of the test results for test STCR-2 showed that the approach guardrail transition attached to a steel bridge rail adequately contained and redirected the vehicle with controlled lateral displacements of the guardrail transition. There were no detached elements nor fragments which showed potential for penetrating the occupant compartment or presented undue hazard to other traffic. Deformations of, or intrusions into, the occupant compartment that could have caused serious injury to the occupants did not occur. The test vehicle did not penetrate nor ride over the

approach guardrail transition and remained upright during and after the collision. Vehicle roll, pitch, and yaw angular displacements were noted, but they were deemed acceptable because they did not adversely influence the occupant risk safety criteria nor cause rollover. After collision, the vehicle's trajectory revealed minimum intrusion into adjacent traffic lanes. In addition, the vehicle's exit angle was less than 60 percent of the impact angle. Therefore, test STCR-2 conducted on the approach guardrail transition attached to a steel bridge rail system was determined to be acceptable according to the TL-2 safety performance criteria provided in NCHRP Report No. 350.

0.000 sec | 0.088 sec | 0.174 sec | 0.300 sec | 0.416 sec

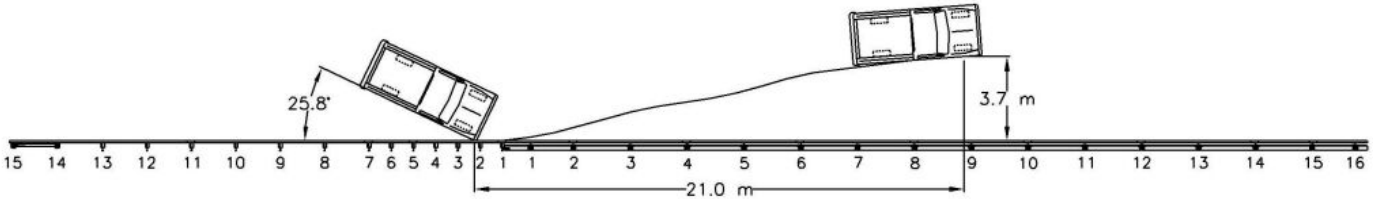

- Test Number STCR-2
- Date 10/14/1998
- Appurtenance . . . . . Approach Guardrail Transition attached to a Steel Bridge Rail with Channel Rail System for Transverse Decks
- Total Length . . . . . 20.96 m
- Steel Thrie Beam Rail
  - Thickness . . . . . 3.42 mm
  - Top Mounting Height . . . . . 804 mm
- Steel W-Beam Rail
  - Thickness . . . . . 2.66 mm
  - Top Mounting Height . . . . . 706 mm
- Steel Posts (Post Nos. 1 - 13)
  - Material . . . . . ASTM A36
    - Post Nos. 1 - 5 . . . . . W152x13.4 by 2,134-mm long
    - Post Nos. 6 - 7 . . . . . W152x13.4 by 1.981-mm long
    - Post Nos. 8 - 13 . . . . . W152x13.4 by 1,829-mm long
- Wood BCT Posts (Post Nos. 14 - 15)
  - Material . . . . . Southern Yellow Pine, Grade No. 1 or Better (CCA)
  - Dimensions . . . . . 140 mm x 191 mm x 1,080 mm
- Wood Spacer Blocks (Post Nos. 1 - 13)
  - Material . . . . . Southern Yellow Pine, Grade No. 1 (CCA)
    - Post Nos. 1 - 5 . . . . . 152 mm x 203 mm x 483 mm
    - Post No. 6 . . . . . 152 mm x 203 mm x 483 mm
    - Post Nos. 7 - 13 . . . . . 152 mm x 203 mm x 368 mm
- Vehicle Model . . . . . 1990 Chevy 2500 ¾-Ton Pickup Truck
  - Curb . . . . . 2,028 kg
  - Test Inertial . . . . . 2,035 kg
  - Gross Static . . . . . 2,035 kg
- Vehicle Speed
  - Impact . . . . . 69.9 km/hr
  - Exit . . . . . 45.5 km/hr
- Vehicle Angle
  - Impact . . . . . 25.8 deg
  - Exit . . . . . 17.6 deg
- Vehicle Snagging . . . . . None
- Vehicle Stability . . . . . Satisfactory
- Effective Coefficient of Friction (μ) 0.42
- Occupant Ridedown Deceleration (10 msec avg.)
  - Longitudinal . . . . . 4.22 < 20 G's
  - Lateral (not required) 6.06
- Occupant Impact Velocity
  - Longitudinal . . . . . 5.15 < 12 m/s
  - Lateral (not required) 5.41
- Vehicle Damage . . . . . Moderate
  - TAD[32] 1-RFQ-4
  - SAE[33] 01-RFEW3
- Vehicle Stopping Distance . . . . . 21.0 m downstream 3.7 m lateral
- Barrier Damage . . . . . Minimal
- Maximum Deflections – Thrie Beam
  - Permanent Set . . . . . 117 mm
  - Dynamic . . . . . 183 mm
- Maximum Deflections – Channel
  - Permanent Set . . . . . 98 mm
  - Dynamic . . . . . 202 mm

Figure 68. Summary of Test Results and Sequential Photographs, Test STCR-2

0.000 sec

0.508 sec

0.110 sec

0.684 sec

0.188 sec

0.756 sec

0.266 sec

0.958 sec

0.348 sec

Figure 69. Additional Sequential Photographs, Test STCR-2

0.000 sec

0.000 sec

0.082 sec

0.059 sec

0.124 sec

0.075 sec

0.238 sec

0.130 sec

0.381 sec

0.349 sec

Figure 70. Additional Sequential Photographs, Test STCR-2

Figure 71. Documentary Photographs, Test STCR-2

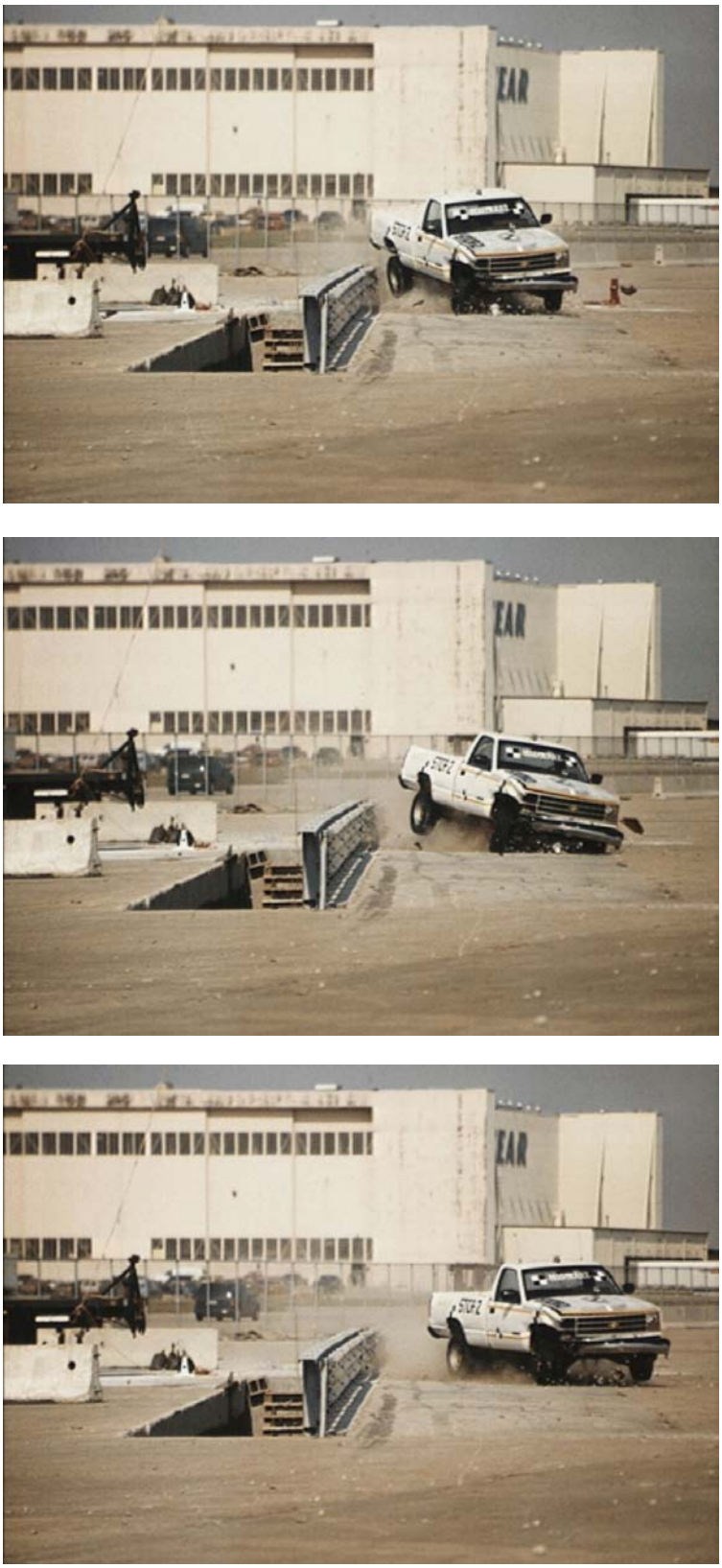

Figure 72. Documentary Photographs, Test STCR-2

Figure 73. Documentary Photographs, Test STCR-2

Figure 74. Impact Locations, Test STCR-2

Figure 75. Final Vehicle Position and Trajectory Marks, Test STCR-2

Figure 76. Barrier Damage, Test STCR-2

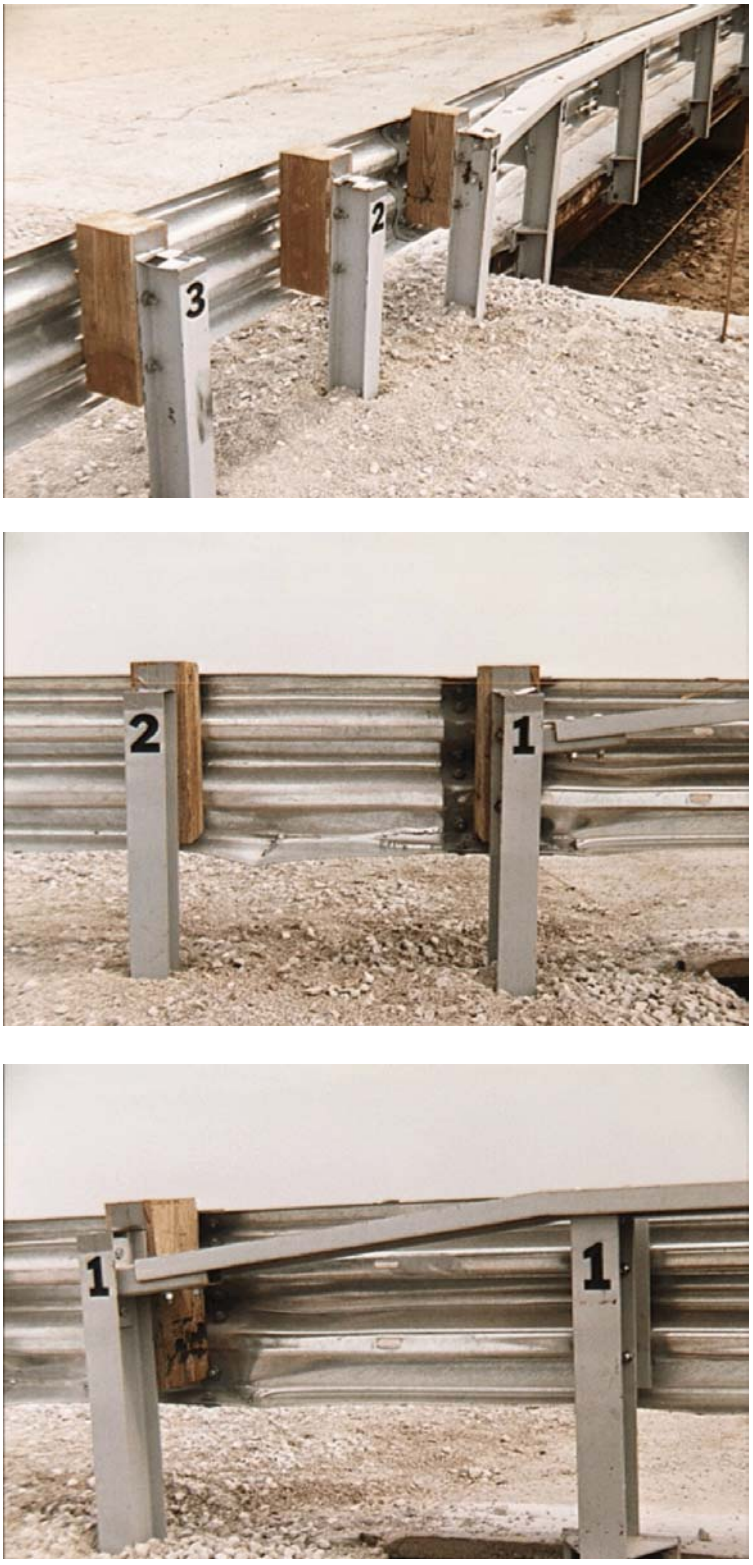

Figure 77. Barrier Damage, Test STCR-2

Figure 78. Guardrail Post Nos. 1 through 3 Damage, Test STCR-2

Figure 79. Bridge Post No. 1 Damage, Test STCR-2

Figure 80. Permanent Set Deformations, Test STCR-2

Figure 81. Vehicle Damage, Test STCR-2

Figure 82. Vehicle Damage, Test STCR-2

Figure 83. Occupant Compartment Deformations, Test STCR-2

11 SUMMARY AND CONCLUSIONS - STEEL SYSTEM

A steel bridge railing system and an attached approach guardrail transition system were successfully developed and crash tested for use on transverse glulam timber deck bridges. Two full-scale vehicle crash tests - one on the bridge railing and one on the approach guardrail transition - were performed and determined to have acceptable safety performance according to TL-2 of NCHRP Report No. 350 (3). A summary of the safety performance evaluations for both crash tests are provided in Table 4.

As previously mentioned, prior to the development of this steel bridge railing system, no other TL-2 railing systems had been developed for use on transverse glulam timber deck bridges. However, this research program clearly demonstrates that crashworthy steel railing systems are feasible for use on these types of bridges. The development of the steel bridge railing and transition system addressed the concerns for aesthetics, economy, material availability, ease of construction, and reasonable margin of structural adequacy. In addition, the steel bridge railing and transition system was relatively easy to install and should have reasonable construction labor costs. This steel railing system should also be adaptable to: (1) other transverse glulam timber deck bridges with thicknesses equal to or greater than 130 mm and with little or no modification; (2) longitudinal glulam timber deck bridges where sufficient deck strength is provided to resist the lateral impact forces; and (3) bridges supporting reinforced concrete decks that are capable of meeting the same lateral impact load requirements.

No significant damage to the test bridge was evident from the vehicle impact tests. For the bridge railing system, damage consisted primarily of permanent deformation of the thrie beam rail, channel rail, wide-flange posts, and rail spacers. Although visual permanent set deformations of the

steel components were found in the vicinity of the impact, all the steel members remained intact and serviceable after the test. Thus, replacement of the bridge railing would be based more on aesthetics than on structural integrity. For the approach guardrail transition system, damaged consisted primarily of deformed thrie beam rail and bridge posts as well as displaced guardrail posts. Although visual permanent set deformations of the thrie beam rail were found in the vicinity of the impact, the rail remained intact and serviceable after the test. Thus, replacement of the guardrail would be based more on aesthetics than on structural integrity.

Therefore, the successful completion of this phase of the research project resulted in a TL-2 steel bridge railing and approach guardrail transition system having acceptable safety performance and meeting current crash test safety standards.

Table 4. NCHRP Report No. 350 TL-2 Evaluation Results - Steel System (Bridge Railing and Transition)

Evaluation Factors	Evaluation Criteria		Test No.	
			STCR-1	STCR-2
Structural Adequacy	A.	Test article should contain and redirect the vehicle; the vehicle should not penetrate, underride, or override the installation although controlled lateral deflection of the test article is acceptable.	S	S
Occupant Risk	D.	Detached elements, fragments or other debris from the test article should not penetrate or show potential for penetrating the occupant compartment, or present an undue hazard to other traffic, pedestrians, or personnel in a work zone. Deformations of, or intrusions into, the occupant compartment that could cause serious injuries should not be permitted.	S	S
	F.	The vehicle should remain upright during and after collision although moderate roll, pitching, and yawing are acceptable.	S	S
Vehicle Trajectory	K.	After collision it is preferable that the vehicle's trajectory not intrude into adjacent traffic lanes.	S	S
	L.	The occupant impact velocity in the longitudinal direction should not exceed 12 m/s and the occupant ridedown acceleration in the longitudinal direction should not exceed 20 g's.	S	S
	M.	The exit angle from the test article preferably should be less than 60 percent of test impact angle, measured at time of vehicle loss of contact with test devise.	S	S

S - Satisfactory
M - Marginal
U - Unsatisfactory
NR - Not Required

12 WOOD SYSTEM DEVELOPMENT

As stated previously, there have been no NCHRP Report No. 350 TL-2 bridge railing systems developed for use on transverse glulam timber deck bridges prior to this research. However, in 1997, a TL-4 wood bridge railing system was developed for use on a transverse deck bridge and successfully full-scale crash tested by MwRSF (1-2,17). Since a wood bridge railing system for transverse decks had successfully met the TL-4 safety performance evaluation of NCHRP Report No. 350, it was determined that concepts from the railing system could be successfully implemented into the design of the TL-2 wood bridge railing system. In addition, concepts from a glulam timber rail without curb system for longitudinal decks, successfully tested to the AASHTO PL-1 safety performance criteria, could also be implemented into the TL-2 design.

The TL-2 wood bridge railing system was configured similarly to the PL-1 glulam timber rail without curb system previously developed for longitudinal decks (5-6,9,17). However, for this system, all wood components were fabricated from glulam timber, whereas the previous system used glulam rail and sawn lumber posts and blocks. From the PL-1 railing system, the steel box that was used to support the posts was replaced with a more-economical steel U-shaped bracket, which attached to the deck surface. In addition, all structural members and the steel hardware were resized to account for the increased post spacing from 1,905 to 2,438 mm. Again, the new post spacing was selected to optimize the design and improve the constructability of the railing system, which was based on 1,219-mm wide deck panels.

13 WOOD SYSTEM DESIGN DETAILS

13.1 Wood Bridge Railing

The bridge railing system consisted of four major components: (1) a rectangular rail; (2) rectangular bridge posts; (3) rail blockouts; and (4) deck mounting plates. Photographs of the bridge railing system are shown in Figures 84 through 88. The overall layout of the bridge railing system is shown in Figure 89. Design details of the bridge railings system are shown in Figures 90 through 95.

The glulam timber for the rail and post members was fabricated with Combination No. 48 SYP material, as specified in AASHTO's *LRFD Bridge Design Specifications*, and it was treated with pentachlorophenol in heavy oil to a minimum net retention of 9.61 kg/m^3 as specified in AWPA Standard C14 (28). The glulam timber for the spacer blocks was fabricated with Combination No. 47 SYP material, as specified by AASHTO, and was treated according to AWPA Standard C14.

The bridge rail was 171-mm wide by 343-mm deep with a 721-mm top mounting height, as measured from the top of the asphalt wearing surface to the top of the bridge rail. Two rail splices were required on the bridge rail to attain the total rail length of approximately 37.24 m. Details for the bridge rail splices are shown in Figure 92. The bridge rail was offset from the posts with spacer blocks measuring 171-mm wide by 191-mm deep by 267-mm long. The bridge rail and spacer blocks were attached to the posts with two 19-mm diameter by 610-mm long ASTM A307 galvanized dome head bolts with lugs at non-splice locations. At all bridge rail splice locations, four 19-mm diameter by 635-mm long ASTM A307 galvanized dome head bolts without lugs were used to attach the rail and spacer blocks to the posts.

Sixteen posts, measuring 171-mm wide by 191-mm deep by 935-mm long, were used to

support the upper rail. Bridge posts were spaced 2,438 mm on centers along the length of the bridge railing, except at each end where the two end posts were spaced 1,829 mm on centers. The lower portion of each post was bolted to two ASTM A36 steel plate assemblies that were connected to the top and bottom surfaces of the bridge deck with vertical bolts, as shown in Figure 93. The top and bottom plate assemblies were attached to each post with three ASTM A307 25-mm diameter x 267-mm long hex head bolts, two bolts for the top plate and one bolt for the bottom plate, as shown in Figure 93. The plate assemblies were attached to the deck with six ASTM A307 22-mm diameter x 197-mm long bolts with 102-mm diameter shear plates located between the upper deck mounting plates and the glulam deck, as shown in Figure 93. The bolt location and spacing are shown in Figure 93 and 94.

The glulam rails were anchored at the downstream end of the bridge railing system with a rigid assembly consisting of welded steel plates and structural steel tubes that were bolted to the rail and anchored to the concrete tarmac. The anchor, as shown in Figures 84, 85, and 88, was necessary to develop the tensile capacity of the rail at the downstream end of the bridge railing system.

A 51-mm thick, concrete wearing surface was placed on top of the transverse glulam deck panels. This deck surface treatment was added in order to represent actual field conditions where an asphalt surface would likely be overlaid on the bridge for resistance to both wear and moisture. For the overlay, a 20.7 MPa concrete mix was used with Type III Portland cement, 9.5-mm minus aggregate, and fiber mesh additive.

Figure 84. Wood Bridge Railing System

Figure 85. Wood Bridge Railing System

Figure 86. Wood Bridge Railing System - Bridge Posts

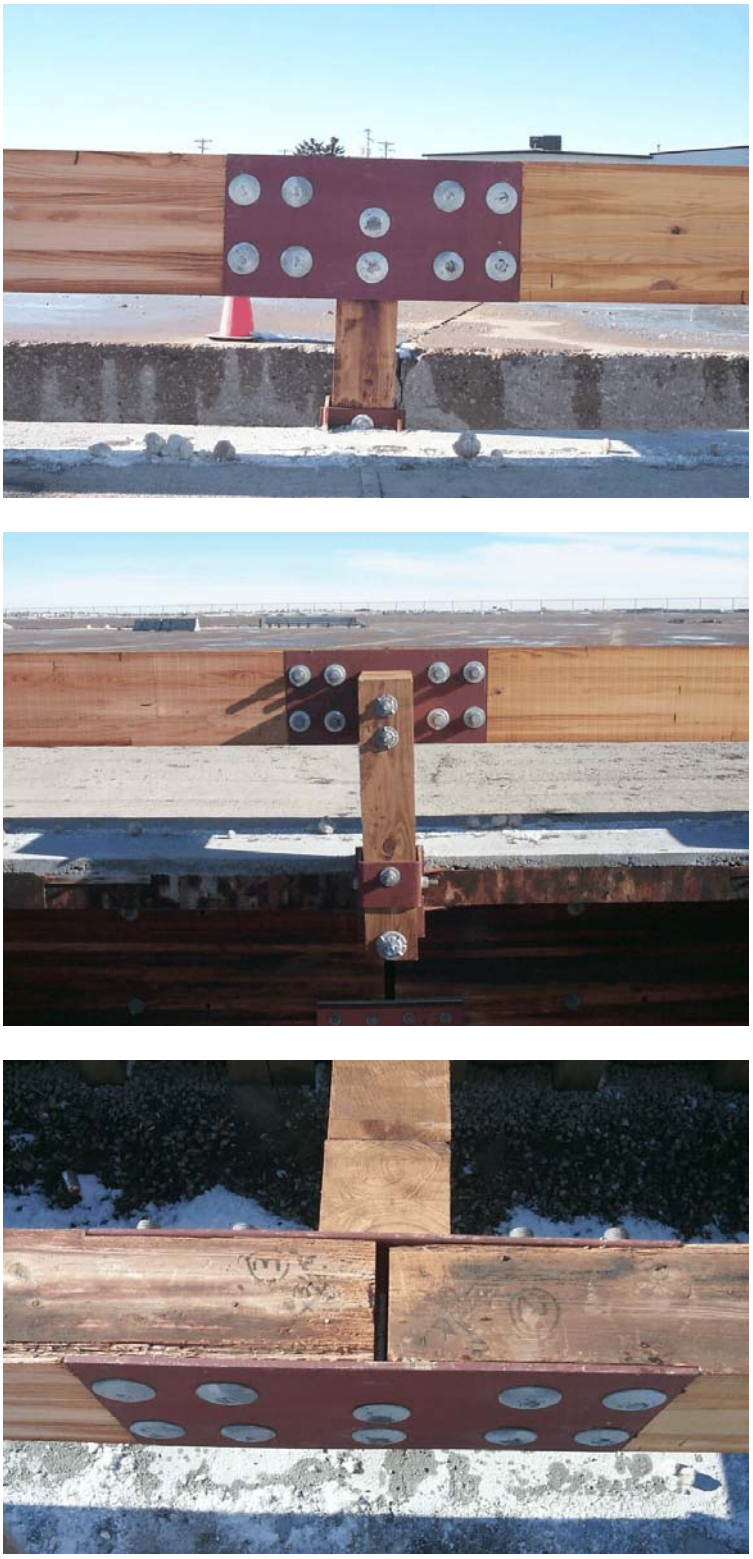

Figure 87. Wood Bridge Railing System - Rail Splices

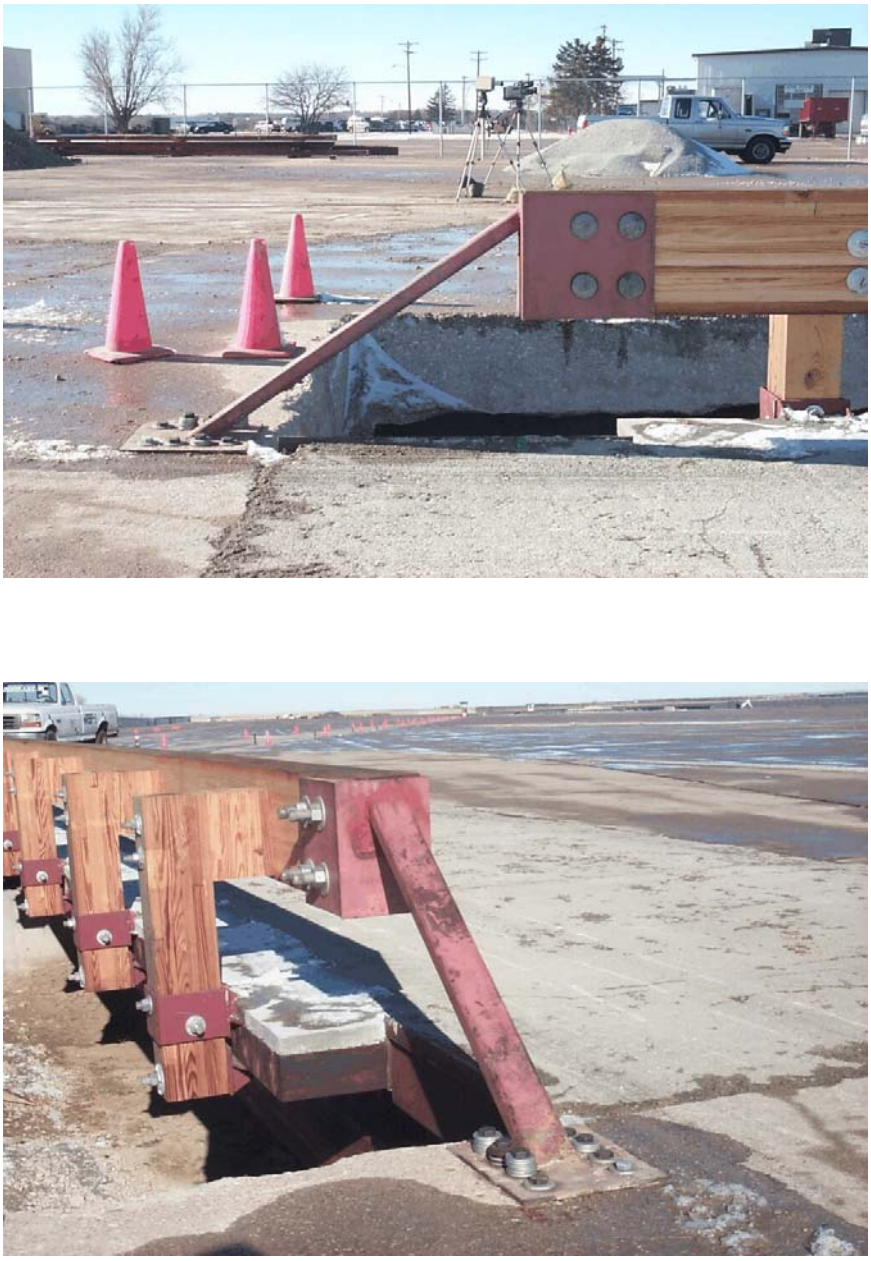

Figure 88. Wood Bridge Railing System - Anchor System

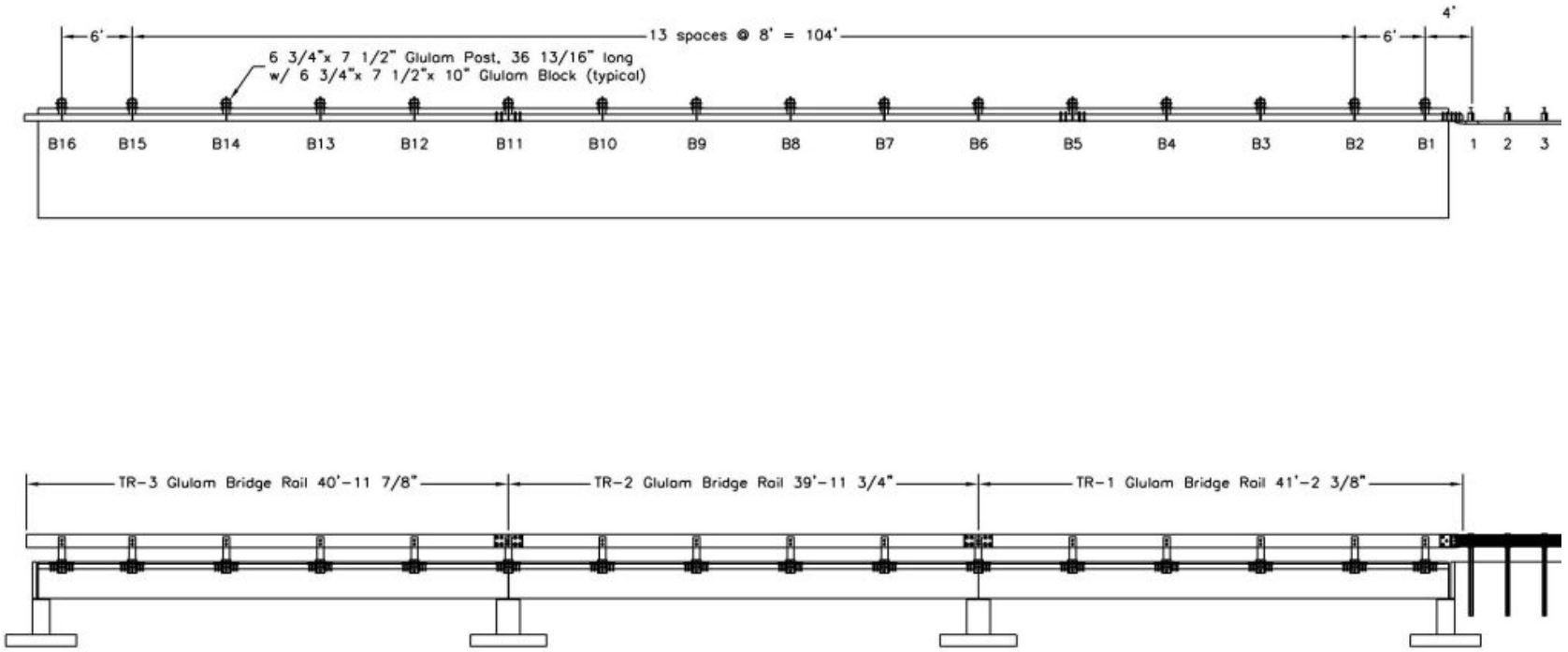

Figure 89. Overall Layout of Wood Bridge Railing System

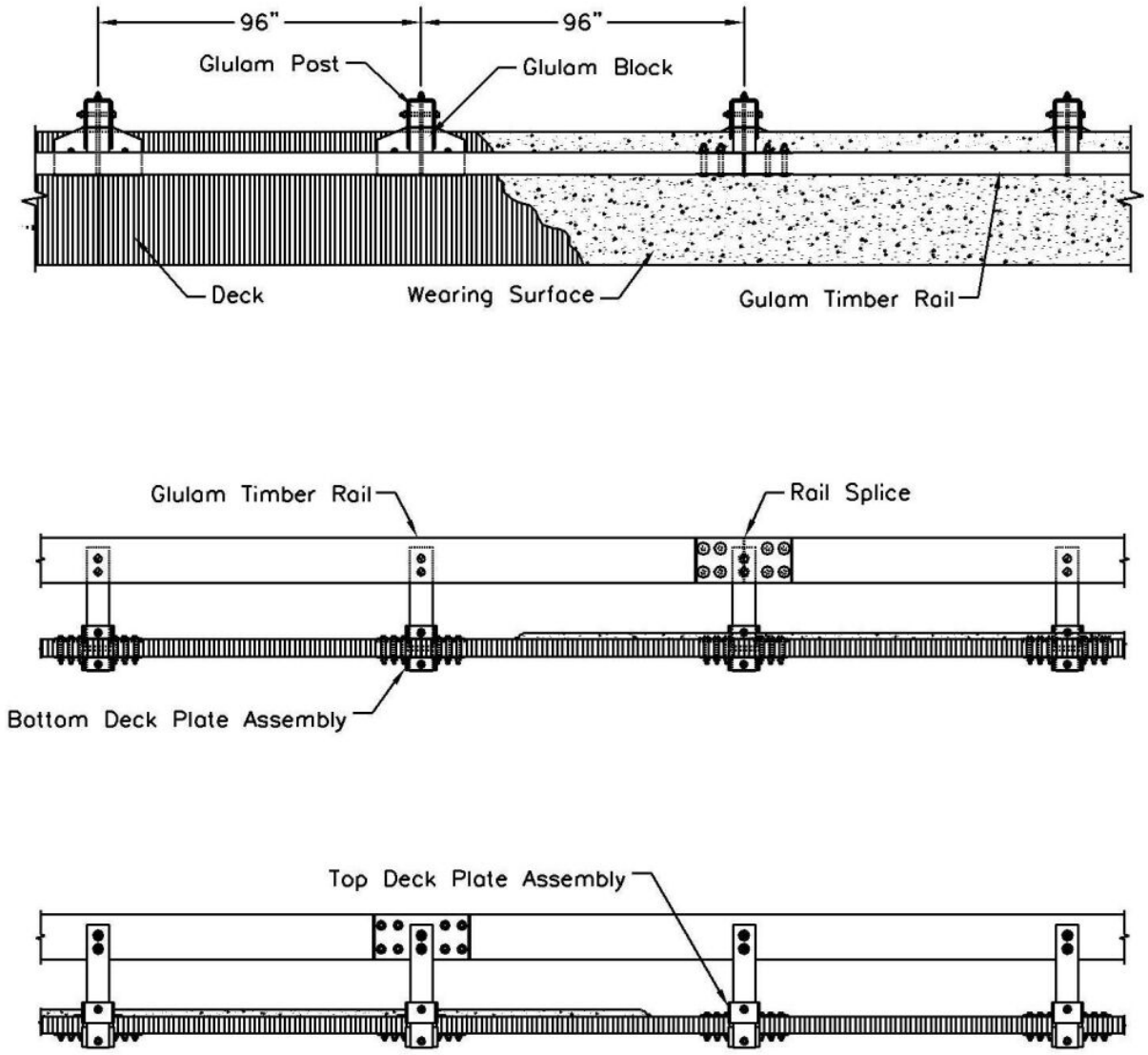

Figure 90. General Configuration of Wood Bridge Railing System

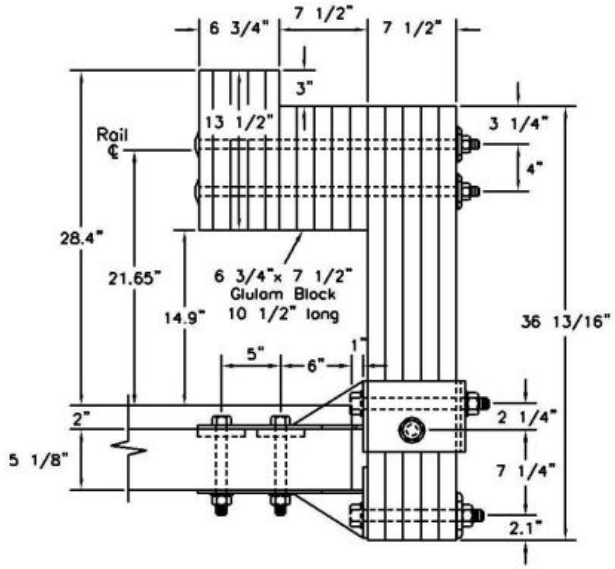

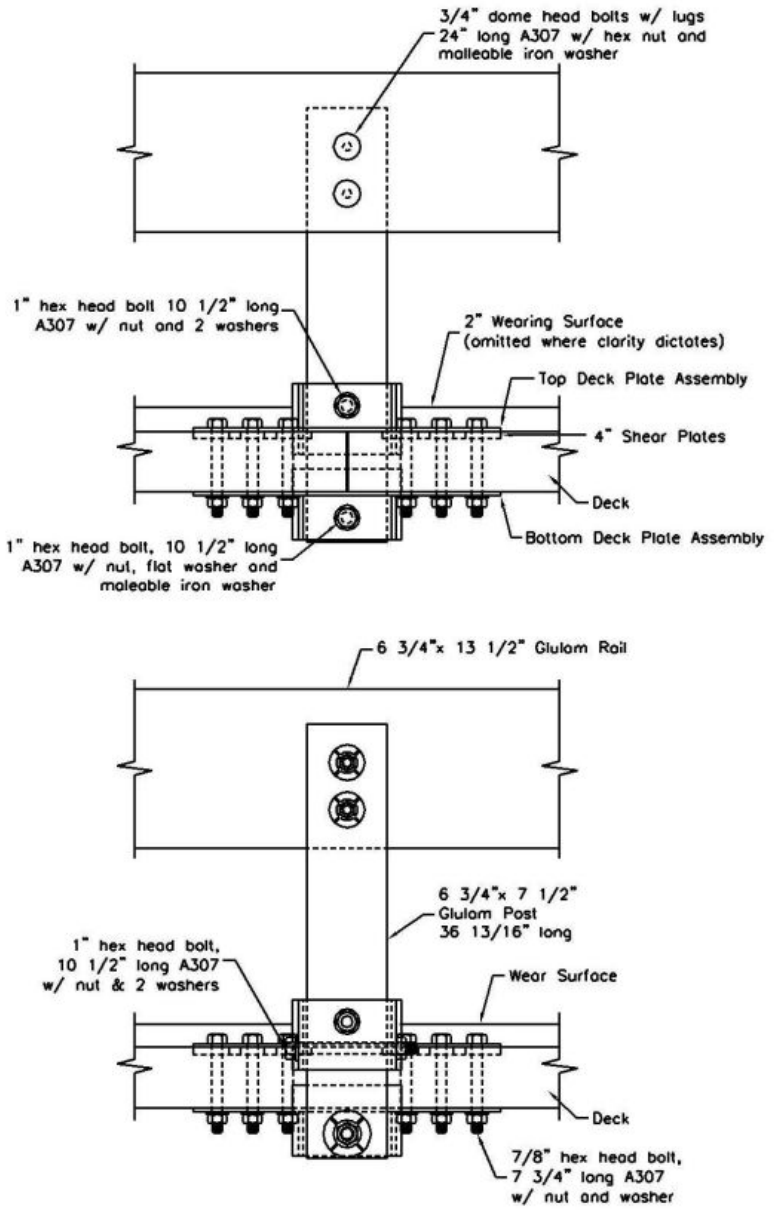

Figure 91. Bridge Railing Design Details - Wood System

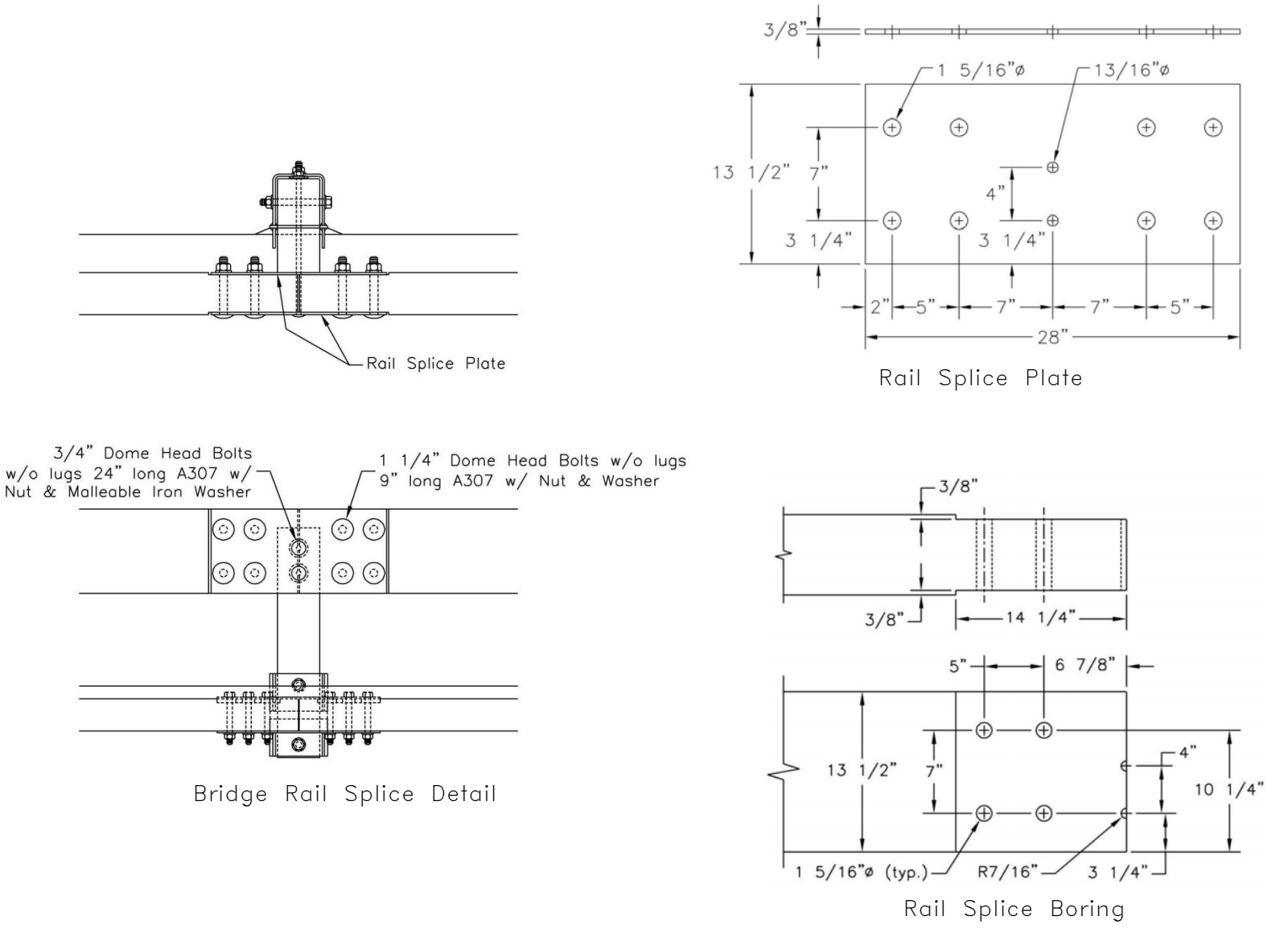

Figure 92. Rail Splice Design Details

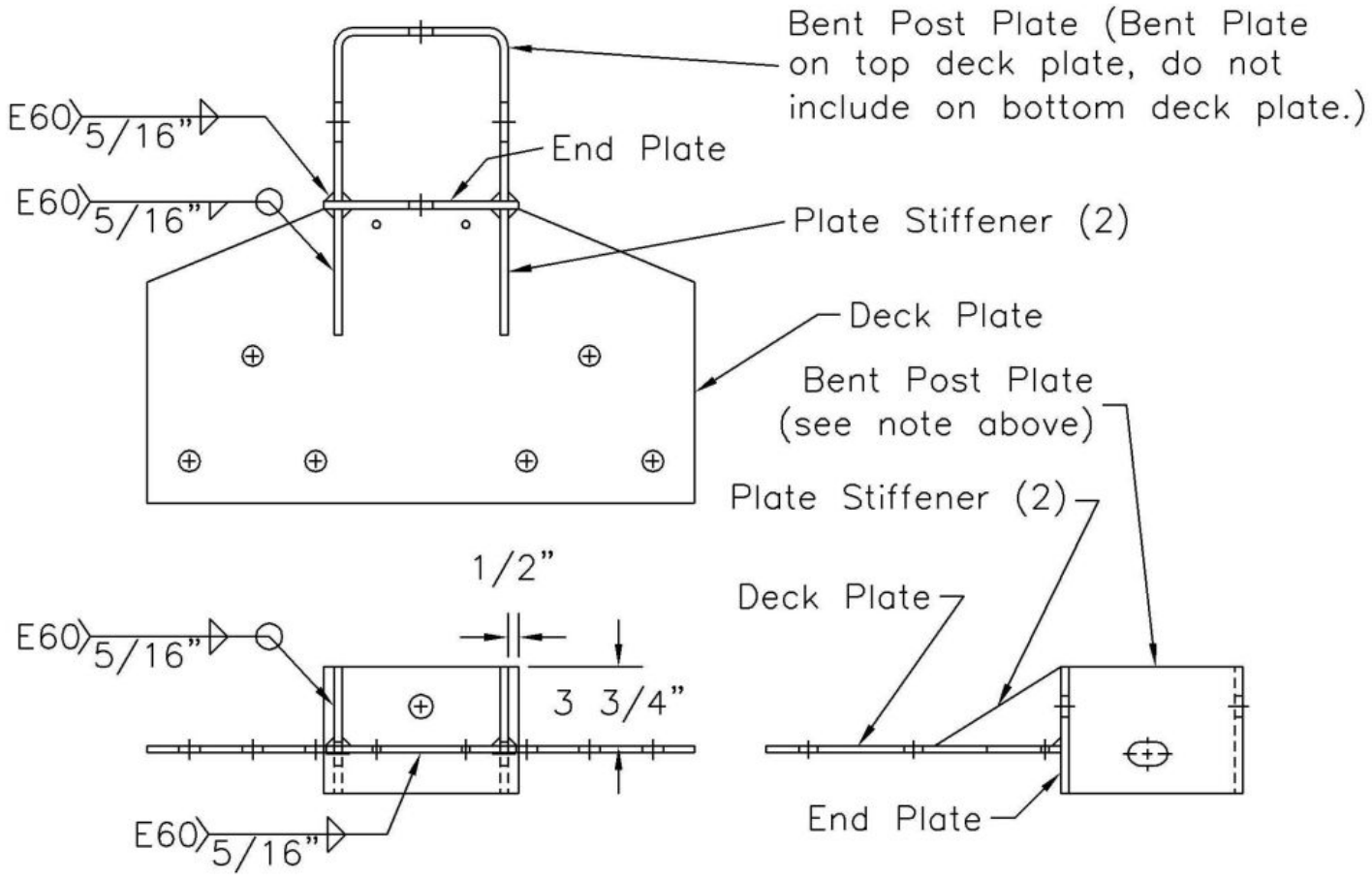

Figure 93. Design Details of Post Plate Assemblies

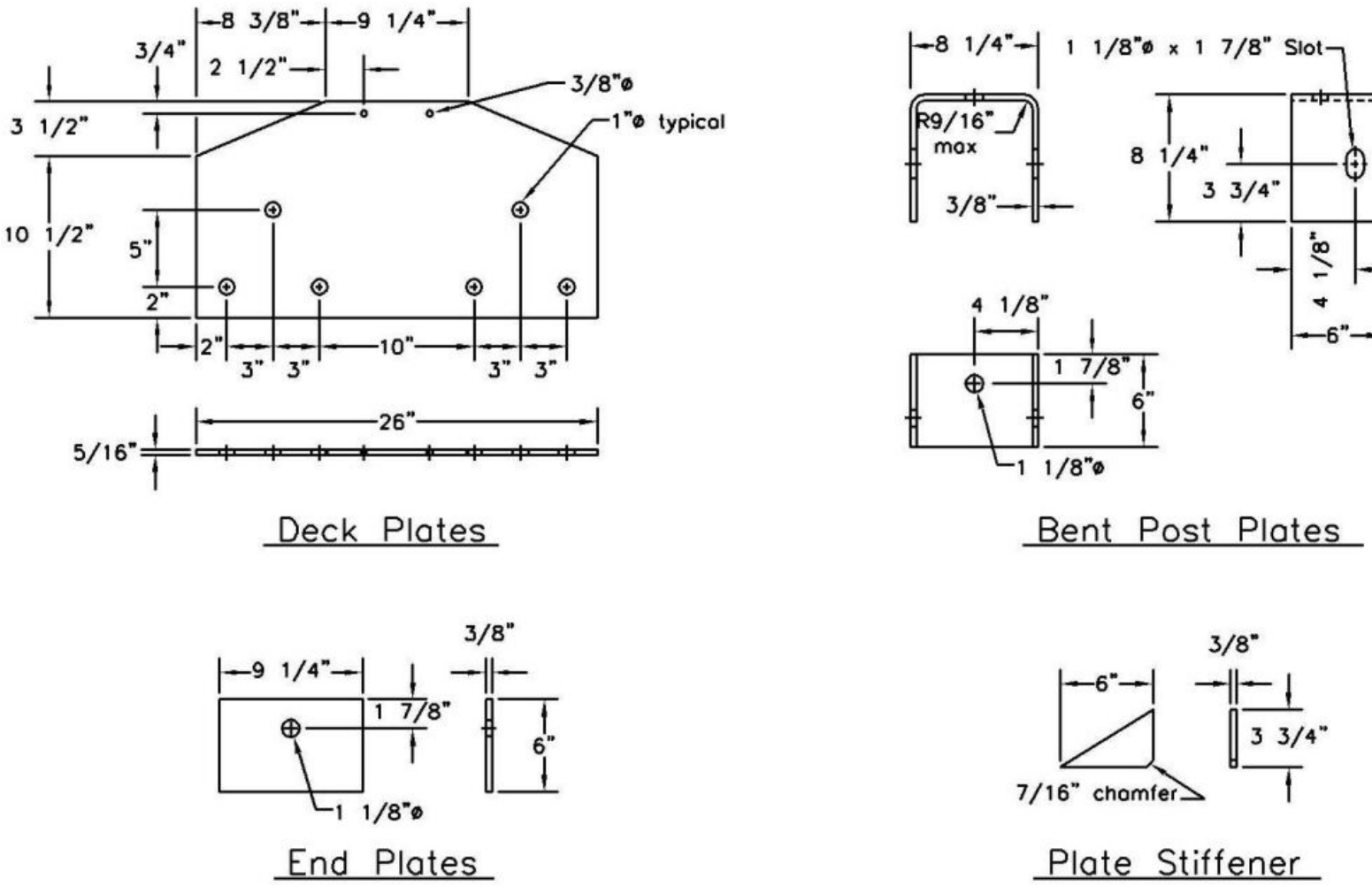

Figure 94. Post Plate Assembly Component Design Details

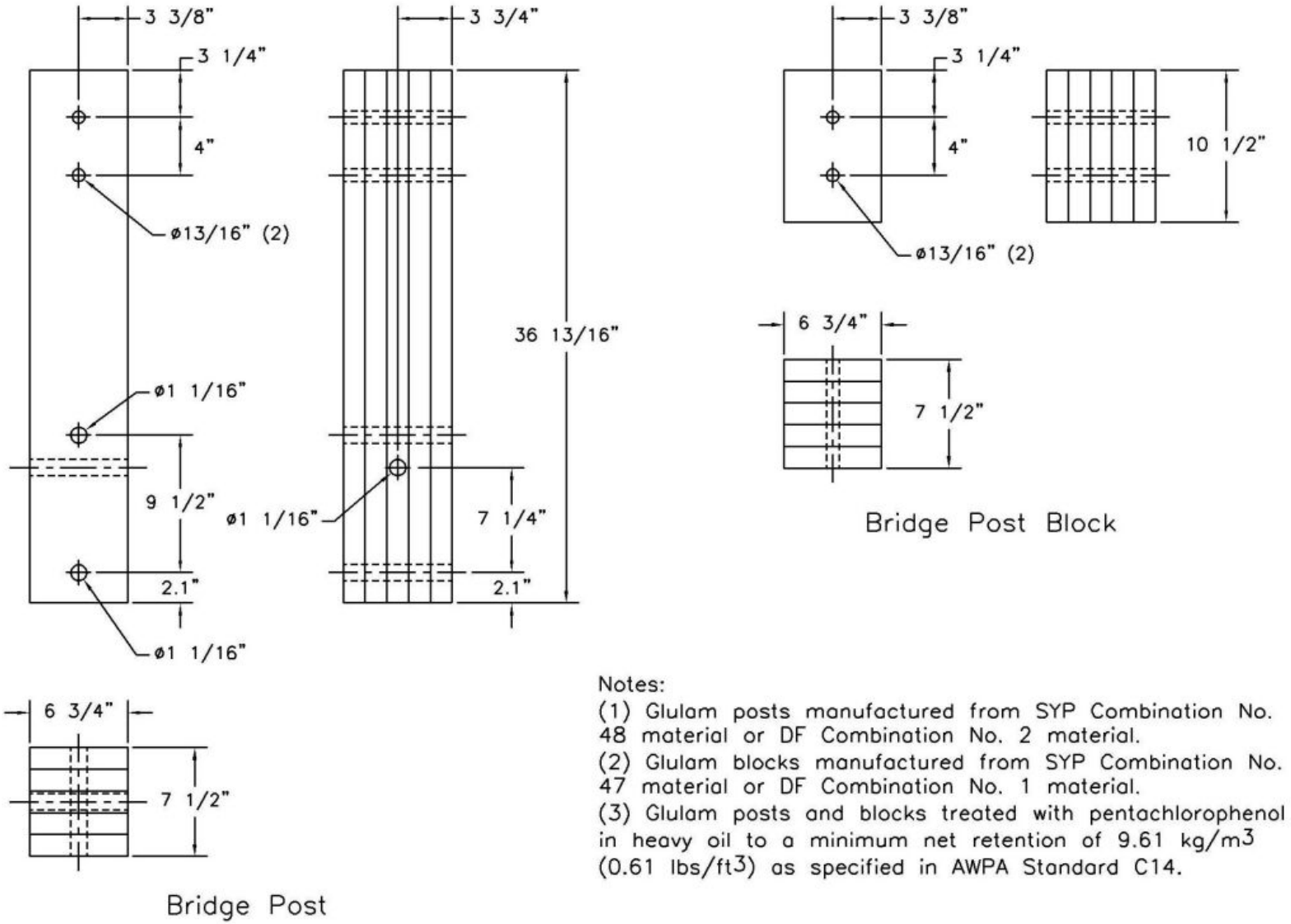

Figure 95. Bridge Post and Spacer Block Design Details

13.2 Approach Guardrail Transition

An approach guardrail transition system was attached to the upstream end of the bridge railing system and was used to connect the standard guardrail to the bridge rail. The approach guardrail transition system consisted of six major components: (1) a W-beam terminal connector; (2) a nested W-beam guardrail section; (3) standard W-beam guardrail; (4) steel guardrail posts; (5) timber blockouts; and (6) a simulated end anchorage system. Photographs of the approach guardrail transition system are shown in Figures 96 through 99. The overall layout of the approach guardrail transition system is shown in Figure 100. Design details of the approach guardrail transition system are provided in Figures 101 through 104.

Nested W-beam guardrail, measuring 2.66-mm thick and 3,810-mm long, was used to span between transition posts no. 1 and 5. A standard 2.66-mm thick W-beam rail, measuring 20,955-mm long, was placed between post nos. 5 and 15. The W-beam rails had a top mounting height of 706 mm, as measured from the roadway surface to the top of the rails. Lap-splice connections between the steel rail sections were configured to reduce vehicle snagging at the splice during the crash tests.

A 3.42-mm thick W-beam terminal connector was used to attach the W-beam rail to the glulam rail of the bridge railing system. Subsequently, the W-beam terminal connector bolted to a 4.76-mm thick steel rail transition plate that mounted to the traffic-side face of the glulam rail.

The system was constructed with fifteen guardrail posts, as shown in Figures 100 and 104. Post nos. 1 through 5 consisted of galvanized, ASTM A36 steel W152x13.4 sections measuring 2,134-mm long. Post nos. 6 and 7 were W152x13.4 steel sections measuring 1,981-mm long. Post nos. 8 through 13 were also W152x13.4 sections but measuring 1,829-mm long. Post nos. 14 and 15 consisted of 140-mm wide by 190-mm deep x 1,080-mm long BCT timber posts and were placed

in steel foundation tubes. The timber posts and foundation tubes were part of an anchorage system used to develop the required tensile capacity of the guardrail at the upstream end of the system.

For post nos. 1 through 13, treated timber blockouts were used to space the W-beam guardrails away from the traffic-side face of each guardrail post. The blockouts were fabricated from SYP, Grade No. 1 material and treated with CCA. For post nos. 1 through 13, a wood blockout, measuring 152-mm wide x 203-mm deep x 368-mm long, was used with W-beam guardrail.

The soil embedment depths of the post nos. 1 through 5, 6 through 7, and 8 through 13 were 1,399 mm, 1,247 mm, and 1,095 mm, as shown in Figure 104. The steel posts were placed in a compacted coarse, crushed limestone material that met Grading B of AASHTO M147-65 (1990) as found in NCHRP Report No. 350.

Figure 96. Approach Guardrail Transition - Front View

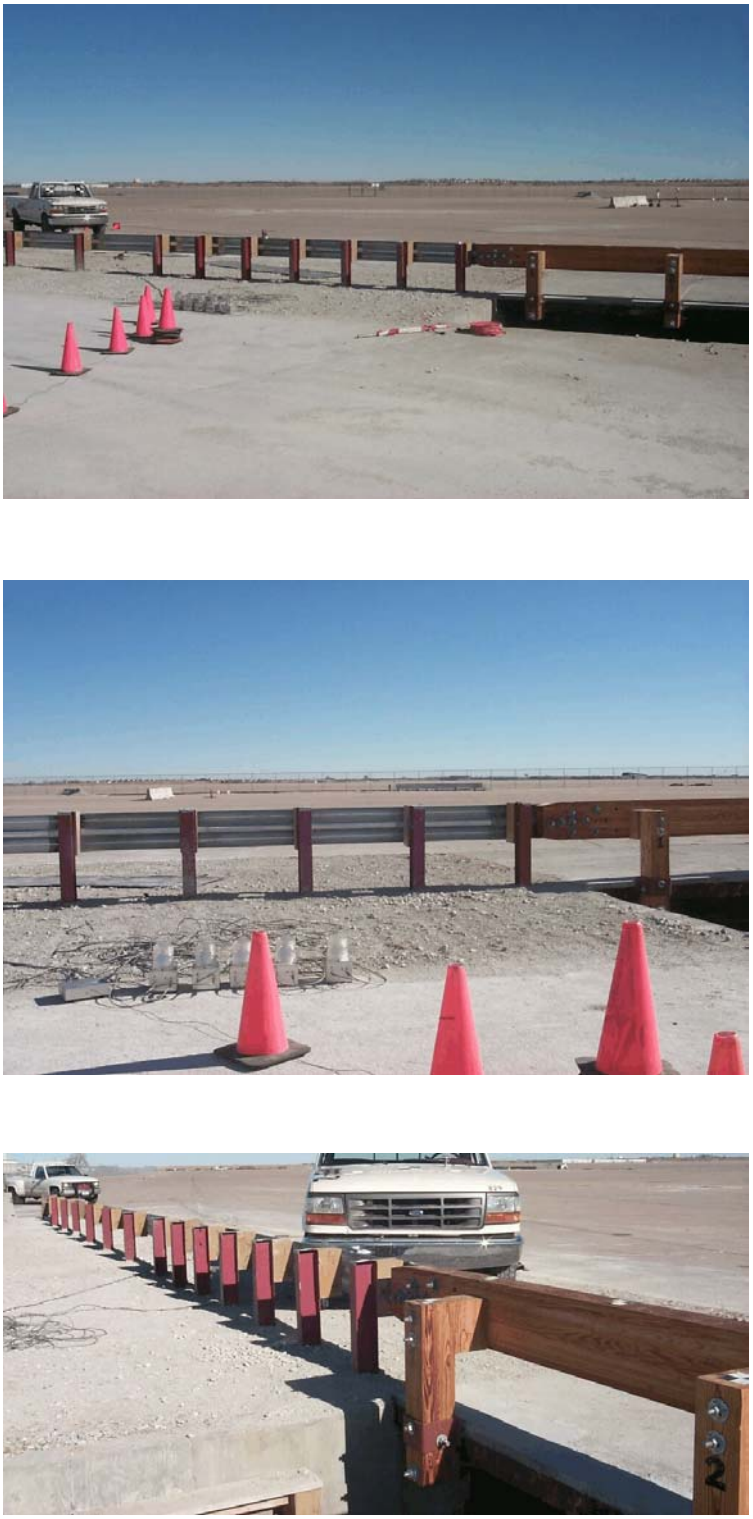

Figure 97. Approach Guardrail Transition - Back View

Figure 98. Approach Guardrail Transition - Parallel View

Figure 99. Connection to Wood Bridge Railing System

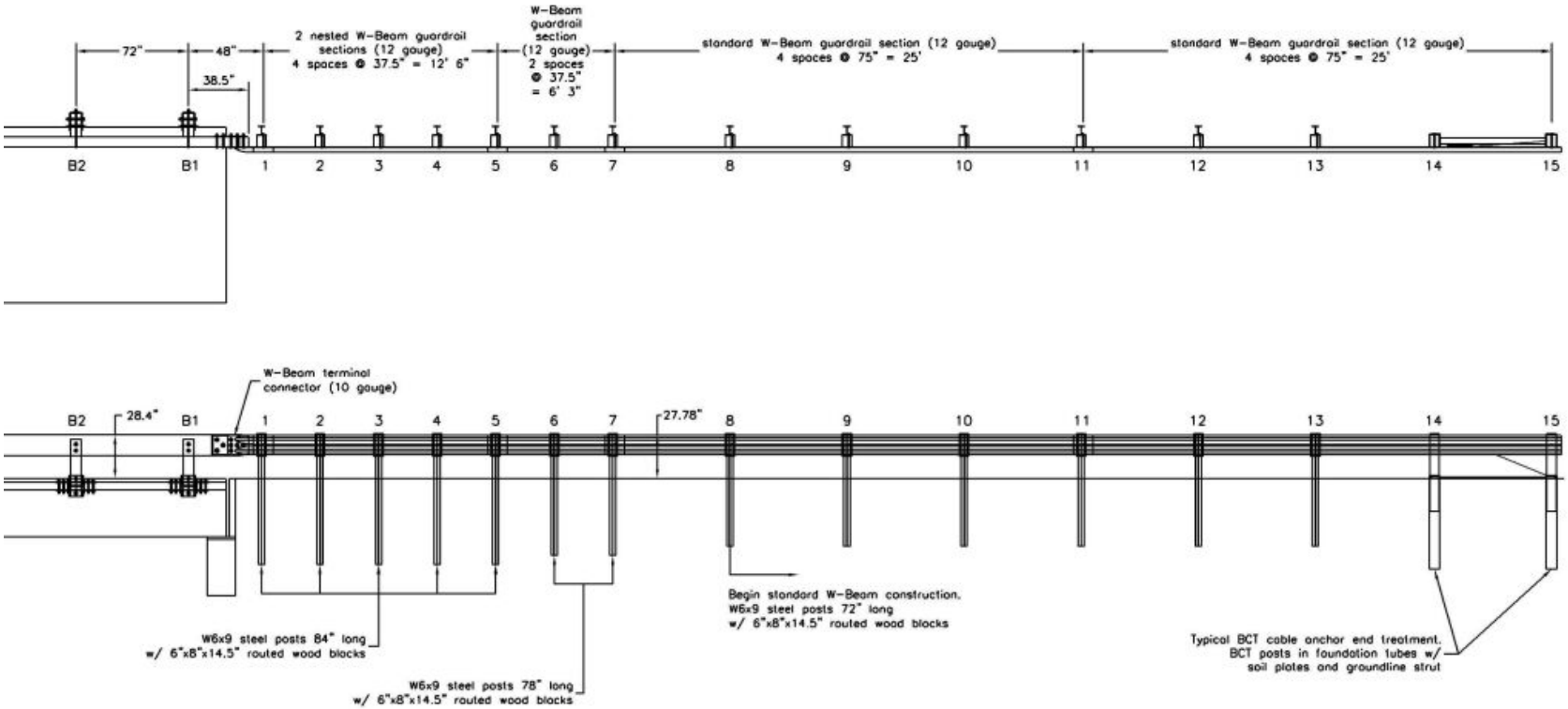

Figure 100. Overall Layout of Approach Guardrail Transition System - Wood System

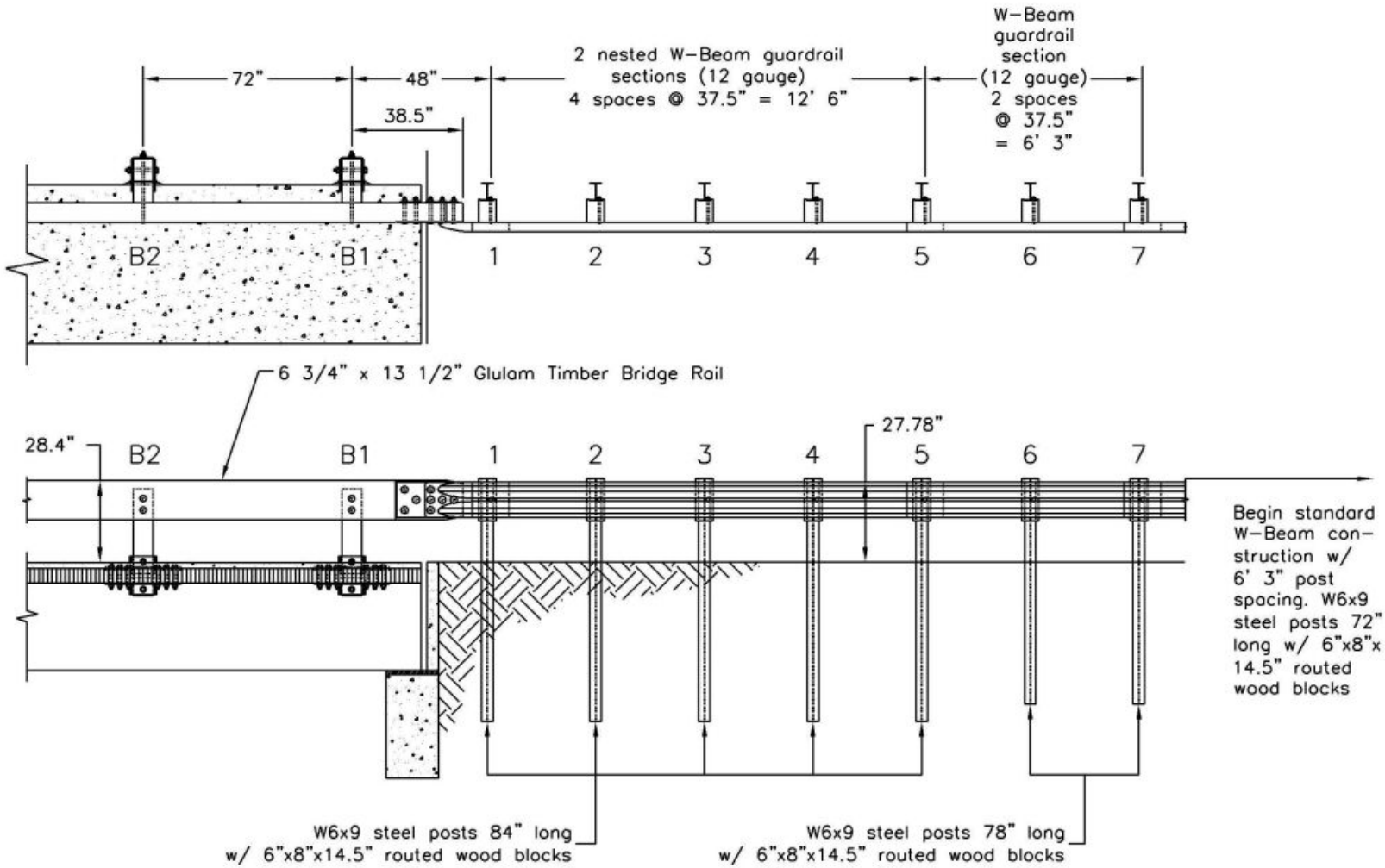

Figure 101. General Configuration of Approach Guardrail Transition System - Wood System

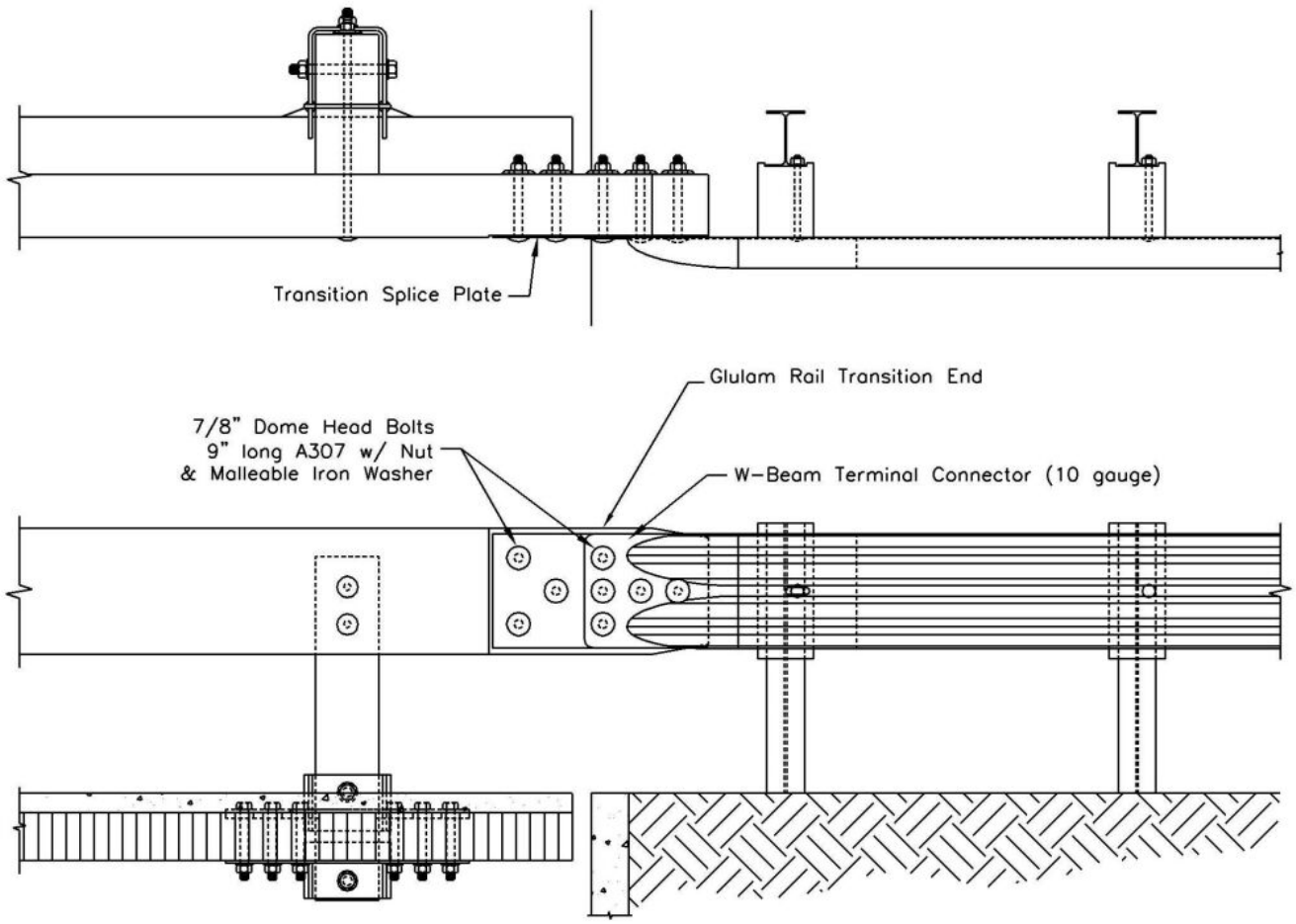

Figure 102. Transition Connection Details - Wood System

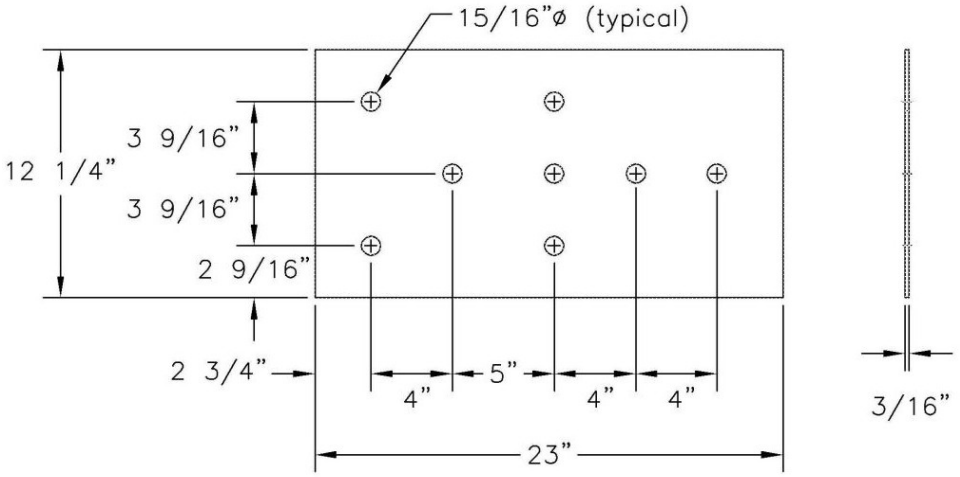

Transition Splice Plate

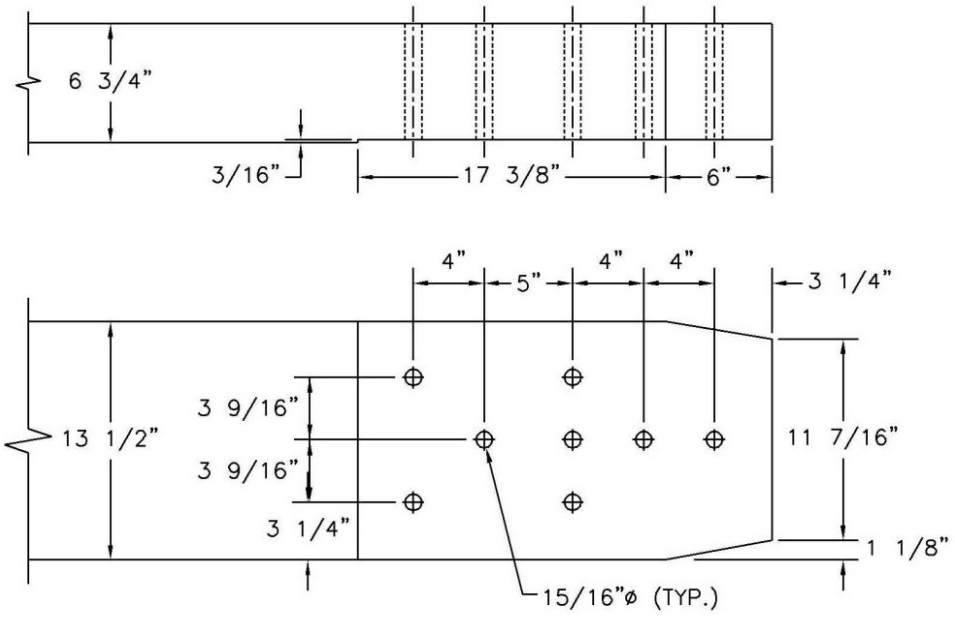

Transition Splice Boring

Figure 103. Transition Splice Plate and Boring Details

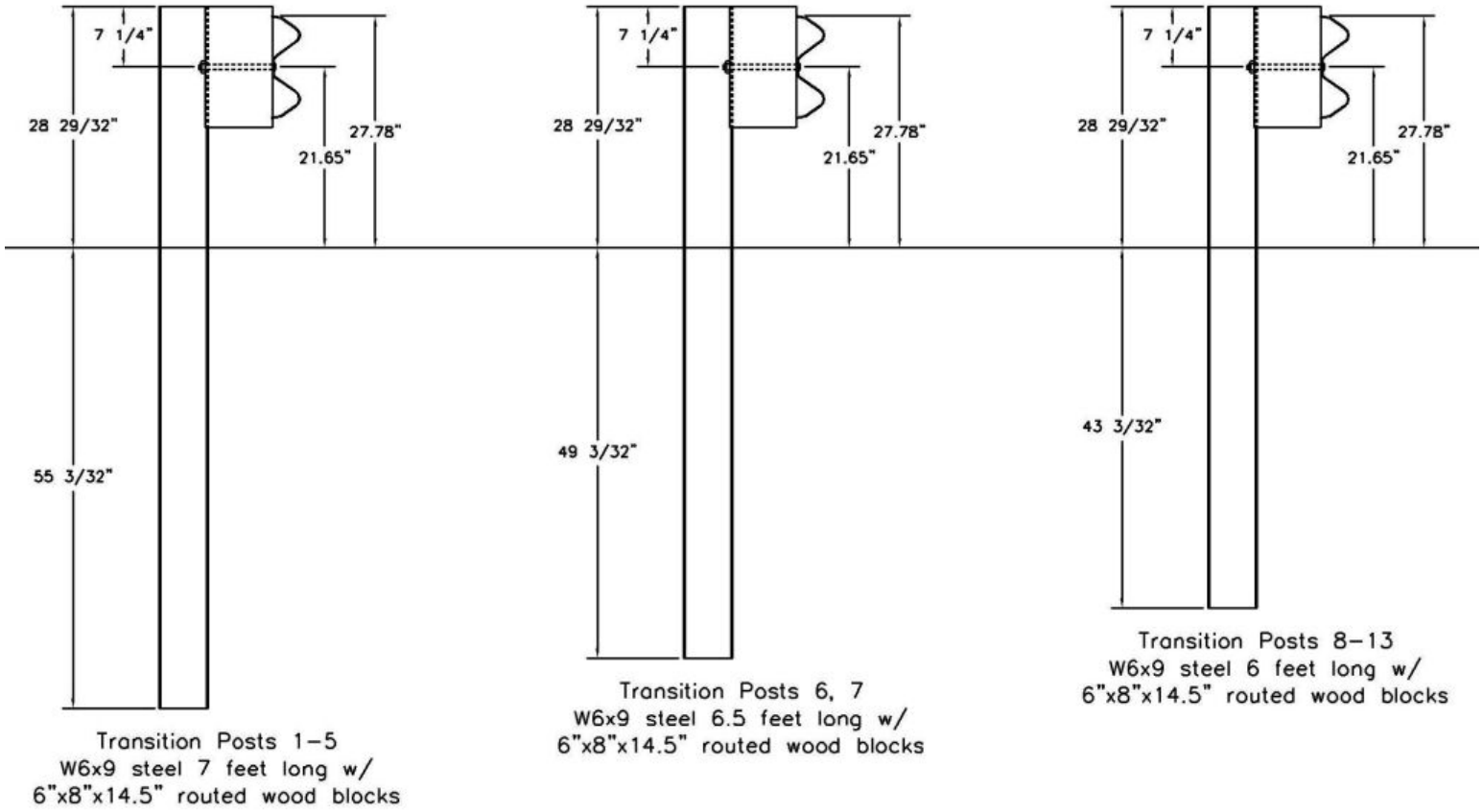

Figure 104. Transition Post Configurations

14 COMPUTER SIMULATION

14.1 Introduction

Computer simulation modeling with BARRIER VII (31) was performed to analyze and predict the dynamic performance of the timber bridge railing and approach guardrail transition systems prior to full-scale vehicle crash testing. The simulations were conducted modeling a 2000-kg pickup truck impacting at a speed of 70.0 km/hr and at an angle of 25 degrees. The BARRIER VII finite element model of the wood bridge railing and approach guardrail transition systems are shown in Appendix J. Typical computer simulation input data files for each system and vehicle are shown in Appendix K. Computer simulation was also used to determine the CIP for the wood bridge railing and approach guardrail transition systems.

14.2 BARRIER VII Results

14.2.1 Bridge Railing Results

The simulation results indicated that the wood bridge railing system described in Section No. 13 would satisfactorily redirect the 2,000-kg pickup truck. In addition, all structural hardware would remain functional during both of the vehicle impacts with the bridge railing system.

For the 2,000-kg pickup truck impact simulation, the CIP was determined to occur with an impact between bridge post nos. 5 and 6 or 914-mm downstream from the centerline of bridge post no. 5 . The maximum dynamic and permanent set deflections of the timber bridge rail, as measured from the roadway surface to the center of the rail, were 225 mm and 106 mm, respectively. The pickup truck became parallel to the bridge railing at 0.264 sec with a velocity of 52.0 km/hr. At 0.398 sec after impact, the pickup truck exited the bridge railing with a velocity of 49.8 km/hr and at an angle of 8.7 degrees.

14.2.2 Approach Guardrail Transition Results

The simulation results indicated that the approach guardrail transition system would satisfactorily redirect the 2,000-kg pickup truck. In addition, all structural hardware would remain functional during both of the vehicle impacts with the approach guardrail transition system.

For the 2,000-kg pickup truck impact simulation, the CIP was determined to occur with an impact between transition post nos. 2 and 3 or 238-mm downstream of transition post no. 3. The maximum dynamic and permanent set deflections of the thrie beam rail, as measured from the roadway surface to the center of the rail, were 137 mm and 91 mm, respectively. The pickup truck became parallel to the bridge railing at 0.256 sec with a velocity of 52.6 km/hr. At 0.356 sec after impact, the pickup truck exited the bridge railing with a velocity of 50.5 km/hr and at an angle of 4.6 degrees.

15 CRASH TEST NO. 1 (WOOD SYSTEM - BRIDGE RAILING)

15.1 Test WRBP-1

The 2,031-kg pickup truck impacted the bridge railing at a speed of 69.0 km/hr and at an angle of 26.2 degrees. A summary of the test results and the sequential photographs are shown in Figure 105. Additional sequential photographs are shown in Figures 106 and 107. Documentary photographs of the crash test are shown in Figures 108 through 110.

15.2 Test Description

Initial impact occurred between bridge post nos. 5 and 6 or 914 mm downstream from bridge post no. 5, as shown in Figure 111. At 0.014 sec after impact, the front bumper encountered major deformation. At 0.018 sec, bridge post nos. 5 and 6 deflected rapidly. At 0.057 sec, the hood and right-front headlight extended over the rail. At 0.074 sec, the right-front corner of the vehicle was located at bridge post no. 6. At 0.078 sec, the front bumper moved toward the left side of the truck. At this same time, bridge post no. 6 reached its maximum deflection. At 0.082 sec, the truck encountered extensive redirection as the right-front fender crushed inward. At 0.135 sec, the left-front tire became airborne. At 0.181 sec, the truck rolled CCW toward the rail. At 0.207 sec, the right-front corner of the vehicle was located at bridge post no. 7. At 0.220 sec, the right-front tire became airborne. At 0.254 sec, the right-front tire lost contact with the rail. At 0.280 sec after impact, the vehicle became parallel to the bridge rail with a velocity of 47.2 km/hr. At 0.289 sec, the right-rear of the truck box contacted the rail. At 0.325 sec, the right-rear tire became airborne. At 0.390 sec, the right-rear corner of the truck box was located at bridge post no. 6. At 0.395 sec, the front of the truck reached its maximum pitch angle. At 0.452 sec, the vehicle exited the bridge railing at a speed of approximately 47.1 km/hr and an angle of 5.9 degrees. At 0.438 sec, the right-

front tire contacted the ground. At 0.579 sec, the left-front tire also contacted the ground. At 0.646 sec, the rear of the truck reached its maximum pitch angle. At 0.679 sec, the truck rolled CW away from the rail. The vehicle's post-impact trajectory is shown in Figure 105. The vehicle came to rest behind the system, approximately 28.9-m downstream from impact and 1.4-m laterally behind a line projected parallel to the traffic-side face of the rail, as shown in Figure 112.

15.3 Bridge Rail Damage

Damage to the bridge railing was moderate as shown in Figures 113 and 114. Significant gouging occurred to the middle of the glulam rail between post nos. 5 and 6, as shown in Figure 113. The gouge mark on the front face of the glulam rail was 483-mm long and approximately 25-mm deep. Black tire marks and scrapes, measuring 3.43-m long, spanned between bridge post nos. 5 and 7. Another set of black tire marks were found on the glulam rail from 1,143-mm upstream of bridge post no. 14 to 762-mm downstream of bridge post no. 14. Tire marks were also found on the downstream end anchor.

No contact marks nor damage was observed on the posts, but movement of transition post no. 1 was evident by the 3-mm soil gap at the front face of this post. The bent post plate at bridge post no. 6 deformed. Permanent set of the guardrail and posts was visible between bridge post nos. 3 and 8.

The maximum lateral permanent set deflections for midspan rail and post locations, as determined from field measurements in the impact region, were approximately 63 mm at 1,219-mm downstream from the centerline of bridge post no. 6 and at the centerline of bridge post no. 6. The maximum dynamic lateral deflections for midspan rail and post locations, as determined from high-speed film analysis, were 145 mm at 1,219-mm downstream from the centerline of bridge post no.

6 and 189 mm at bridge post no. 6, respectively. The effective coefficient of friction was determined to be approximately 0.48.

15.4 Vehicle Damage

Exterior vehicle damage was moderate, as shown in Figures 115 and 116. Vehicle damage occurred to several body locations, such as to the right side of the pickup box, right-side quarter panels, front bumper, and right-side wheels and rims. The right corner of the front bumper and quarter panels were crushed inward due to contact with the rail, as shown in Figure 115. The right-front wheel assembly deformed inward toward the firewall, as shown in Figure 115. The right-front steel rim was deformed, and the tire was deflated, as shown in Figures 115 and 116. Both the right- and left-side doors were jarred open. The right-side door also encountered a tear in the sheet metal near the lower-front portion of the door. The cab's right side encountered a tear in the sheet metal near the rear of the door. The right side of the box was deformed inward on both sides of the right-rear tire. The right side of the rear bumper was deformed and ripped. Light scuff marks were found on the right-rear tire but no rim nor axle damage occurred. No occupant compartment damage occurred, and all window glass remained undamaged.

15.5 Occupant Risk Values

The longitudinal and lateral occupant impact velocities were determined to be 5.47 m/sec and 5.45 m/sec, respectively. The maximum 0.010-sec average occupant ridedown decelerations in the longitudinal and lateral directions were 3.86 g's and 6.28 g's, respectively. It is noted that the occupant impact velocities and occupant ridedown decelerations were within the suggested limits provided in NCHRP Report No. 350. The results of the occupant risk, determined from accelerometer data, are summarized in Figure 105. Results are shown graphically in Appendix L.

Due to technical difficulties, the rate transducer did not collect the roll, pitch, and yaw data. However, the roll, pitch, and yaw data were collected from film analysis and are shown graphically in Appendix M.

15.6 Discussion

The analysis of the test results for test WRBP-1 showed that the glulam bridge railing adequately contained and redirected the vehicle with controlled lateral displacement of the bridge rail. There were no detached elements nor fragments which showed potential for penetrating the occupant compartment or presented undue hazard to other traffic. Deformations of, or intrusions into, the occupant compartment that could have caused serious injury to the occupants did not occur. The test vehicle did not penetrate nor ride over the bridge rail and remained upright both during and after the collision. Vehicle roll, pitch, and yaw angular displacements were noted, but they were deemed acceptable. After collision, the vehicle's trajectory revealed minimum intrusion into adjacent traffic lanes. In addition, the vehicle's exit angle was less than 60 percent of the impact angle. Therefore, test WRBP-1 conducted on the glulam bridge rail system was determined to be acceptable according to the TL-2 safety performance criteria provided in NCHRP Report No. 350.

15.7 Barrier Instrumentation Results

For test WRBP-1, strain gauges were located on selected components of the steel bridge railing system. The results of the strain gauge analysis are summarized in Table 5. Results of the strain gauge analysis are also shown graphically in Appendix N.

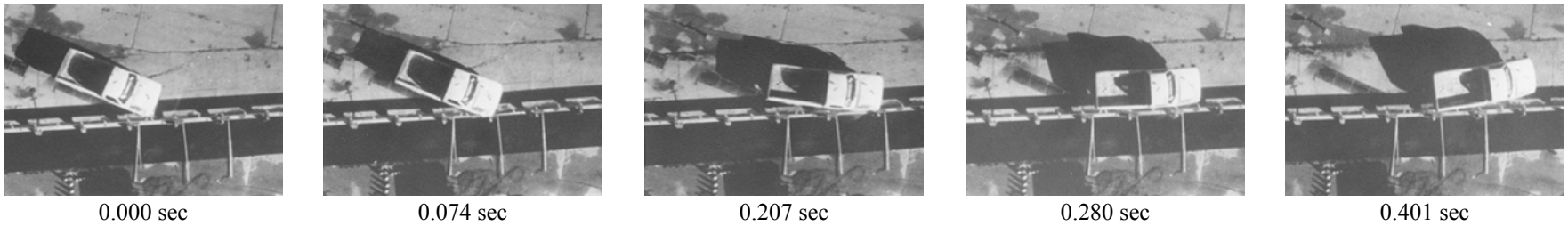

0.000 sec | 0.074 sec | 0.207 sec | 0.280 sec | 0.401 sec

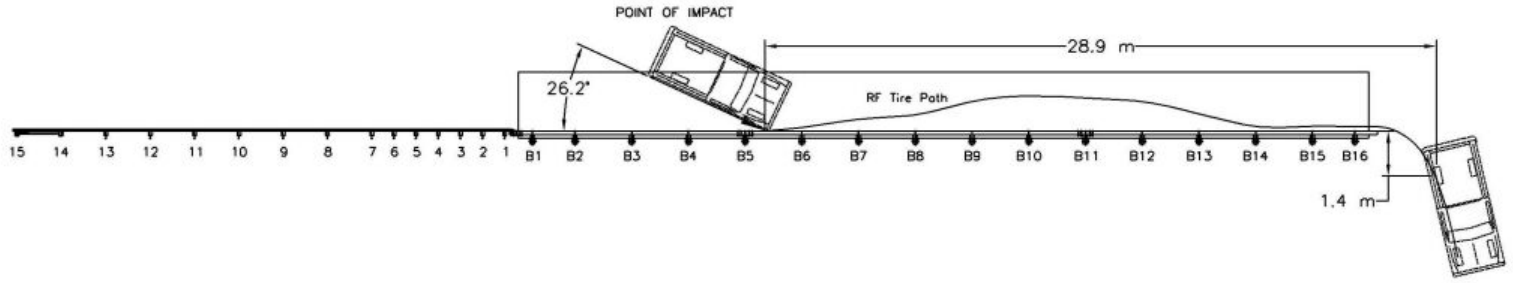

- Test Number WRBP-1
- Date 12/15/99
- Appurtenance . . . . . Wood Bridge Rail System for Transverse Decks
- Total Length . . . . . 37.24 m
- Wood Rail
  - Material . . . . . Southern Yellow Pine, Combination No. 48
  - Dimensions . . . . . 171 mm x 343 mm x 37.24 m
  - Top Mounting Height . . . . . 721 mm
- Rail Wood Post Nos. 1-16
  - Material . . . . . Southern Yellow Pine, Combination No. 48
  - Dimensions . . . . . 171 mm x 191 mm x 935 mm
- Rail Wood Spacer Blocks Nos. 1-16
  - Material . . . . . Southern Yellow Pine, Combination No. 47
  - Dimensions . . . . . 171 mm x 191 mm x 267 mm
- Vehicle Model . . . . . 1994 Ford F-250 3/4 Ton Pickup Truck
  - Curb . . . . . 2,045 kg
  - Test Inertial . . . . . 2,031 kg
  - Gross Static . . . . . 2,031 kg
- Vehicle Speed
  - Impact . . . . . 69.0 km/hr
  - Exit . . . . . 47.1 km/hr
- Vehicle Angle
  - Impact 26.2deg
  - Exit . . . . . 5.9 deg
- Vehicle Snagging . . . . . None
- Vehicle Stability . . . . . Satisfactory
- Effective Coefficient of Friction (μ) 0.48
- Occupant Ridedown Deceleration (10 msec avg.)
  - Longitudinal . . . . . 3.86 < 20 G's
  - Lateral (not required) 6.28
- Occupant Impact Velocity
  - Longitudinal . . . . . 5.47 < 12 m/s
  - Lateral (not required) 5.45
- Vehicle Damage . . . . . Moderate
  - TAD[32] 1-RFQ-3/1-RD-4
  - SAE[33] 01-RDES3
- Vehicle Stopping Distance . . . . . 28.9 m downstream
  1.4 m laterally behind
- Bridge Rail Damage . . . . . Moderate
- Maximum Deflections
  - Permanent Set . . . . . est. 63 mm
  - Dynamic . . . . . 189 mm

Figure 105. Summary of Test Results and Sequential Photographs, Test WRBP-1

0.000 sec

0.438 sec

0.088 sec

0.579 sec

0.181 sec

0.679 sec

0.269 sec

0.862 sec

Figure 106. Additional Sequential Photographs, Test WRBP-1

0.000 sec

0.000 sec

0.082 sec

0.084 sec

0.133 sec

0.139 sec

0.197 sec

0.221 sec

0.238 sec

0.290 sec

Figure 107. Additional Sequential Photographs, Test WRBP-1

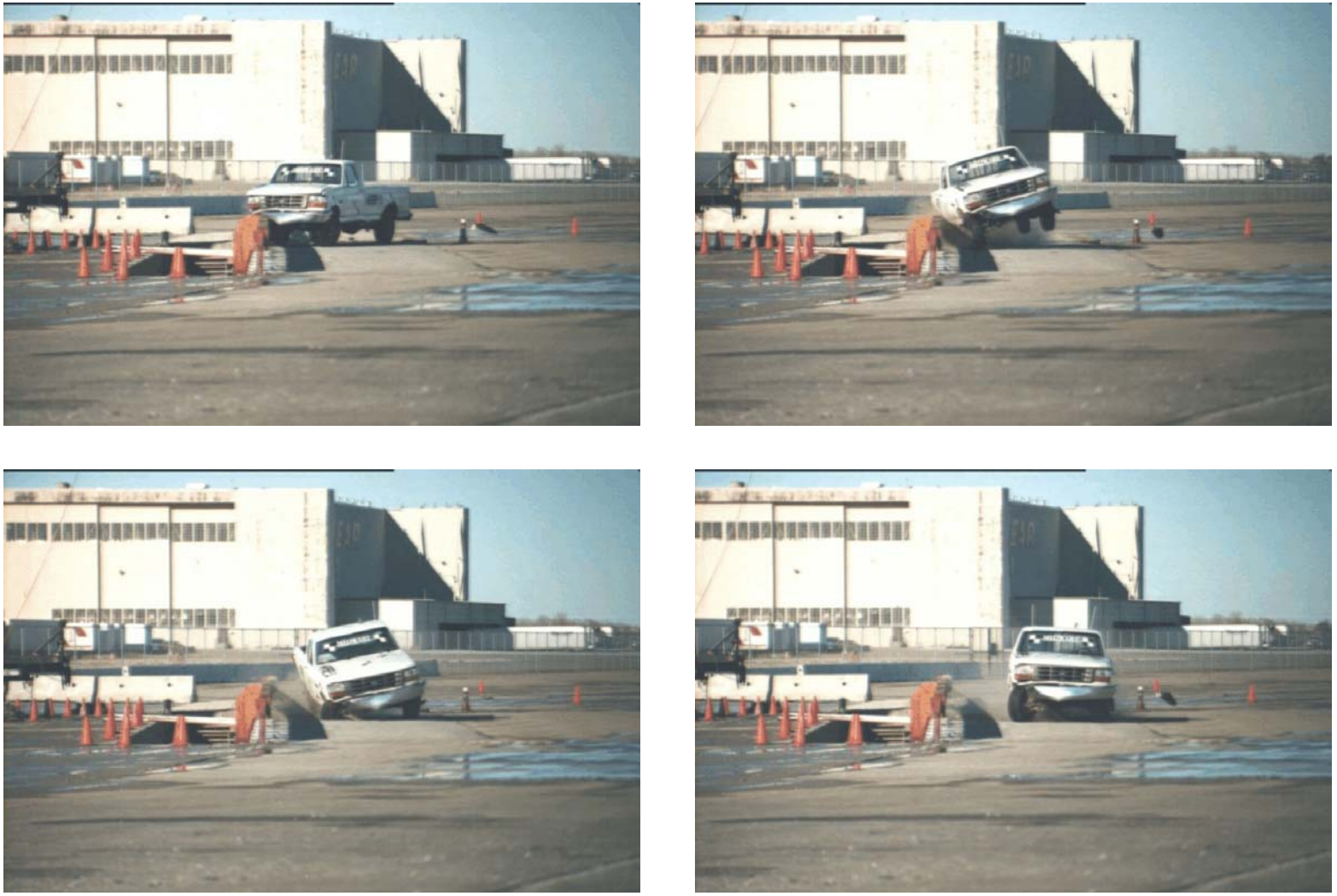

Figure 108. Documentary Photographs, Test WRBP-1

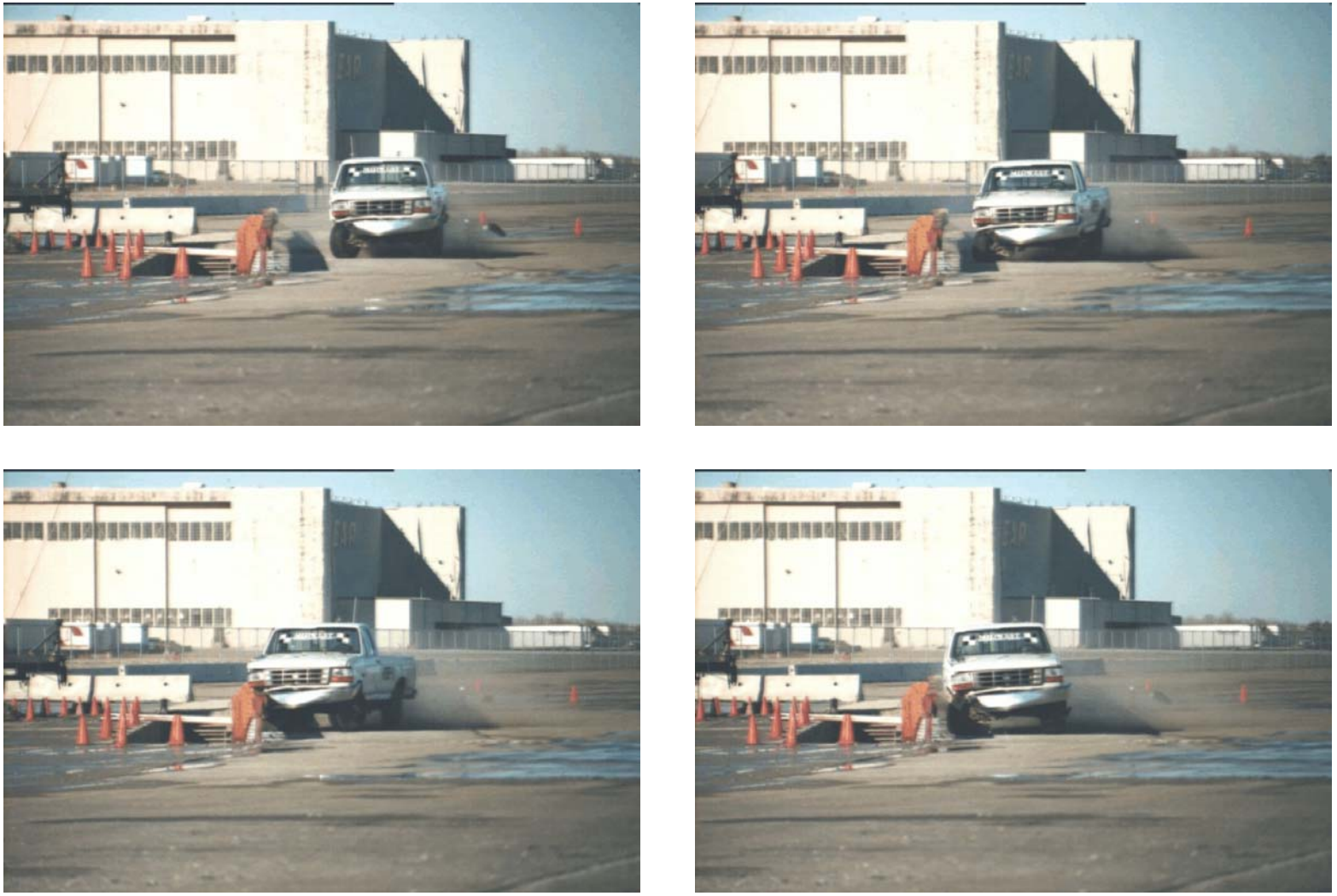

Figure 109. Documentary Photographs, Test WRBP-1

Figure 110. Documentary Photographs, Test WRBP-1

Figure 111. Impact Locations, Test WRBP-1

Figure 112. Final Vehicle Position and Trajectory Marks, Test WRBP-1

Figure 113. Barrier Damage, Test WRBP-1

Figure 114. Typical Post Damage, Test WRBP-1

Figure 115. Vehicle Damage, Test WRBP-1

Figure 116. Vehicle Damage, Test WRBP-1

Table 5. Strain Gauge and String Potentiometer Results, Test WRBP-1

Strain Gauge No.	Gauge Location	Maximum μ Strain[1] (mm/mm)	Maximum Stress[2] (MPa)	Comments
1	Top Plate No. 5	1238	256.1	Upstream bolt in row closest to post - perpendicular to rail
2	Top Plate No. 5	1243	257.0	Downstream bolt in row closest to post - perpendicular to rail
3	Top Plate No. 5	470	97.3	Most upstream bolt in row furthest from post - perpendicular to rail
4	Top Plate No. 5	55	11.4	Between gauges at upstream bolts in row furthest from post - perpendicular to rail
5	Top Plate No. 5	553	114.4	Upstream bolt near middle in row furthest from post - perpendicular to rail
6	Top Plate No. 5	802	165.9	Downstream bolt near middle in row furthest from post - perpendicular to rail
7	Top Plate No. 5	173	35.9	Between gauges at downstream bolts in row furthest from post - perpendicular to rail
8	Top Plate No. 5	601	124.3	Most downstream bolt in row furthest from post - perpendicular to rail
9	Top Plate No. 6	1991	Plate Yield	Upstream bolt in row closest to post - perpendicular to rail
10	Top Plate No. 6	1985	Plate Yield	Downstream bolt in row closest to post - perpendicular to rail
11	Top Plate No. 6	1924	Plate Yield	Most upstream bolt in row furthest from post - perpendicular to rail
12	Top Plate No. 6	459	94.9	Between gauges at upstream bolts in row furthest from post - perpendicular to rail
13	Top Plate No. 6	982	203.1	Upstream bolt near middle in row furthest from post - perpendicular to rail
14	Top Plate No. 6	900	186.1	Downstream bolt near middle in row furthest from post - perpendicular to rail
15	Top Plate No. 6	642	133.0	Between gauges at downstream bolts in row furthest from post - perpendicular to rail
16	Top Plate No. 6	836	172.9	Most downstream bolt in row furthest from post - perpendicular to rail
17	Top Plate No. 7	1397	228.9	Upstream bolt in row closest to post - perpendicular to rail
18	Top Plate No. 7	1993	Plate Yield	Downstream bolt in row closest to post - perpendicular to rail
19	Top Plate No. 7	450	93.2	Most upstream bolt in row furthest from post - perpendicular to rail
20	Top Plate No. 7	73	15.1	Between gauges at upstream bolts in row furthest from post - perpendicular to rail
21	Top Plate No. 7	334	69.1	Upstream bolt near middle in row furthest from post - perpendicular to rail
25	Bent Post Plate No. 6	554	114.6	Above slot on upstream side
26	Bent Post Plate No. 6	695	143.8	Above slot on downstream side

[1] - All strain values are shown as the absolute value only.
[2] - For plates, elastic stress values are shown as the absolute value only and calculated by multiplying the strain by the modulus of elasticity equal to 207,000 MPa (30,000 ksi). Minimum yield stress for the plates is 248 MPa (36 ksi).
NA - Not available or not applicable.

16 CRASH TEST NO. 2 (WOOD SYSTEM - APPROACH GUARDRAIL TRANSITION)

16.1 Test WRBP-2

The 2,011-kg pickup truck impacted the approach guardrail transition at a speed of 71.6 km/hr and at an angle of 26.3 degrees. A summary of the test results and the sequential photographs are shown in Figure 117. Additional sequential photographs are shown in Figures 118 and 119. Documentary photographs of the crash test are shown in Figures 120 and 121.

16.2 Test Description

Initial impact occurred between transition post nos. 2 and 3 or 238 mm downstream from transition post no. 3, as shown in Figures 122. At 0.015 sec, transition post nos. 2 and 3 rotated backward. At 0.020 sec after impact, the front bumper deformed extensively and was pushed toward the left side of the vehicle. At 0.041 sec, the right-front tire contacted the rail. At 0.061 sec, the deformed right-front corner of the vehicle was located at transition post no. 2 and a gap formed between the cab and the back of the hood. At 0.065 sec, the right-front corner of the hood extended over the rail. At 0.077 sec, the right-front fender deformed into the door. At 0.088 sec, the right-front corner of the vehicle was positioned at transition post no. 1 as the grill began to disengage from the truck. At 0.101 sec, the front fender snagged on the wood blockout at transition post no. 1. At 0.108 sec, redirection of the truck began. At 0.117 sec, the right-side door deformed. At 0.124 sec, the left-front tire became airborne. At 0.132 sec, the left-rear tire became airborne. At 0.147 sec, the left-front corner of the vehicle was located at bridge post no. 1 as the right-side headlight was dislodged. At 0.191 sec, the right-front tire became airborne. At 0.248 sec, the left-front corner of the vehicle was positioned at bridge post no. 2. At 0.261 sec after impact, the vehicle became parallel to the rail with a velocity of 55.9 km/hr. At 0.269 sec, the rear end of the truck contacted

the rail. At 0.274 sec, the right-front tire contacted the ground. At 0.277 sec, the right-rear corner of the box was located at transition post no. 3. At 0.281 sec, transition post no. 2 rotated backward due to the impact from the rear of the truck. At 0.324 sec, the right-rear corner of the box was located at transition post no. 2. At 0.329 sec, the grill completely detached from the truck. At 0.389 sec, the right-rear corner of the box was at transition post no. 1. The vehicle exited the bridge railing at a speed of approximately 54.6 km/hr and an angle of 3.5 degrees at 0.422 sec. At 0.432 sec, the left-front tire contacted the ground. At 0.616 sec, the left-rear tire contacted the ground. The vehicle's post-impact trajectory is shown in Figure 117. The vehicle came to rest against the traffic-side face of the system approximately 29.7-m downstream from impact, as shown in Figure 123.

16.3 Bridge Rail and Approach Guardrail Transition Damage

Damage to the approach guardrail transition and bridge railing was minimal, as shown in Figures 124 through 127. Damage consisted mostly of deformed thrie beam, displaced guardrail posts, and contact marks on a thrie beam section and wood rail section. The physical damage to the thrie beam rail was found between transition post no. 3 and bridge post no. 1, as shown in Figure 124. The thrie beam damaged consisted of moderate deformation and flattening of the impacted section of rail between transition post nos. 2 and 3. A 127-mm long gouge was found in the lower corrugation at the impact location. Contact marks were found on the guardrail from 187-mm downstream of transition post no. 3 through bridge post no. 1. Contact marks were also found on the blockouts at transition post nos. 1 and 2. Minor scrape marks were found on the top of a wood bridge rail section from the upstream end of the rail to bridge post no. 1.

No contact marks nor damage was observed on the transition posts, but movement of the posts was evident by the 13-mm, 13-mm, and 3-mm soil gaps at the front faces of transition post

nos. 2, 3, and 4, respectively. A 13-mm soil gap was also found at the back face of transition post no. 2. Transition post no. 1 and 5 through 15 along with all the bridge posts did not move. No significant system damage occurred upstream of transition post no. 4 nor downstream of bridge post no. 1.

The maximum lateral permanent set deflections for rail and post locations, as determined from field measurements in the impact region, were approximately 29 mm at transition post no. 2. The maximum dynamic lateral deflections for rail and post locations, as determined from high-speed film analysis, were 125 mm and 109 mm at transition post no.2, respectively. The effective coefficient of friction was determined to be approximately 0.26.

16.4 Vehicle Damage

Exterior vehicle damage was moderate, as shown in Figures 128 and 129. Vehicle damage occurred to several body locations, such as right-side door and quarter panels, front and rear bumpers, right-side wheels and rims, steel frame and suspension, and windshield. The right corner of the rear bumper was deformed inward, and the box was twisted, as shown in Figure 128. The right-front quarter panel was crushed inward and downward, as shown in Figures 128 and 129. Contact marks from interaction with the wood bridge rail were on the right-front quarter panel and door. The right-side door was also deformed and was ajar at the top. The right-side of the front bumper was deformed inward while the entire bumper was shifted toward the vehicle's left side, as shown in Figure 128 and 129. The right-front wheel assembly was deformed toward the firewall, and the lower cast suspension member fractured at the inner connection. The right-front tire disengaged from the steel rim which was severely deformed. The grill disengaged from the truck. The right-side headlight assembly was damaged severely. Minor cracking was observed in the

lower-right side of the front windshield. There was no intrusion nor deformation of the occupant compartment.

16.5 Occupant Risk Values

The longitudinal and lateral occupant impact velocities were determined to be 4.43 m/sec and 6.42 m/sec, respectively. The maximum 0.010-sec average occupant ridedown decelerations in the longitudinal and lateral directions were 5.51 g's and 9.74 g's, respectively. It is noted that the occupant impact velocities and occupant ridedown decelerations were within the suggested limits provided in NCHRP Report No. 350. The results of the occupant risk, determined from accelerometer data, are summarized in Figure 117. Results are shown graphically in Appendix O. Due to technical difficulties, the rate transducer did not collect the roll, pitch, and yaw data. However, the roll, pitch, and yaw data were collected from film analysis and are shown graphically in Appendix P.

16.6 Discussion

The analysis of the test results for test WRBP-2 showed that the approach guardrail transition attached to a glulam bridge rail adequately contained and redirected the vehicle with controlled lateral displacement of the guardrail transition. There were no detached elements nor fragments which showed potential for penetrating the occupant compartment or presented undue hazard to other traffic. Deformations of, or intrusion into, the occupant compartment that could have caused serious injury did not occur. The test vehicle did not penetrate nor ride over the approach guardrail transition and remained upright both during and after the collision. Vehicle roll, pitch, and yaw angular displacements were noted, but they were deemed acceptable. After collision, the vehicle's trajectory revealed minimum intrusion into adjacent traffic lanes. In addition, the vehicle's exit

angle was less than 60 percent of the impact angle. Therefore, test WRBP-2 conducted on the approach guardrail transition attached to a glulam bridge rail system was determined to be acceptable according to the TL-2 safety performance criteria provided in NCHRP Report No. 350.

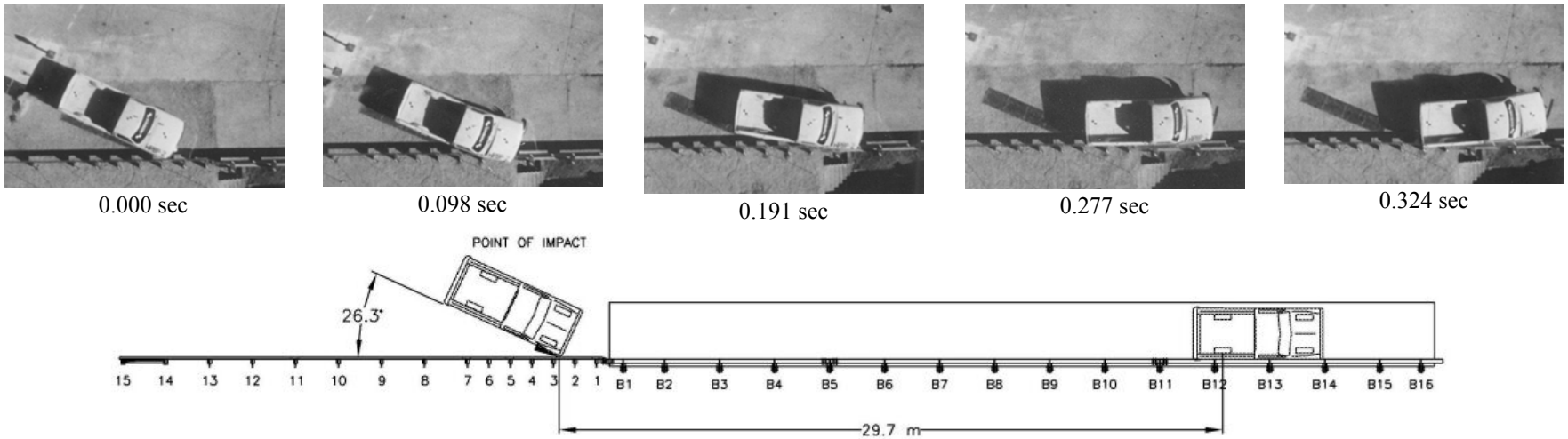

- Test Number WRBP-2
- Date 2/03/00
- Appurtenance . . . . . Approach Guardrail Transition attached to a Wood Bridge Rail System for Transverse Decks
- Total Length . . . . . 24.77 m
- Steel W-Beam Rail (Nested)
  - Thickness . . . . . 2.66 mm
  - Top Mounting Height . . . . . 706 mm
- Steel W-Beam Rail
  - Thickness . . . . . 2.66 mm
  - Top Mounting Height . . . . . 706 mm
- Steel Posts
  - Post Nos. 1 -5 . . . . . W152x13.4 by 2,134-mm long
  - Post Nos. 6 - 7 . . . . . W152x13.4 by 1,981-mm long
  - Post Nos. 8 - 13 . . . . . W152x13.4 by 1,829-mm long
- Wood Posts
  - Post Nos. 14 - 15 (BCT) . . . . . 140 mm x 190 mm by 1,080 mm long
- Wood Spacer Blocks
  - Post Nos. 1 - 13 . . . . . 152 mm x 203 mm by 368-mm long
- Vehicle Model . . . . . 1993 Ford F-250 ¾-Ton Pickup Truck
  - Curb . . . . . 2,092 kg
  - Test Inertial . . . . . 2,011 kg
  - Gross Static . . . . . 2,011 kg
- Vehicle Speed
  - Impact . . . . . 71.6 km/hr
  - Exit . . . . . 54.6 km/hr
- Vehicle Angle
  - Impact . . . . . 26.3 deg
  - Exit . . . . . 3.5 deg
- Vehicle Snagging . . . . . None
- Vehicle Stability . . . . . Satisfactory
- Effective Coefficient of Friction (μ) 0.26
- Occupant Ridedown Deceleration (10 msec avg.)
  - Longitudinal . . . . . 5.51 < 20 G's
  - Lateral (not required) 9.74
- Occupant Impact Velocity
  - Longitudinal . . . . . 4.43 < 12 m/s
  - Lateral (not required) 6.42
- Vehicle Damage . . . . . Moderate
  - TAD[32] 1-RFQ-3/1-RD-2
  - SAE[33] 01-RDES3
- Vehicle Stopping Distance . . . . . 29.7 m downstream
  0.0 m lateral
- Barrier Damage . . . . . Minor
- Maximum Deflections
  - Permanent Set . . . . . 29 mm
  - Dynamic . . . . . 125 mm

Figure 117. Summary of Test Results and Sequential Photographs, Test WRBP-2

0.000 sec

0.237 sec

0.041 sec

0.368 sec

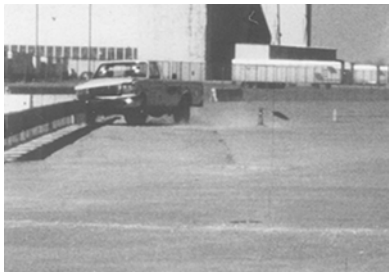

0.088 sec

0.531 sec

0.135 sec

0.711 sec

Figure 118. Additional Sequential Photographs, Test WRBP-2

0.000 sec

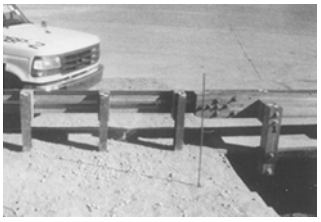

0.000 sec

0.065 sec

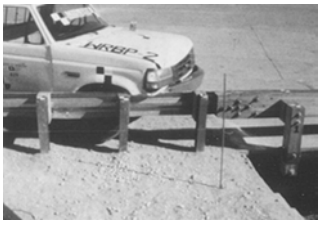

0.062 sec

0.130 sec

0.101 sec

0.195 sec

0.167 sec

0.314sec

0.272 sec

Figure 119. Additional Sequential Photographs, Test WRBP-2

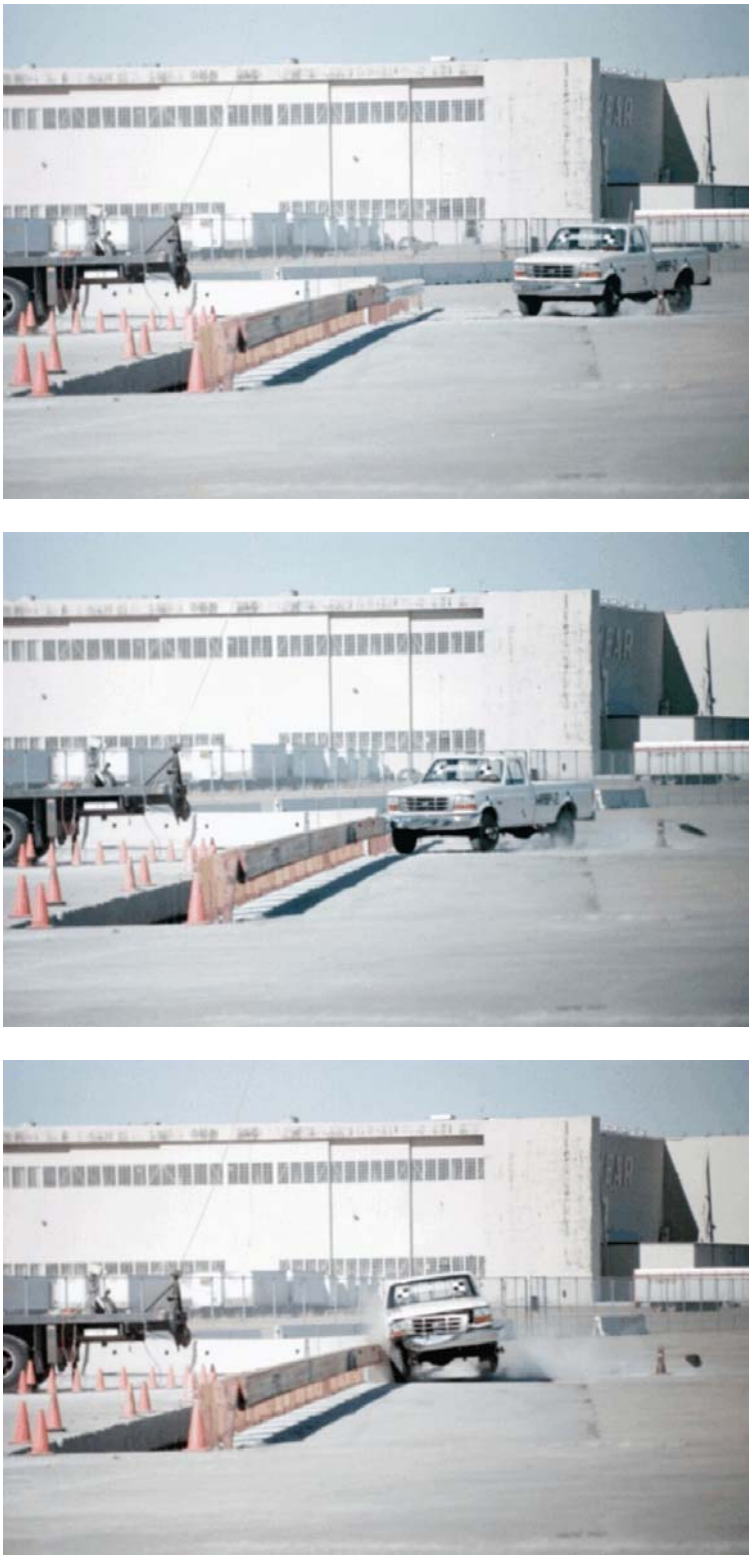

Figure 120. Documentary Photographs, Test WRBP-2

Figure 121. Documentary Photographs, Test WRBP-2

Figure 122. Impact Locations, Test WRBP-2

Figure 123. Final Vehicle Position, Test WRBP-2

Figure 124. Barrier Damage, Test WRBP-2

Figure 125. Barrier Damage, Test WRBP-2

Figure 126. Barrier Damage, Test WRBP-2

Figure 127. Permanent Set Deflections, Test WRBP-2

Figure 128. Vehicle Damage, Test WRBP-2

Figure 129. Vehicle Damage, Test WRBP-2

17 SUMMARY AND CONCLUSIONS - WOOD SYSTEM

A wood bridge railing system and an attached approach guardrail transition system were successfully developed and crash tested for use on transverse glulam timber deck bridges. Two full-scale vehicle crash tests - one on the bridge railing and one on the approach guardrail transition - were performed and determined to have acceptable safety performance according to TL-2 of NCHRP Report No. 350 (3). A summary of the safety performance evaluations for both crash tests are provided in Table 6.

As previously mentioned, prior to the development of this wood bridge railing system, no other TL-2 railing systems had been developed for use on transverse glulam timber deck bridges except for the steel bridge railings system developed within the scope of this study. However, this research program clearly demonstrates that crashworthy wood railing systems are feasible for use on these types of bridges. The development of the wood bridge railing and transition system addressed the concerns for aesthetics, economy, material availability, ease of construction, and reasonable margin of structural adequacy. In addition, the wood bridge railing and transition systems were relatively easy to install and should have reasonable construction labor costs. This wood railing system should also be adaptable to: (1) other transverse glulam timber deck bridges with thicknesses equal to or greater than 130 mm and with little or no modification; (2) longitudinal glulam timber deck bridges where sufficient deck strength is provided to resist the lateral impact forces; and (3) bridges supporting reinforced concrete decks that are capable of meeting the same lateral impact load requirements.

No significant damage to the test bridge was evident from the vehicle impact tests. For the wood bridge railing system, damage consisted primarily of rail gouging and scraping, as well as

permanent set deformations of the steel deck mounting plates. All glulam timber railings remained intact and serviceable after the tests. Thus, railing replacement would not be considered necessary except to provide improved aesthetics. For the approach guardrail transition system, damage consisted primarily of deformed W-beam rail and displaced guardrail posts. Although visual permanent set deformations of the W-beam rail were found in the vicinity of the impact, the rail remained intact and serviceable after the test. Thus, replacement of the guardrail would be based more on aesthetics than on structural integrity.

Therefore, the successful completion of this phase of the research project resulted in a TL-2 wood bridge railing and approach guardrail transition system having acceptable safety performance and meeting current crash test safety standards.

Table 6. NCHRP Report No. 350 TL-2 Evaluation Results - Wood System (Bridge Railing and Transition)

Evaluation Factors	Evaluation Criteria		Test No.	
			WRBP-1	WRBP-2
Structural Adequacy	A.	Test article should contain and redirect the vehicle; the vehicle should not penetrate, underride, or override the installation although controlled lateral deflection of the test article is acceptable.	S	S
Occupant Risk	D.	Detached elements, fragments or other debris from the test article should not penetrate or show potential for penetrating the occupant compartment, or present an undue hazard to other traffic, pedestrians, or personnel in a work zone. Deformations of, or intrusions into, the occupant compartment that could cause serious injuries should not be permitted.	S	S
	F.	The vehicle should remain upright during and after collision although moderate roll, pitching, and yawing are acceptable.	S	S
Vehicle Trajectory	K.	After collision it is preferable that the vehicle's trajectory not intrude into adjacent traffic lanes.	S	S
	L.	The occupant impact velocity in the longitudinal direction should not exceed 12 m/s and the occupant ridedown acceleration in the longitudinal direction should not exceed 20 g's.	S	S
	M.	The exit angle from the test article preferably should be less than 60 percent of test impact angle, measured at time of vehicle loss of contact with test devise.	S	S

S - Satisfactory
M - Marginal
U - Unsatisfactory
NR - Not Required

18 RECOMMENDATIONS

As stated previously, both the steel and wood bridge railing systems for use with transverse timber deck bridges were instrumented with sensors on key components of the railing systems in an attempt to measure the actual forces imparted into the bridge deck. The researchers deemed that the dynamic load information was necessary because additional economy could be provided by down-sizing specific structural components. Following the analysis of the crash test and instrumentation results, it was determined that the bridge railing and transition systems performed well as designed, and that no design changes were necessary. Finally, it is recommended that FHWA approve the TL-2 steel bridge railing and approach guardrail transition systems and the TL-2 wood bridge railing and approach guardrail transition systems for use on Federal-aid highways.

For the steel system, eight 22-mm diameter ASTM A307 bolts were used to attach the steel mounting plates to the top and bottom surfaces of the timber deck. Measured strain readings on the plates near the outer bolt locations were found to be significantly lower than those observed near the central bolt locations. In addition, no bearing deformations of the deck mounting plates and vertical bolts, nor damage to the timber deck near the shear connectors, was found. Therefore, the researchers believed that the TL-2 steel bridge railing system would have performed in a acceptable manner if each deck plate had been attached with only six vertical bolts instead of eight. It is noted that strain gauge results were used similarly when the number of vertical bolts was reduced in the TL-4 steel bridge railing system (1). However, for a reduction of two vertical bolts, there exists the potential for a slight increase in deck damage as well as increased difficulty in removing and repairing the plates and bolts following an impact.

For the wood system, six 22-mm-diameter ASTM A307 bolts were used to attach the steel

mounting plates to the top and bottom surfaces of the timber deck. For the three top plates that were instrumented, measured strain readings showed that the load was better distributed throughout each plate and to all six of the vertical bolts. Thus, no design changes were believed to be necessary.

19 REFERENCES

1. Polivka, K.A., Faller, R.K., Rosson, B.T., Fowler, M.D., Keller, E.A. *Two Test Level 4 Bridge Railing and Transition Systems for Transverse Glue-Laminated Timber Decks*, Report Submitted to the United States Department of Agriculture-Forest Service-Forest Products Laboratory, Transportation Report No. TRP-03-71-01, Performed by the Midwest Roadside Safety Facility, Civil Engineering Department, University of Nebraska-Lincoln, January 2002.

2. Faller, R.K., Ritter, M.A., Rosson, B.T., Fowler, M.D., and Duwadi, S.R., *Two Test Level 4 Bridge Railing and Transition Systems for Transverse Timber Deck Bridges*, Transportation Research Record No. 1696, Transportation Research Board, National Research Council, Washington, D.C., 2000.

3. Ross, H.E., Sicking, D.L., Zimmer, R.A. and Michie, J.D., *Recommended Procedures for the Safety Performance Evaluation of Highway Features*, National Cooperative Highway Research Program (NCHRP) Report No. 350, Transportation Research Board, Washington, D.C., 1993.

4. *Guide Specifications for Bridge Railings*, American Association of State Highway and Transportation Officials, Washington, D.C., 1989.

5. Faller, R.K., Ritter, M.A., Holloway, J.C., Pfeifer, B.G., and B.T. Rosson, *Performance Level 1 Bridge Railings for Timber Decks*, Transportation Research Record No. 1419, Transportation Research Board, National Research Council, Washington D.C., 1993.

6. Ritter, M.A., Lee, P.D.H., Faller, R.K., Rosson, B.T., and S.R. Duwaldi, *Plans for Crash Tested Bridge Railings for Longitudinal Wood Decks*, General Technical Report No. FPL-GTR-87, United States Department of Agriculture, Forest Service, Forest Products Laboratory, Madison, Wisconsin, September 1995.

7. Ritter, M.A. and R.K. Faller, *Crashworthy Bridge Railings for Longitudinal Wood Decks*, Paper presented by Ritter at the 1994 Pacific Timber Engineering Conference, Gold Coast, Australia, July 11-15, 1994.

8. Ritter, M.A., Faller, R.K., and Duwaldi, S.R., *Crash-Tested Bridge Railings for Timber Bridges*, Presented by Ritter at the Fourth International Bridge Engineering Conference, Volume 2, Conference Proceedings 7, San Francisco, California, August 28-30, 1995, Transportation Research Board, Washington, D.C., August 1995.

9. Faller, R.K., Rosson, B.T., Ritter, M.A., Lee, P.D.H., and Duwadi, S.R., *Railing Systems for Longitudinal Timber Deck Bridges*, Presented at the National Conference on Wood Transportation Structures, Madison, Wisconsin, October 23-25, 1996, General Technical Report No. FPL-GTR-94, United States Department of Agriculture - Forest Service - Forest Products Laboratory and Federal Highway Administration, October 1996.

10. Rosson, B.T., Faller, R.K., and M.A. Ritter, *Performance Level 2 and Test Level 4 Bridge Railings for Timber Decks*, Transportation Research Record No. 1500, Transportation Research Board, National Research Council, Washington D.C., 1995.

11. Faller, R.K., Rosson, B.T., Ritter, M.A., and Sicking, D.L., *Design and Evaluation of Two Low-Volume Bridge Railings*, Presented at the Sixth International Conference on Low-Volume Roads, Volume 2, Conference Proceedings 6, University of Minnesota, Minneapolis, Minnesota, June 25-29, 1995, Transportation Research Board, Washington, D.C., June 1995.

12. Ritter, M.A., Faller, R.K., Sicking, D.L., and Bunnell, S., *Development of Low-Volume Curb-Type Bridge Railings for Timber Bridge Decks*, Draft Report Submitted to the United Sates Department of Agriculture-Forest Service-Forest Products Laboratory, Transportation Report No. TRP-03-31-93, Midwest Roadside Safety Facility, University of Nebraska-Lincoln, December 1993.

13. Faller, R.K., Soyland, K., Rosson, B.T., Stutzman, T.M., *TL-1 Curb-Type Bridge Railing for Longitudinal Glulam Timber Decks Located on Low-Volume Roads*, Draft Report Submitted to the United States Department of Agriculture-Forest Service-Forest Products Laboratory, Transportation Research Report No. TRP-03-54-96, Performed by the Midwest Roadside Safety Facility, Civil Engineering Department, University of Nebraska-Lincoln, April 1996.

14. Faller, R.K., Rosson, B.T., and Fowler, M.D., *Top-Mounted W-Beam Bridge Railing for Longitudinal Glulam Timber Decks Located on Low-Volume Roads*, Draft Report Submitted to the United Sates Department of Agriculture-Forest Service-Forest Products Laboratory, Transportation Report No. TRP-03-61-96, Midwest Roadside Safety Facility, University of Nebraska-Lincoln, September 1996.

15. Faller, R.K., and Rosson, B.T., *Development of a Flexible Bridge Railing for Longitudinal Timber Decks*, Draft Report Submitted to the United Sates Department of Agriculture-Forest Service-Forest Products Laboratory, Transportation Report No. TRP-03-62-96, Midwest Roadside Safety Facility, University of Nebraska-Lincoln, June 1997.

16. Ritter, M.A., Faller, R.K., Bunnell, S., Lee, P.D.H., and Rosson, B.T. *Plans for Crash-Tested Railings for Longitudinal Wood Decks on Low-Volume Roads.* General Technical Report No. FPL-GTR-107, United States Department of Agriculture, Forest Service, Forest Products Laboratory, Madison, Wisconsin, September 1998.

17. Faller, R.K., Rosson, B.T., Ritter, M.A., and Duwadi, S.R. *Railing Systems for Use on Timber Deck Bridges.* Transportation Research Record No. 1656, Transportation Research Board, National Research Council, Washington D.C., 1999.

18. Fowler, M.D. *Design and Testing of a Test Level 4 Bridge Railing for Transverse Glulam Timber Deck Bridges*. M.S. Thesis. University of Nebraska, Lincoln, 1997.

19. Ritter, M.A., Faller, R.K., Lee, P.D.H., Rosson, B.T., and Duwadi, S.R. *Plans for Crash-Tested Wood Bridge Railings for Concrete Decks*. General Technical Report FPL-GTR-108. USDA Forest Service, 1998.

20. Hancock, K.L., Hansen, A.G. and J.B. Mayer, *Aesthetic Bridge Rails, Transitions, and Terminals for Park Roads and Parkways*, Report No. FHWA-RD-90-052, Submitted to the Office of Safety and Traffic Operations R&D, Federal Highway Administration, Performed by the Scientex Corporation, May 1990.

21. Raju, P.R., GangaRao, H.V.S., Mak, K.K. and D.C. Alberson, *Timber Bridge Rail Testing and Evaluation: Timber Bridge Rail, Posts, and Deck on Steel Stringers*, Final Report, Volume 1, Constructed Facilities Center, West Virginia University, Morgantown, WV, October 1993.

22. Raju, P.R., GangaRao, H.V.S., Mak, K.K. and D.C. Alberson, *Timber Bridge Rail and Transition Rail Testing and Evaluation: Glulam Bridge Rail and Deck on Glulam Stringers*, Final Report, Volume 2, Constructed Facilities Center, West Virginia University, Morgantown, WV, October 1993.

23. Raju, P.R., GangaRao, H.V.S., Mak, K.K. and D.C. Alberson, *Timber Bridge Rail and Transition Rail Testing and Evaluation: W-Beam Steel Rail, Timber Posts and Glulam Deck on Steel Stringers*, Final Report, Volume 3, Constructed Facilities Center, West Virginia University, Morgantown, WV, October 1993.

24. Raju, P.R., GangaRao, H.V.S., Duwaldi, S.R. and H.K. Thippeswamy, *Development and Testing of Timber Bridge and Transition Rails for Transverse Glued-Laminated Bridge Decks*, Transportation Research Record No. 1460, Transportation Research Board, National Research Council, Washington D.C., 1994.

25. Buth, C.E., Campise, W.L., Griffin, III, L.I., Love, M.L., and Sicking, D.L., *Performance Limits of Longitudinal Barrier Systems - Volume I - Summary Report*, Report No. FHWA/RD-86/153, Submitted to the Office of Safety and Traffic Operations, Federal Highway Administration, Performed by Texas Transportation Institute, May 1986.

26. Ivey, D.L., Robertson, R., and Buth, C.E., *Test and Evaluation of W-Beam and Thrie-Beam Guardrails*, Report No. FHWA/RD-82/071, Submitted to the Office of Research, Federal Highway Administration, Performed by Texas Transportation Institute, March 1986.

27. Ross, H.E., Jr., Perera, H.S., Sicking, D.L., and Bligh, R.P., *Roadside Safety Design for Small Vehicles*, National Cooperative Highway Research Program (NCHRP) Report No. 318, Transportation Research Board, Washington, D.C., May 1989.

28. *American Wood-Preservers' Association Book of Standards*, American Wood-Preservers' Association, Woodstock, Md., 1991.

29. Hinch, J., Yang, T-L, and Owings, R., *Guidance Systems for Vehicle Testing*, ENSCO, Inc., Springfield, VA, 1986.

30. *Center of Gravity Test Code - SAE J874 March 1981*, SAE Handbook Vol. 4, Society of Automotive Engineers, Inc., Warrendale, Pennsylvania, 1986.

31. Powell, G.H., *BARRIER VII: A Computer Program For Evaluation of Automobile Barrier Systems*, Prepared for: Federal Highway Administration, Report No. FHWA RD-73-51, April 1973.

32. *Vehicle Damage Scale for Traffic Investigators*, Second Edition, Technical Bulletin No. 1, Traffic Accident Data (TAD) Project, National Safety Council, Chicago, Illinois, 1971.

33. *Collision Deformation Classification - Recommended Practice J224 March 1980*, Handbook Volume 4, Society of Automotive Engineers (SAE), Warrendale, Pennsylvania, 1985.

20 APPENDICES

APPENDIX A

Strain Gauge Locations – Test STCR-1

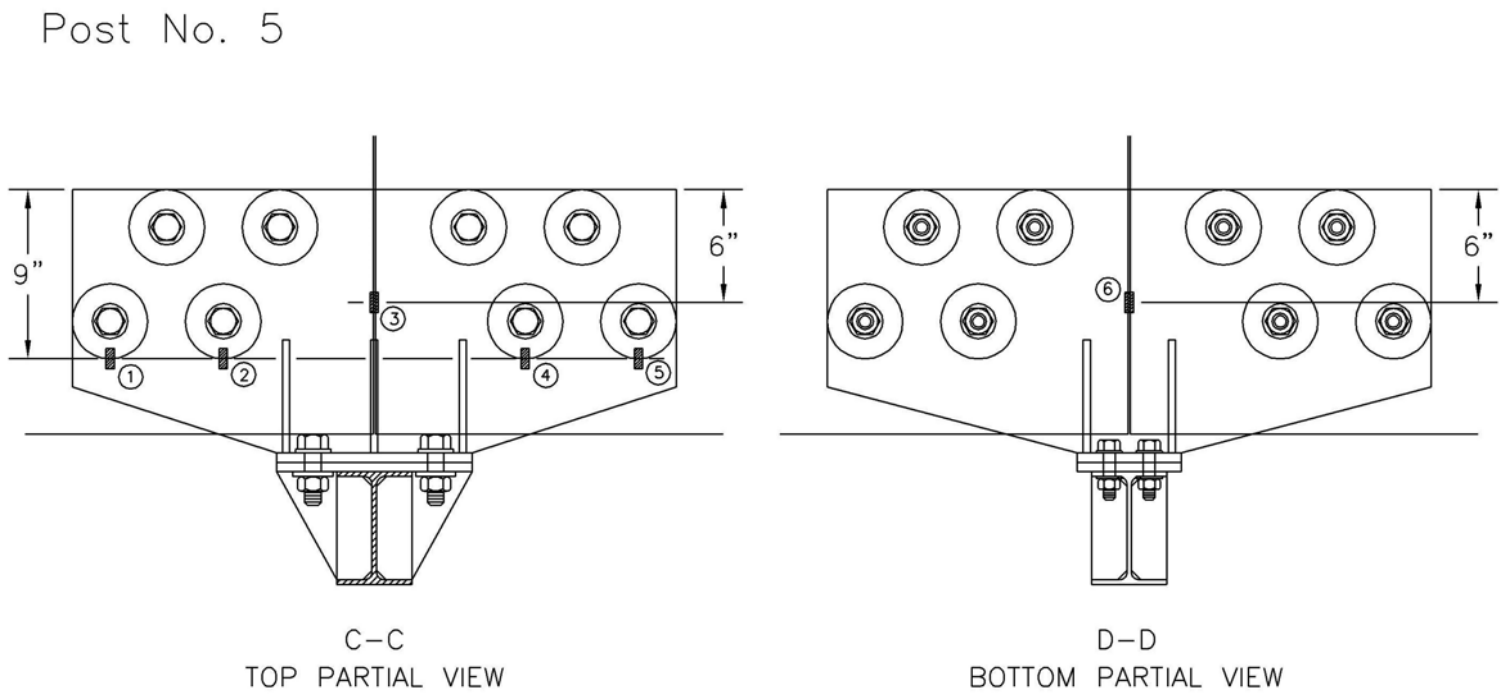

Figure A-1. Strain Gauge Nos. 1 through 6 Locations, Test STCR-1

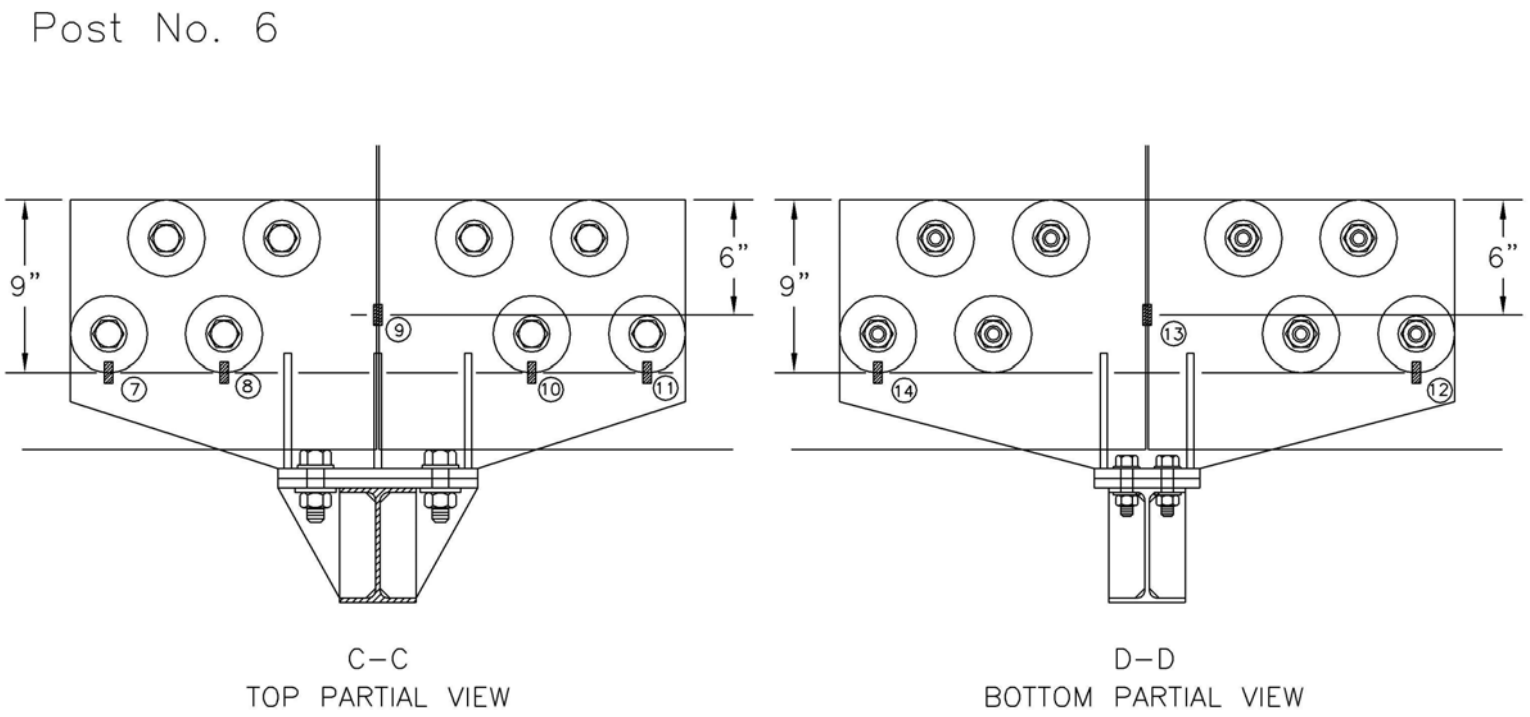

Figure A-2. Strain Gauge Nos. 7 through 16 Location, Test STCR-1

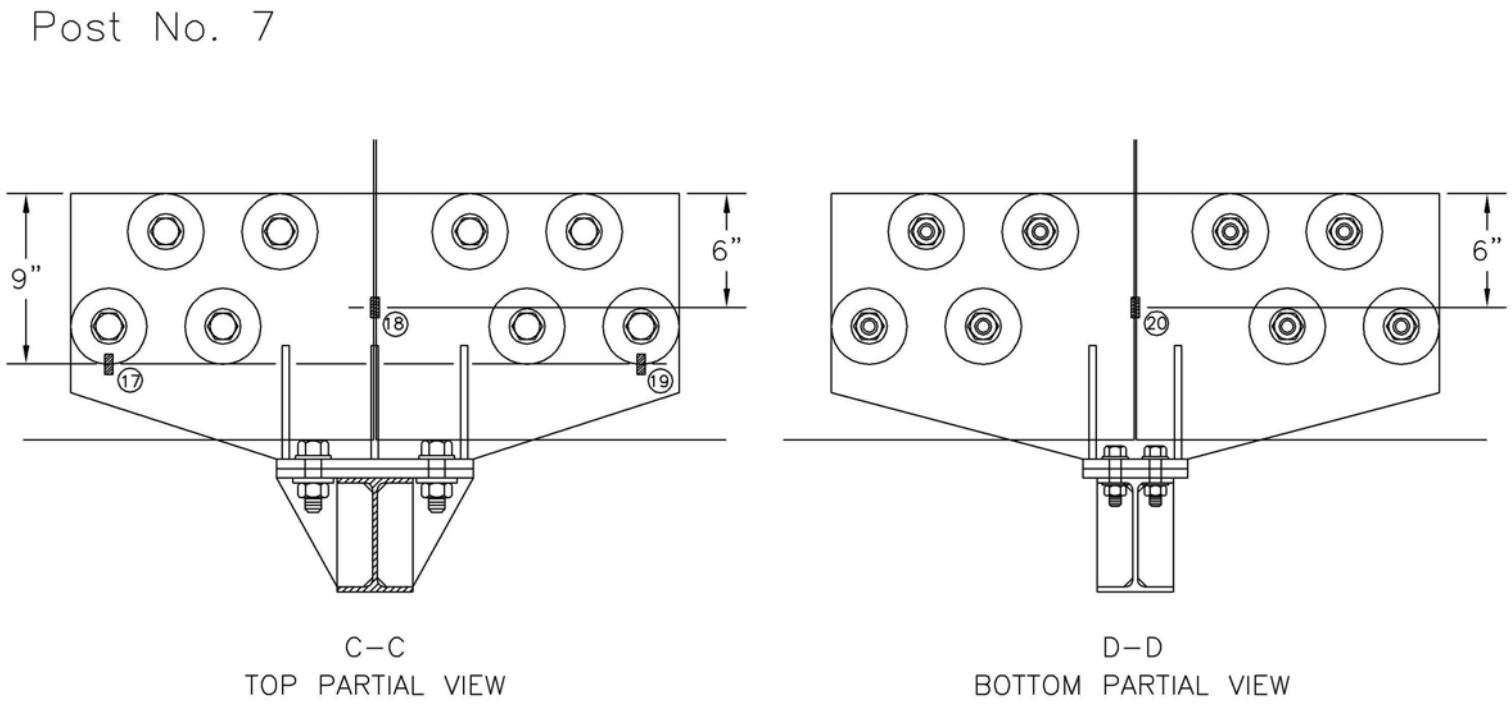

Figure A-3. Strain Gauge Nos. 17 through 20 Locations, Test STCR-1

APPENDIX B

Strain Gauge Locations – Test WRBP-1

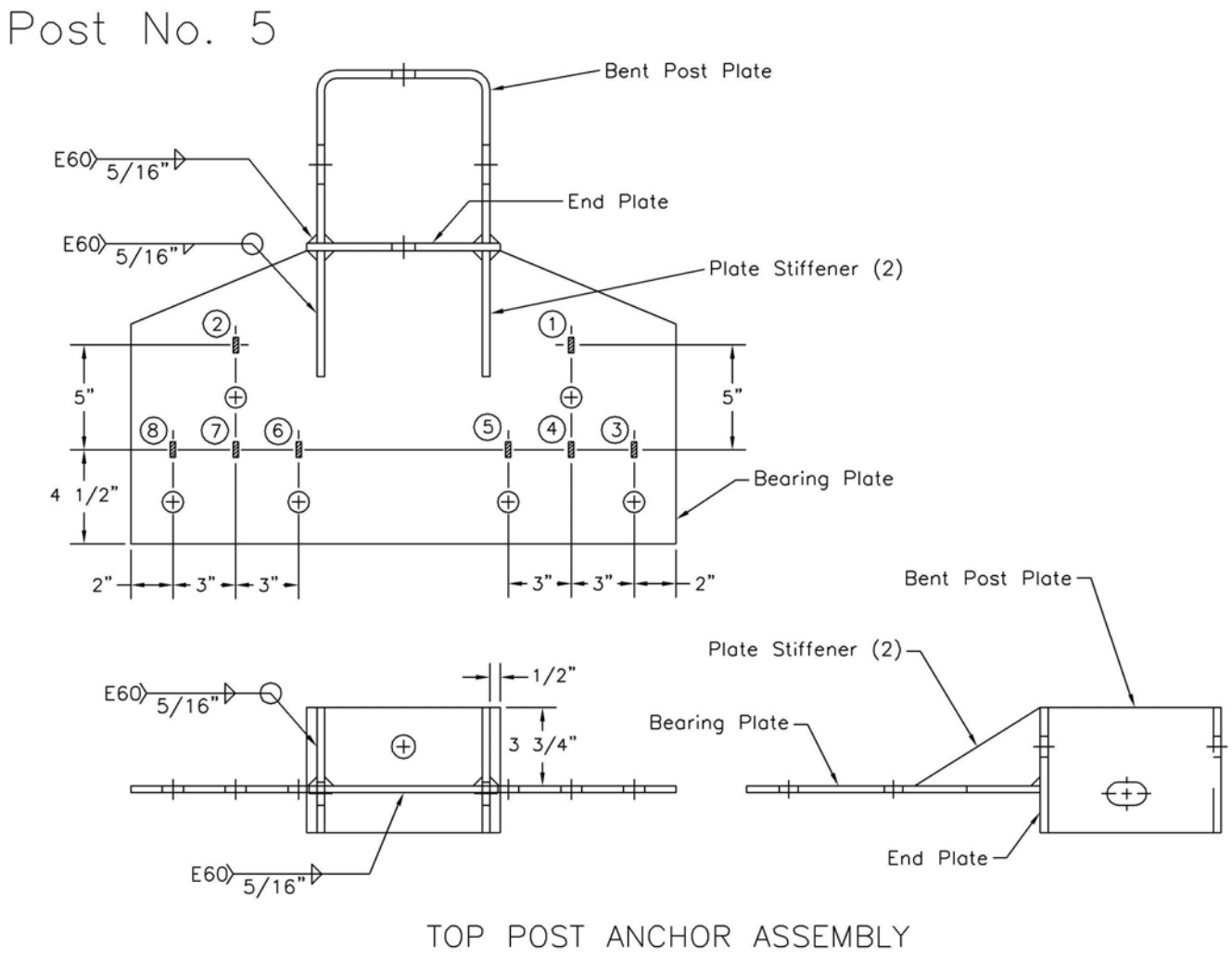

Figure B-1. Strain Gauge Nos. 1 through 8 Locations, Test WRBP-1

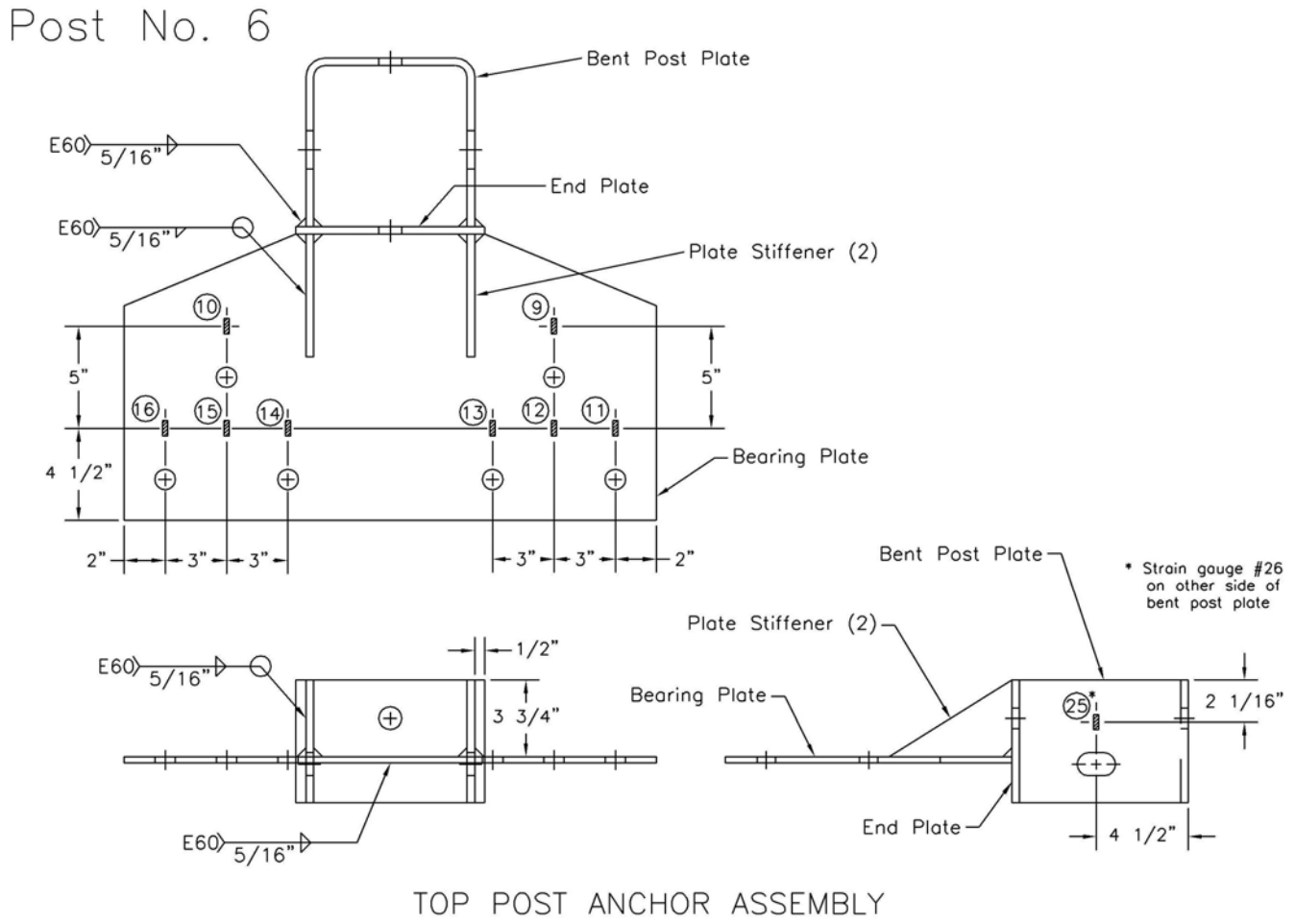

Figure B-2. Strain Gauge Nos. 9 through 16 and 25 through 26 Locations, Test WRBP-1

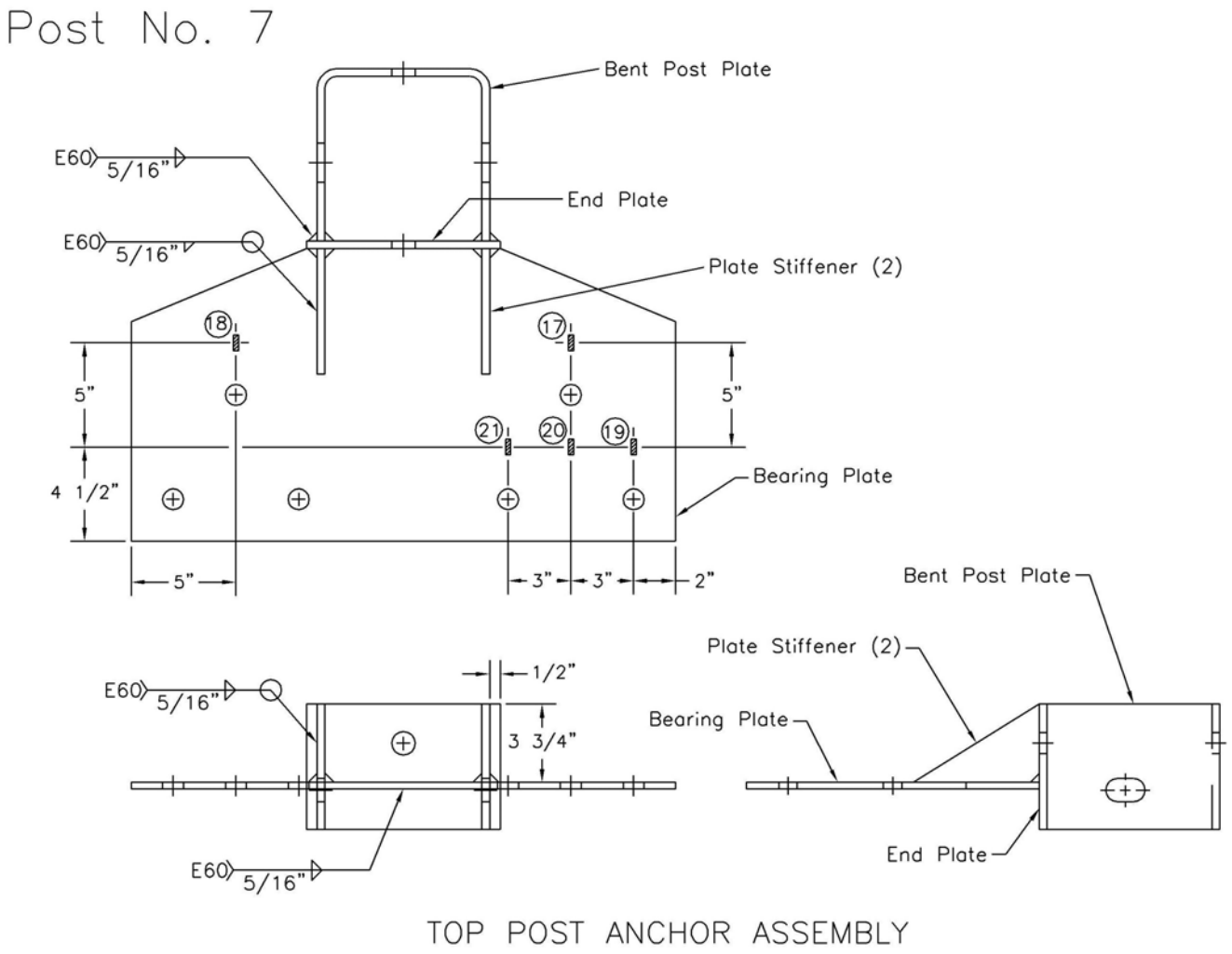

Figure B-3. Strain Gauge Nos. 17 through 21 Locations, Test WRBP-1

APPENDIX C

BARRIER VII Computer Models - Steel System

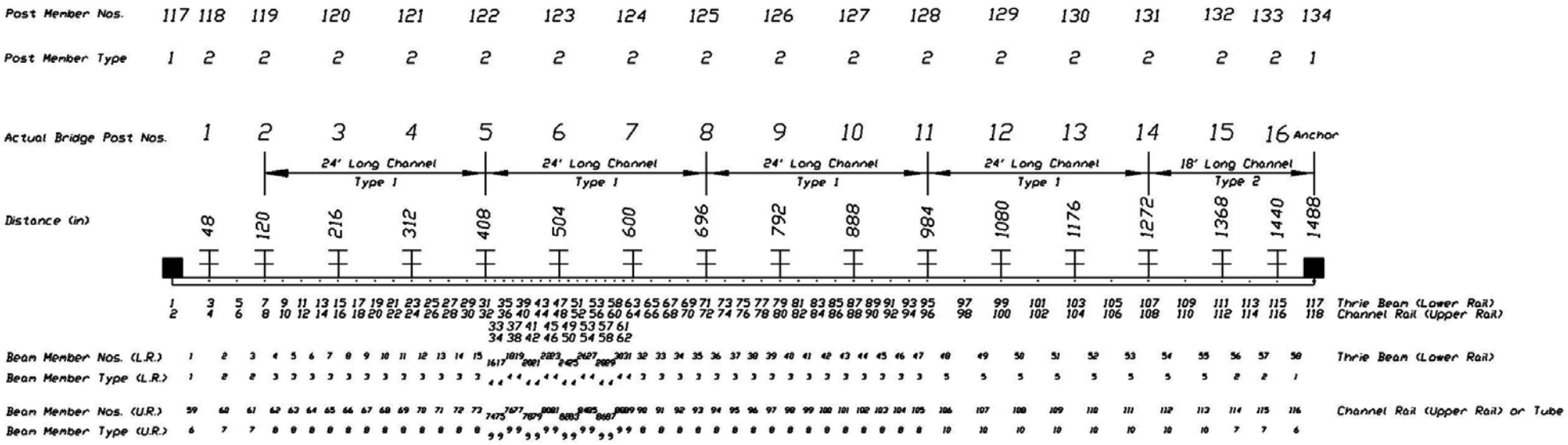

Figure C-1. Model of the Steel Bridge Railing System

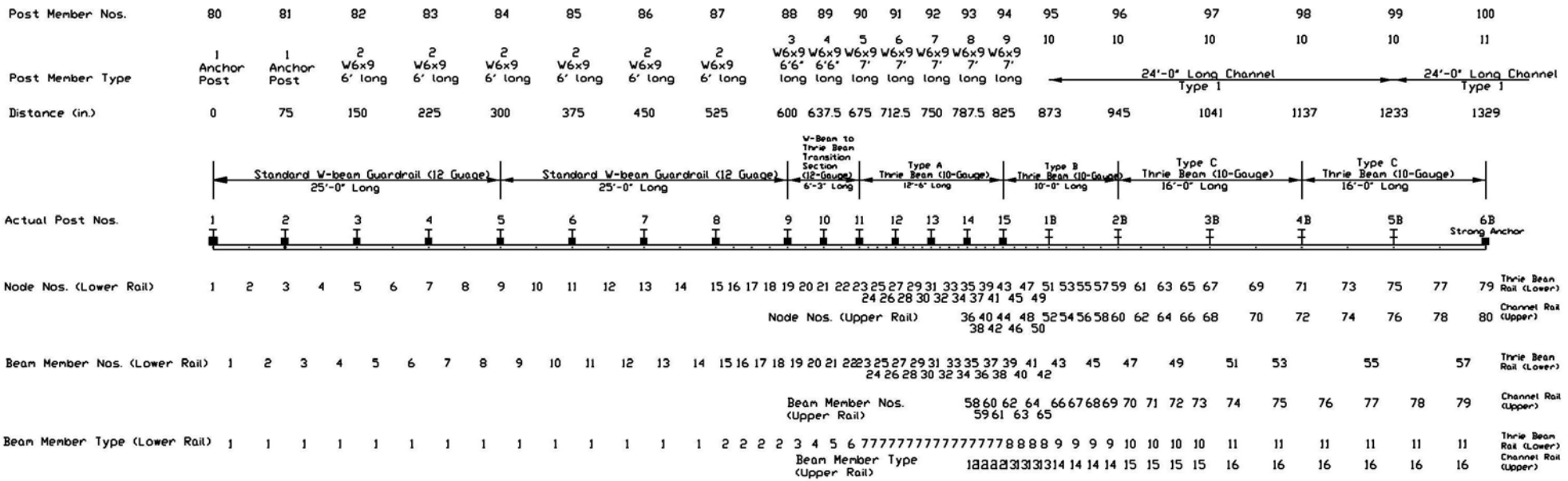

Figure C-2. Model of the Approach Guardrail System attached to the Steel Bridge Railing

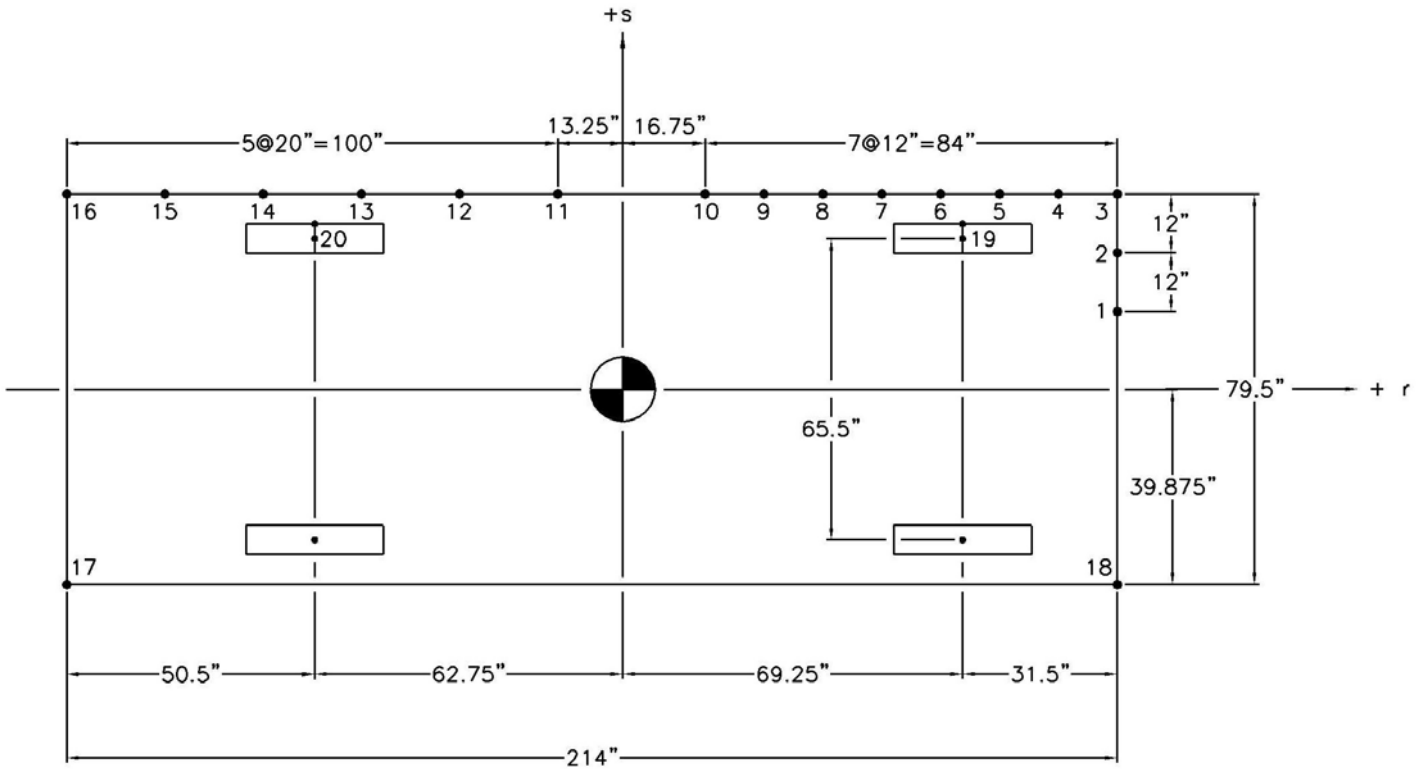

Figure C-3. Idealized Finite Element, 2 Dimensional Vehicle Model for the 2,000-kg Pickup Truck

APPENDIX D

Typical BARRIER VII Input Data Files - Steel System

Note that the example BARRIER VII input data files included in Appendix D corresponds with the critical impact point for tests STCR-1 and STCR-2, respectively.

```
USFS TL-2 STEEL BRIDGE RAIL (TRANSVERSE DECK PROJECT) - RUN11C - NODE 35/36 (10-GA. THRIE BEAM AND CHANNEL RAIL 8x11.5)
  118   18   12    2  134   24    2    0
    0.0001    0.0001      0.60 1100    0       1.0    1
    1    5    5    5    5    5    1
    1       0.0       0.0
    2       0.0       0.0
    3     48.00       0.0
    4     48.00       0.0
    7    120.00       0.0
    8    120.00       0.0
   31    408.00       0.0
   32    408.00       0.0
   64    600.00       0.0
   63    600.00       0.0
   95    984.00       0.0
   96    984.00       0.0
  111   1368.00       0.0
  112   1368.00       0.0
  115   1440.00       0.0
  116   1440.00       0.0
  117   1488.00       0.0
  118   1488.00       0.0
    3    7    1    2       0.0
    4    8    1    2       0.0
    7   31   11    2       0.0
    8   32   11    2       0.0
   31   63   15    2       0.0
   32   64   15    2       0.0
   63   95   15    2       0.0
   64   96   15    2       0.0
   95  111    7    2       0.0
   96  112    7    2       0.0
  111  115    1    2       0.0
  112  116    1    2       0.0
    1   59      0.35
  117  115  113  111  109  107  105  103  101   99
   97   95   93   91   89   87   85   83   81   79
   77   75   73   71   69   67   65   63   61   59
   57   55   53   51   49   47   45   43   41   39
   37   35   33   31   29   27   25   23   21   19
   17   15   13   11    9    7    5    3    1
    2   59      0.35
  118  116  114  112  110  108  106  104  102  100
   98   96   94   92   90   88   86   84   82   80
   78   76   74   72   70   68   66   64   62   60
   58   56   54   52   50   48   46   44   42   40
   38   36   34   32   30   28   26   24   22   20
   18   16   14   12   10    8    6    4    2
  100   10
    1      4.82      4.00     48.00   30000.0     13.95     200.0     140.0 0.10 10-Gauge Thrie Beam
    2      4.82      4.00     36.00   30000.0     13.95     200.0     140.0 0.10 10-Gauge Thrie Beam
    3      4.82      4.00     24.00   30000.0     13.95     200.0     140.0 0.10 10-Gauge Thrie Beam
    4      4.82      4.00     12.00   30000.0     13.95     200.0     140.0 0.10 10-Gauge Thrie Beam
    5      4.82      4.00     48.00   30000.0     13.95     200.0     140.0 0.10 10-Gauge Thrie Beam
    6      32.6      3.38     48.00   30000.0     11.50       5.0    343.80 0.10 C8x11.5 Channel Rail
    7      32.6      3.38     36.00   30000.0     11.50       5.0    343.80 0.10 C8x11.5 Channel Rail
    8      32.6      3.38     24.00   30000.0     11.50       5.0    343.80 0.10 C8x11.5 Channel Rail
    9      32.6      3.38     12.00   30000.0     11.50       5.0    343.80 0.10 C8x11.5 Channel Rail
   10      32.6      3.38     48.00   30000.0     11.50       5.0    343.80 0.10 C8x11.5 Channel Rail
  300    2
    1     21.65     29.68    1000.0    1000.0     250.0   10000.0   10000.0 0.10 Simulated Strong Anchor Post
     200.0     200.0       2.0       2.0
    2     21.65     29.68      26.52     10.00      32.0    125.28    448.20 0.10 W6x12 Steel Post
       40.0      40.0       5.0      10.0
    1    1    3              101       0.0       0.0       0.0
    2    3    5    3    2  102       0.0       0.0       0.0
    4    7    9   15    2  103       0.0       0.0       0.0
   16   31   33   31    2  104       0.0       0.0       0.0
   32   63   65   47    2  103       0.0       0.0       0.0
   48   95   97   55    2  105       0.0       0.0       0.0
   56  111  113   57    2  102       0.0       0.0       0.0
   58  115  117             101       0.0       0.0       0.0
   59    2    4             106       0.0       0.0       0.0
   60    4    6   61    2  107       0.0       0.0       0.0
   62    8   10   73    2  108       0.0       0.0       0.0
   74   32   34   89    2  109       0.0       0.0       0.0
   90   64   66  105    2  108       0.0       0.0       0.0
  106   96   98  113    2  110       0.0       0.0       0.0
  114  112  114  115    2  107       0.0       0.0       0.0
  116  116  118             106       0.0       0.0       0.0
  117    1    2             301       0.0       0.0       0.0       0.0       0.0
  118    3    4  119    4  302       0.0       0.0       0.0       0.0       0.0
  120   15   16  122    8  302       0.0       0.0       0.0       0.0       0.0
```

```
123   47   48  124   16  302       0.0       0.0       0.0       0.0       0.0
125   71   72  128    8  302       0.0       0.0       0.0       0.0       0.0
129   99  100  132    4  302       0.0       0.0       0.0       0.0       0.0
133  115  116             302       0.0       0.0       0.0       0.0       0.0
134  117  118             301       0.0       0.0       0.0       0.0       0.0
  4400.0   40000.0   20    6    4    0    1
  1     0.055      0.12      6.00      17.0
  2     0.057      0.15      7.00      18.0
  3     0.062      0.18     10.00      12.0
  4     0.110      0.35     12.00       6.0
  5      0.35      0.45      6.00       5.0
  6      1.45      1.50     15.00       1.0
  1    100.75    15.875    1       12.0    1    1    0    0
  2    100.75    27.875    1       12.0    1    1    0    0
  3    100.75    39.875    2       12.0    1    1    0    0
  4     88.75    39.875    2       12.0    1    1    0    0
  5     76.75    39.875    2       12.0    1    1    0    0
  6     64.75    39.875    2       12.0    1    1    0    0
  7     52.75    39.875    2       12.0    1    1    0    0
  8     40.75    39.875    2       12.0    1    1    0    0
  9     28.75    39.875    2       12.0    1    1    0    0
 10     16.75    39.875    2       12.0    1    1    0    0
 11    -13.25    39.875    3       12.0    1    1    0    0
 12    -33.25    39.875    3       12.0    1    1    0    0
 13    -53.25    39.875    3       12.0    1    1    0    0
 14    -73.25    39.875    3       12.0    1    1    0    0
 15    -93.25    39.875    3       12.0    1    1    0    0
 16   -113.25    39.875    4       12.0    1    1    0    0
 17   -113.25   -39.875    4       12.0    0    0    0    0
 18    100.75   -39.875    1       12.0    0    0    0    0
 19     69.25     37.75     5        1.0    1    1    0    0
 20    -62.75     37.75     6        1.0    1    1    0    0
  1     69.25     32.75       0.0       608.
  2     69.25    -32.75       0.0       608.
  3    -62.75     32.75       0.0       492.
  4    -62.75    -32.75       0.0       492.
  1       0.0       0.0
  3    432.00       0.0      25.0     43.50       0.0       0.0       1.0
```

```
USFS TL-2 STEEL TRANSITION (TRANSVERSE DECK PROJECT) - NTRUN22 - NODE 34 (10-GA. THRIE BEAM AND CHANNEL RAIL C8x11.5)
   80   29   27    2  100   29    2    0
    0.0001    0.0001      0.60  300    0       1.0    1
    1    5    5    5    5    5    1
    1       0.0       0.0
    3      75.0       0.0
    5     150.0       0.0
    7     225.0       0.0
    9     300.0       0.0
   11     375.0       0.0
   13     450.0       0.0
   15     525.0       0.0
   19     600.0       0.0
   21    637.50       0.0
   23     675.0       0.0
   27    712.50       0.0
   31     750.0       0.0
   35    787.50       0.0
   36    787.50       0.0
   43     825.0       0.0
   44     825.0       0.0
   51     873.0       0.0
   52     873.0       0.0
   59     945.0       0.0
   60     945.0       0.0
   67    1041.0       0.0
   68    1041.0       0.0
   71    1137.0       0.0
   72    1137.0       0.0
   75    1233.0       0.0
   76    1233.0       0.0
   79    1329.0       0.0
   80    1329.0       0.0
    1    3    1    1       0.0
    3    5    1    1       0.0
    5    7    1    1       0.0
    7    9    1    1       0.0
    9   11    1    1       0.0
   11   13    1    1       0.0
   13   15    1    1       0.0
   15   19    3    1       0.0
   19   21    1    1       0.0
   21   23    1    1       0.0
   23   27    3    1       0.0
   27   31    3    1       0.0
   31   35    3    1       0.0
   35   43    3    2       0.0
   43   51    3    2       0.0
   51   59    3    2       0.0
   59   67    3    2       0.0
   67   71    1    2       0.0
   71   75    1    2       0.0
   75   79    1    2       0.0
   36   44    3    2       0.0
   44   52    3    2       0.0
   52   60    3    2       0.0
   60   68    3    2       0.0
   68   72    1    2       0.0
   72   76    1    2       0.0
   76   80    1    2       0.0
    1   57      0.35
   79   77   75   73   71   69   67   65   63   61
   59   57   55   53   51   49   47   45   43   41
   39   37   35   34   33   32   31   30   29   28
   27   26   25   24   23   22   21   20   19   18
   17   16   15   14   13   12   11   10    9    8
    7    6    5    4    3    2    1
    2   23      0.35
   80   78   76   74   72   70   68   66   64   62
   60   58   56   54   52   50   48   46   44   42
   40   38   36
  100   16
    1      2.30      1.99     37.50   30000.0      6.92      99.5      68.5 0.10 12-Gauge W-Beam
    2      2.30      1.99     18.75   30000.0      6.92      99.5      68.5 0.10 12-Gauge W-Beam
    3     2.475     2.125     18.75   30000.0     7.405    106.25     73.75 0.10 12-Gauge W-Beam to Thrie Beam Transition
    4      2.84      2.40     18.75   30000.0     8.375     120.0      84.0 0.10 12-Gauge W-Beam to Thrie Beam Transition
    5     3.205      2.68     18.75   30000.0      9.35     134.0      94.0 0.10 12-Gauge W-Beam to Thrie Beam Transition
    6     3.575      2.96     18.75   30000.0    10.325     148.0    104.25 0.10 12-Gauge W-Beam to Thrie Beam Transition
    7      4.82      4.00     9.375   30000.0     13.95     200.0     140.0 0.10 10-Gauge Thrie Beam
    8      4.82      4.00     12.00   30000.0     13.95     200.0     140.0 0.10 10-Gauge Thrie Beam
    9      4.82      4.00     18.00   30000.0     13.95     200.0     140.0 0.10 10-Gauge Thrie Beam
   10      4.82      4.00     24.00   30000.0     13.95     200.0     140.0 0.10 10-Gauge Thrie Beam
   11      4.82      4.00     48.00   30000.0     13.95     200.0     140.0 0.10 10-Gauge Thrie Beam
```

```
 12      32.6      3.38     9.375   30000.0      1.00       1.0      1.00 0.10  C8x11.5 Channel Rail with Reduced Properties
 13      32.6      3.38     12.00   30000.0     11.50       5.0    343.80 0.10  C8x11.5 Channel Rail
 14      32.6      3.38     18.00   30000.0     11.50       5.0    343.80 0.10  C8x11.5 Channel Rail
 15      32.6      3.38     24.00   30000.0     11.50       5.0    343.80 0.10  C8x11.5 Channel Rail
 16      32.6      3.38     48.00   30000.0     11.50       5.0    343.80 0.10  C8x11.5 Channel Rail
300   11
  1     21.65       0.0    1000.0    1000.0     250.0   10000.0   10000.0 0.10  Strong Post Anchor
   200.0     200.0       2.0       2.0
  2     21.65       0.0      4.00      4.00      54.0     92.88    270.62 0.10  W6x9 by 6' Long
     6.0      15.0      16.0      16.0
  3     21.65       0.0      4.00      4.00      58.5     92.88    270.62 0.10  W6x9 by 6.5' Long
     6.0      15.0      16.0      16.0
  4     21.65       0.0      4.00      4.00      58.5     92.88    270.62 0.10  W6x9 by 6.5' Long
     6.0      15.0      16.0      16.0
  5     21.65       0.0       8.0       8.0      63.0     92.88    336.42 0.10  W6x9 by 7' Long
    10.0      20.0      16.0      16.0
  6     21.65       0.0       8.0       8.0      63.0     92.88    336.42 0.10  W6x9 by 7' Long
    10.0      20.0      16.0      16.0
  7     21.65       0.0       8.0       8.0      63.0     92.88    336.42 0.10  W6x9 by 7' Long
    10.0      20.0      16.0      16.0
  8     21.65     29.68       8.0       8.0      63.0     92.88    336.42 0.10  W6x9 by 7' Long
    10.0      20.0      16.0      16.0
  9     21.65     29.68       8.0       8.0      63.0     92.88    336.42 0.10  W6x9 by 7' Long
    10.0      20.0      16.0      16.0
 10     21.65     29.68     26.52     10.00      32.0    125.28    448.20 0.10  W6x12 Bridge Post
    40.0      40.0       5.0      10.0
 11     21.65     29.68    1000.0    1000.0     250.0   10000.0   10000.0 0.10  Strong Post Anchor
   200.0     200.0       2.0       2.0
  1    1    2   14    1  101       0.0       0.0       0.0
 15   15   16   18    1  102       0.0       0.0       0.0
 19   19   20         1  103       0.0       0.0       0.0
 20   20   21         1  104       0.0       0.0       0.0
 21   21   22         1  105       0.0       0.0       0.0
 22   22   23         1  106       0.0       0.0       0.0
 23   23   24   34    1  107       0.0       0.0       0.0
 35   35   37   38    2  107       0.0       0.0       0.0
 39   43   45   42    2  108       0.0       0.0       0.0
 43   51   53   46    2  109       0.0       0.0       0.0
 47   59   61   50    2  110       0.0       0.0       0.0
 51   67   69   57    2  111       0.0       0.0       0.0
 58   36   38   61    2  112       0.0       0.0       0.0
 62   44   46   65    2  113       0.0       0.0       0.0
 66   52   54   69    2  114       0.0       0.0       0.0
 70   60   62   73    2  115       0.0       0.0       0.0
 74   68   70   79    2  116       0.0       0.0       0.0
 80    1        81    2  301       0.0       0.0       0.0       0.0       0.0
 82    3        87    2  302       0.0       0.0       0.0       0.0       0.0
 88   19                 303       0.0       0.0       0.0       0.0       0.0
 89   21                 304       0.0       0.0       0.0       0.0       0.0
 90   23                 305       0.0       0.0       0.0       0.0       0.0
 91   27                 306       0.0       0.0       0.0       0.0       0.0
 92   31                 307       0.0       0.0       0.0       0.0       0.0
 93   35   36            308       0.0       0.0       0.0       0.0       0.0
 94   43   44            309       0.0       0.0       0.0       0.0       0.0
 95   51   52   97    8  310       0.0       0.0       0.0       0.0       0.0
 98   71   72   99    4  310       0.0       0.0       0.0       0.0       0.0
100   79   80            311       0.0       0.0       0.0       0.0       0.0
  4400.0   40000.0   20    6    4    0    1
  1     0.055      0.12      6.00      17.0
  2     0.057      0.15      7.00      18.0
  3     0.062      0.18     10.00      12.0
  4     0.110      0.35     12.00       6.0
  5      0.35      0.45      6.00       5.0
  6      1.45      1.50     15.00       1.0
  1    100.75    15.875    1      12.0    1    0    0    0
  2    100.75    27.875    1      12.0    1    0    0    0
  3    100.75    39.875    2      12.0    1    0    0    0
  4     88.75    39.875    2      12.0    1    0    0    0
  5     76.75    39.875    2      12.0    1    0    0    0
  6     64.75    39.875    2      12.0    1    0    0    0
  7     52.75    39.875    2      12.0    1    0    0    0
  8     40.75    39.875    2      12.0    1    0    0    0
  9     28.75    39.875    2      12.0    1    0    0    0
 10     16.75    39.875    2      12.0    1    0    0    0
 11    -13.25    39.875    3      12.0    1    0    0    0
 12    -33.25    39.875    3      12.0    1    0    0    0
 13    -53.25    39.875    3      12.0    1    0    0    0
 14    -73.25    39.875    3      12.0    1    0    0    0
 15    -93.25    39.875    3      12.0    1    0    0    0
 16   -113.25    39.875    4      12.0    1    0    0    0
 17   -113.25   -39.875    4      12.0    0    0    0    0
 18    100.75   -39.875    1      12.0    0    0    0    0
 19     69.25     37.75    5       1.0    1    0    0    0
```

```
20    -62.75     37.75    6       1.0    1    0    0    0
 1     69.25     32.75       0.0       608.
 2     69.25    -32.75       0.0       608.
 3    -62.75     32.75       0.0       492.
 4    -62.75    -32.75       0.0       492.
 1       0.0       0.0
 3   778.125       0.0      25.0     43.50       0.0       0.0       1.0
```

APPENDIX E

Accelerometer Data Analysis - Test STCR-1

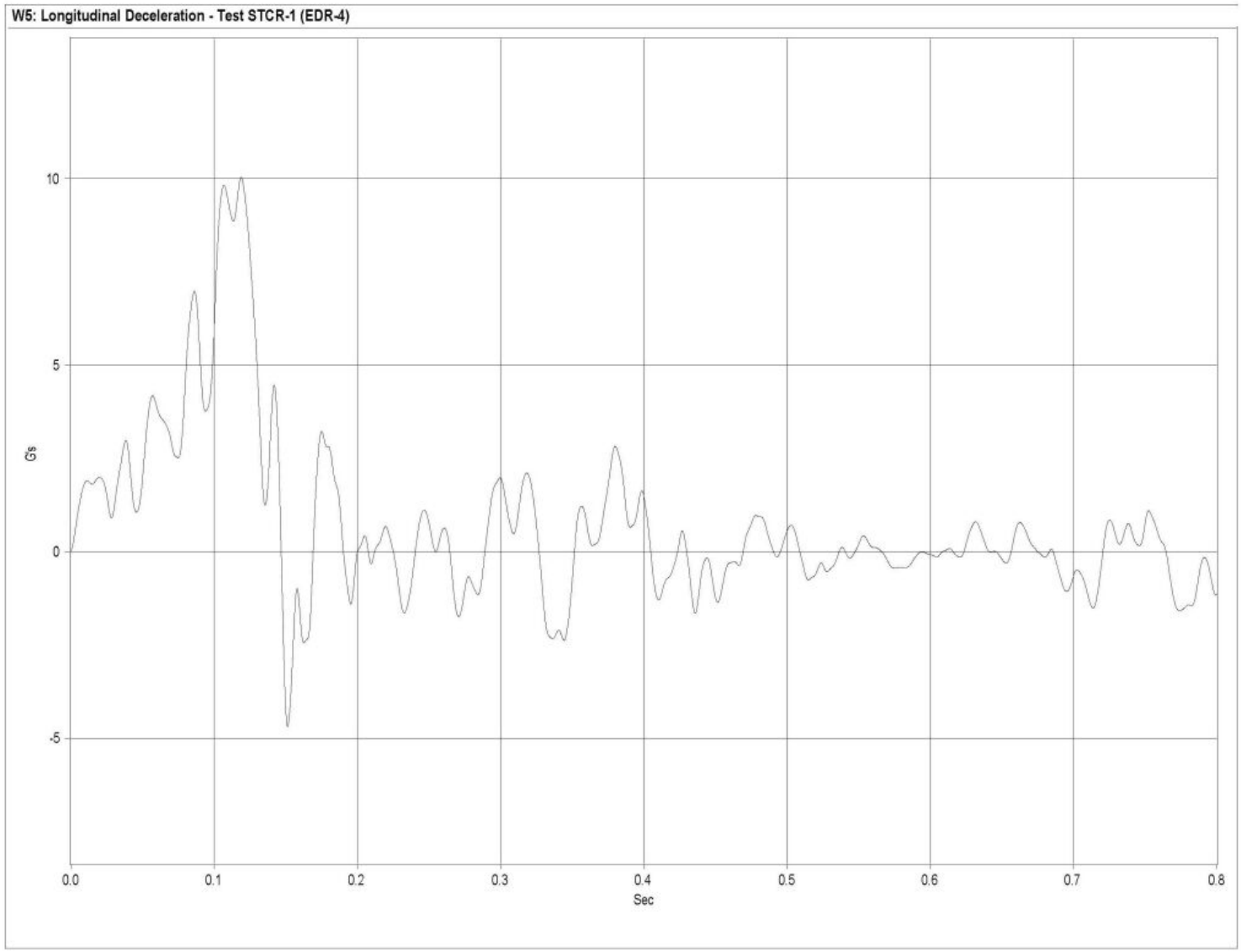

Figure E-1. Graph of Longitudinal Deceleration, Test STCR-1

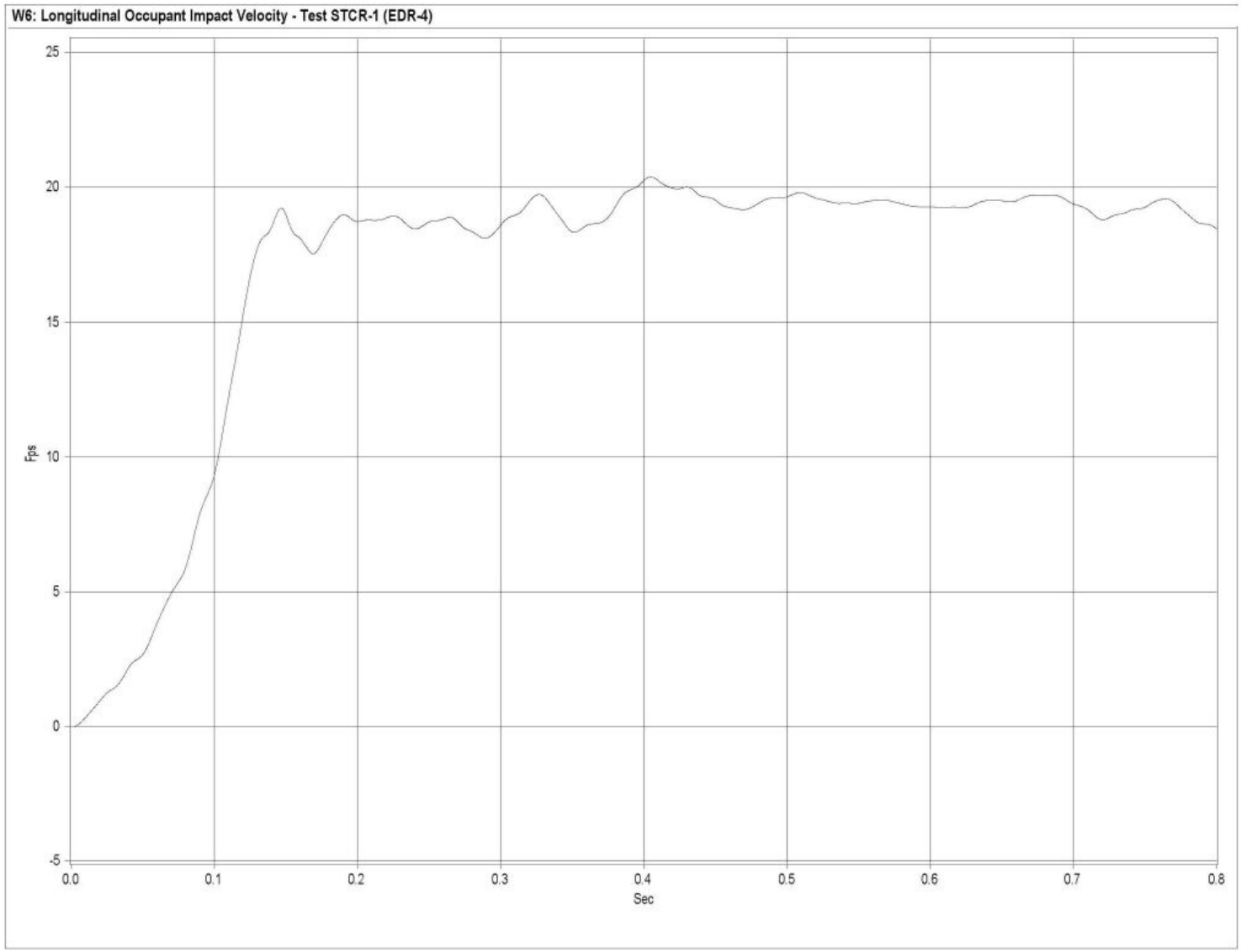

Figure E-2. Graph of Longitudinal Occupant Impact Velocity, Test STCR-1

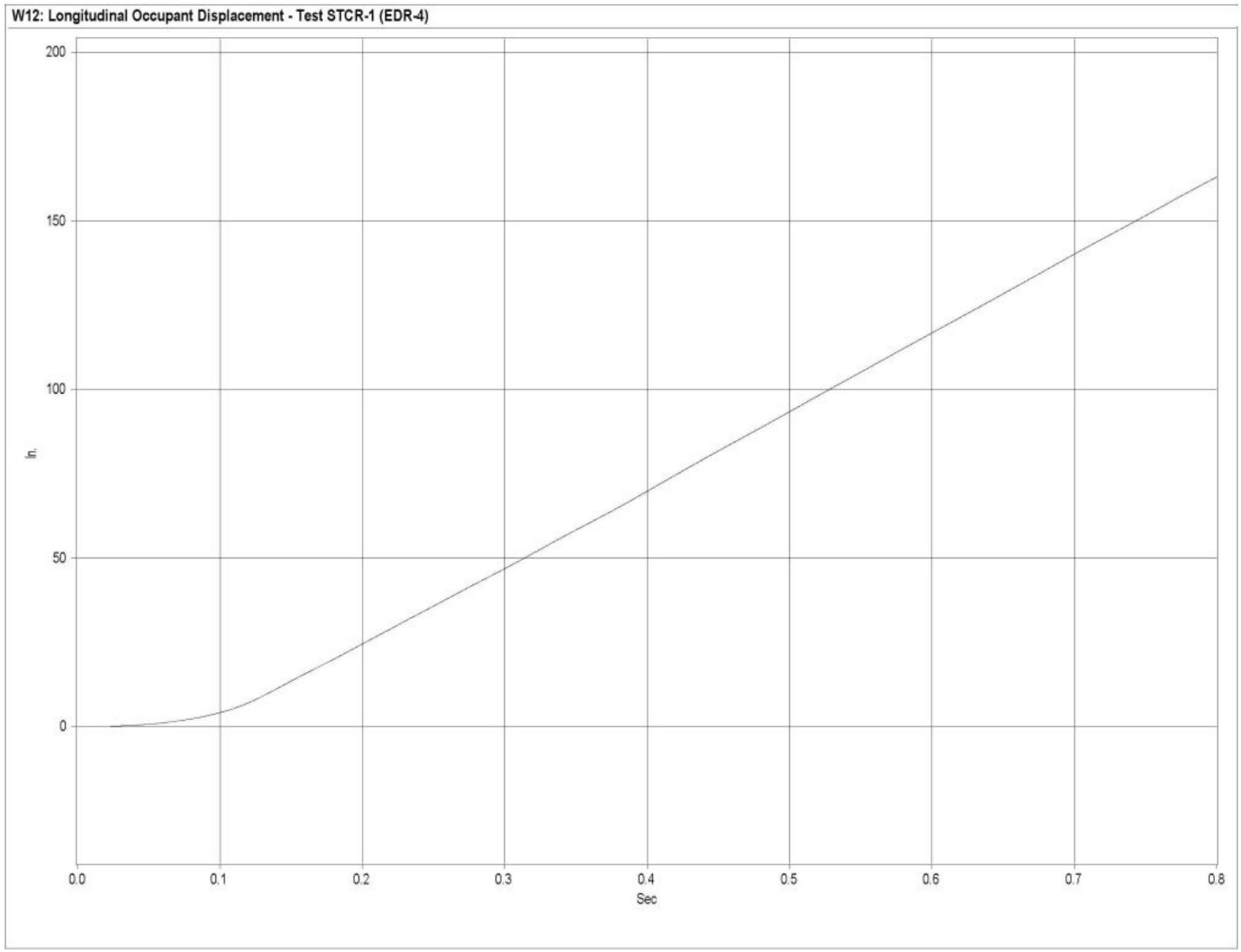

Figure E-3. Graph of Longitudinal Occupant Displacement, Test STCR-1

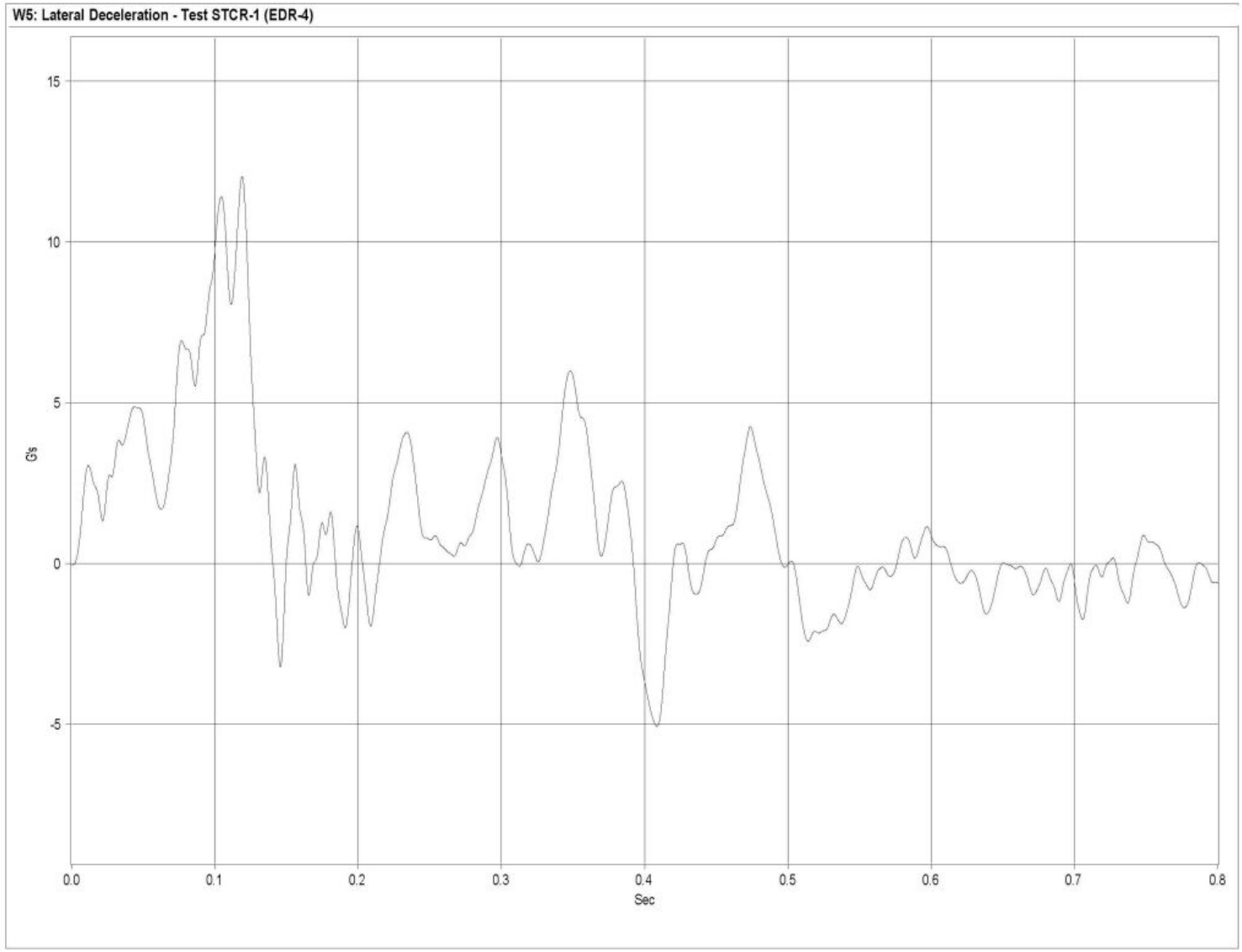

Figure E-4. Graph of Lateral Deceleration, Test STCR-1

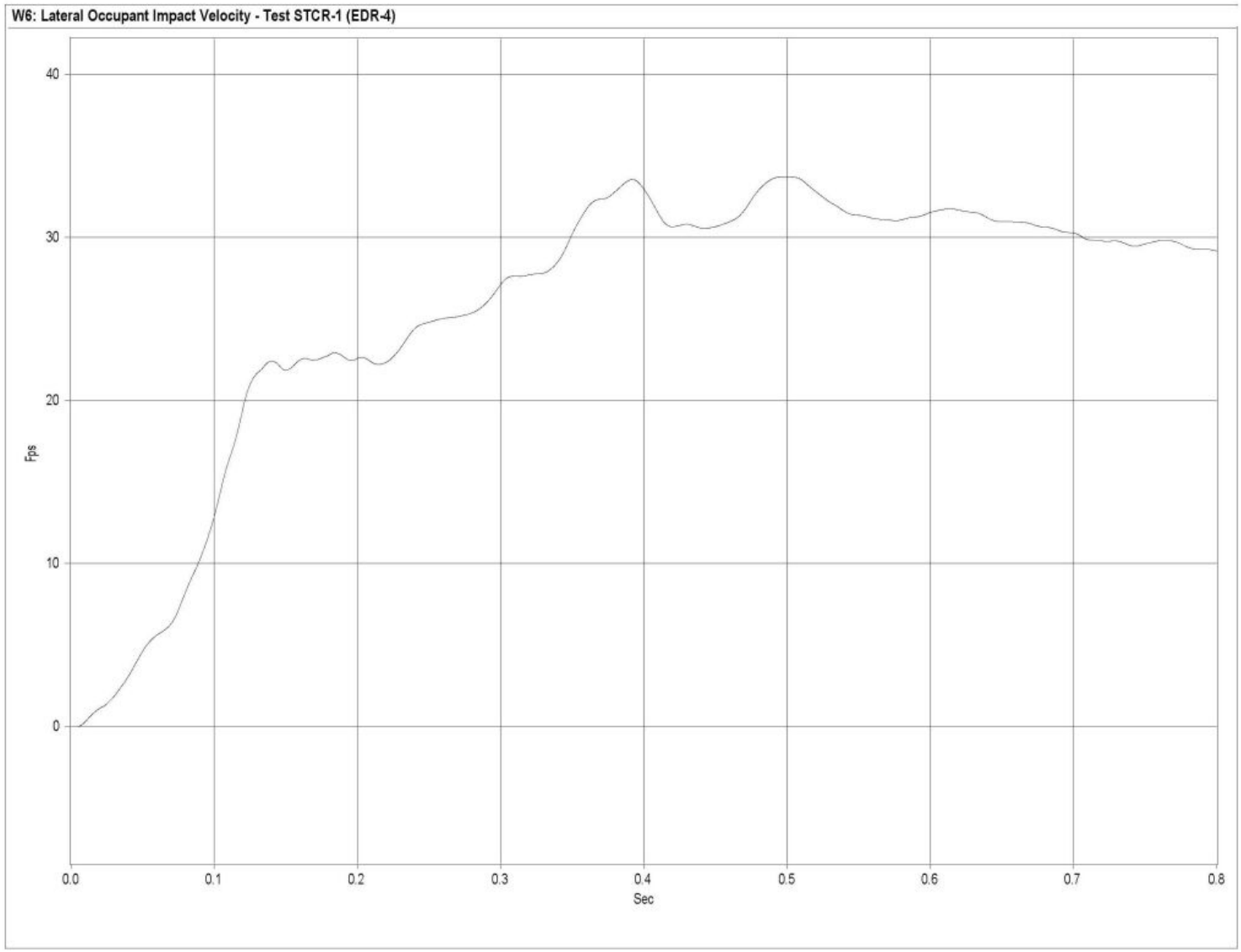

Figure E-5. Graph of Lateral Occupant Impact Velocity, Test STCR-1

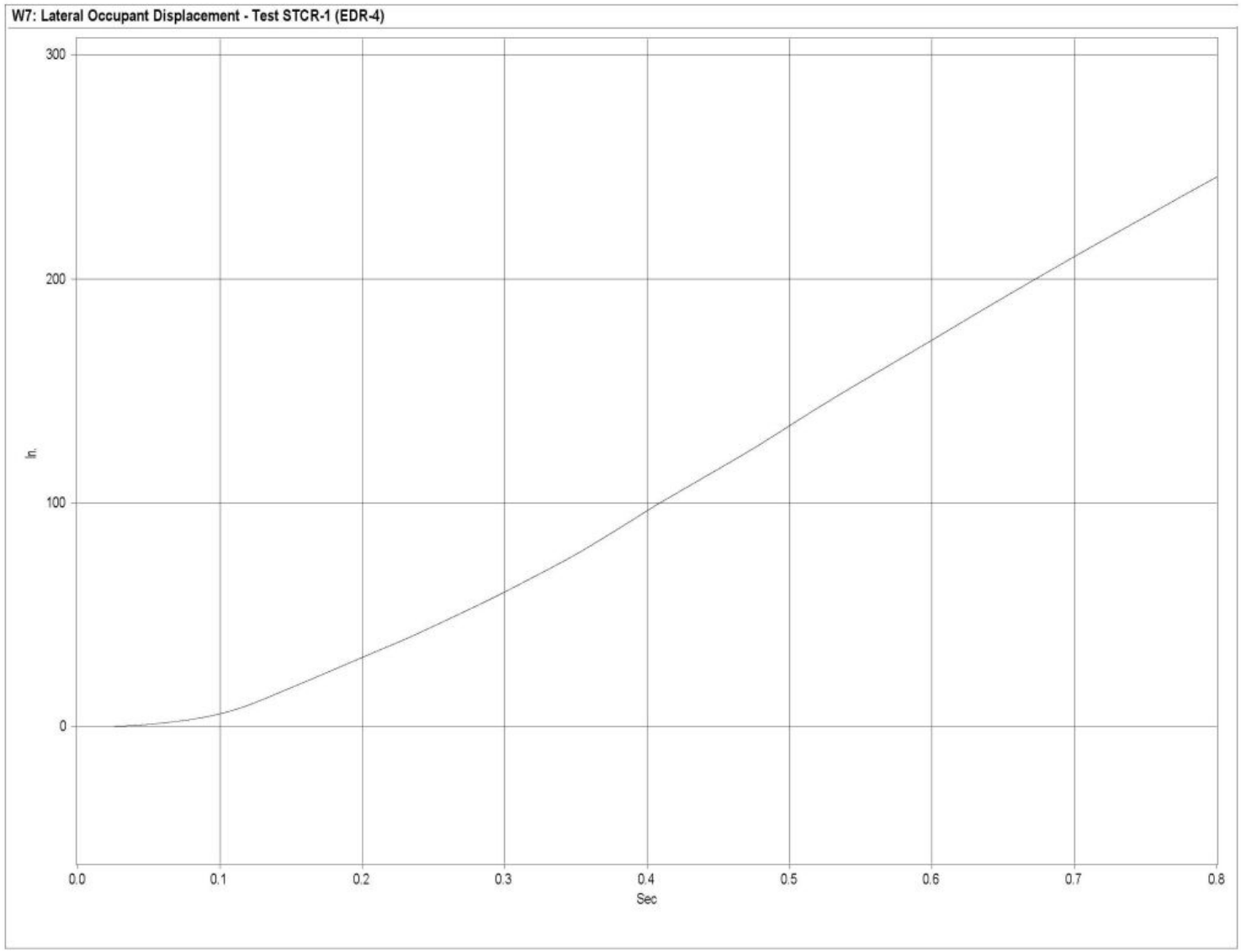

Figure E-6. Graph of Lateral Occupant Displacement, Test STCR-1

APPENDIX F

Roll, Pitch, and Yaw Data Analysis - Test STCR-1

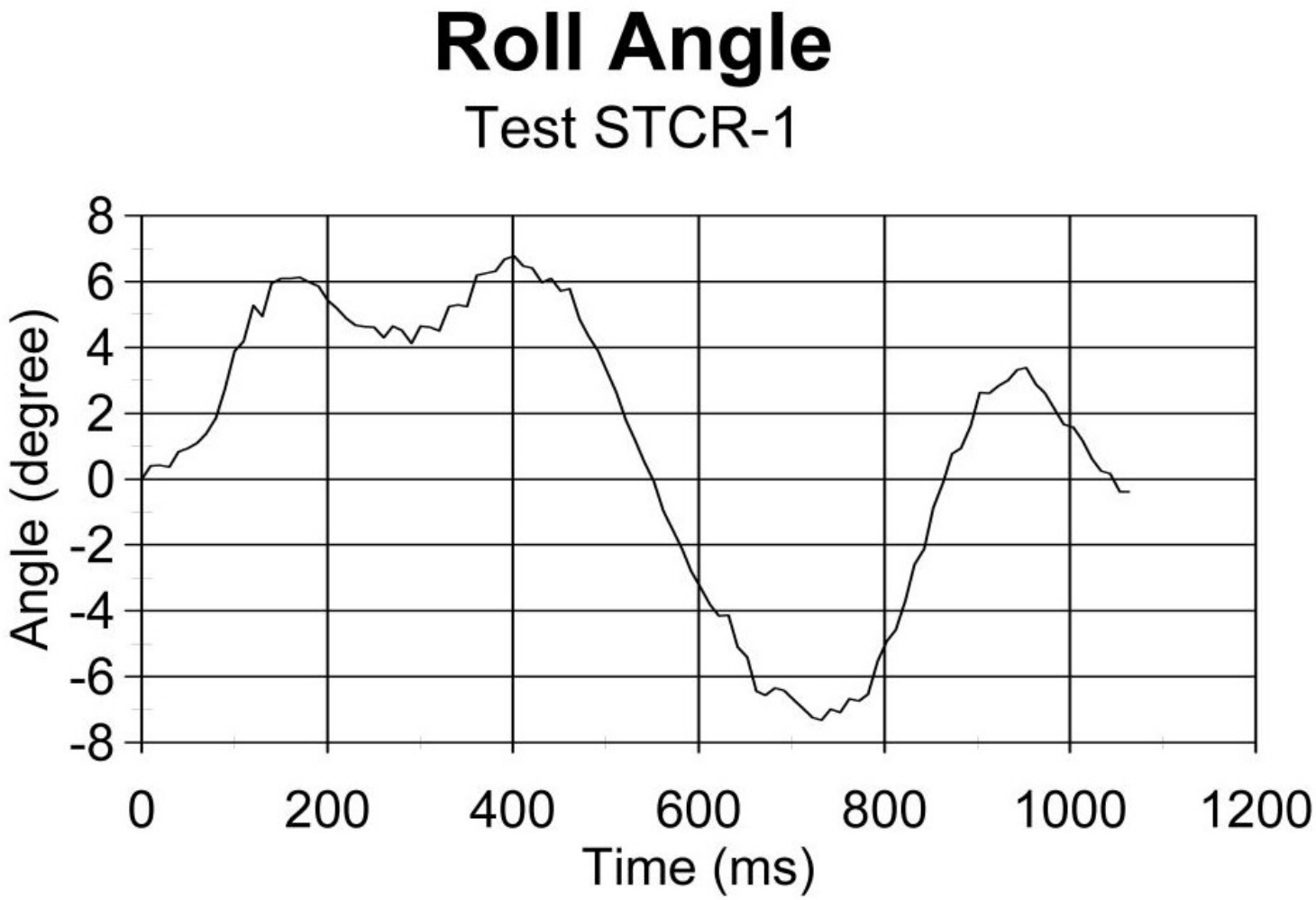

Figure F-1. Graph of Roll Angular Displacements, Test STCR-1

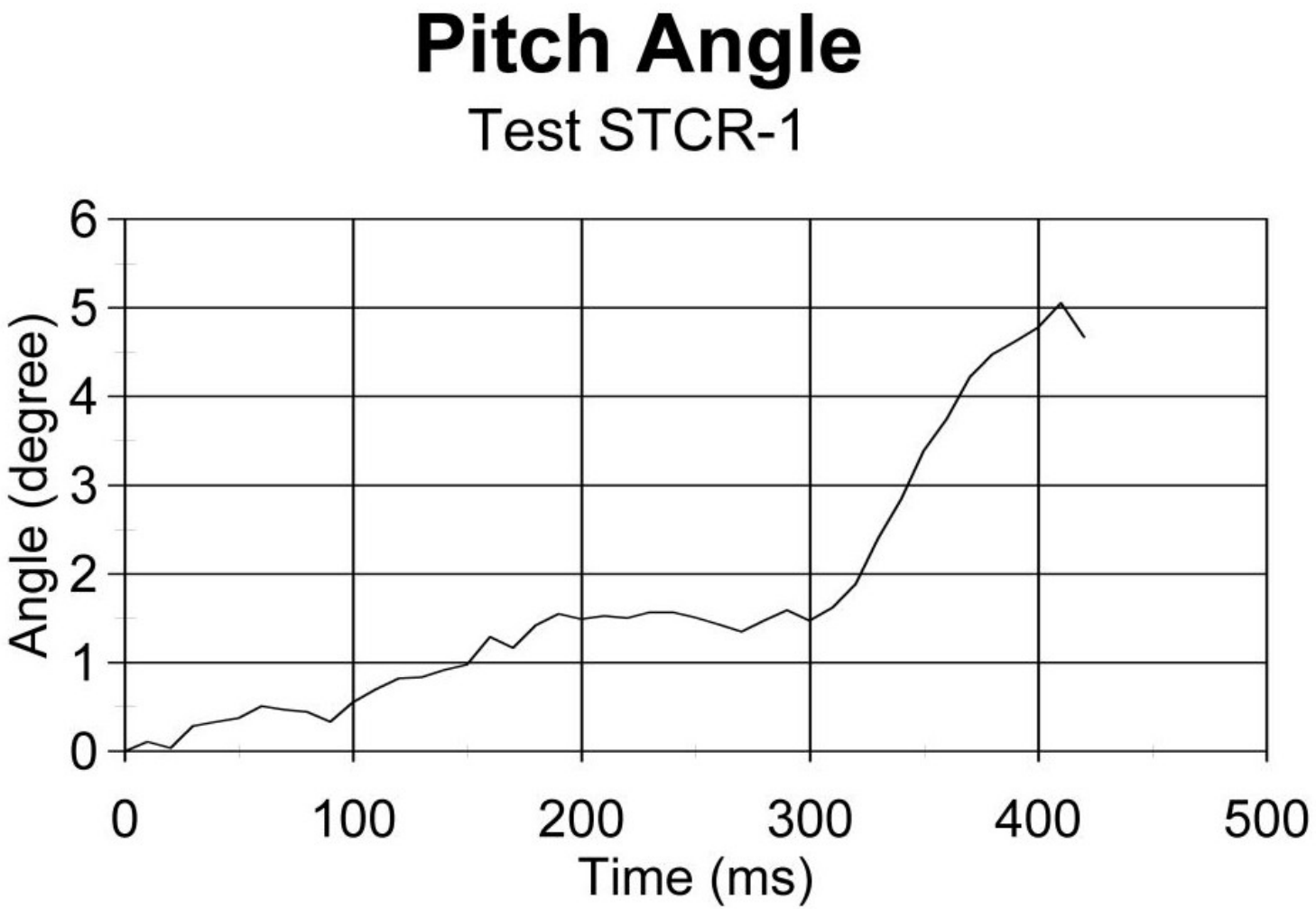

Figure F-2. Graph of Pitch Angular Displacements, Test STCR-1

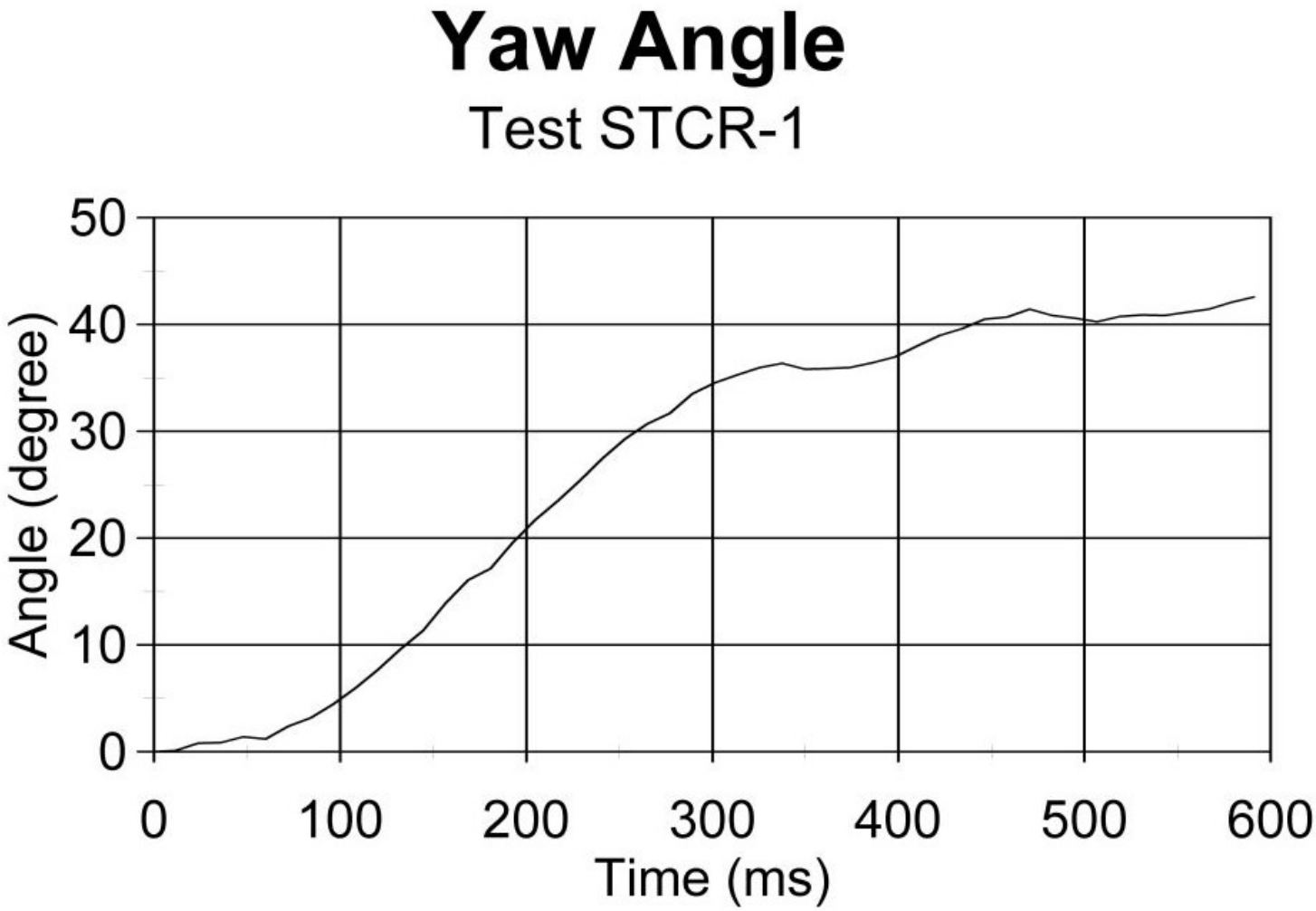

Figure F-3. Graph of Yaw Angular Displacements, Test STCR-1

APPENDIX G

Strain Gauge Data Analysis - Test STCR-1

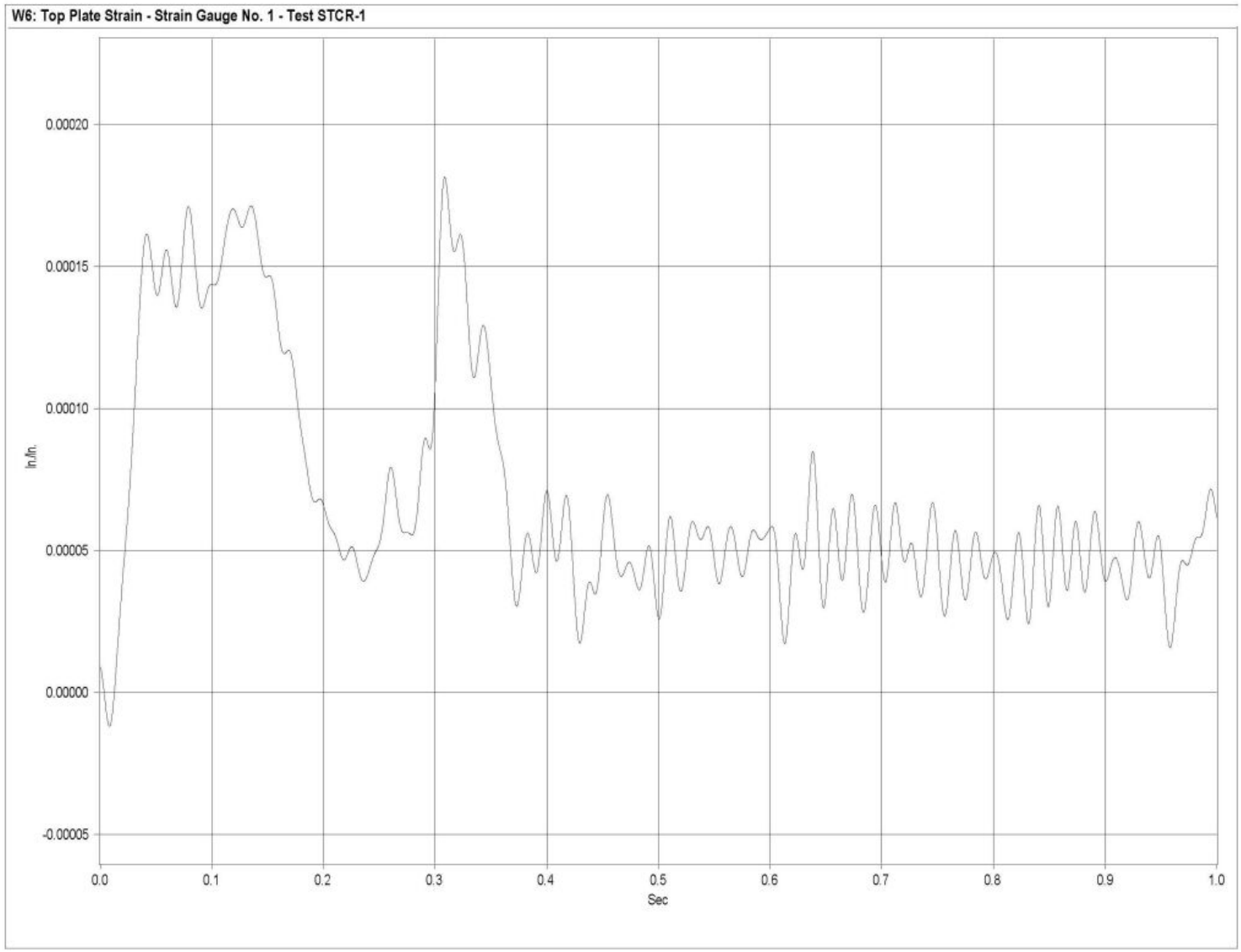

Figure G-1. Graph of Top Plate Post No. 5 - Stain Gauge No. 1 Perpendicular to Rail - Strain, Test STCR-1

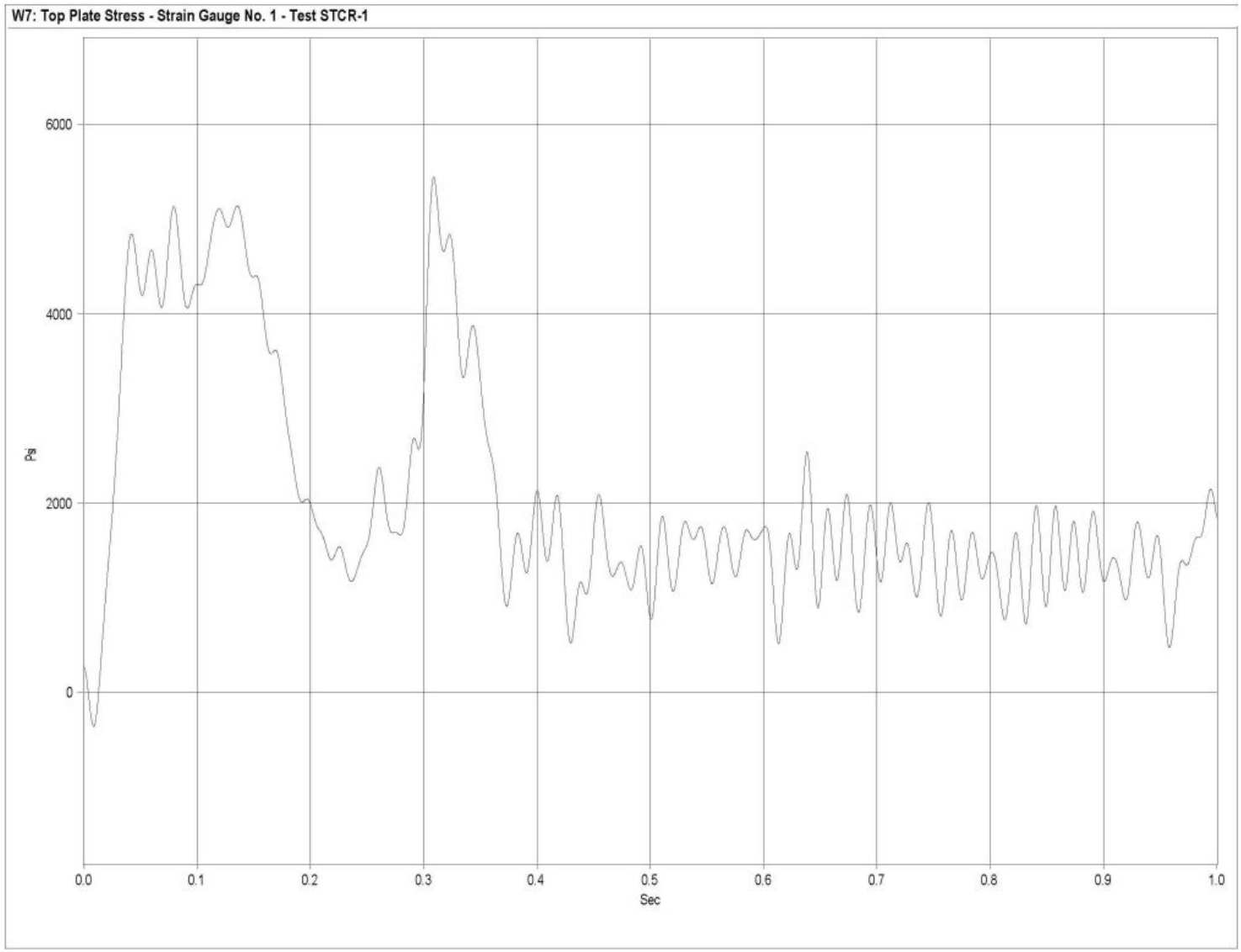

Figure G-2. Graph of Top Plate Post No. 5 - Stain Gauge No. 1 Perpendicular to Rail - Stress, Test STCR-1

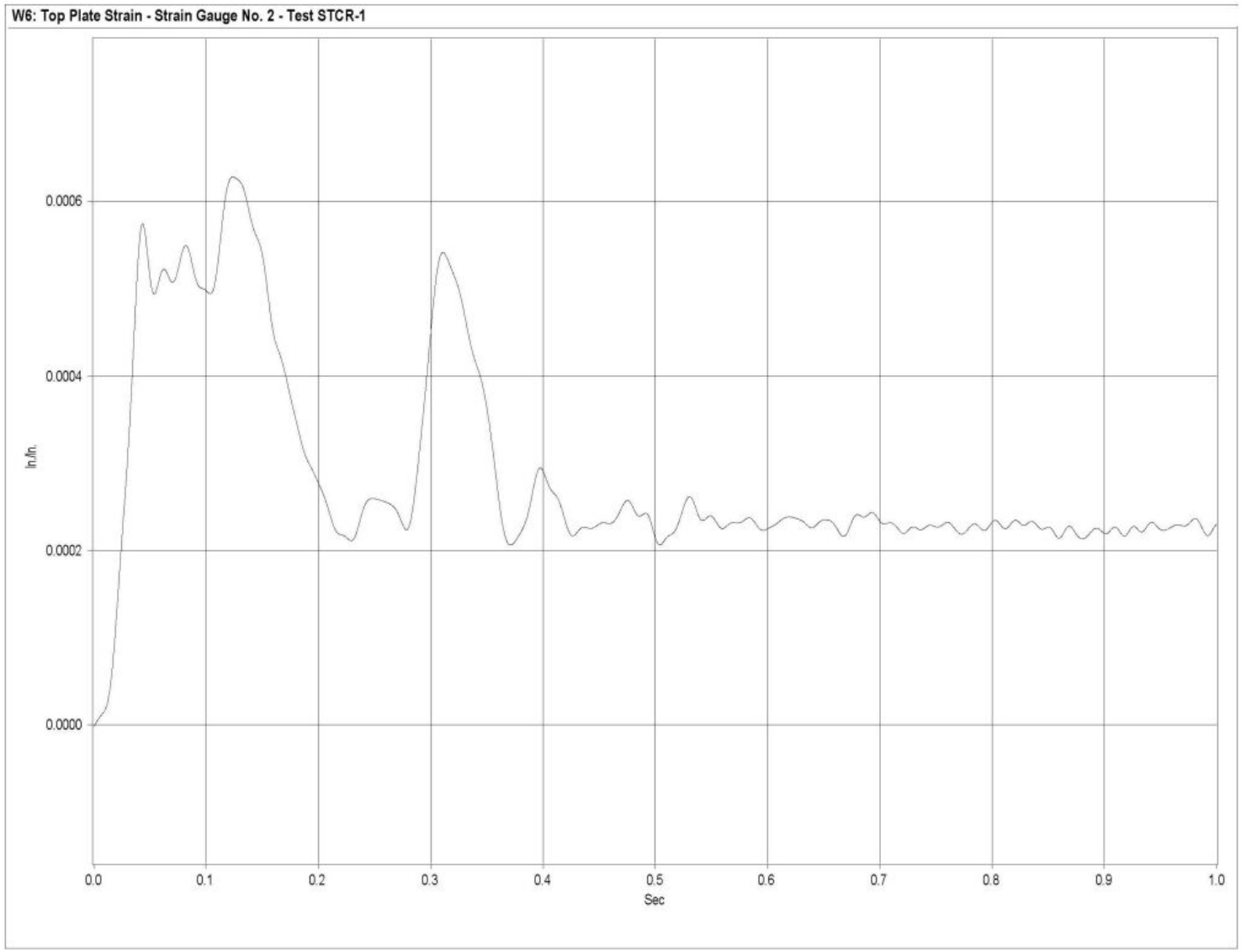

Figure G-3. Graph of Top Plate Post No. 5 - Stain Gauge No. 2 Perpendicular to Rail - Strain, Test STCR-1

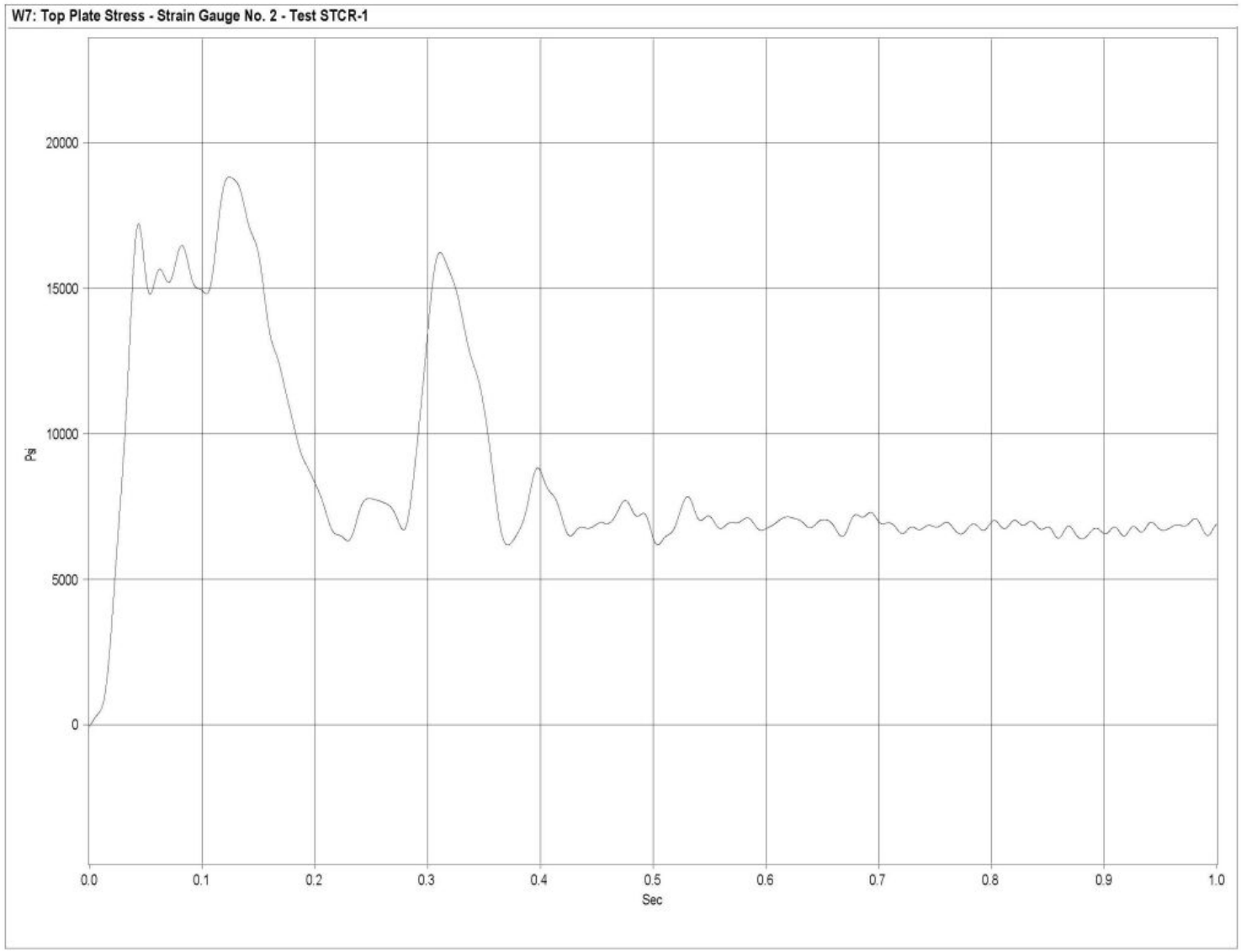

Figure G-4. Graph of Top Plate Post No. 5 - Stain Gauge No. 2 Perpendicular to Rail - Stress, Test STCR-1

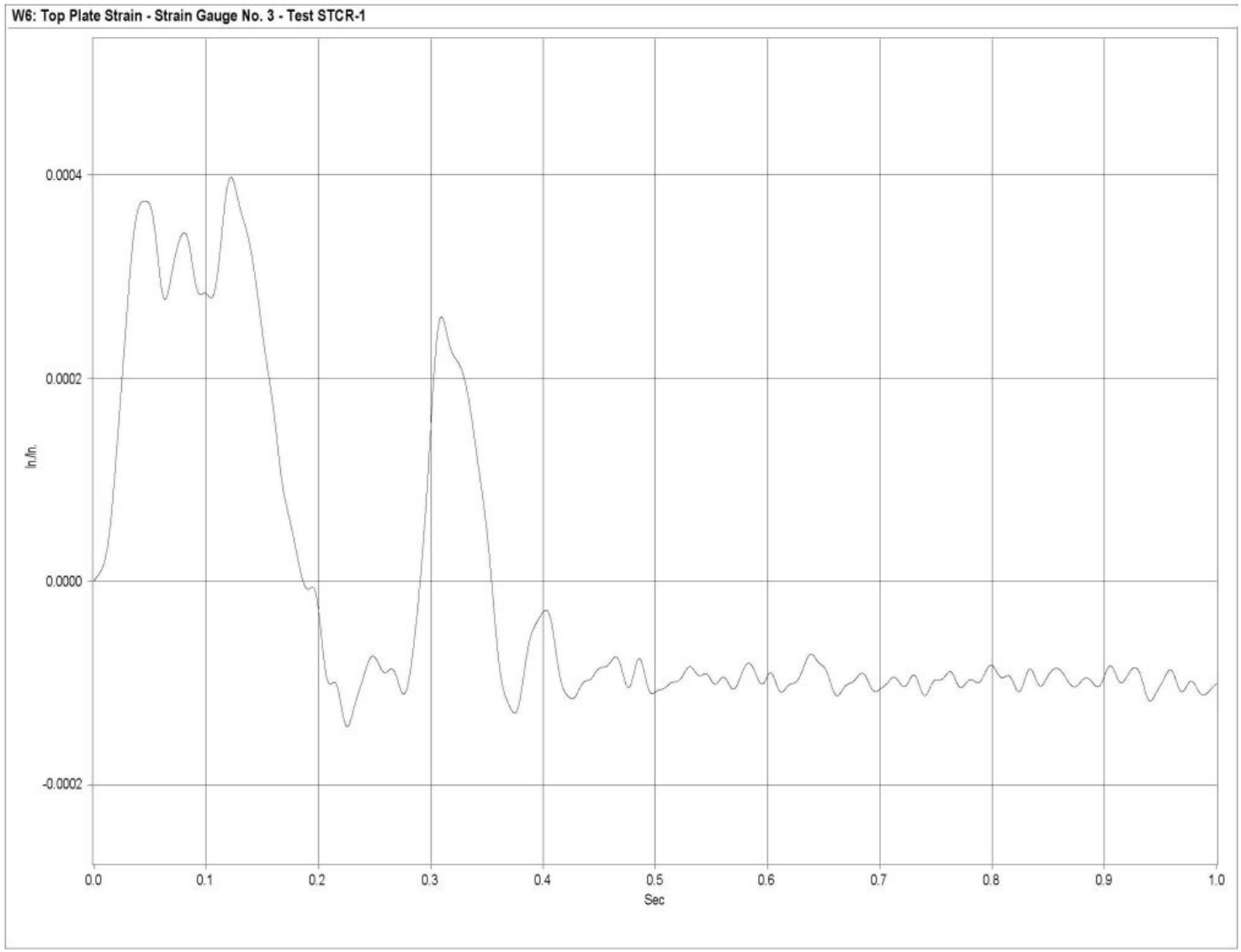

Figure G-5. Graph of Top Plate Post No. 5 - Stain Gauge No. 3 Perpendicular to Rail - Strain, Test STCR-1

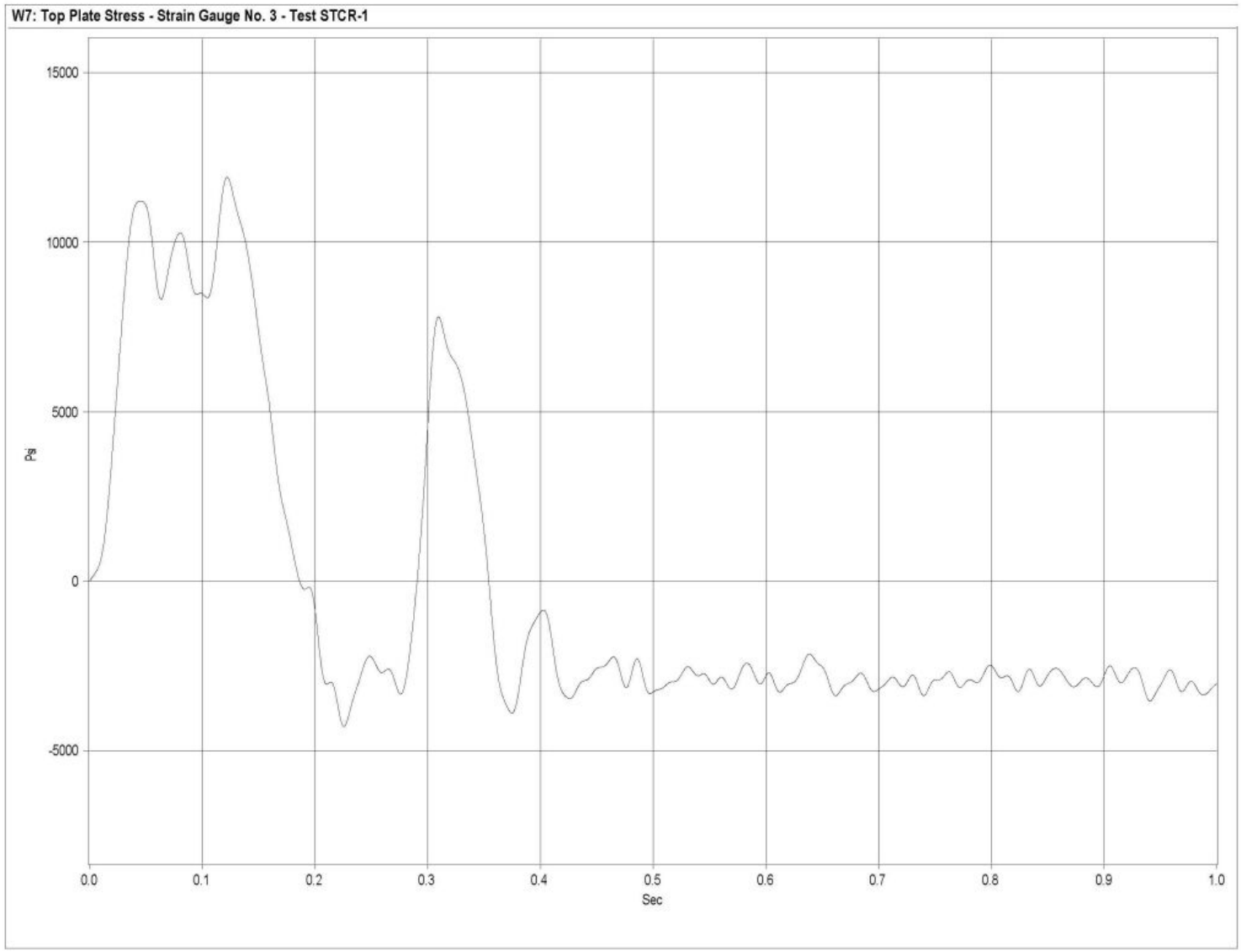

Figure G-6. Graph of Top Plate Post No. 5 - Stain Gauge No. 3 Perpendicular to Rail - Stress, Test STCR-1

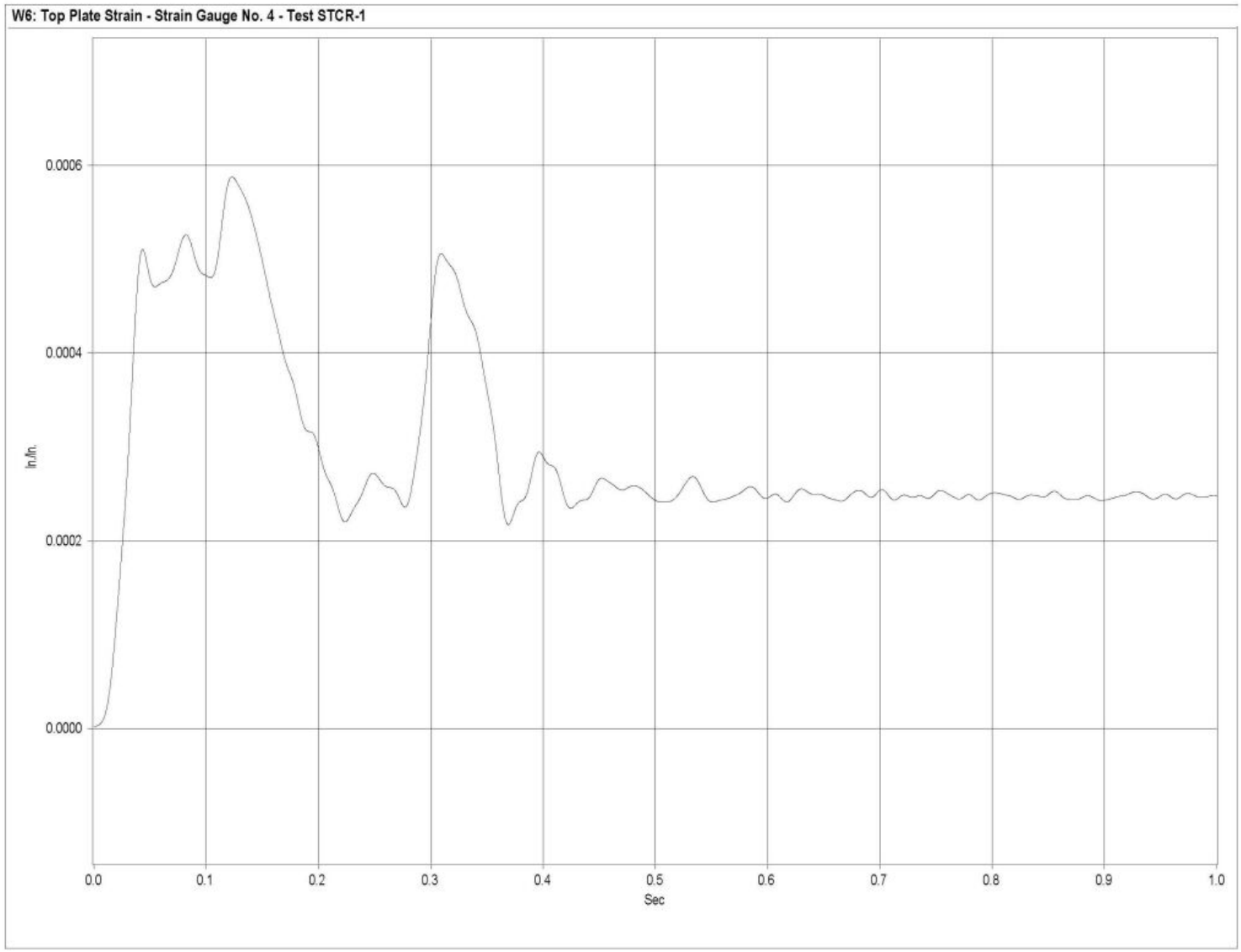

Figure G-7. Graph of Top Plate Post No. 5 - Stain Gauge No. 4 Perpendicular to Rail - Strain, Test STCR-1

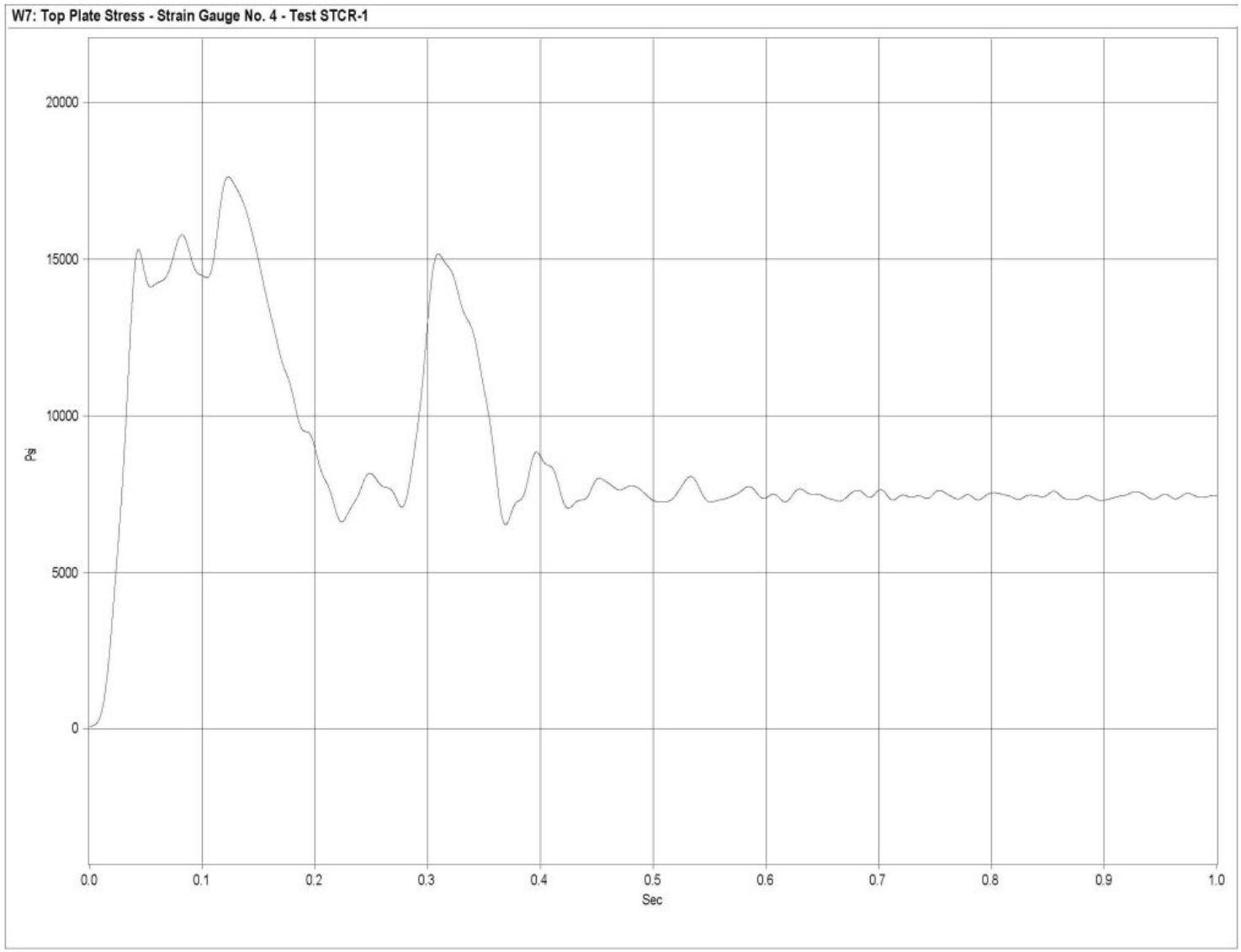

Figure G-8. Graph of Top Plate Post No. 5 - Stain Gauge No. 4 Perpendicular to Rail - Stress, Test STCR-1

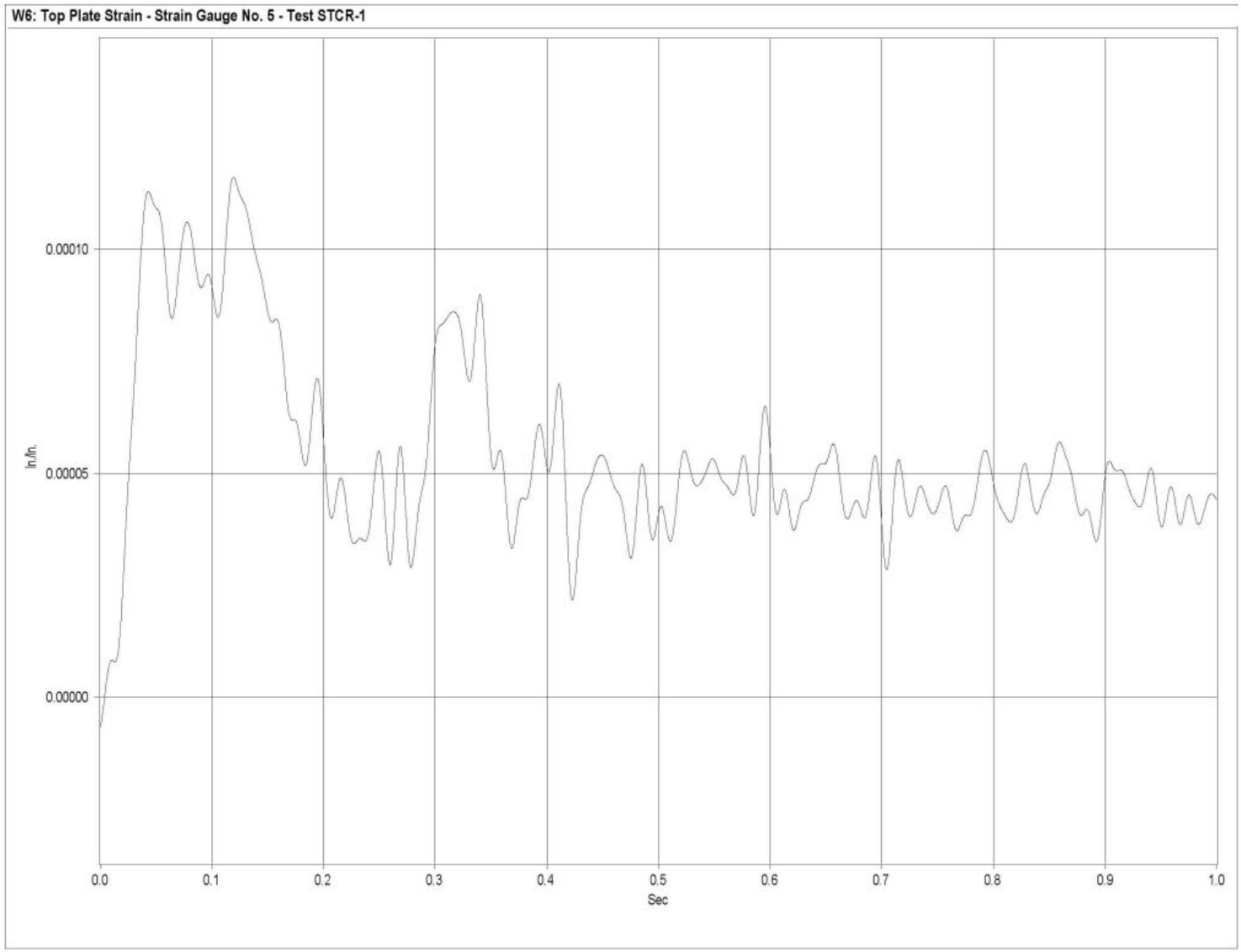

Figure G-9. Graph of Top Plate Post No. 5 - Stain Gauge No. 5 Perpendicular to Rail - Strain, Test STCR-1

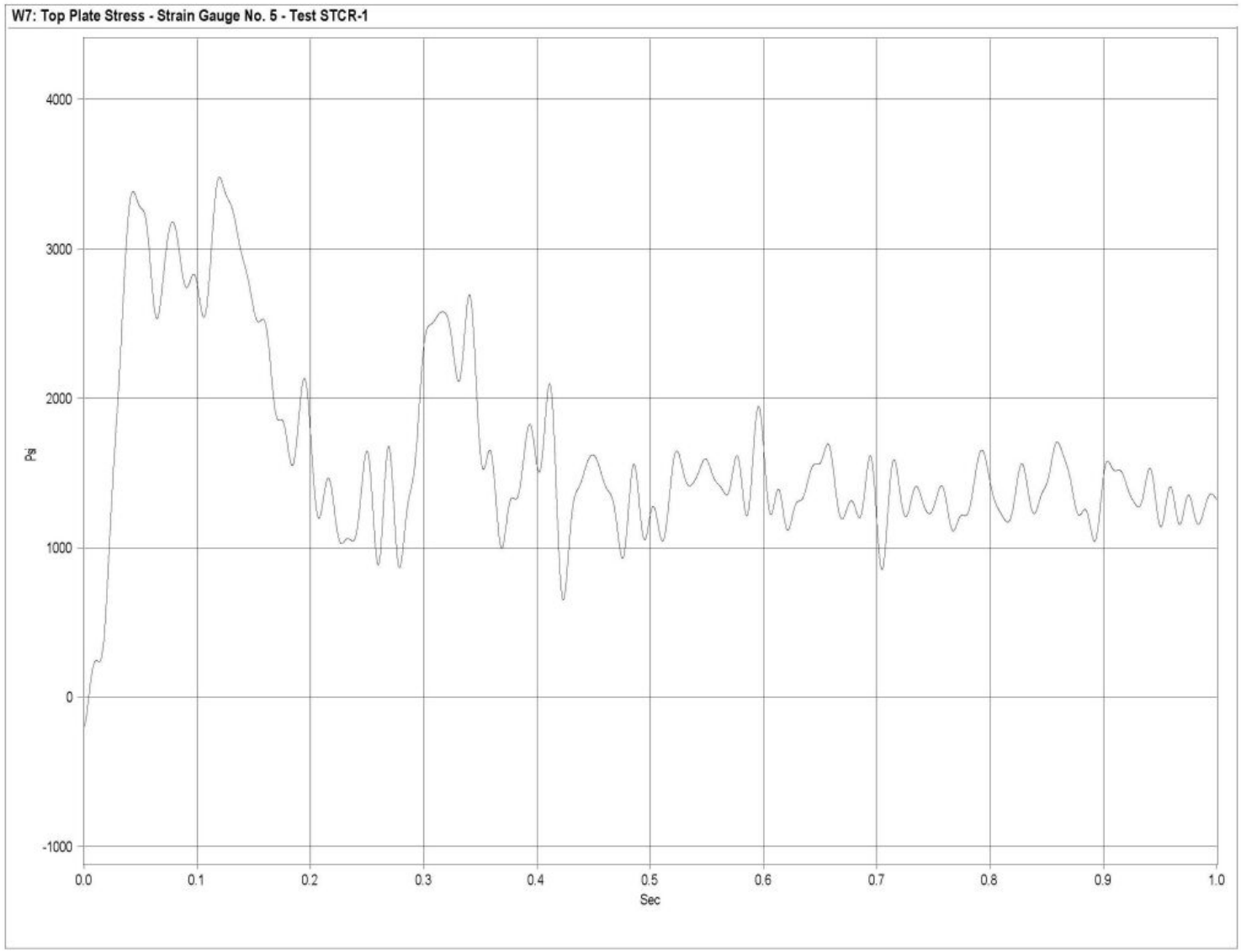

Figure G-10. Graph of Top Plate Post No. 5 - Stain Gauge No. 5 Perpendicular to Rail - Stress, Test STCR-1

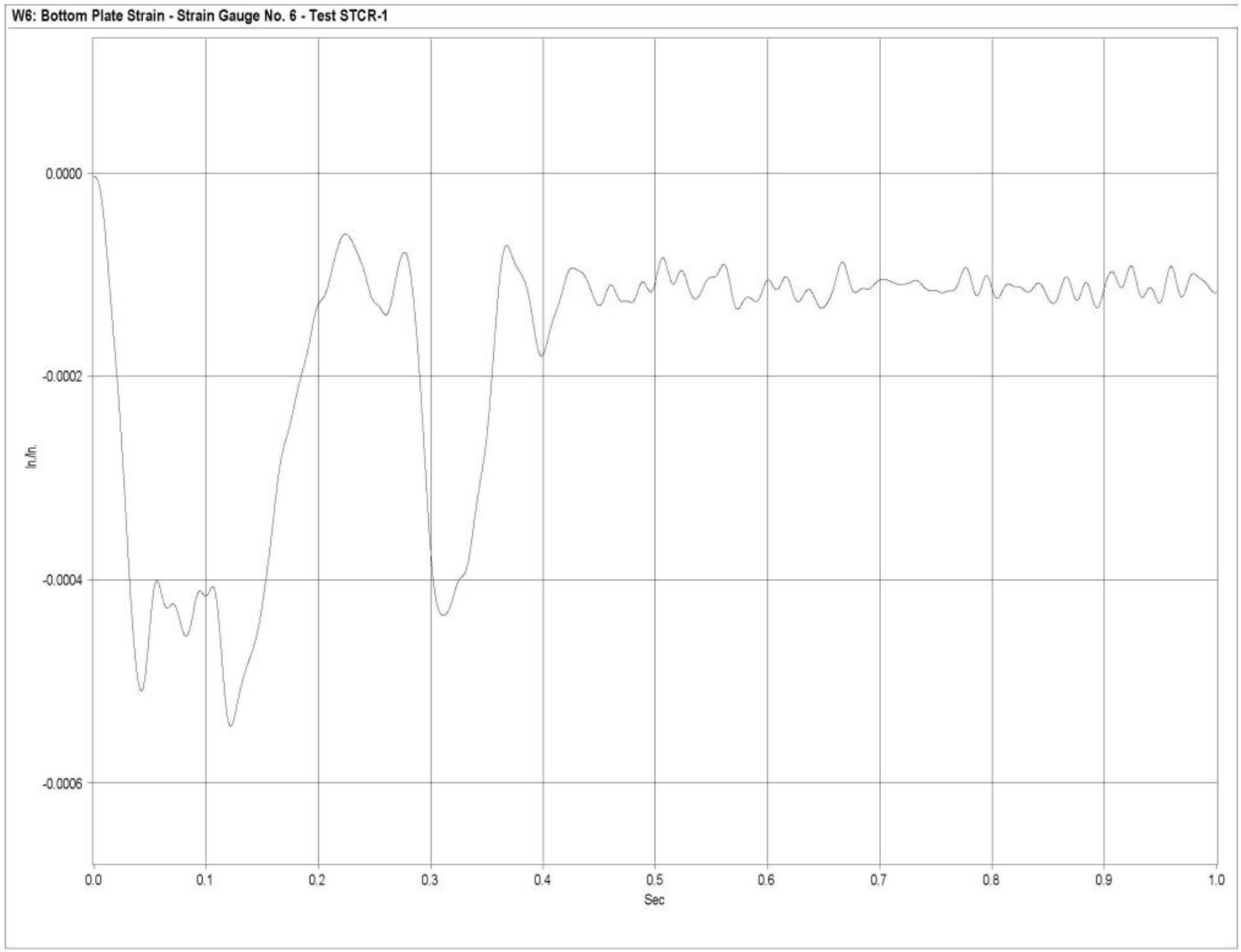

Figure G-11. Graph of Bottom Plate Post No. 5 - Stain Gauge No. 6 Perpendicular to Rail - Strain, Test STCR-1

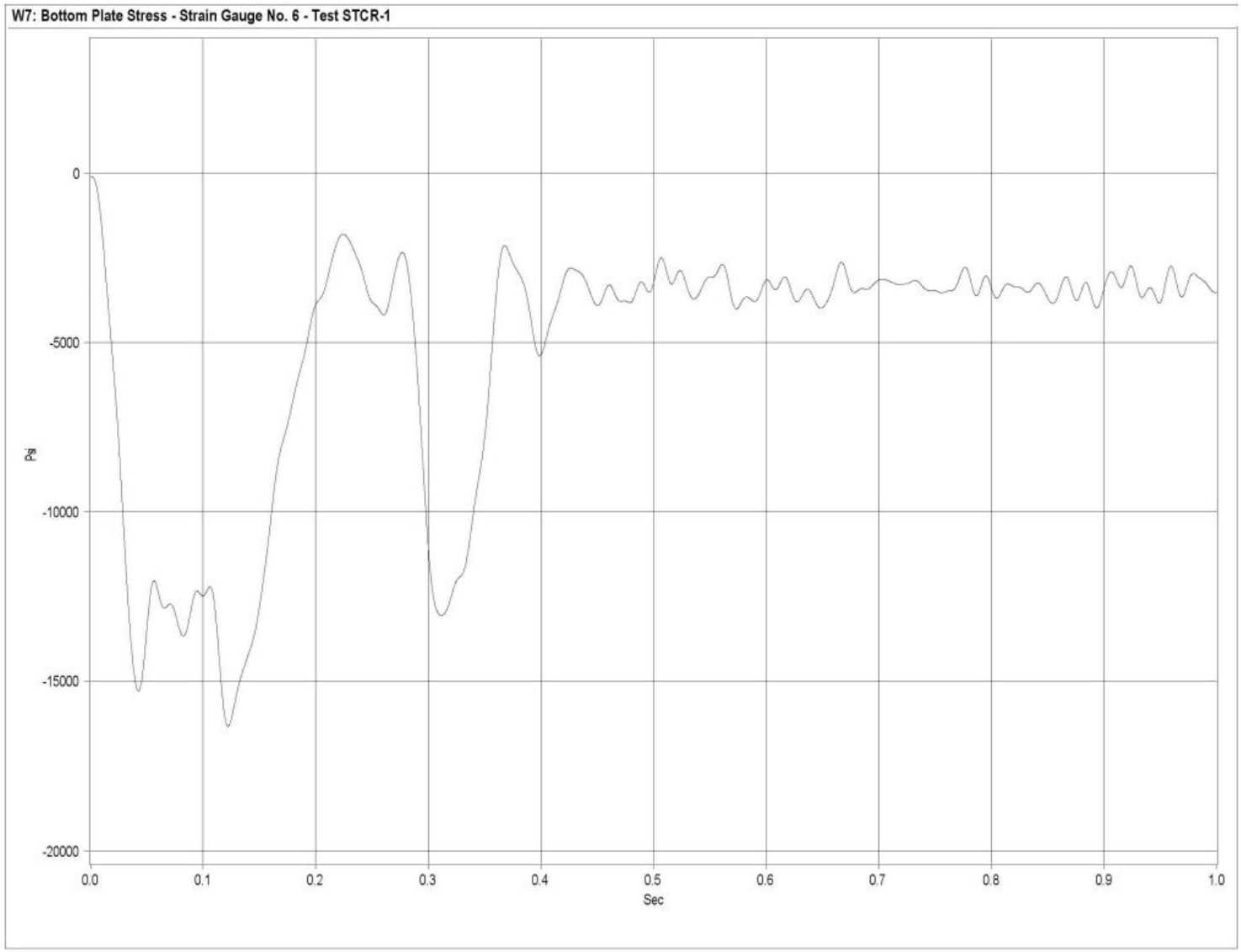

Figure G-12. Graph of Bottom Plate Post No. 5 - Stain Gauge No. 6 Perpendicular to Rail - Stress, Test STCR-1

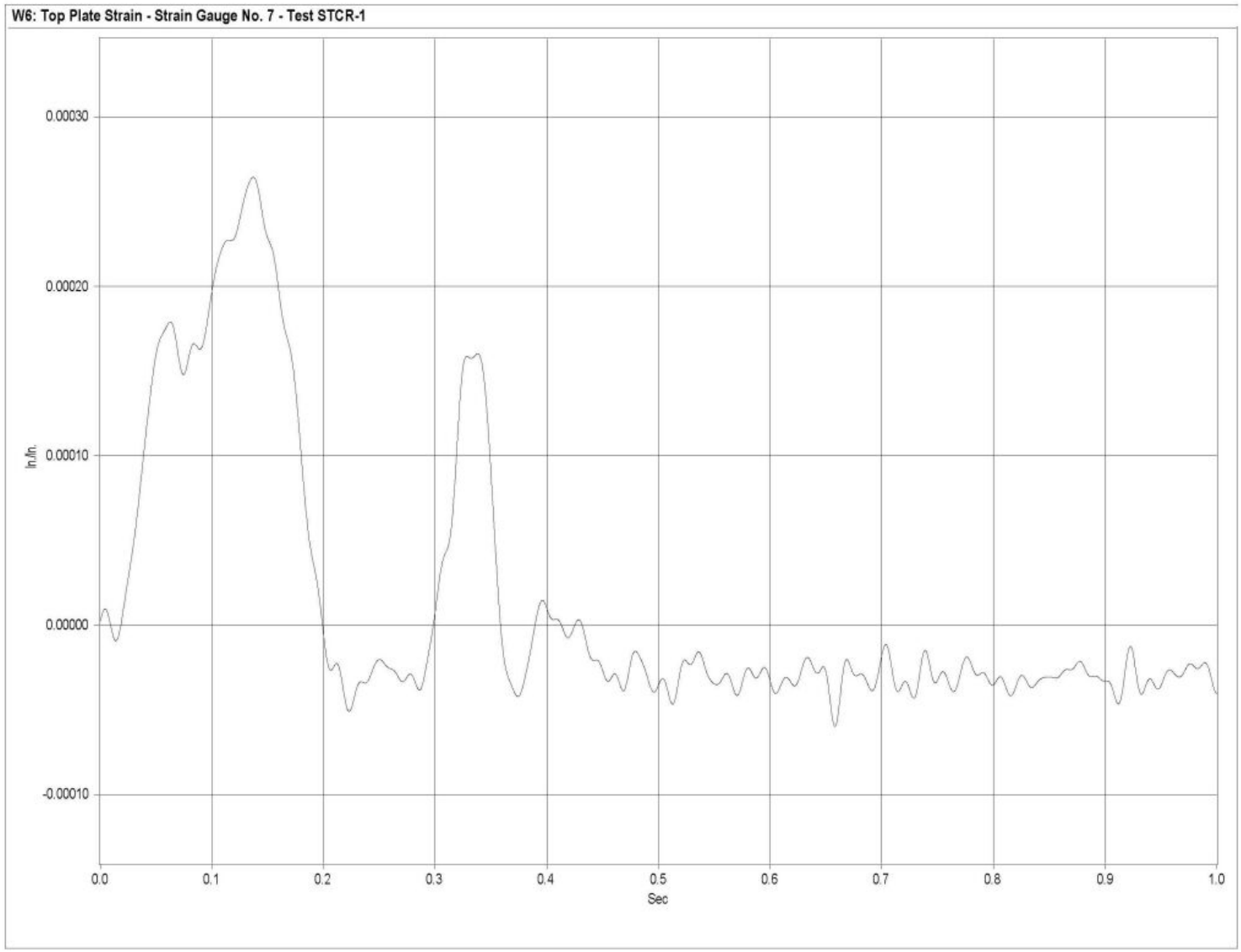

Figure G-13. Graph of Top Plate Post No. 6 - Stain Gauge No. 7 Perpendicular to Rail - Strain, Test STCR-1

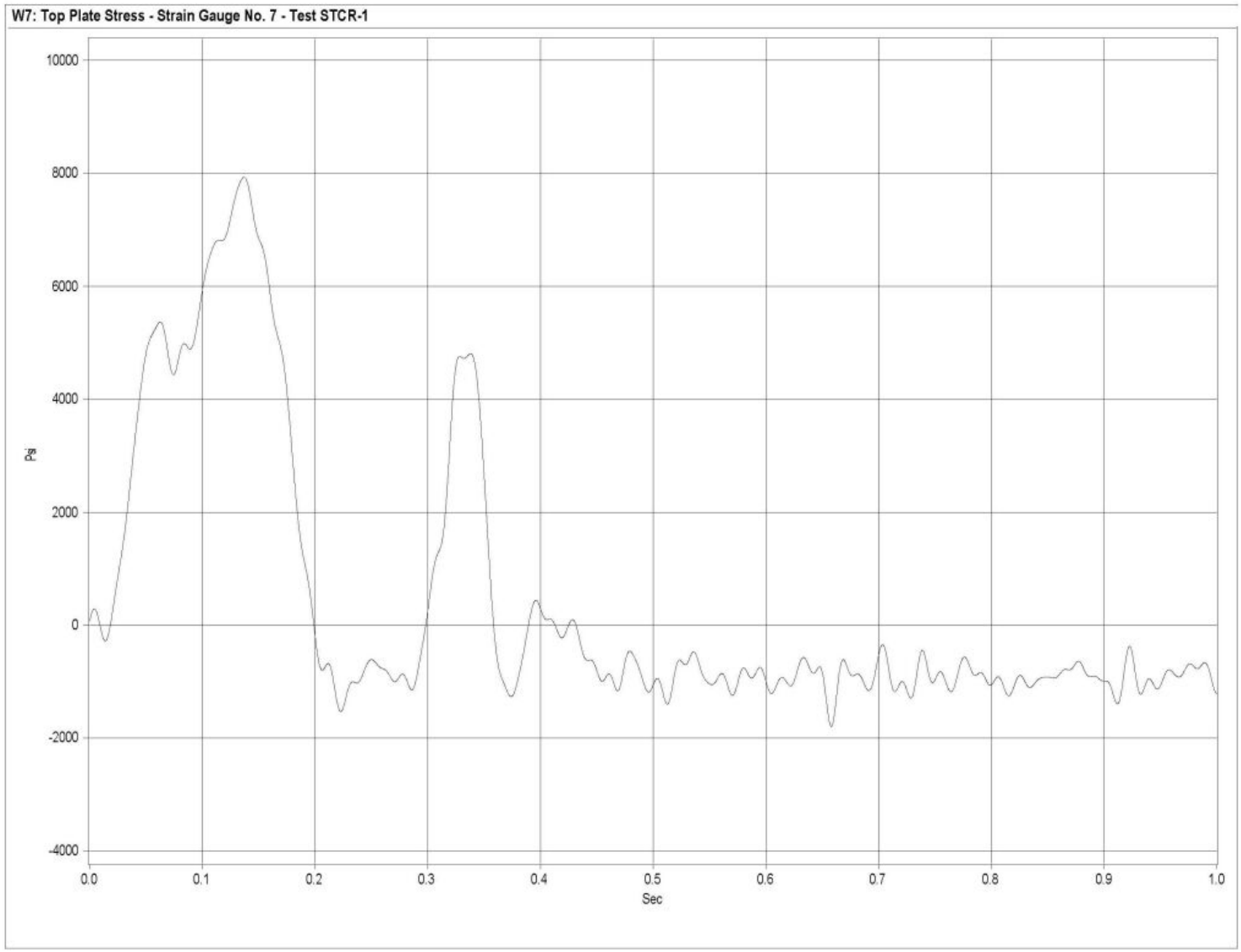

Figure G-14. Graph of Top Plate Post No. 6 - Stain Gauge No. 7 Perpendicular to Rail - Stress, Test STCR-1

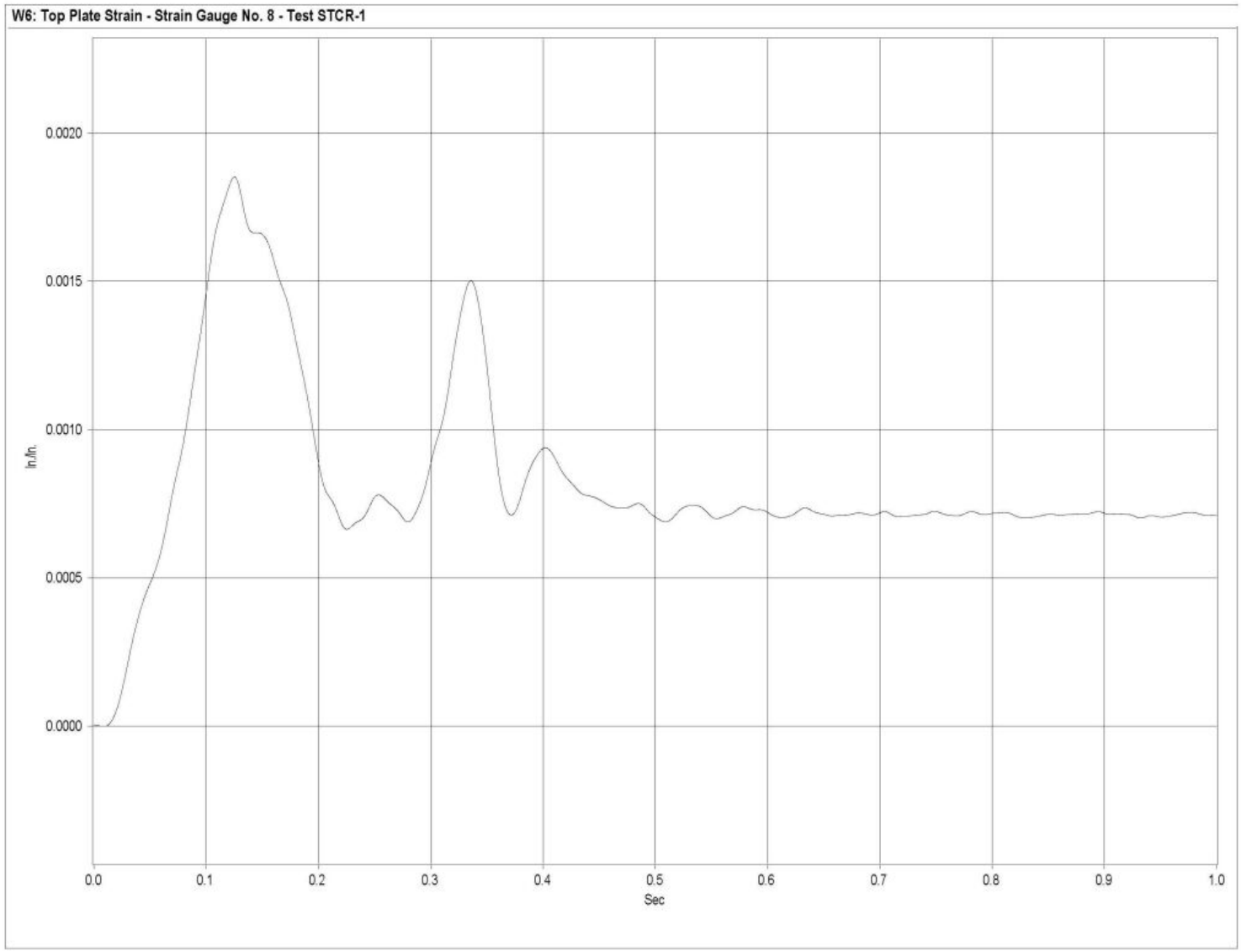

Figure G-15. Graph of Top Plate Post No. 6 - Stain Gauge No. 8 Perpendicular to Rail - Strain, Test STCR-1

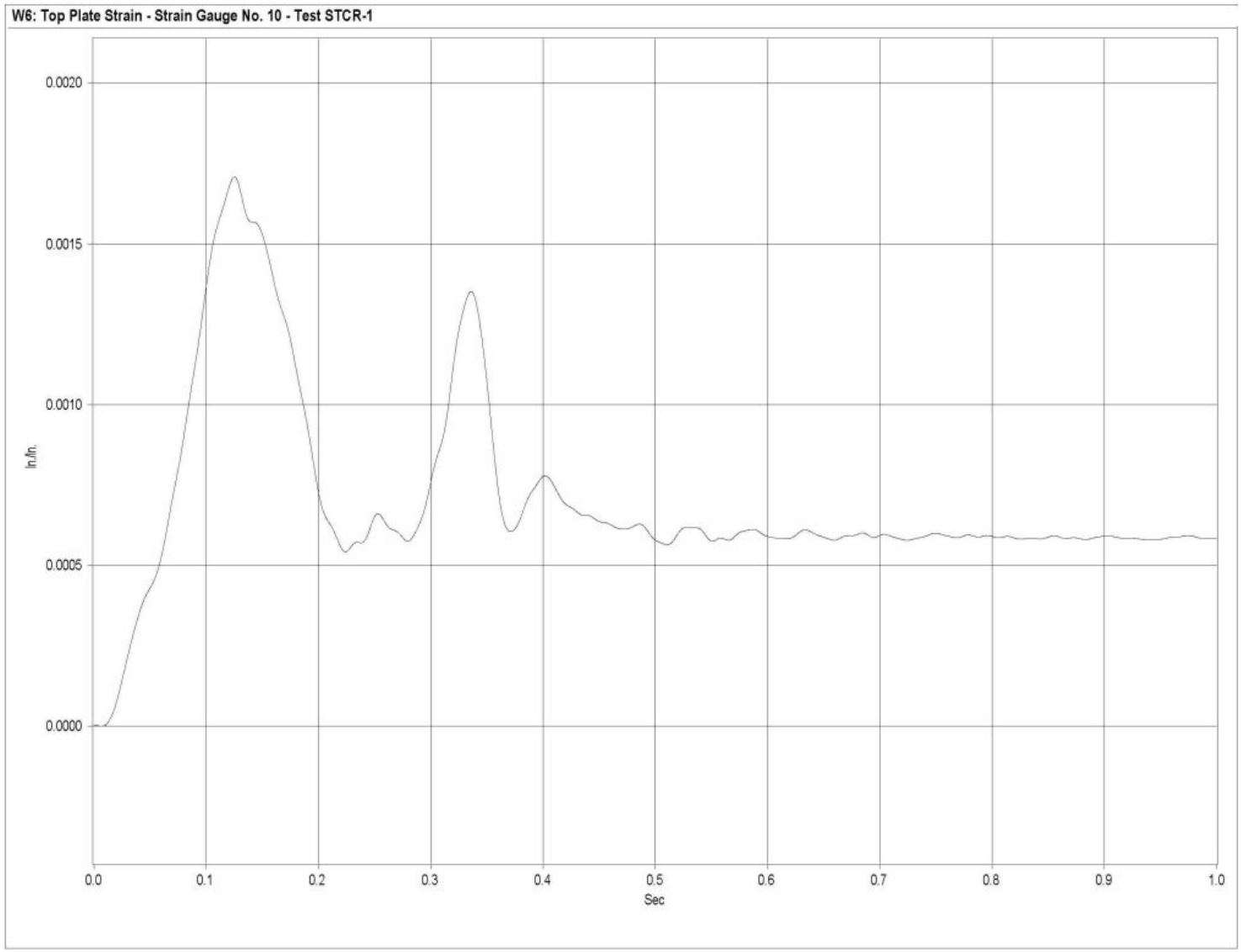

Figure G-16. Graph of Top Plate Post No. 6 - Stain Gauge No. 10 Perpendicular to Rail - Strain, Test STCR-1

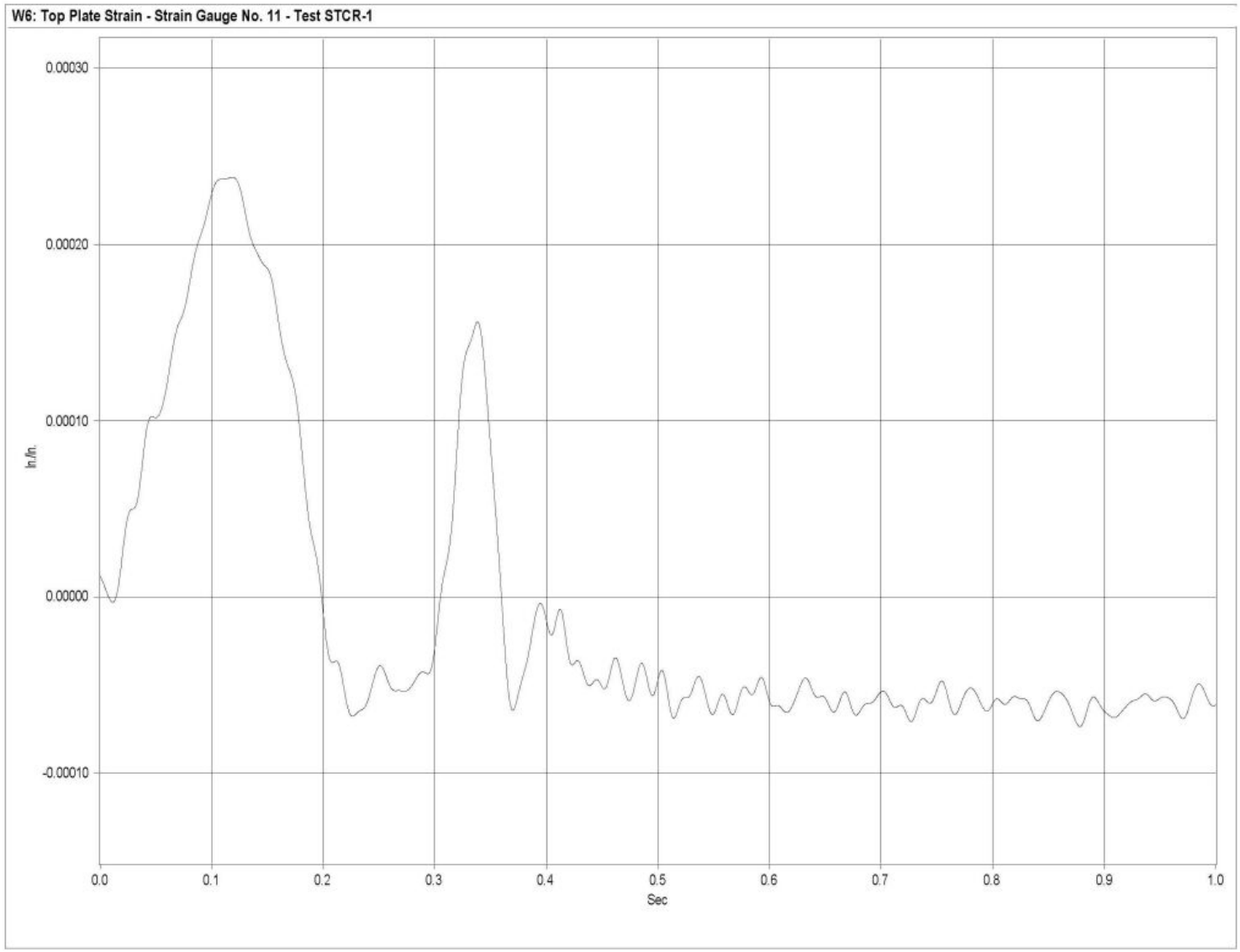

Figure G-17. Graph of Top Plate Post No. 6 - Stain Gauge No. 11 Perpendicular to Rail - Strain, Test STCR-1

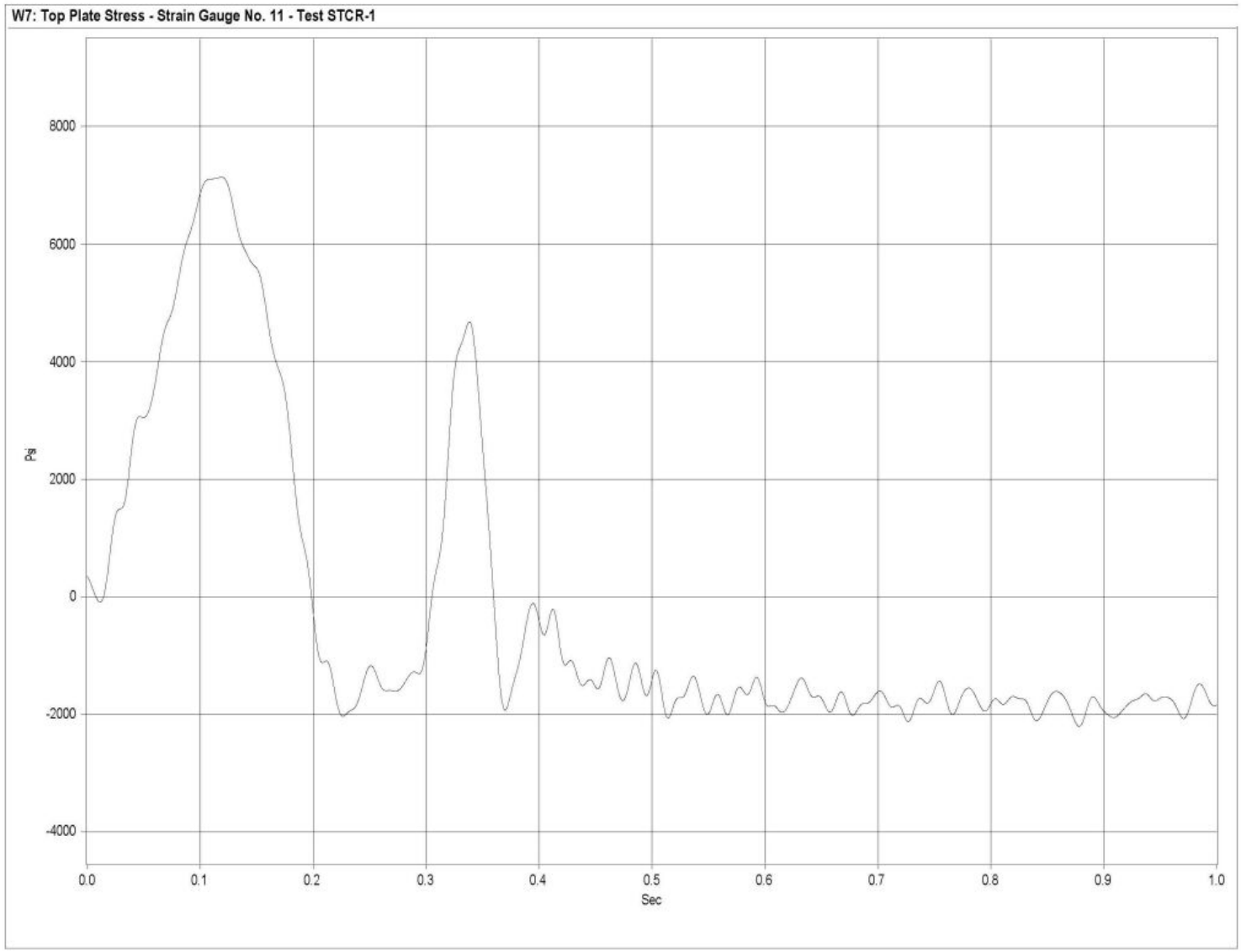

Figure G-18. Graph of Top Plate Post No. 6 - Stain Gauge No. 11 Perpendicular to Rail - Stress, Test STCR-1

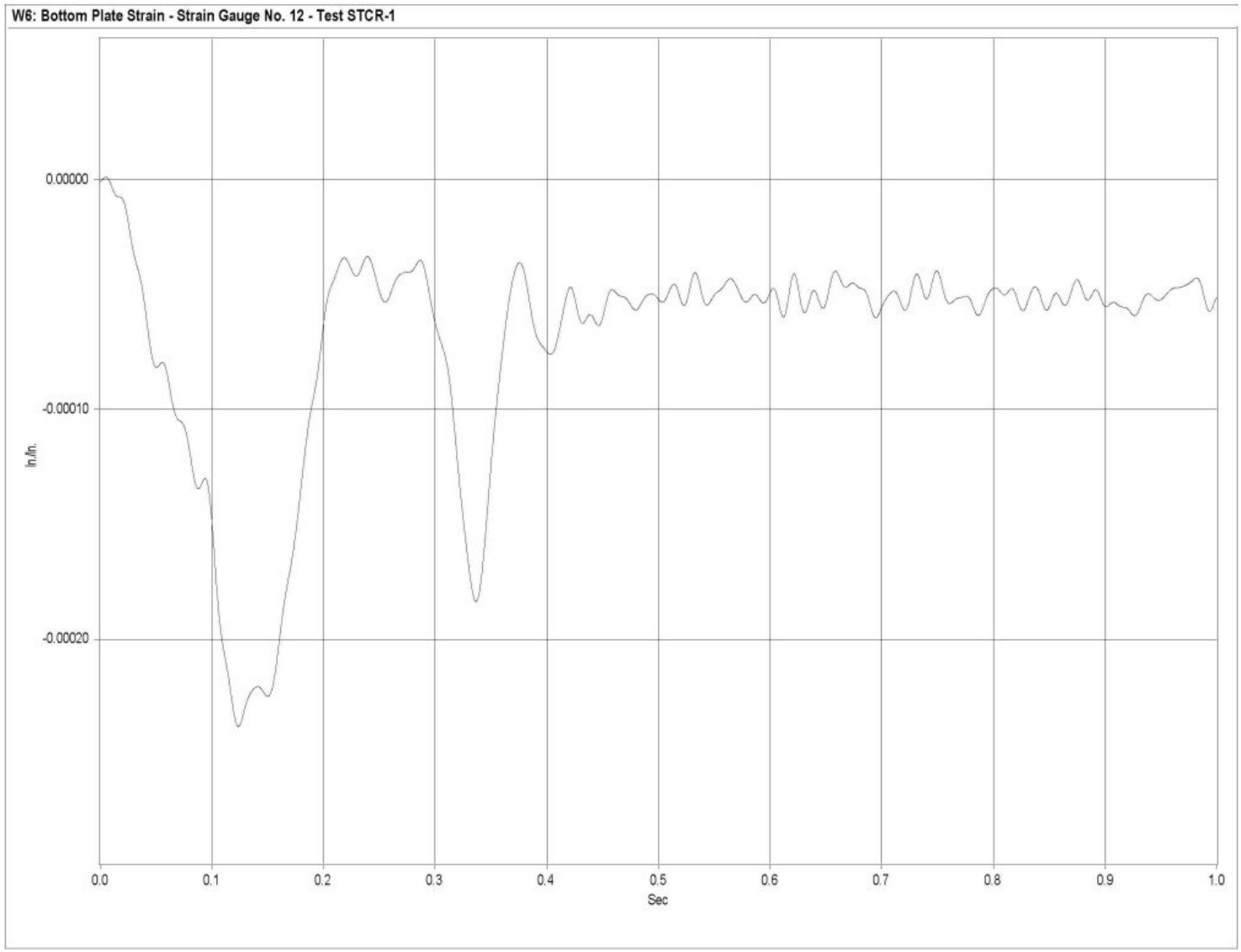

Figure G-19. Graph of Bottom Plate Post No. 6 - Stain Gauge No. 12 Perpendicular to Rail - Strain, Test STCR-1

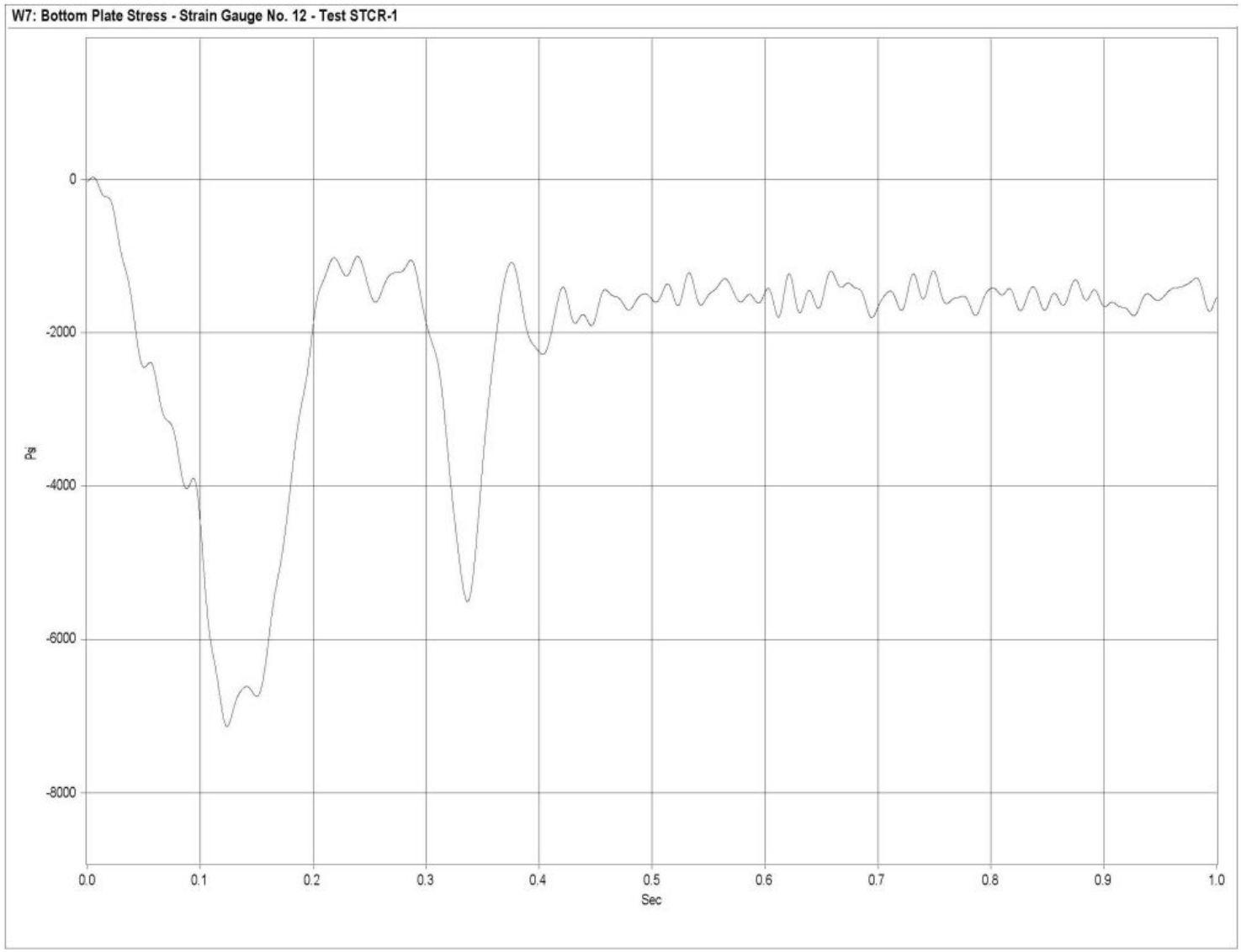

Figure G-20. Graph of Bottom Plate Post No. 6 - Stain Gauge No. 12 Perpendicular to Rail - Stress, Test STCR-1

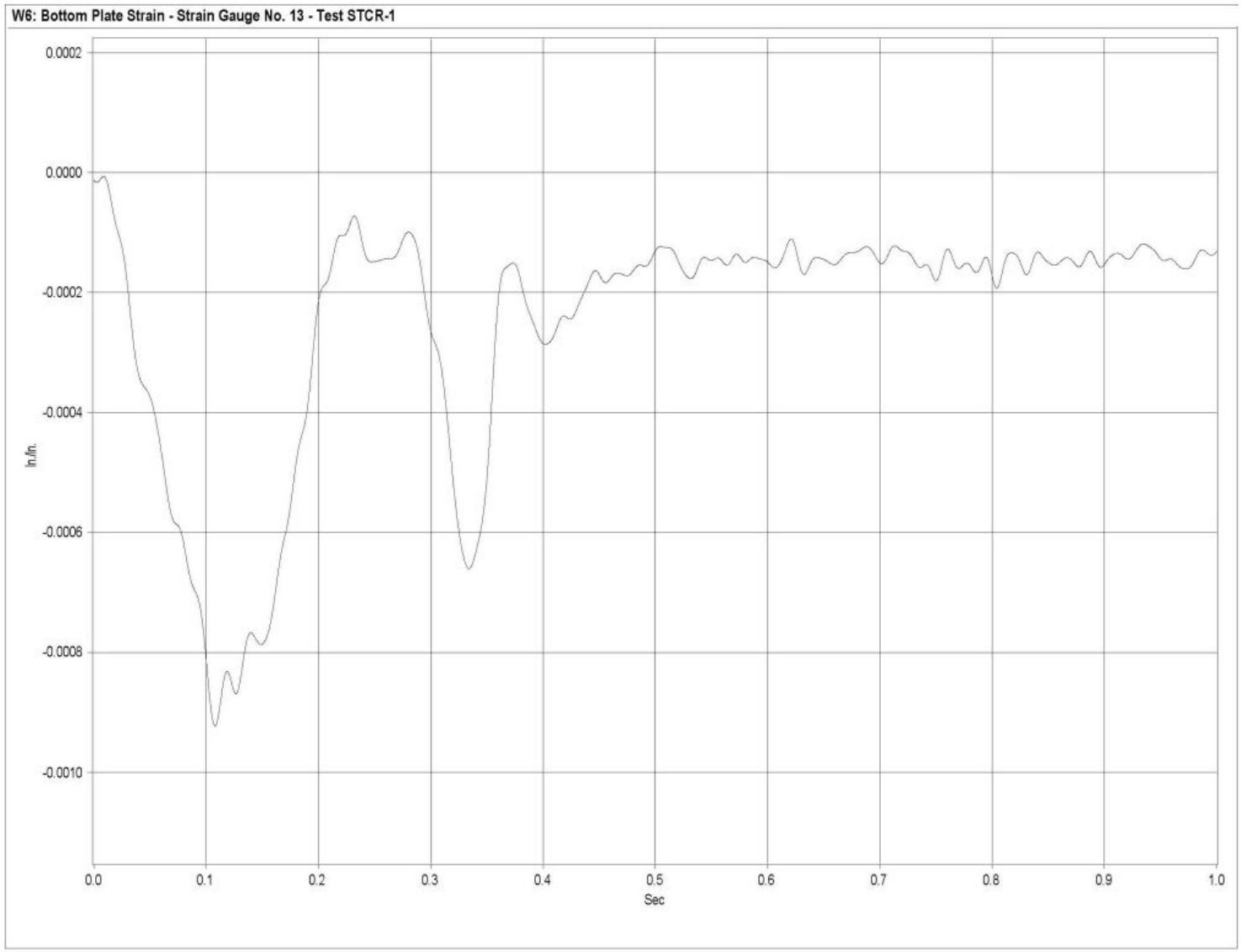

Figure G-21. Graph of Bottom Plate Post No. 6 - Stain Gauge No. 13 Perpendicular to Rail - Strain, Test STCR-1

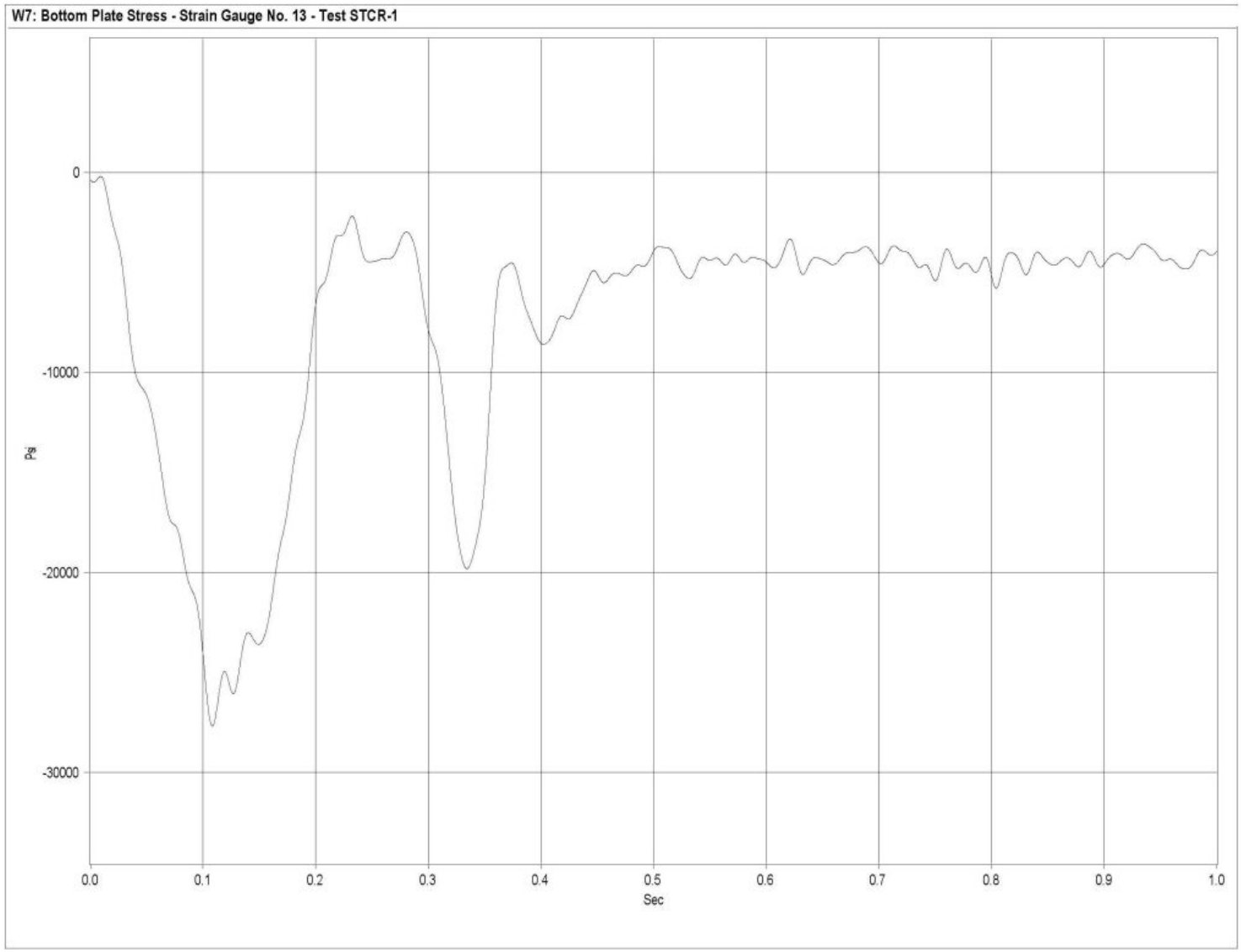

Figure G-22. Graph of Bottom Plate Post No. 6 - Stain Gauge No. 13 Perpendicular to Rail - Stress, Test STCR-1

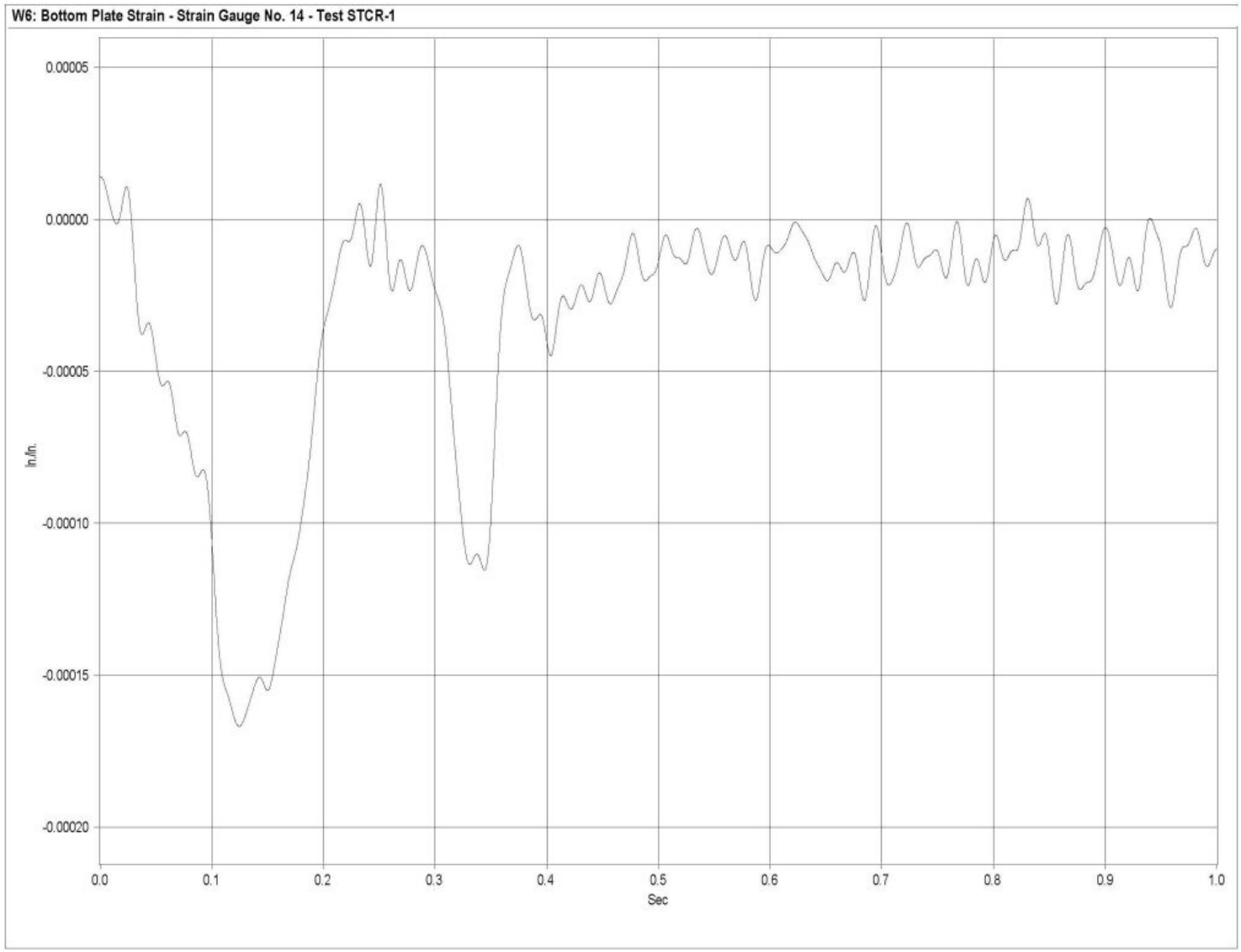

Figure G-23. Graph of Bottom Plate Post No. 5 - Stain Gauge No. 14 Perpendicular to Rail - Strain, Test STCR-1

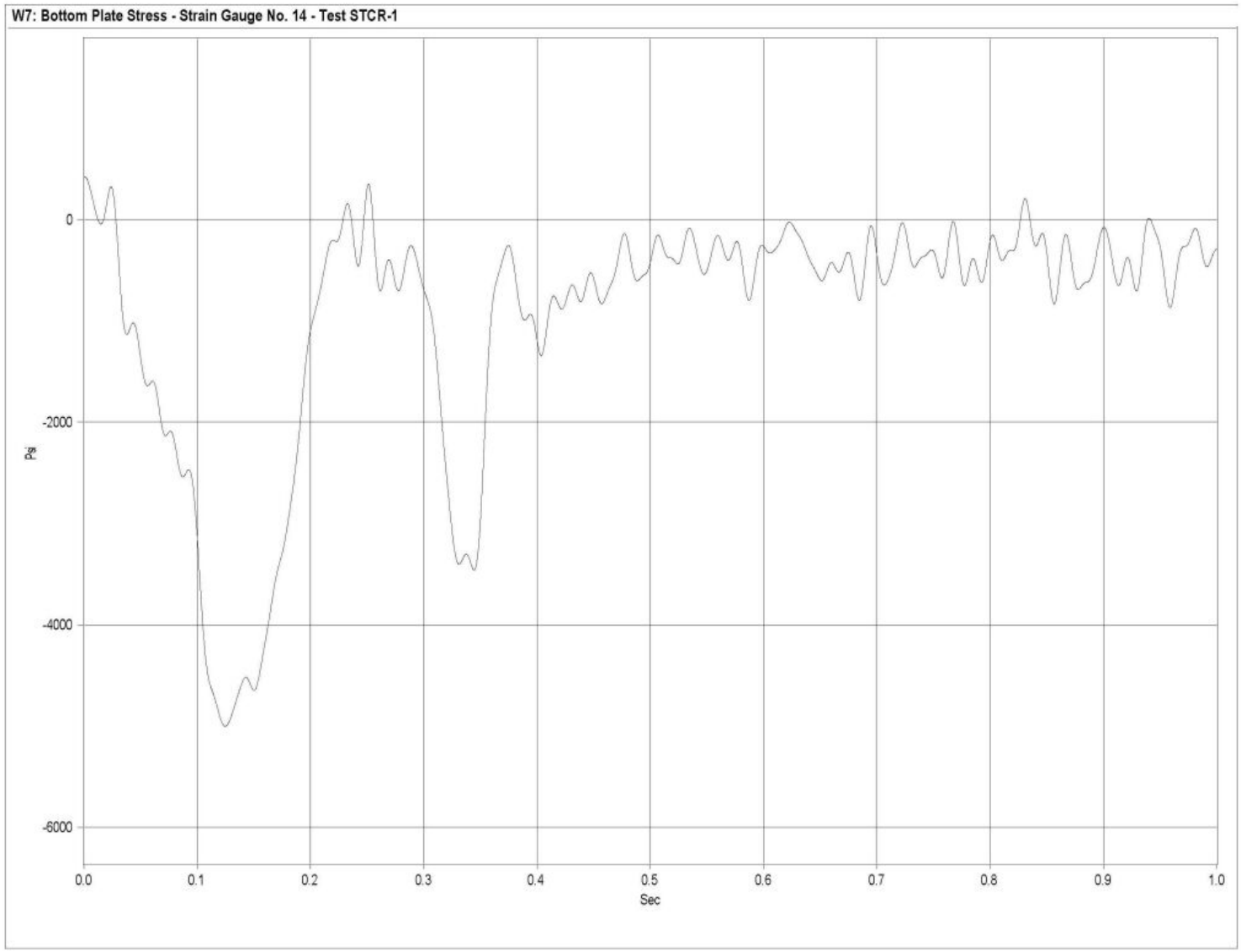

Figure G-24. Graph of Bottom Plate Post No. 6 - Stain Gauge No. 14 Perpendicular to Rail - Stress, Test STCR-1

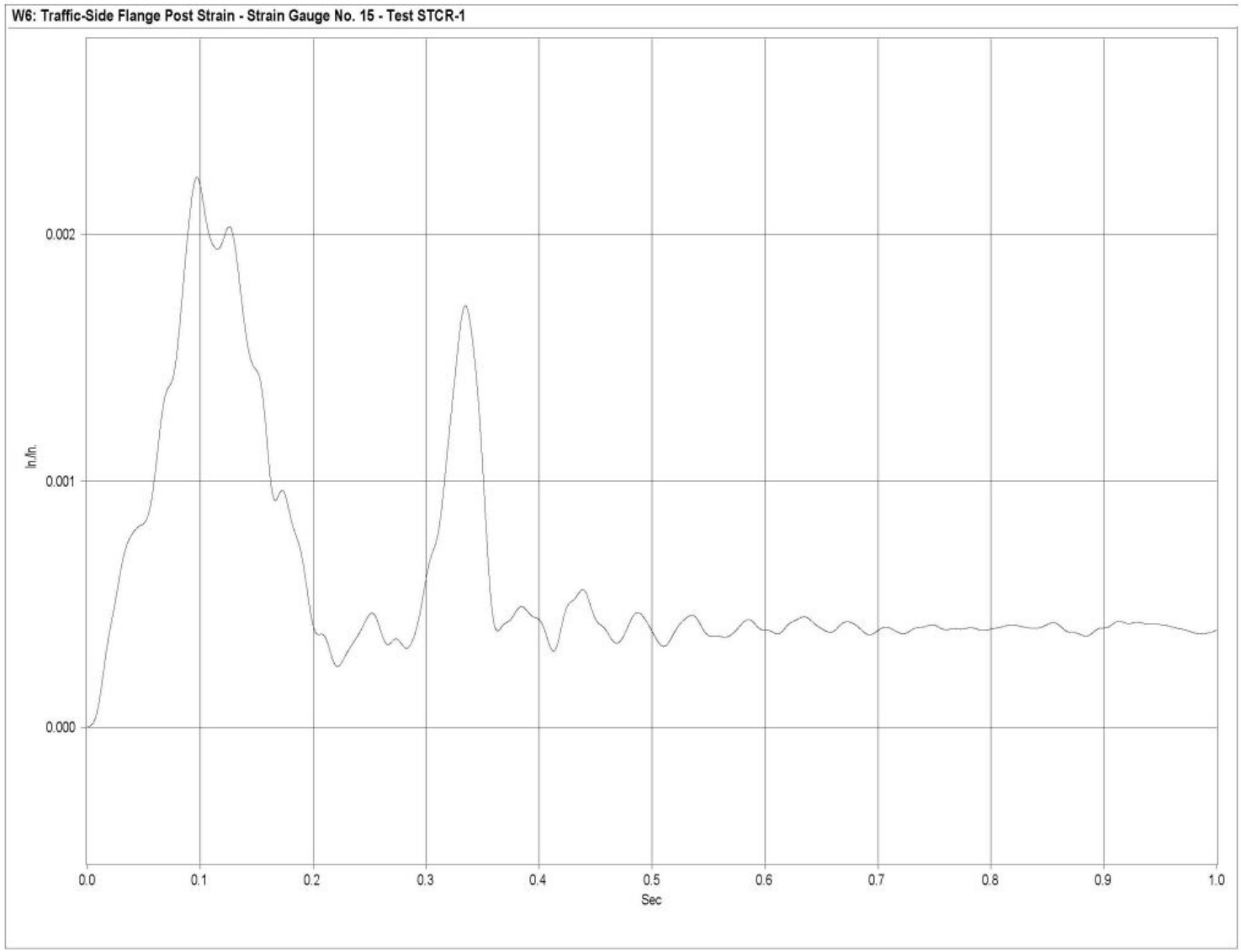

Figure G-25. Graph of Traffic-Side Flange Post No. 6 - Stain Gauge No. 15 - Strain, Test STCR-1

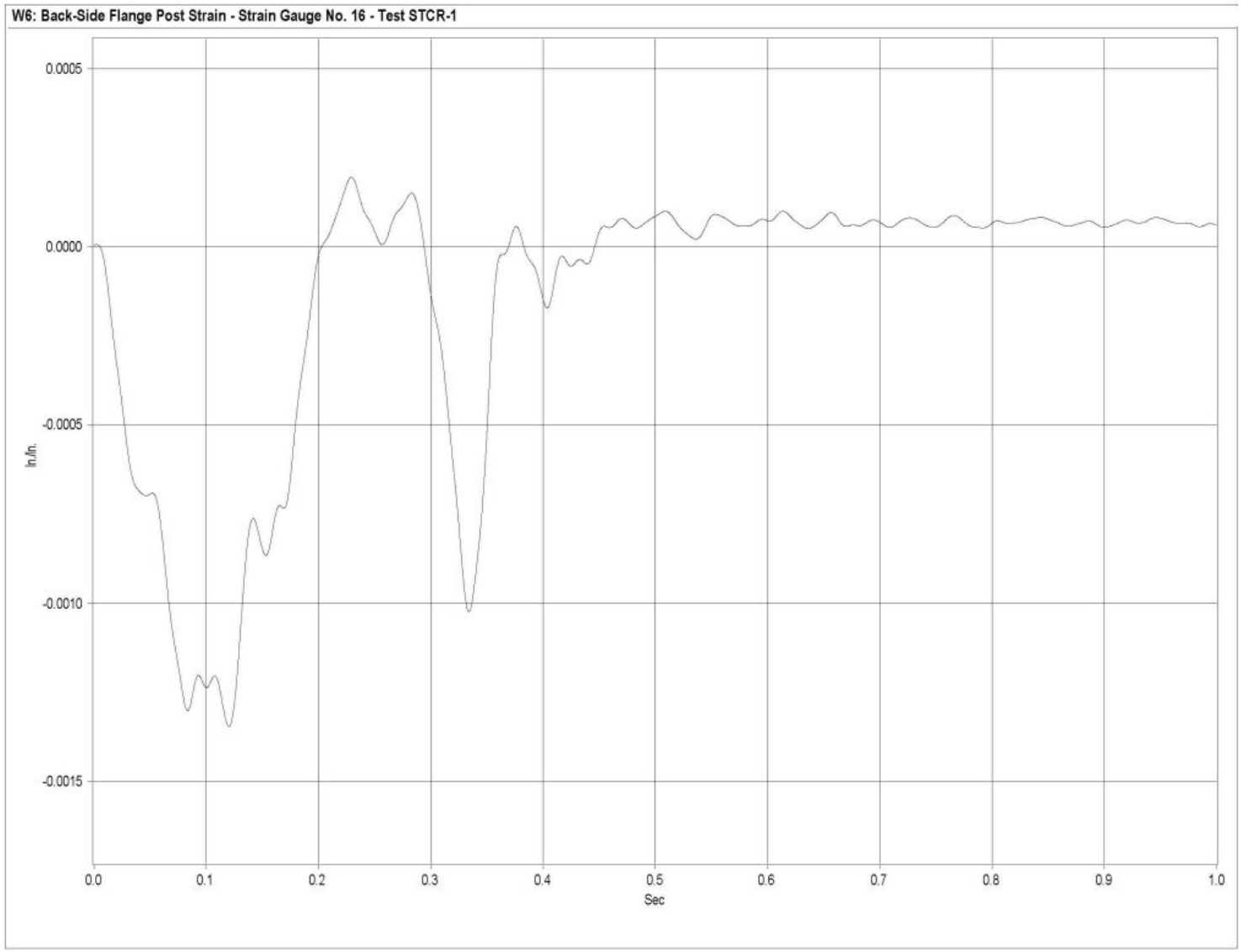

Figure G-26. Graph of Back-Side Flange Post No. 6 - Stain Gauge No. 16 - Strain, Test STCR-1

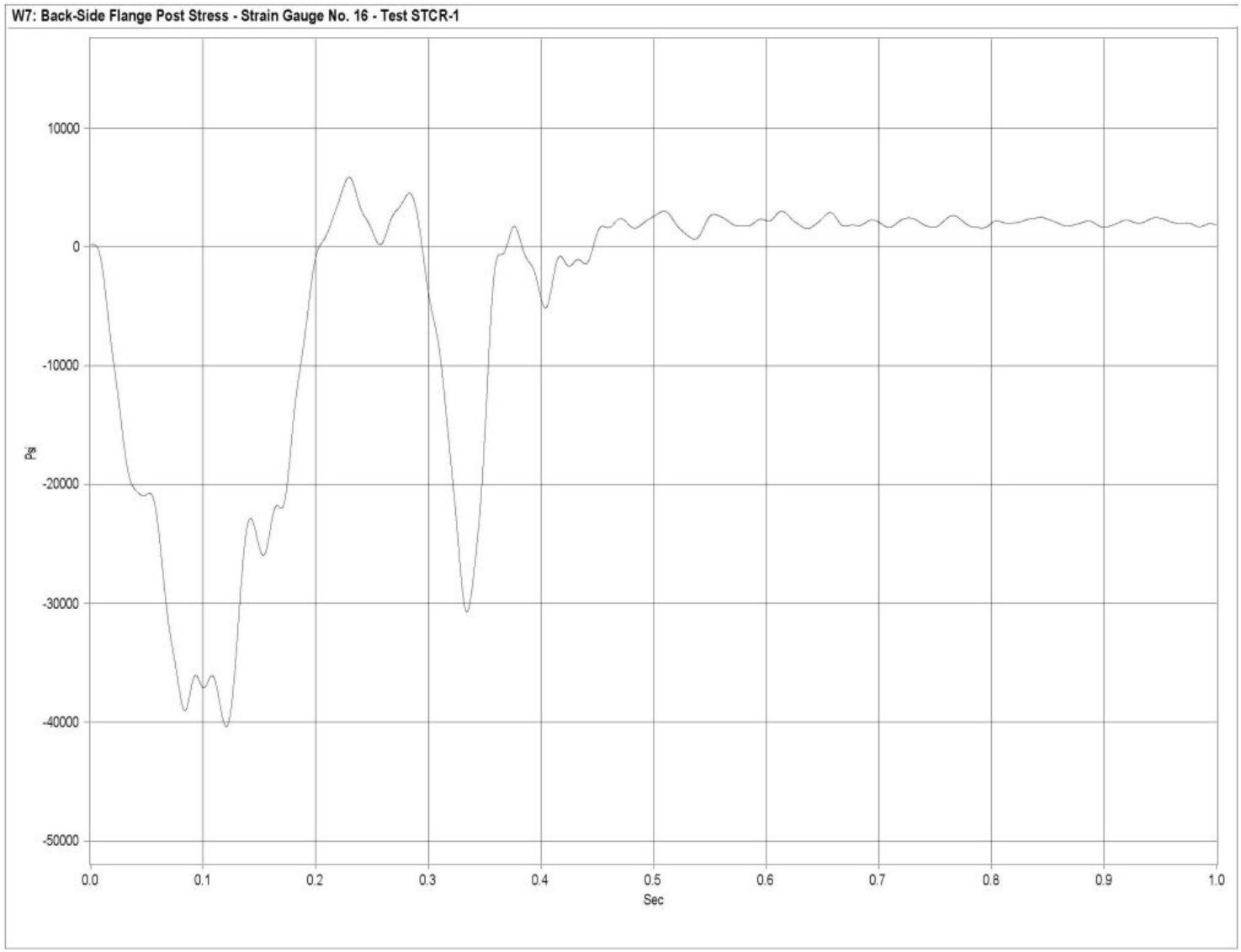

Figure G-27. Graph of Back-Side Flange Post No. 6 - Stain Gauge No. 16 - Stress, Test STCR-1

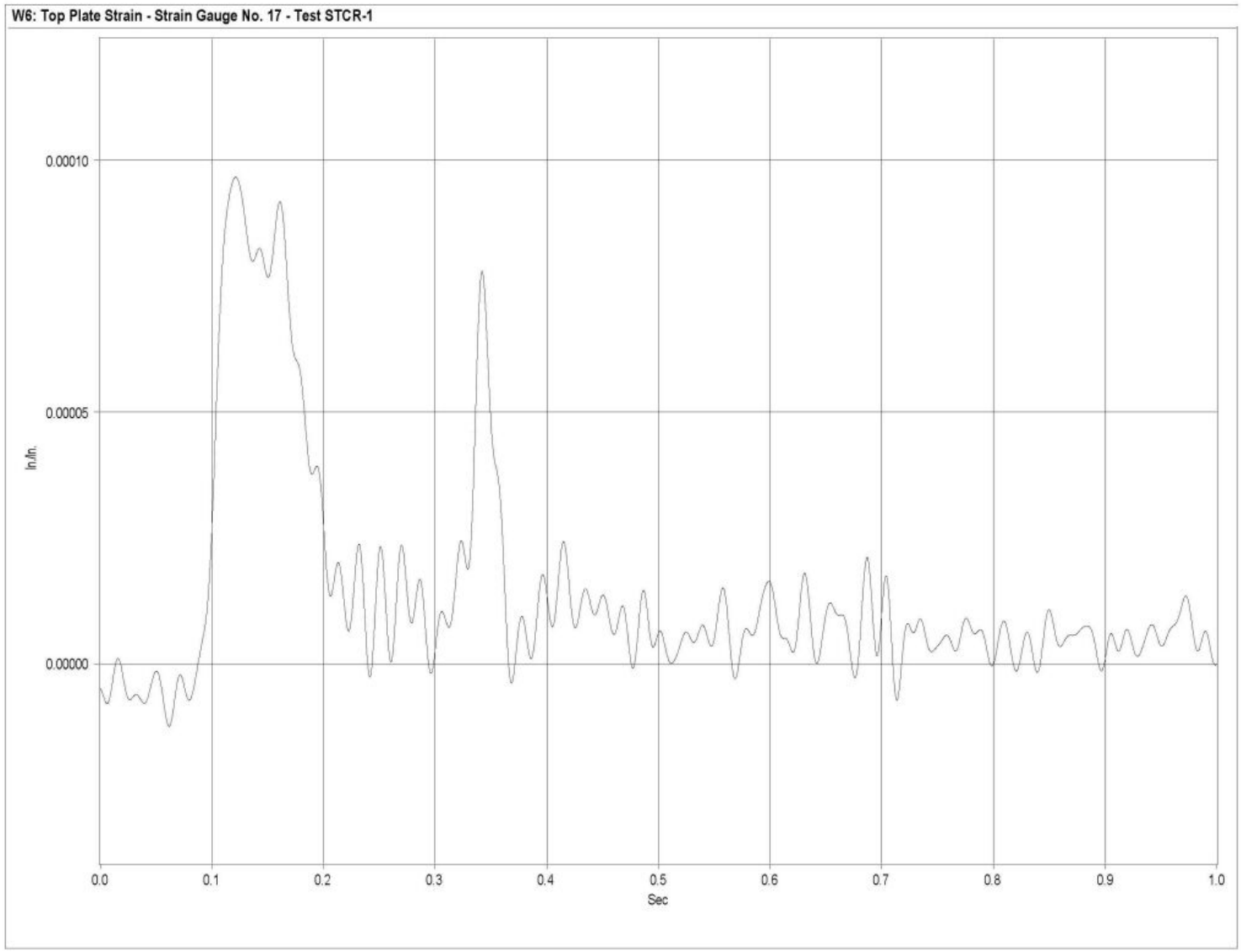

Figure G-28. Graph of Top Plate Post No. 7 - Stain Gauge No. 17 Perpendicular to Rail - Strain, Test STCR-1

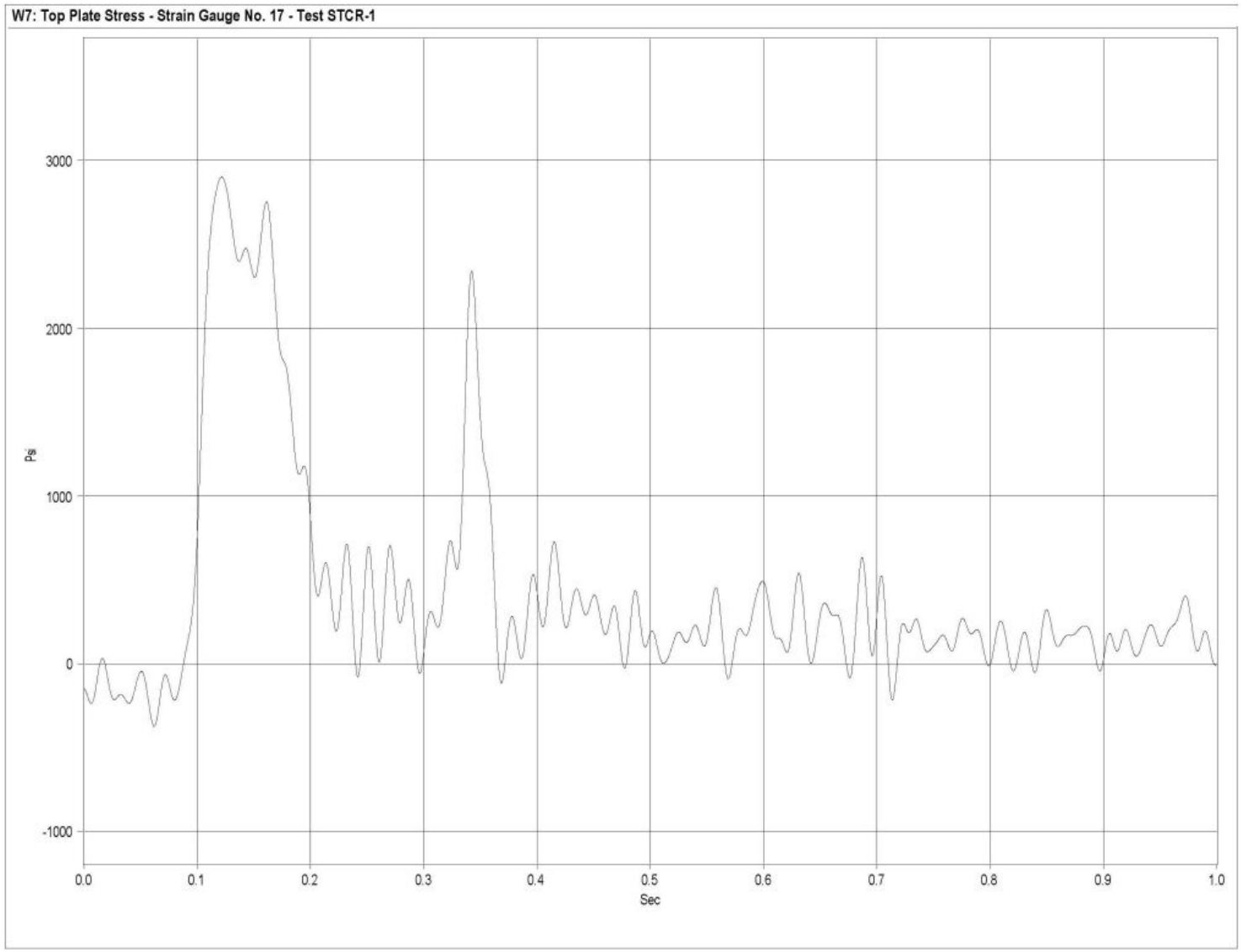

Figure G-29. Graph of Top Plate Post No. 7 - Stain Gauge No. 17 Perpendicular to Rail - Stress, Test STCR-1

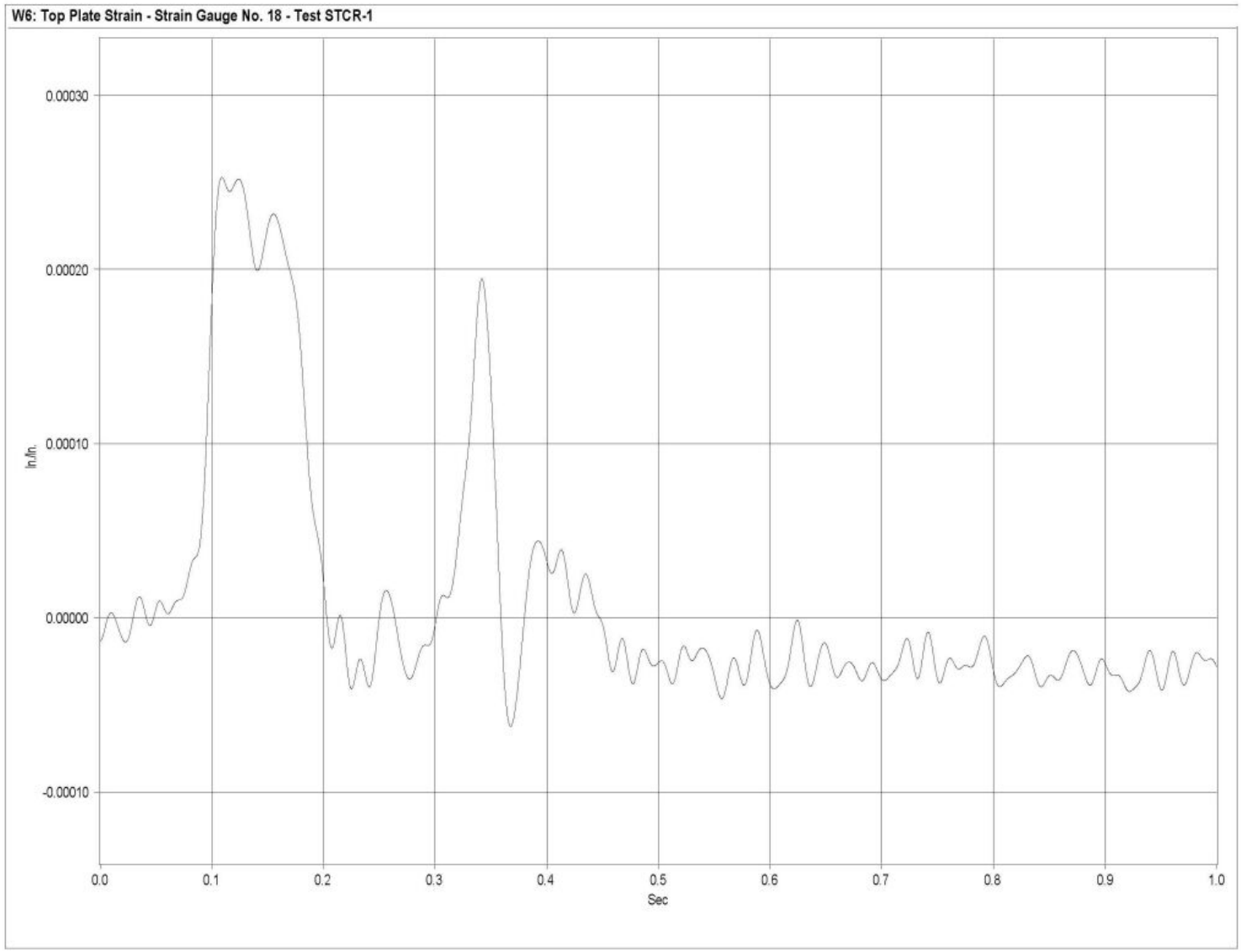

Figure G-30. Graph of Top Plate Post No. 7 - Stain Gauge No. 18 Perpendicular to Rail - Strain, Test STCR-1

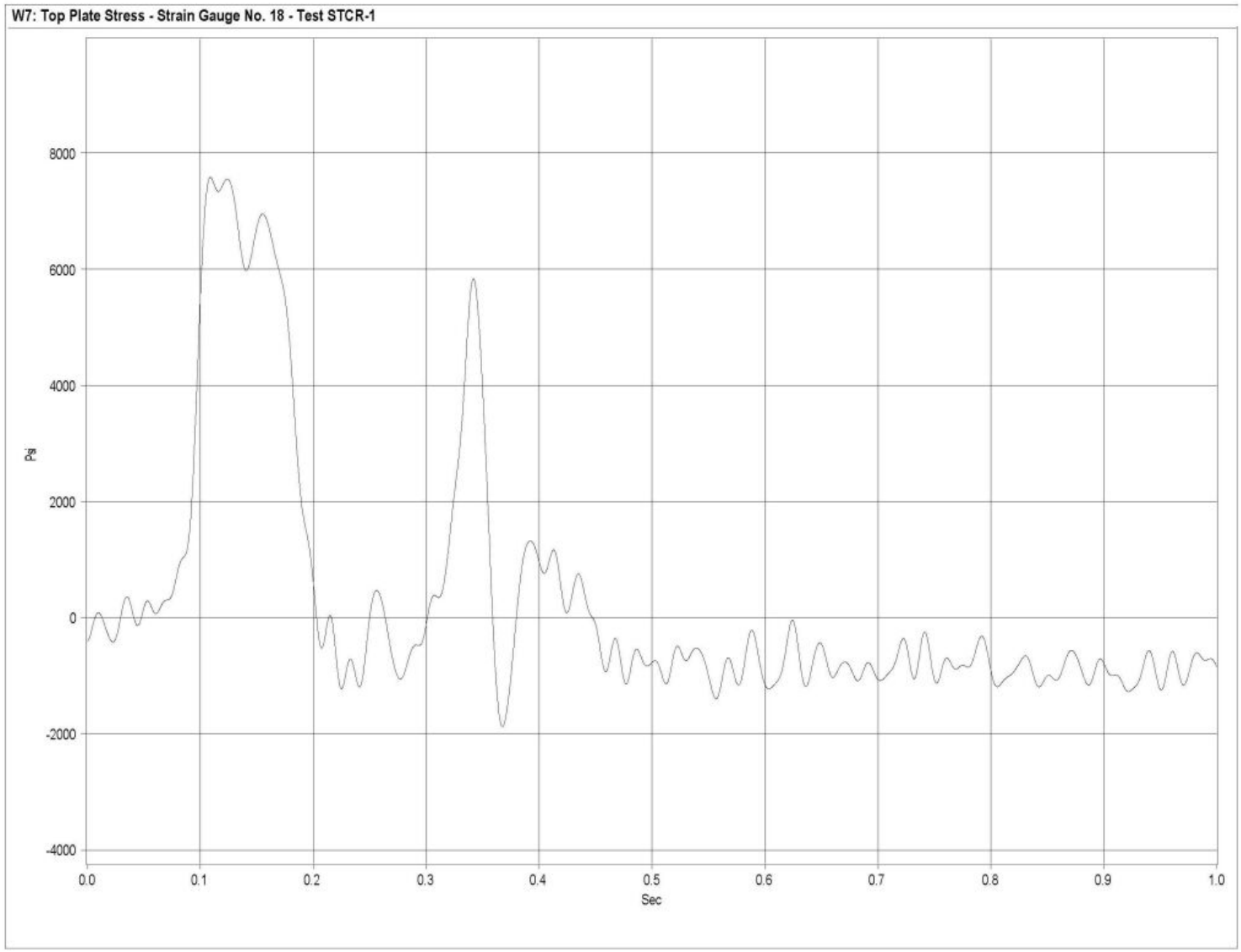

Figure G-31. Graph of Top Plate Post No. 7 - Stain Gauge No. 18 Perpendicular to Rail - Stress, Test STCR-1

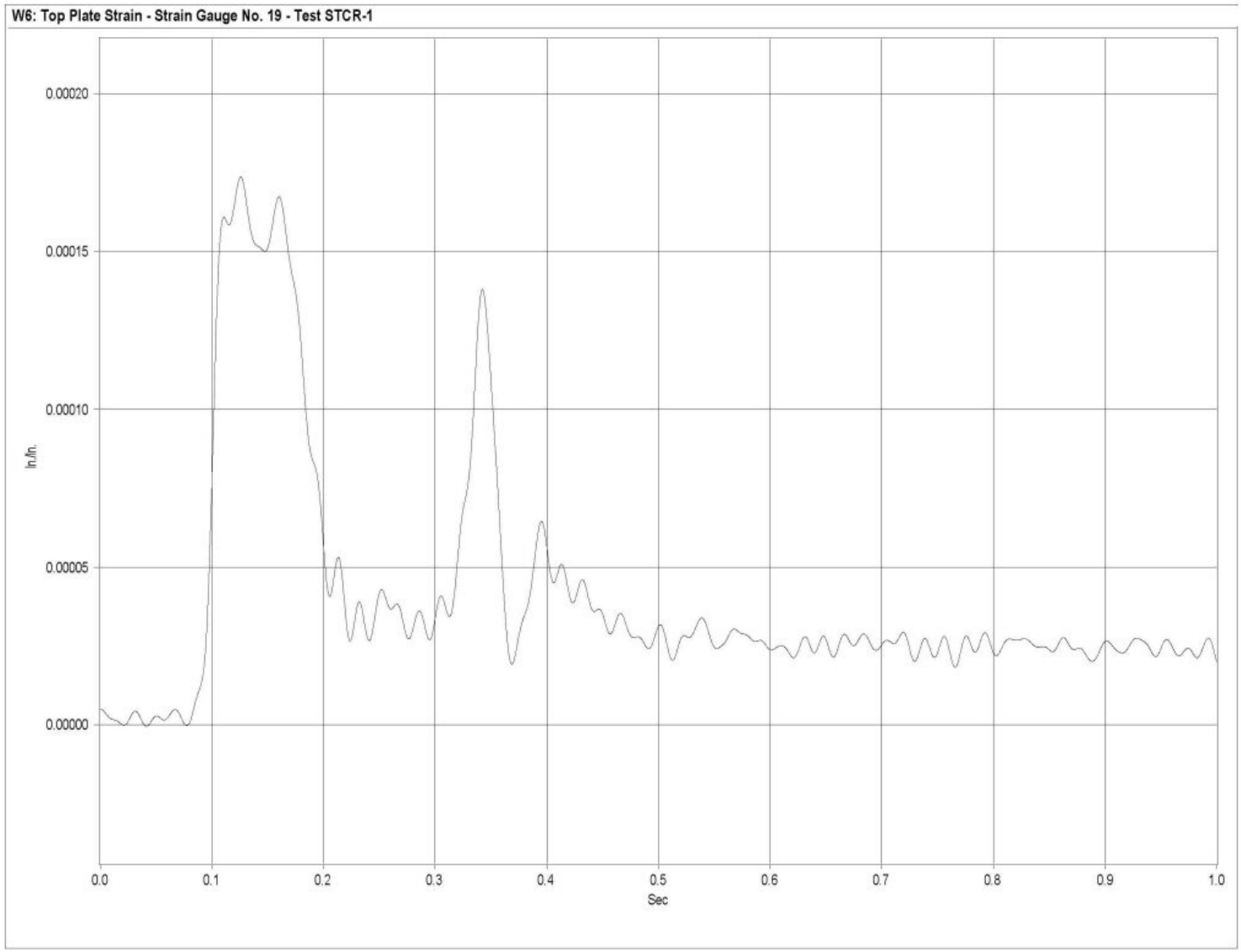

Figure G-32. Graph of Top Plate Post No. 7 - Stain Gauge No. 19 Perpendicular to Rail - Strain, Test STCR-1

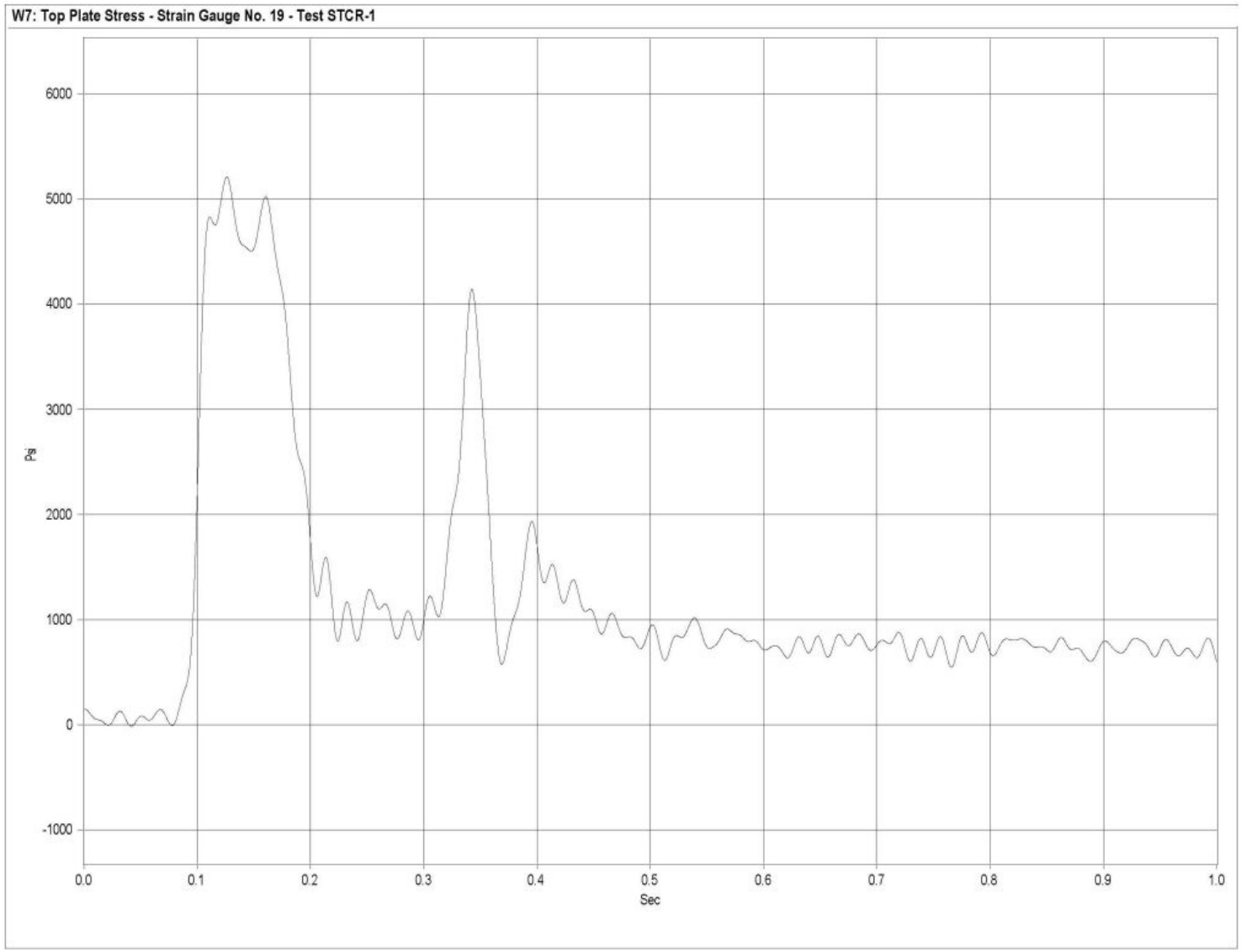

Figure G-33. Graph of Top Plate Post No. 7 - Stain Gauge No. 19 Perpendicular to Rail - Stress, Test STCR-1

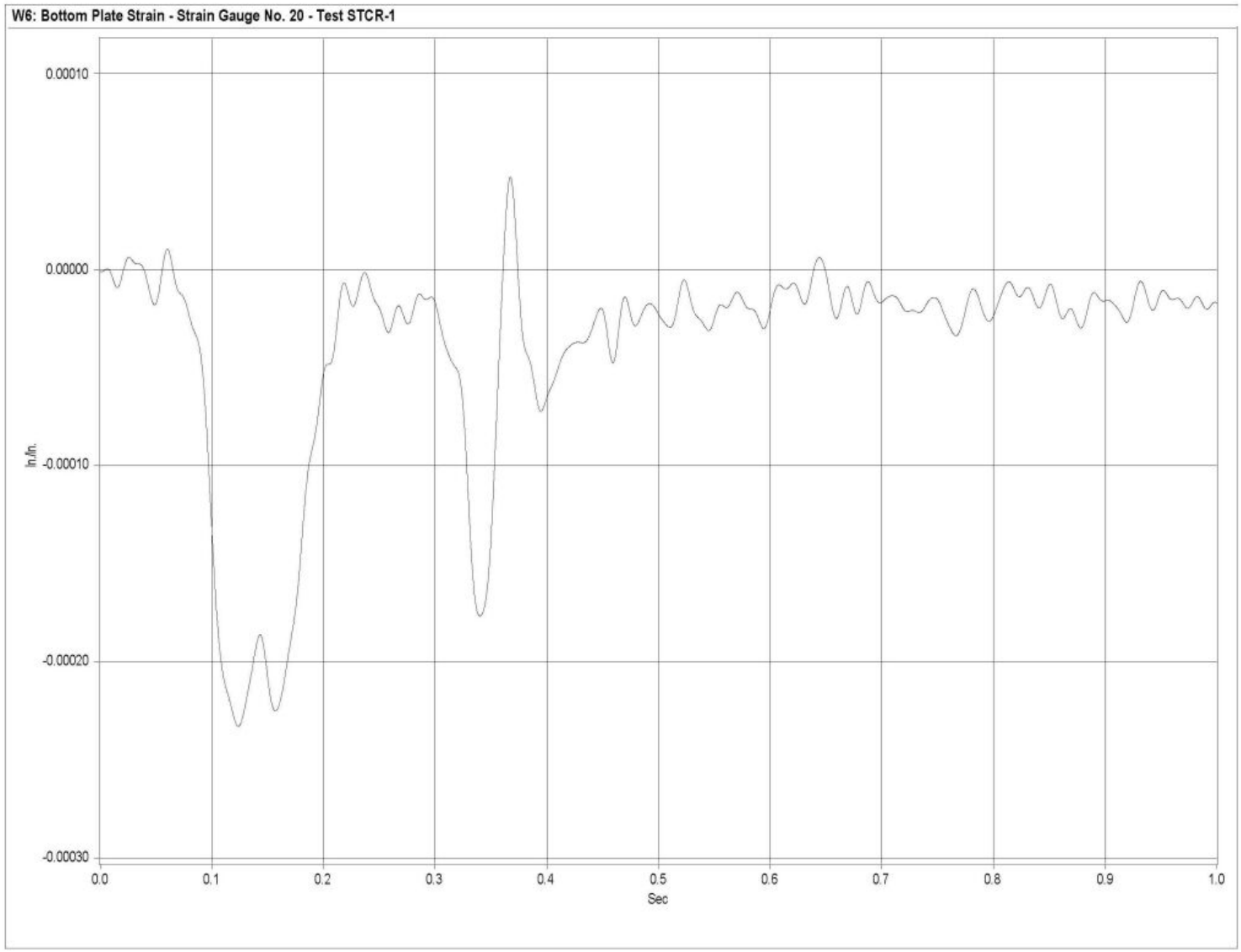

Figure G-34. Graph of Bottom Plate Post No. 7 - Stain Gauge No. 20 Perpendicular to Rail - Strain, Test STCR-1

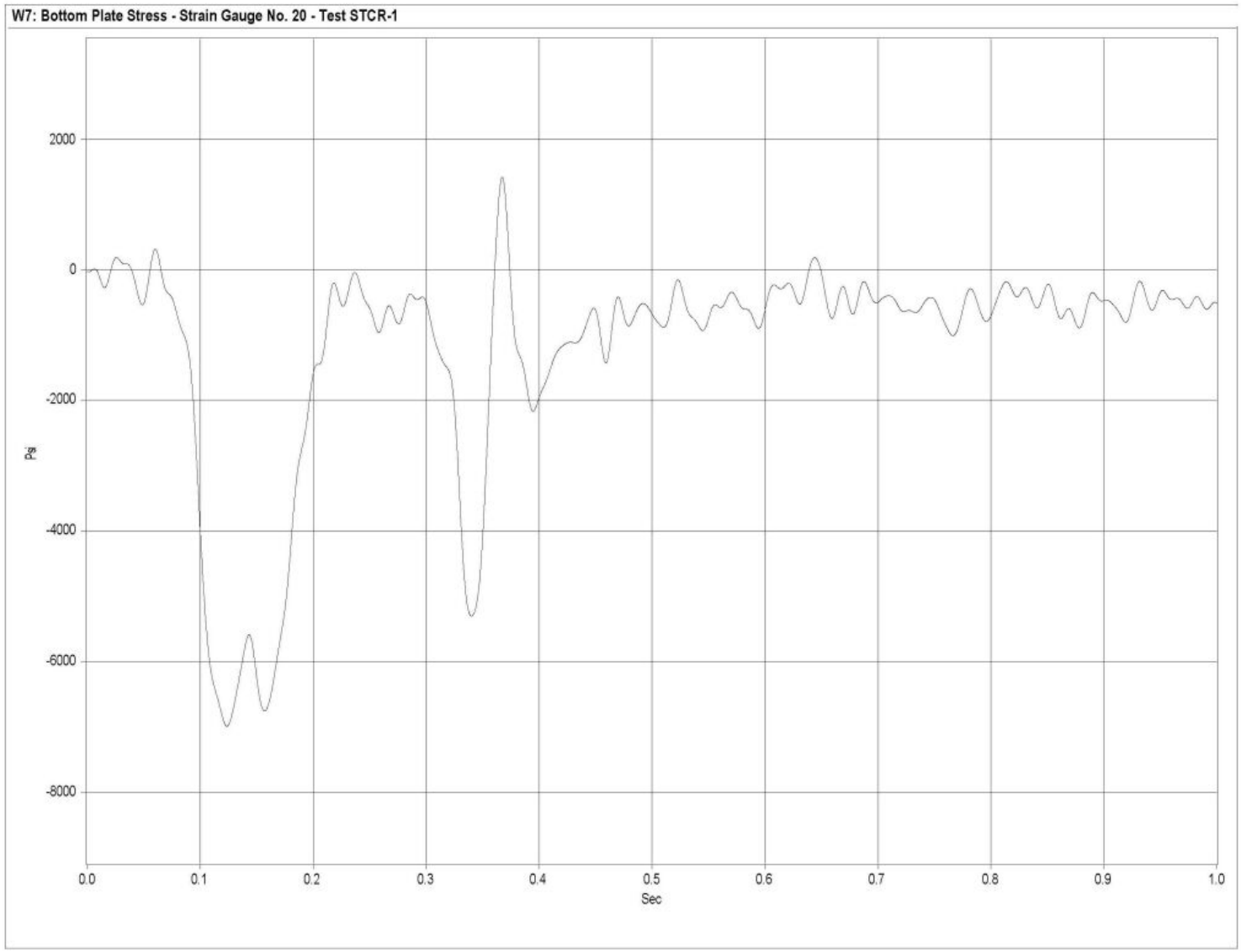

Figure G-35. Graph of Bottom Plate Post No. 7 - Stain Gauge No. 20 Perpendicular to Rail - Stress, Test STCR-1

APPENDIX H

Accelerometer Data Analysis - Test STCR-2

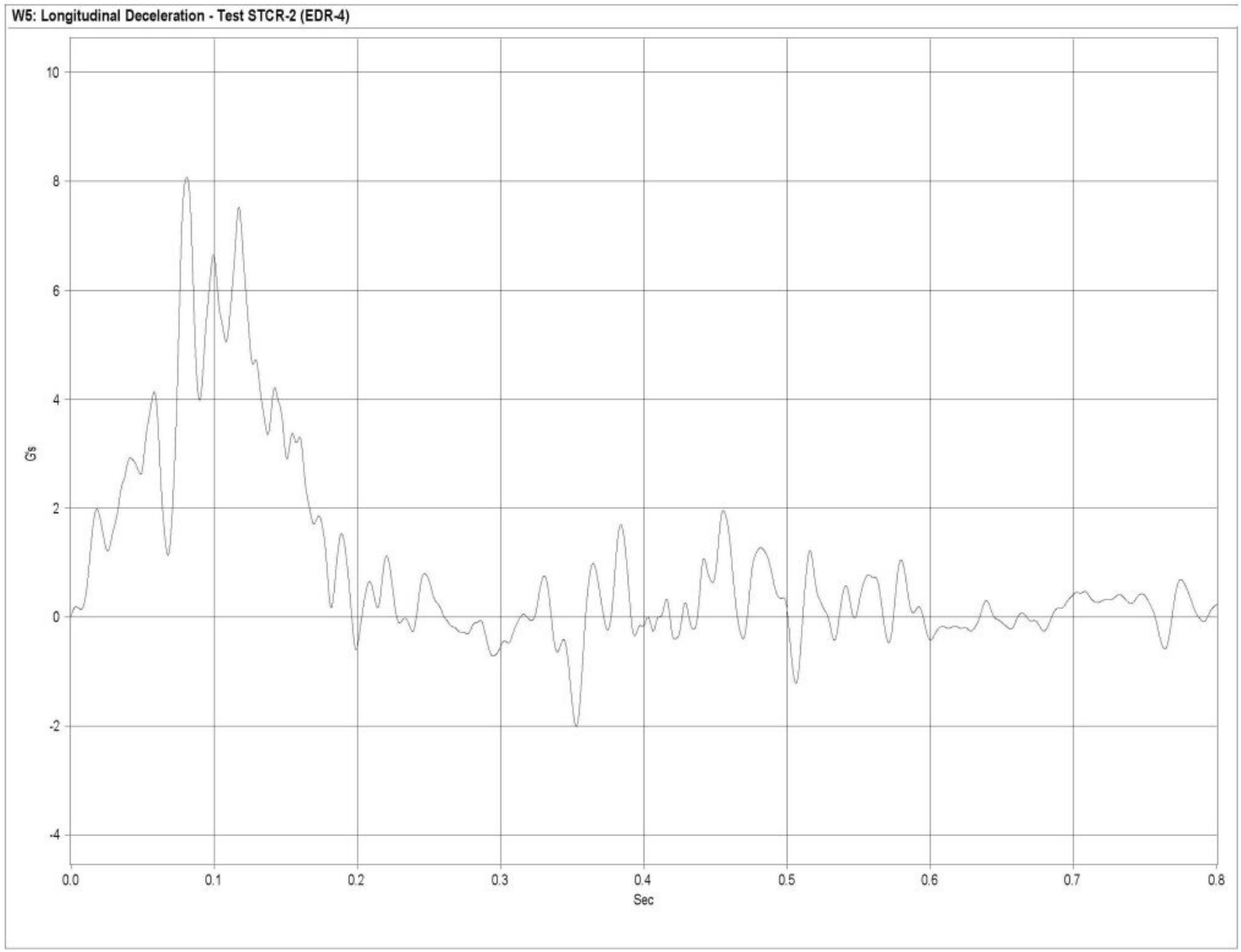

Figure H-1. Graph of Longitudinal Deceleration, Test STCR-2

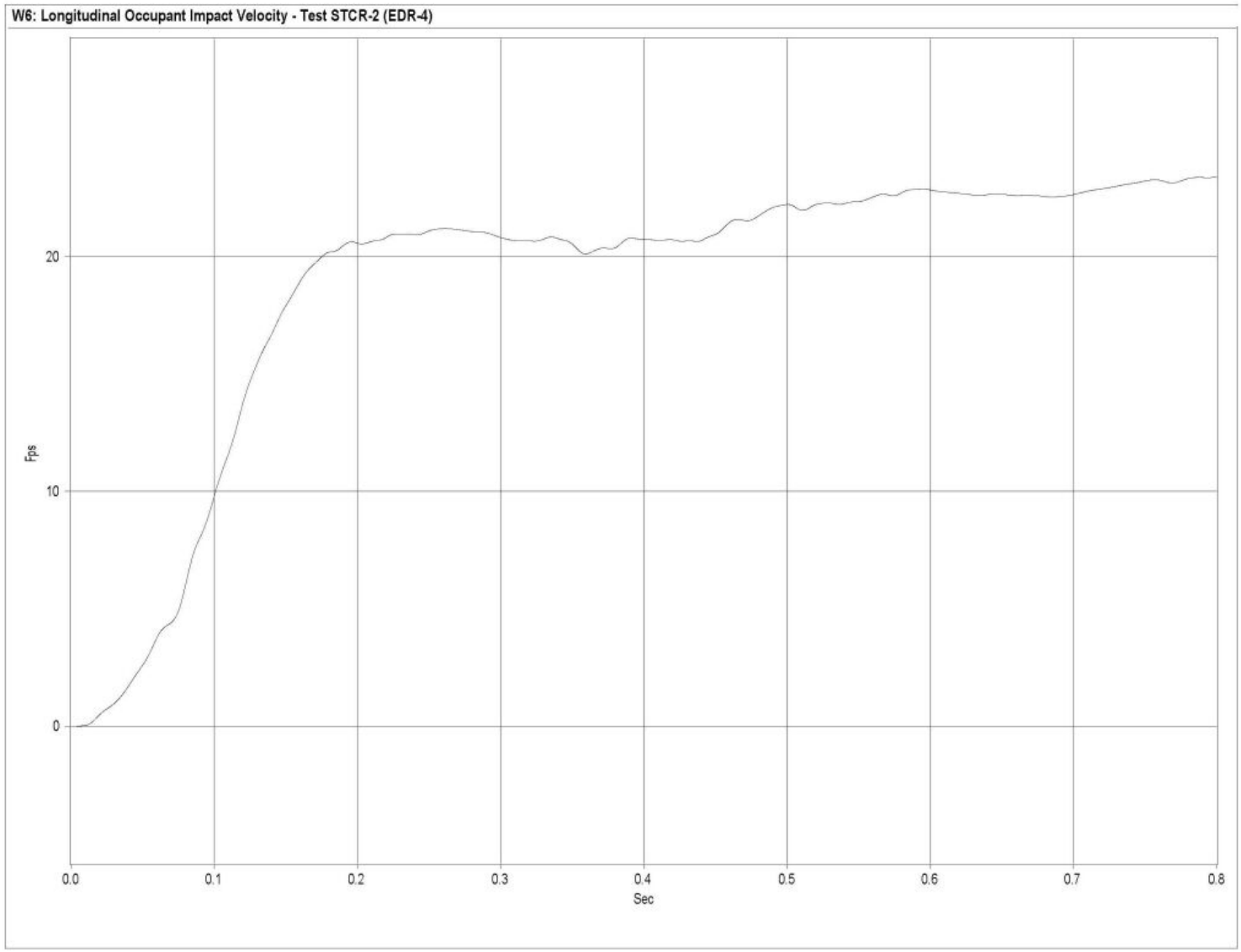

Figure H-2. Graph of Longitudinal Occupant Impact Velocity, Test STCR-2

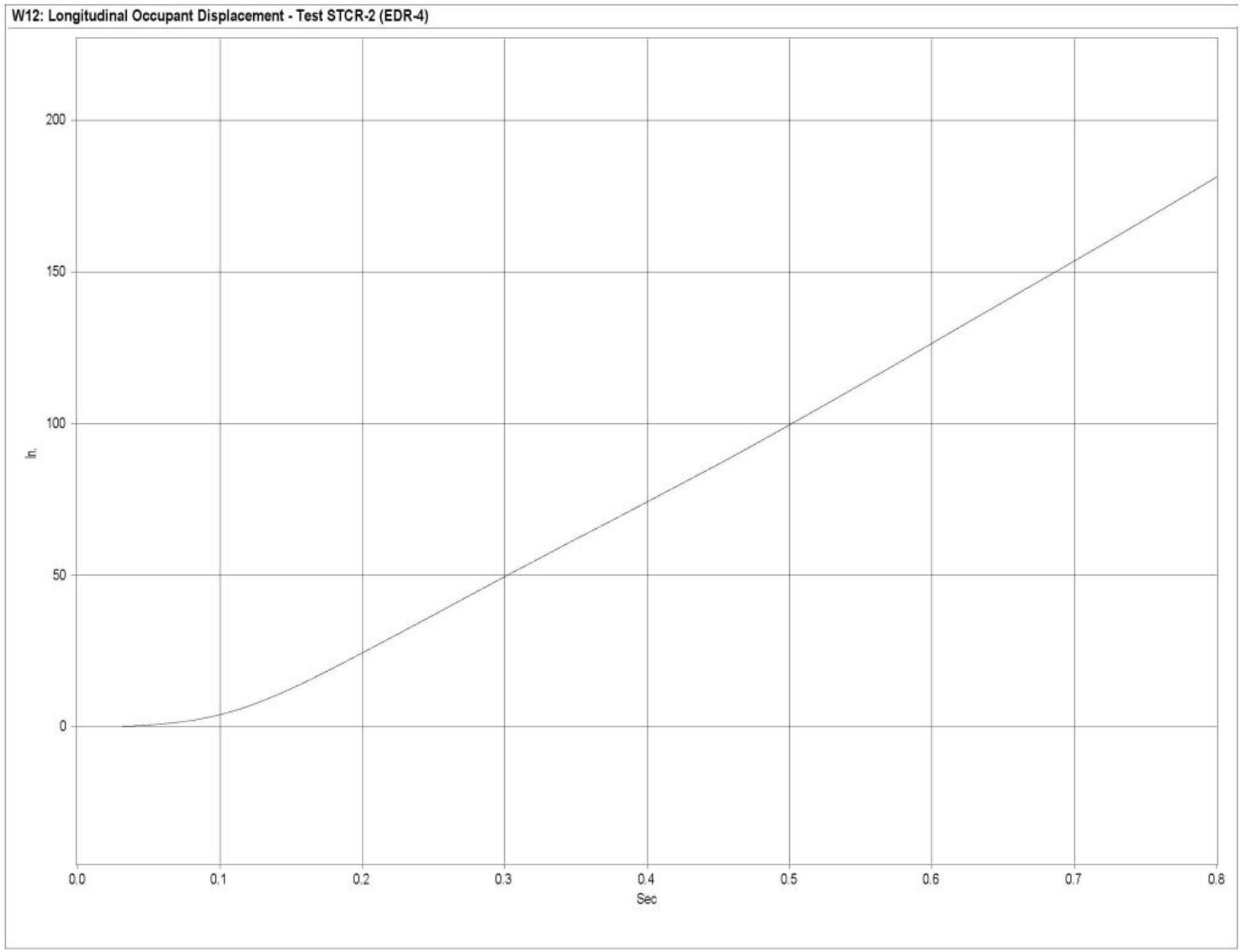

Figure H-3. Graph of Longitudinal Occupant Displacement, Test STCR-2

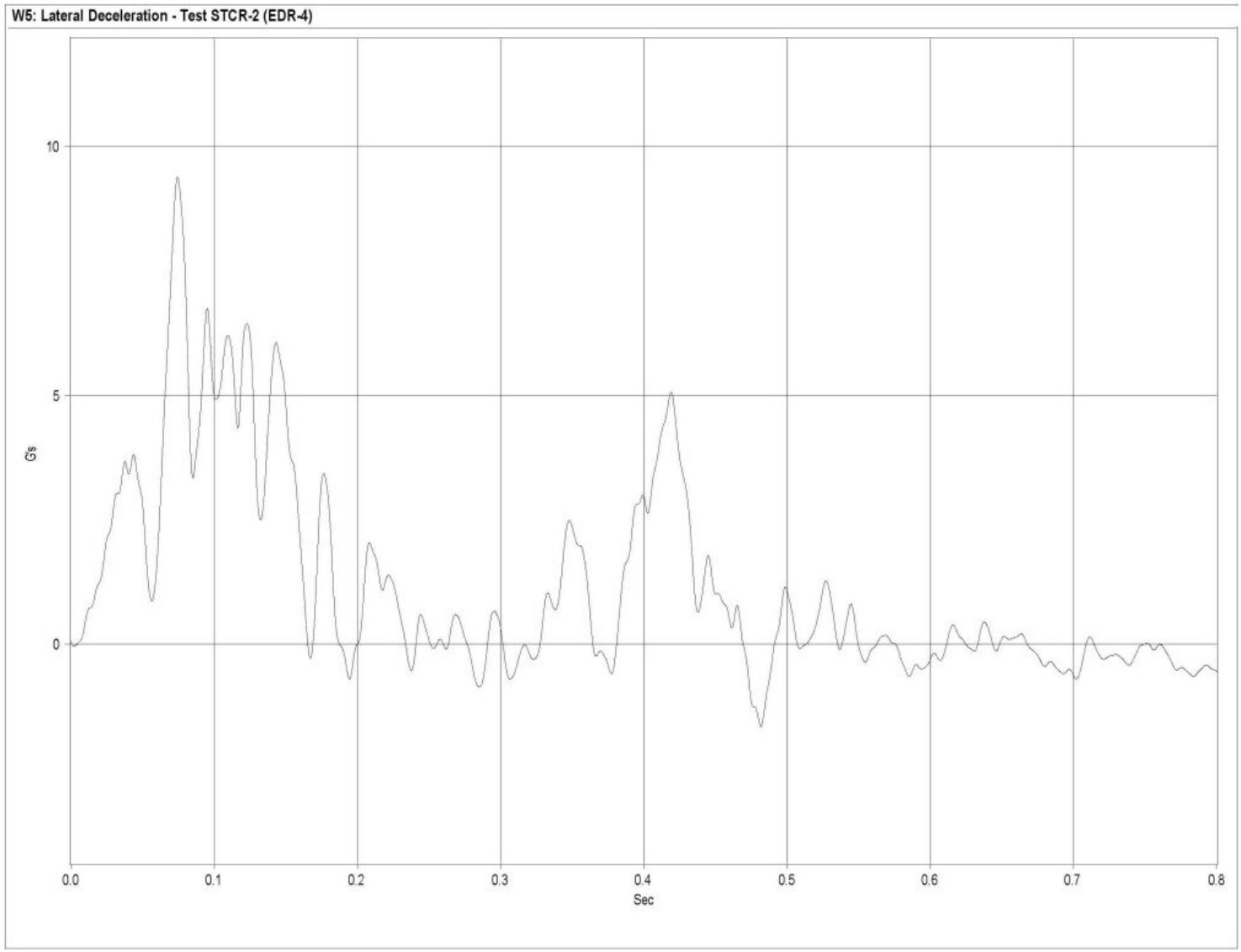

Figure H-4. Graph of Lateral Deceleration, Test STCR-2

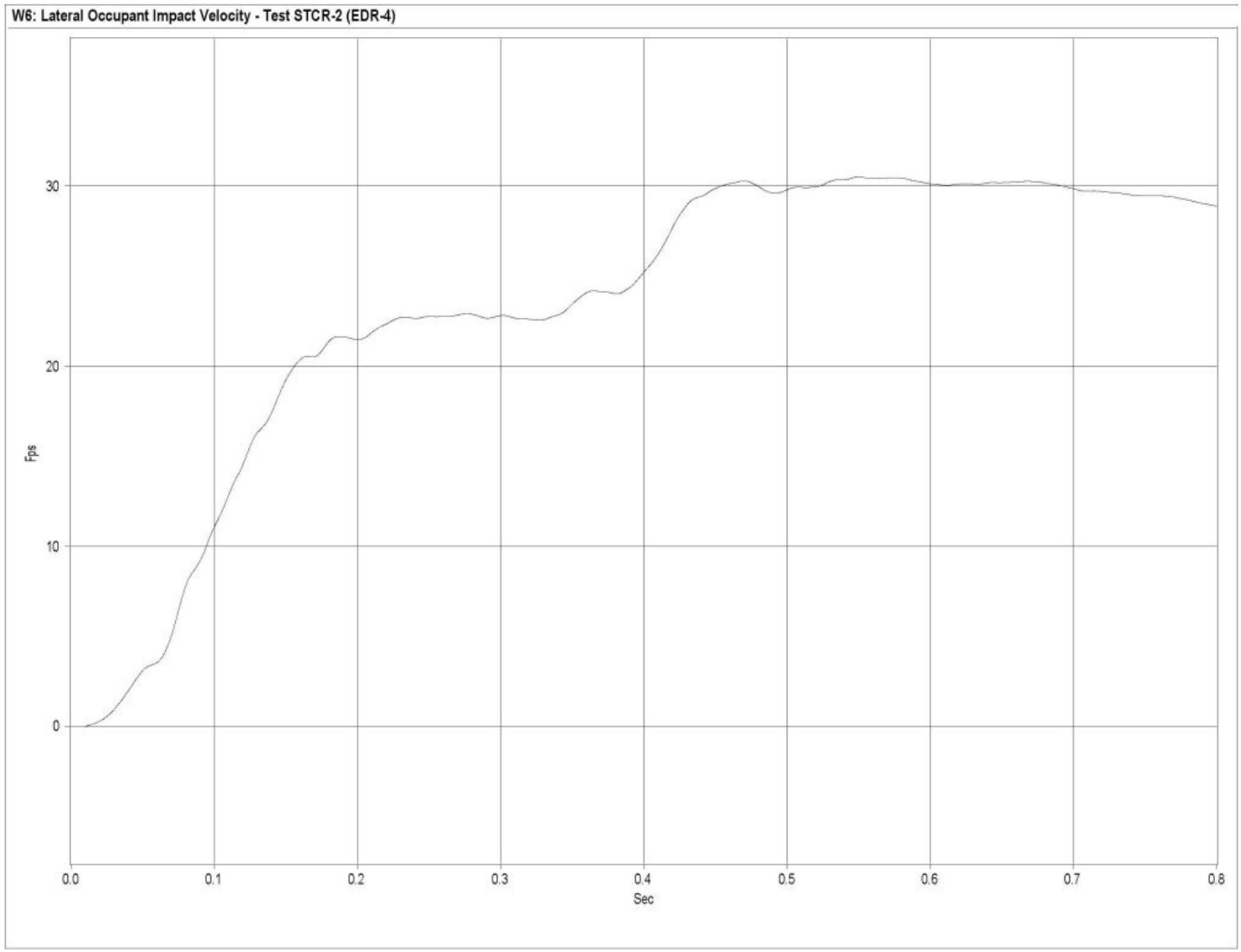

Figure H-5. Graph of Lateral Occupant Impact Velocity, Test STCR-2

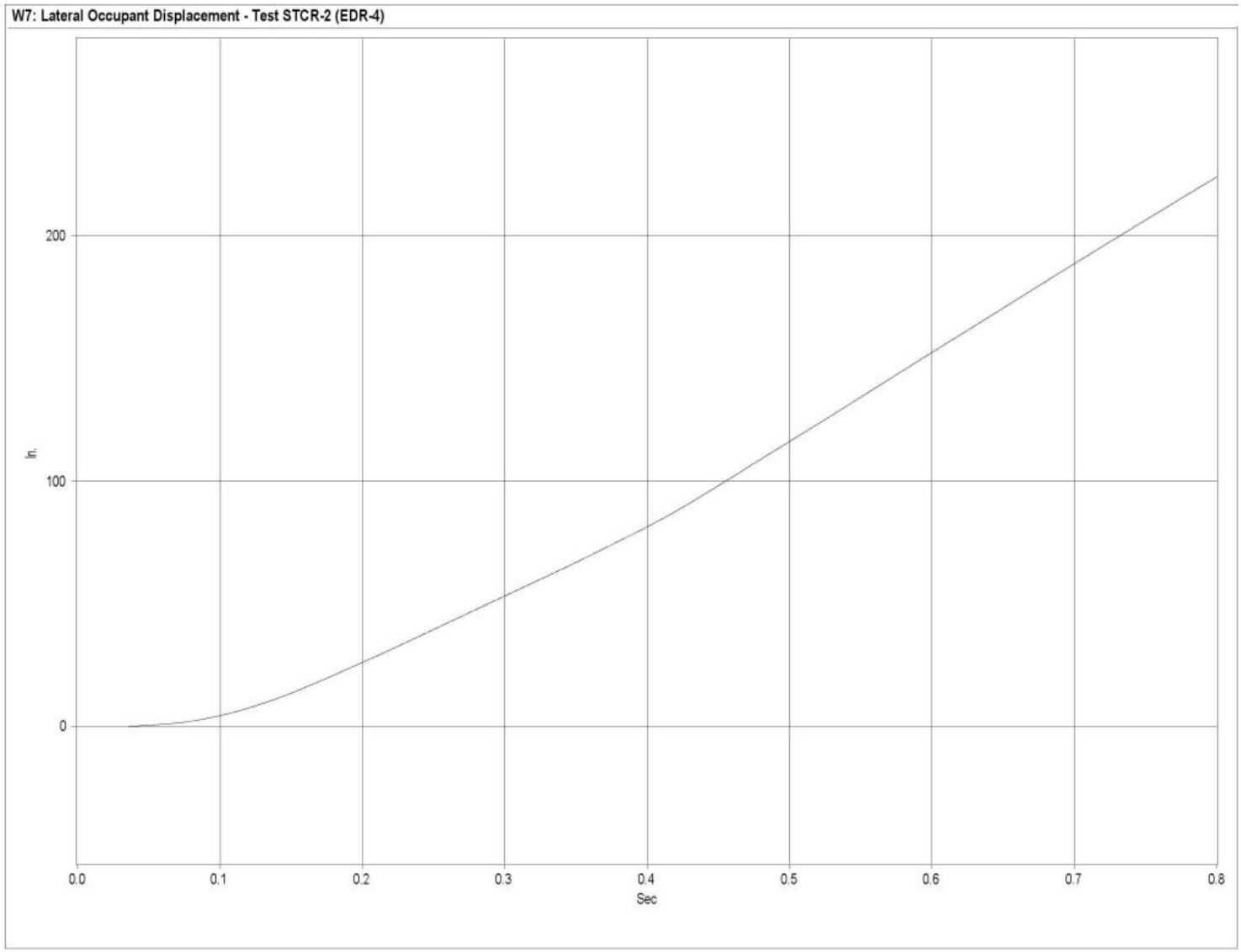

Figure H-6. Graph of Lateral Occupant Displacement, Test STCR-2

APPENDIX I

Roll, Pitch, and Yaw Data Analysis - Test STCR-2

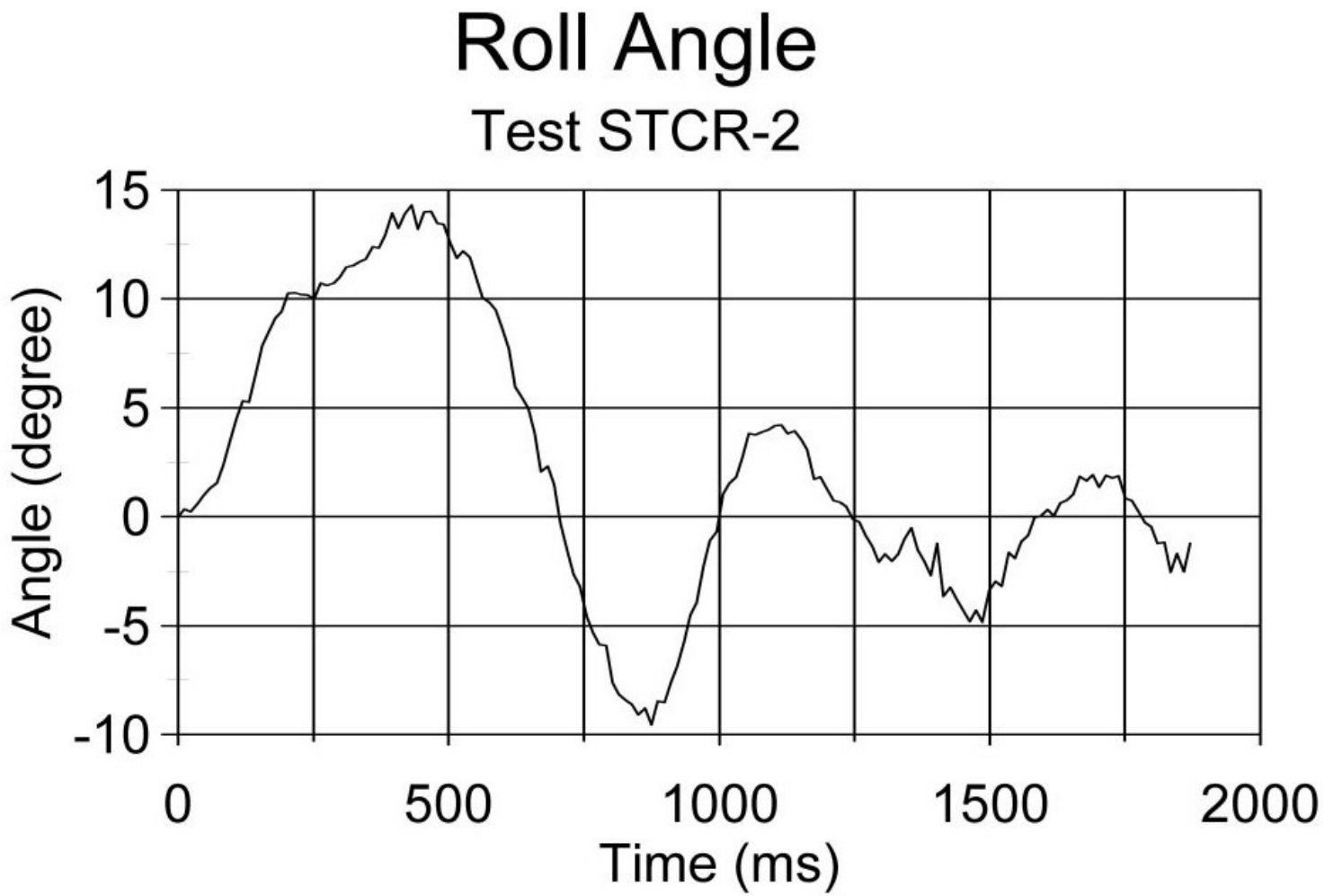

Figure I-1. Graph of Roll Angular Displacements, Test STCR-2

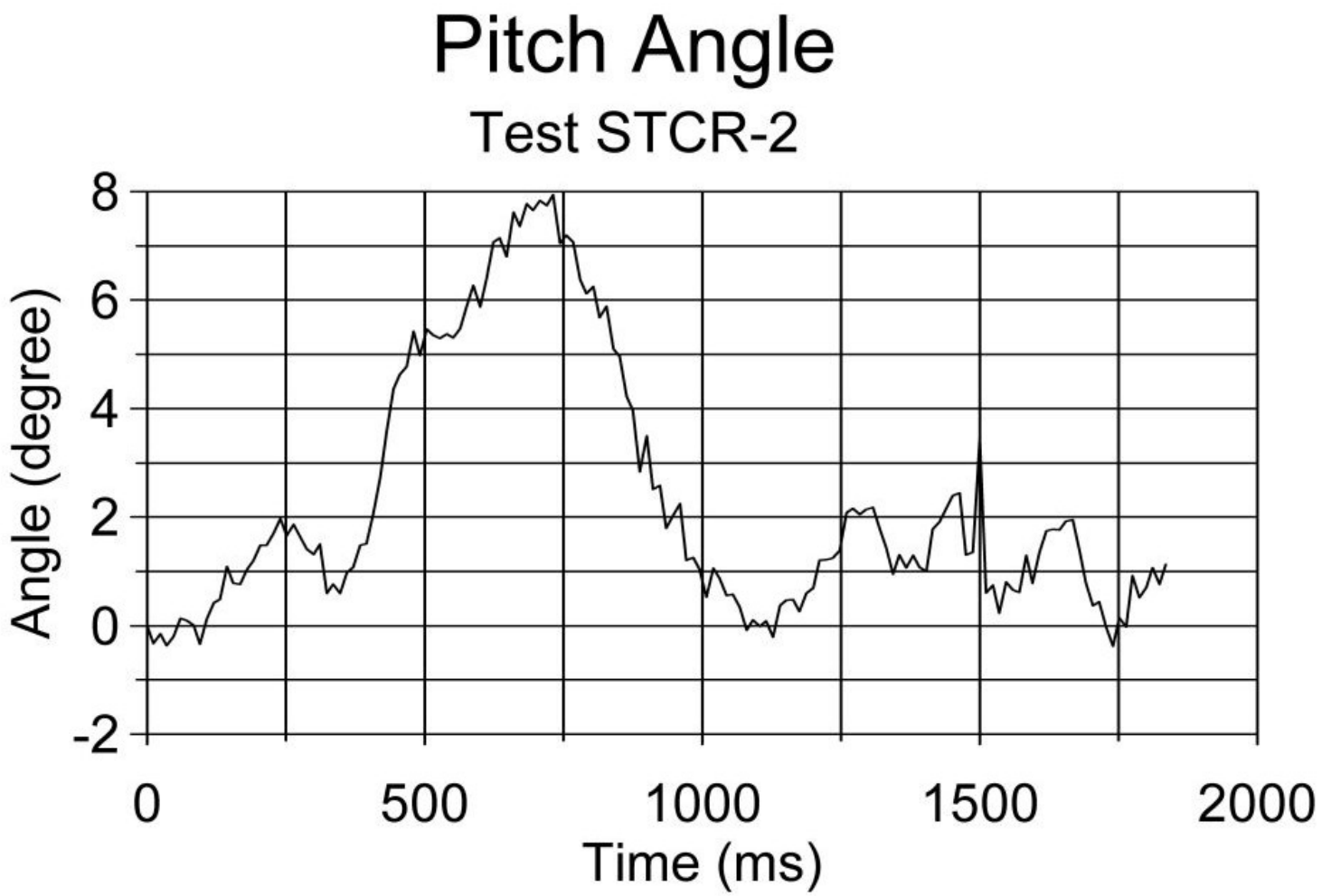

Figure I-2. Graph of Pitch Angular Displacements, Test STCR-2

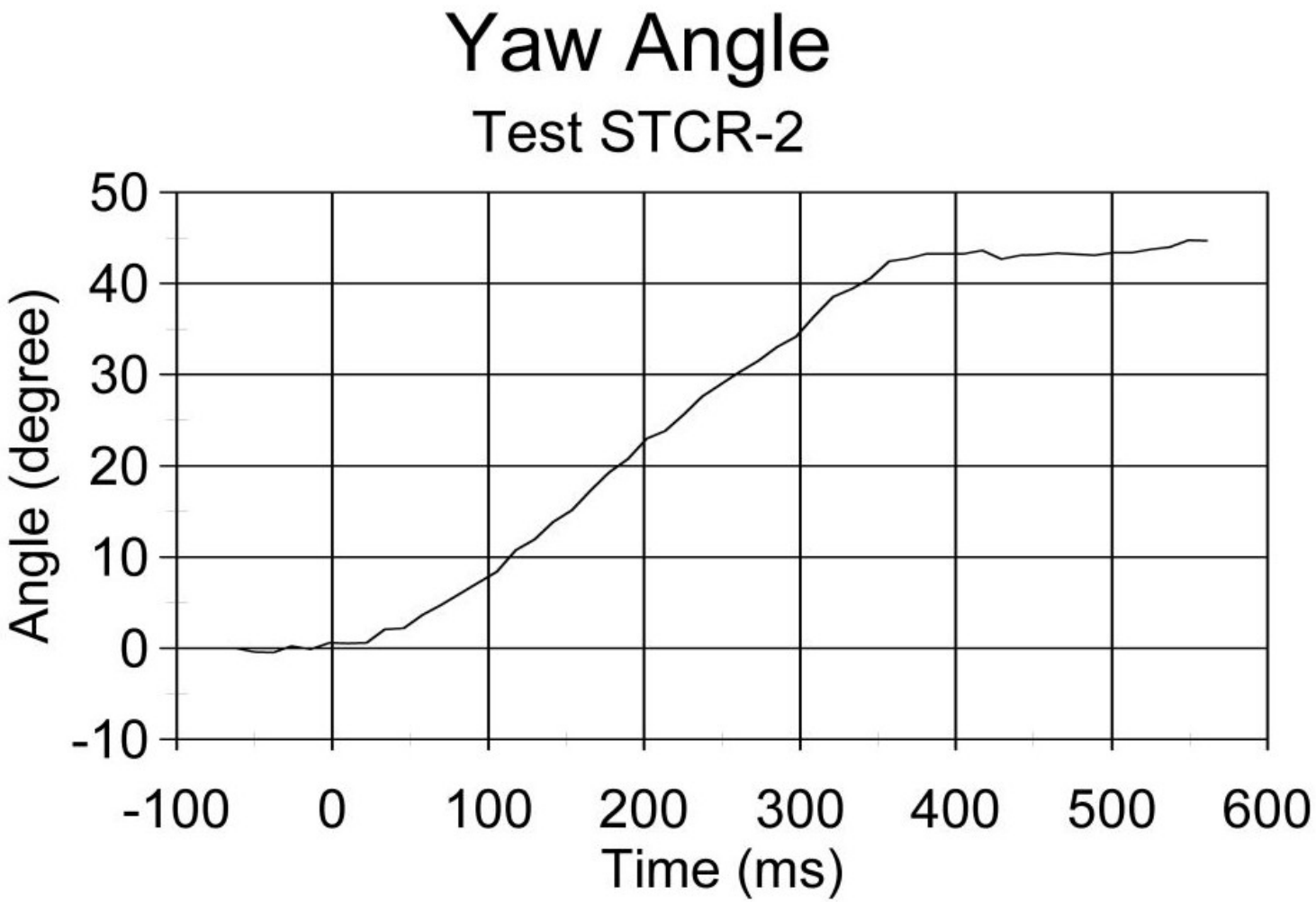

Figure I-3. Graph of Yaw Angular Displacements, Test STCR-2

APPENDIX J

BARRIER VII Computer Models - Wood System

Figure J-1. Model of the Steel Bridge Railing and Approach Guardrail System attached to the Steel Bridge Railing

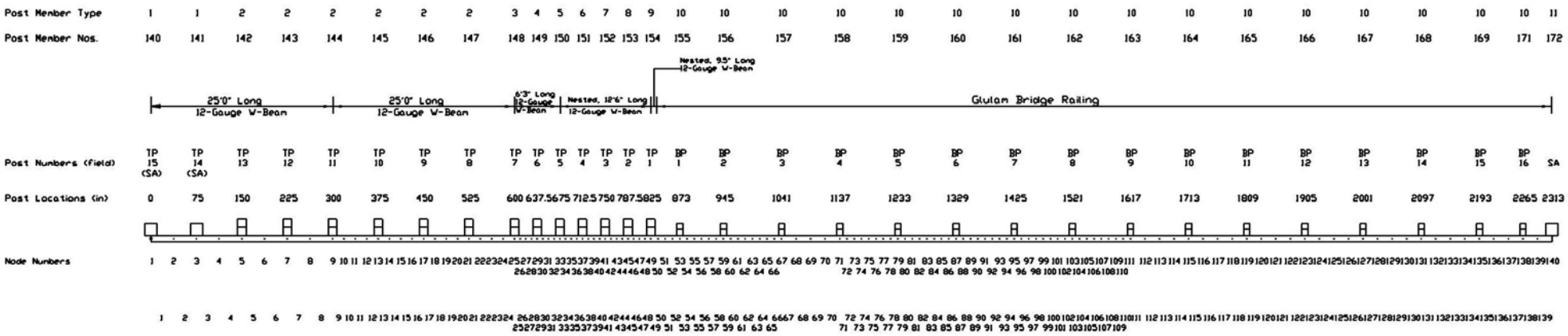

Figure J-1. Model of the Wood Bridge Railing and Approach Guardrail System Attached to the Wood Bridge Railing

APPENDIX K

Typical BARRIER VII Input Data Files - Wood System

Note that the example BARRIER VII input data files included in Appendix K corresponds with the critical impact point for tests WRBP-1 and WRBP-2, respectively.

```
USFS TL-2 GLULAM BRIDGE RAIL and TRANSITION (TRANSVERSE DECK PROJECT) - BR4.DAT - NODE 82
  140   35   30    1  171   30    2    0
    0.0001    0.0001      0.60  800    0       1.0    1
    1    5    5    5    5    5    1
    1       0.0       0.0
    3      75.0       0.0
    5     150.0       0.0
    7     225.0       0.0
    9     300.0       0.0
   13     375.0       0.0
   17     450.0       0.0
   21     525.0       0.0
   25     600.0       0.0
   29    637.50       0.0
   33     675.0       0.0
   37    712.50       0.0
   41     750.0       0.0
   45    787.50       0.0
   49     825.0       0.0
   50     834.5       0.0
   51     847.3       0.0
   52     860.2       0.0
   53     873.0       0.0
   59     945.0       0.0
   67    1041.0       0.0
   71    1137.0       0.0
   79    1233.0       0.0
   87    1329.0       0.0
   95    1425.0       0.0
  103    1521.0       0.0
  111    1617.0       0.0
  115    1713.0       0.0
  119    1809.0       0.0
  123    1905.0       0.0
  127    2001.0       0.0
  131    2097.0       0.0
  135    2193.0       0.0
  138    2265.0       0.0
  140    2313.0       0.0
    1    3    1    1       0.0
    3    5    1    1       0.0
    5    7    1    1       0.0
    7    9    1    1       0.0
    9   13    3    1       0.0
   13   17    3    1       0.0
   17   21    3    1       0.0
   21   25    3    1       0.0
   25   29    3    1       0.0
   29   33    3    1       0.0
   33   37    3    1       0.0
   37   41    3    1       0.0
   41   45    3    1       0.0
   45   49    3    1       0.0
   53   59    5    1       0.0
   59   67    7    1       0.0
   67   71    3    1       0.0
   71   79    7    1       0.0
   79   87    7    1       0.0
   87   95    7    1       0.0
   95  103    7    1       0.0
  103  111    7    1       0.0
  111  115    3    1       0.0
  115  119    3    1       0.0
  119  123    3    1       0.0
  123  127    3    1       0.0
  127  131    3    1       0.0
  131  135    3    1       0.0
  135  138    2    1       0.0
  138  140    1    1       0.0
    1  140      0.35
  140  139  138  137  136  135  134  133  132  131
  130  129  128  127  126  125  124  123  122  121
  120  119  118  117  116  115  114  113  112  111
  110  109  108  107  106  105  104  103  102  101
  100   99   98   97   96   95   94   93   92   91
   90   89   88   87   86   85   84   83   82   81
   80   79   78   77   76   75   74   73   72   71
   70   69   68   67   66   65   64   63   62   61
   60   59   58   57   56   55   54   53   52   51
   50   49   48   47   46   45   44   43   42   41
   40   39   38   37   36   35   34   33   32   31
   30   29   28   27   26   25   24   23   22   21
   20   19   18   17   16   15   14   13   12   11
```

```
 10    9    8    7    6    5    4    3    2    1
100    8
  1      2.30      1.99     37.50   30000.0      6.92      99.5      68.5 0.10 12-Gauge W-Beam
  2      2.30      1.99     18.75   30000.0      6.92      99.5      68.5 0.10 12-Gauge W-Beam
  3      2.30      1.99     9.375   30000.0      6.92      99.5      68.5 0.10 12-Gauge W-Beam
  4      4.60      3.98     9.375   30000.0     13.84     199.0     137.0 0.10 Nested 12-Gauge W-Beam
  5      4.60      3.98      9.50   30000.0     13.84     199.0     137.0 0.10 Nested 12-Gauge W-Beam
  6    345.99    91.125    12.833    1417.0     31.64    150.36    522.83 0.10 6.75x13.5 Glulam Rail
  7    345.99    91.125     12.00    1417.0     31.64    150.36    522.83 0.10 6.75x13.5 Glulam Rail
  8    345.99    91.125     24.00    1417.0     31.64    150.36    522.83 0.10 6.75x13.5 Glulam Rail
300   11
  1     21.65       0.0    1000.0    1000.0     250.0   10000.0   10000.0 0.10 Strong Post Anchor
   200.0     200.0       2.0       2.0
  2     21.65       0.0      4.00      4.00      54.0     92.88    270.62 0.10 W6x9 by 6' Long
     6.0      15.0      16.0      16.0
  3     21.65       0.0       8.0       8.0      63.0     92.88    336.42 0.10 W6x9 by 7' Long
     6.0      15.0      16.0      16.0
  4     21.65       0.0       8.0       8.0      63.0     92.88    336.42 0.10 W6x9 by 7' Long
     6.0      15.0      16.0      16.0
  5     21.65       0.0       8.0       8.0      63.0     92.88    336.42 0.10 W6x9 by 7' Long
    10.0      20.0      16.0      16.0
  6     21.65       0.0       8.0       8.0      63.0     92.88    336.42 0.10 W6x9 by 7' Long
    10.0      20.0      16.0      16.0
  7     21.65       0.0       8.0       8.0      63.0     92.88    336.42 0.10 W6x9 by 7' Long
    10.0      20.0      16.0      16.0
  8     21.65       0.0       8.0       8.0      63.0     92.88    336.42 0.10 W6x9 by 7' Long
    10.0      20.0      16.0      16.0
  9     21.65       0.0       8.0       8.0      63.0     92.88    336.42 0.10 W6x9 by 7' Long
    10.0      20.0      16.0      16.0
 10     21.65       0.0       3.6       4.5      54.2    437.36    487.12 0.10 6.75x7.5 Glulam Bridge Post w/ Hole
    30.0      30.0       5.6       5.0
 11     21.65       0.0    1000.0    1000.0     250.0   10000.0   10000.0 0.10 Strong Post Anchor
   200.0     200.0       2.0       2.0
  1    1    2    8    1  101       0.0       0.0       0.0
  9    9   10   24    1  102       0.0       0.0       0.0
 25   25   26   32    1  103       0.0       0.0       0.0
 33   33   34   48    1  104       0.0       0.0       0.0
 49   49   50         1  105       0.0       0.0       0.0
 50   50   51   52    1  106       0.0       0.0       0.0
 53   53   54   58    1  107       0.0       0.0       0.0
 59   59   60   66    1  107       0.0       0.0       0.0
 67   67   68   70    1  108       0.0       0.0       0.0
 71   71   72  110    1  107       0.0       0.0       0.0
111  111  112  134    1  108       0.0       0.0       0.0
135  135  136  137    1  108       0.0       0.0       0.0
138  138  139  139    1  108       0.0       0.0       0.0
140    1      141    2  301       0.0       0.0       0.0       0.0       0.0
142    5      144    2  302       0.0       0.0       0.0       0.0       0.0
145   13      147    4  302       0.0       0.0       0.0       0.0       0.0
148   25                303       0.0       0.0       0.0       0.0       0.0
149   29                304       0.0       0.0       0.0       0.0       0.0
150   33                305       0.0       0.0       0.0       0.0       0.0
151   37                306       0.0       0.0       0.0       0.0       0.0
152   41                307       0.0       0.0       0.0       0.0       0.0
153   45                308       0.0       0.0       0.0       0.0       0.0
154   49                309       0.0       0.0       0.0       0.0       0.0
155   53                310       0.0       0.0       0.0       0.0       0.0
156   59                310       0.0       0.0       0.0       0.0       0.0
157   67                310       0.0       0.0       0.0       0.0       0.0
158   71      163    8  310       0.0       0.0       0.0       0.0       0.0
164  115      168    4  310       0.0       0.0       0.0       0.0       0.0
169  135      170    3  310       0.0       0.0       0.0       0.0       0.0
171  140                311       0.0       0.0       0.0       0.0       0.0
  4400.0   40000.0   20    6    4    0    1
  1     0.055      0.12      6.00      17.0
  2     0.057      0.15      7.00      18.0
  3     0.062      0.18     10.00      12.0
  4     0.110      0.35     12.00       6.0
  5      0.35      0.45      6.00       5.0
  6      1.45      1.50     15.00       1.0
  1    100.75    15.875    1      12.0    1    0    0    0
  2    100.75    27.875    1      12.0    1    0    0    0
  3    100.75    39.875    2      12.0    1    0    0    0
  4     88.75    39.875    2      12.0    1    0    0    0
  5     76.75    39.875    2      12.0    1    0    0    0
  6     64.75    39.875    2      12.0    1    0    0    0
  7     52.75    39.875    2      12.0    1    0    0    0
  8     40.75    39.875    2      12.0    1    0    0    0
  9     28.75    39.875    2      12.0    1    0    0    0
 10     16.75    39.875    2      12.0    1    0    0    0
 11    -13.25    39.875    3      12.0    1    0    0    0
 12    -33.25    39.875    3      12.0    1    0    0    0
 13    -53.25    39.875    3      12.0    1    0    0    0
```

```
14    -73.25    39.875    3      12.0    1    0    0    0
15    -93.25    39.875    3      12.0    1    0    0    0
16   -113.25    39.875    4      12.0    1    0    0    0
17   -113.25   -39.875    4      12.0    0    0    0    0
18    100.75   -39.875    1      12.0    0    0    0    0
19     69.25     37.75    5       1.0    1    0    0    0
20    -62.75     37.75    6       1.0    1    0    0    0
 1     69.25     32.75       0.0      608.
 2     69.25    -32.75       0.0      608.
 3    -62.75     32.75       0.0      492.
 4    -62.75    -32.75       0.0      492.
 1       0.0       0.0
 3    1269.0       0.0      25.0     43.50       0.0       0.0       1.0
```

```
USFS TL-2 GLULAM BRIDGE RAIL and TRANSITION (TRANSVERSE DECK PROJECT) - TR4.DAT - NODE 42
  140   35   30    1  171   30    2    0
    0.0001    0.0001      0.60 1500    0       1.0    1
    1    5    5    5    5    5    1
    1       0.0       0.0
    3      75.0       0.0
    5     150.0       0.0
    7     225.0       0.0
    9     300.0       0.0
   13     375.0       0.0
   17     450.0       0.0
   21     525.0       0.0
   25     600.0       0.0
   29    637.50       0.0
   33     675.0       0.0
   37    712.50       0.0
   41     750.0       0.0
   45    787.50       0.0
   49     825.0       0.0
   50     834.5       0.0
   51     847.3       0.0
   52     860.2       0.0
   53     873.0       0.0
   59     945.0       0.0
   67    1041.0       0.0
   71    1137.0       0.0
   79    1233.0       0.0
   87    1329.0       0.0
   95    1425.0       0.0
  103    1521.0       0.0
  111    1617.0       0.0
  115    1713.0       0.0
  119    1809.0       0.0
  123    1905.0       0.0
  127    2001.0       0.0
  131    2097.0       0.0
  135    2193.0       0.0
  138    2265.0       0.0
  140    2313.0       0.0
    1    3    1    1       0.0
    3    5    1    1       0.0
    5    7    1    1       0.0
    7    9    1    1       0.0
    9   13    3    1       0.0
   13   17    3    1       0.0
   17   21    3    1       0.0
   21   25    3    1       0.0
   25   29    3    1       0.0
   29   33    3    1       0.0
   33   37    3    1       0.0
   37   41    3    1       0.0
   41   45    3    1       0.0
   45   49    3    1       0.0
   53   59    5    1       0.0
   59   67    7    1       0.0
   67   71    3    1       0.0
   71   79    7    1       0.0
   79   87    7    1       0.0
   87   95    7    1       0.0
   95  103    7    1       0.0
  103  111    7    1       0.0
  111  115    3    1       0.0
  115  119    3    1       0.0
  119  123    3    1       0.0
  123  127    3    1       0.0
  127  131    3    1       0.0
  131  135    3    1       0.0
  135  138    2    1       0.0
  138  140    1    1       0.0
    1  140      0.35
  140  139  138  137  136  135  134  133  132  131
  130  129  128  127  126  125  124  123  122  121
  120  119  118  117  116  115  114  113  112  111
  110  109  108  107  106  105  104  103  102  101
  100   99   98   97   96   95   94   93   92   91
   90   89   88   87   86   85   84   83   82   81
   80   79   78   77   76   75   74   73   72   71
   70   69   68   67   66   65   64   63   62   61
   60   59   58   57   56   55   54   53   52   51
   50   49   48   47   46   45   44   43   42   41
   40   39   38   37   36   35   34   33   32   31
   30   29   28   27   26   25   24   23   22   21
   20   19   18   17   16   15   14   13   12   11
```

```
 10    9    8    7    6    5    4    3    2    1
100    8
  1      2.30      1.99     37.50   30000.0      6.92      99.5      68.5 0.10 12-Gauge W-Beam
  2      2.30      1.99     18.75   30000.0      6.92      99.5      68.5 0.10 12-Gauge W-Beam
  3      2.30      1.99     9.375   30000.0      6.92      99.5      68.5 0.10 12-Gauge W-Beam
  4      4.60      3.98     9.375   30000.0     13.84     199.0     137.0 0.10 Nested 12-Gauge W-Beam
  5      4.60      3.98      9.50   30000.0     13.84     199.0     137.0 0.10 Nested 12-Gauge W-Beam
  6    345.99    91.125    12.833    1417.0     31.64    150.36    522.83 0.10 6.75x13.5 Glulam Rail
  7    345.99    91.125     12.00    1417.0     31.64    150.36    522.83 0.10 6.75x13.5 Glulam Rail
  8    345.99    91.125     24.00    1417.0     31.64    150.36    522.83 0.10 6.75x13.5 Glulam Rail
300   11
  1     21.65       0.0    1000.0    1000.0     250.0   10000.0   10000.0 0.10 Strong Post Anchor
   200.0     200.0       2.0       2.0
  2     21.65       0.0      4.00      4.00      54.0     92.88    270.62 0.10 W6x9 by 6' Long
     6.0      15.0      16.0      16.0
  3     21.65       0.0       8.0       8.0      63.0     92.88    336.42 0.10 W6x9 by 7' Long
     6.0      15.0      16.0      16.0
  4     21.65       0.0       8.0       8.0      63.0     92.88    336.42 0.10 W6x9 by 7' Long
     6.0      15.0      16.0      16.0
  5     21.65       0.0       8.0       8.0      63.0     92.88    336.42 0.10 W6x9 by 7' Long
    10.0      20.0      16.0      16.0
  6     21.65       0.0       8.0       8.0      63.0     92.88    336.42 0.10 W6x9 by 7' Long
    10.0      20.0      16.0      16.0
  7     21.65       0.0       8.0       8.0      63.0     92.88    336.42 0.10 W6x9 by 7' Long
    10.0      20.0      16.0      16.0
  8     21.65       0.0       8.0       8.0      63.0     92.88    336.42 0.10 W6x9 by 7' Long
    10.0      20.0      16.0      16.0
  9     21.65       0.0       8.0       8.0      63.0     92.88    336.42 0.10 W6x9 by 7' Long
    10.0      20.0      16.0      16.0
 10     21.65       0.0       3.6       4.5      54.2    437.36    487.12 0.10 6.75x7.5 Glulam Bridge Post w/ Hole
    30.0      30.0       5.6       5.0
 11     21.65       0.0    1000.0    1000.0     250.0   10000.0   10000.0 0.10 Strong Post Anchor
   200.0     200.0       2.0       2.0
  1    1    2    8    1  101        0.0        0.0        0.0
  9    9   10   24    1  102        0.0        0.0        0.0
 25   25   26   32    1  103        0.0        0.0        0.0
 33   33   34   48    1  104        0.0        0.0        0.0
 49   49   50         1  105        0.0        0.0        0.0
 50   50   51   52    1  106        0.0        0.0        0.0
 53   53   54   58    1  107        0.0        0.0        0.0
 59   59   60   66    1  107        0.0        0.0        0.0
 67   67   68   70    1  108        0.0        0.0        0.0
 71   71   72  110    1  107        0.0        0.0        0.0
111  111  112  134    1  108        0.0        0.0        0.0
135  135  136  137    1  108        0.0        0.0        0.0
138  138  139  139    1  108        0.0        0.0        0.0
140    1      141    2  301        0.0        0.0        0.0        0.0        0.0
142    5      144    2  302        0.0        0.0        0.0        0.0        0.0
145   13      147    4  302        0.0        0.0        0.0        0.0        0.0
148   25                303        0.0        0.0        0.0        0.0        0.0
149   29                304        0.0        0.0        0.0        0.0        0.0
150   33                305        0.0        0.0        0.0        0.0        0.0
151   37                306        0.0        0.0        0.0        0.0        0.0
152   41                307        0.0        0.0        0.0        0.0        0.0
153   45                308        0.0        0.0        0.0        0.0        0.0
154   49                309        0.0        0.0        0.0        0.0        0.0
155   53                310        0.0        0.0        0.0        0.0        0.0
156   59                310        0.0        0.0        0.0        0.0        0.0
157   67                310        0.0        0.0        0.0        0.0        0.0
158   71      163    8  310        0.0        0.0        0.0        0.0        0.0
164  115      168    4  310        0.0        0.0        0.0        0.0        0.0
169  135      170    3  310        0.0        0.0        0.0        0.0        0.0
171  140                311        0.0        0.0        0.0        0.0        0.0
  4400.0   40000.0   20    6    4    0    1
  1     0.055      0.12      6.00      17.0
  2     0.057      0.15      7.00      18.0
  3     0.062      0.18     10.00      12.0
  4     0.110      0.35     12.00       6.0
  5      0.35      0.45      6.00       5.0
  6      1.45      1.50     15.00       1.0
  1    100.75    15.875    1      12.0    1    0    0    0
  2    100.75    27.875    1      12.0    1    0    0    0
  3    100.75    39.875    2      12.0    1    0    0    0
  4     88.75    39.875    2      12.0    1    0    0    0
  5     76.75    39.875    2      12.0    1    0    0    0
  6     64.75    39.875    2      12.0    1    0    0    0
  7     52.75    39.875    2      12.0    1    0    0    0
  8     40.75    39.875    2      12.0    1    0    0    0
  9     28.75    39.875    2      12.0    1    0    0    0
 10     16.75    39.875    2      12.0    1    0    0    0
 11    -13.25    39.875    3      12.0    1    0    0    0
 12    -33.25    39.875    3      12.0    1    0    0    0
 13    -53.25    39.875    3      12.0    1    0    0    0
```

```
14    -73.25    39.875    3      12.0    1    0    0    0
15    -93.25    39.875    3      12.0    1    0    0    0
16   -113.25    39.875    4      12.0    1    0    0    0
17   -113.25   -39.875    4      12.0    0    0    0    0
18    100.75   -39.875    1      12.0    0    0    0    0
19     69.25     37.75    5       1.0    1    0    0    0
20    -62.75     37.75    6       1.0    1    0    0    0
 1     69.25     32.75       0.0      608.
 2     69.25    -32.75       0.0      608.
 3    -62.75     32.75       0.0      492.
 4    -62.75    -32.75       0.0      492.
 1       0.0       0.0
 3   759.375       0.0      25.0     43.50       0.0       0.0       1.0
```

APPENDIX L

Accelerometer Data Analysis - Test WRBP-1

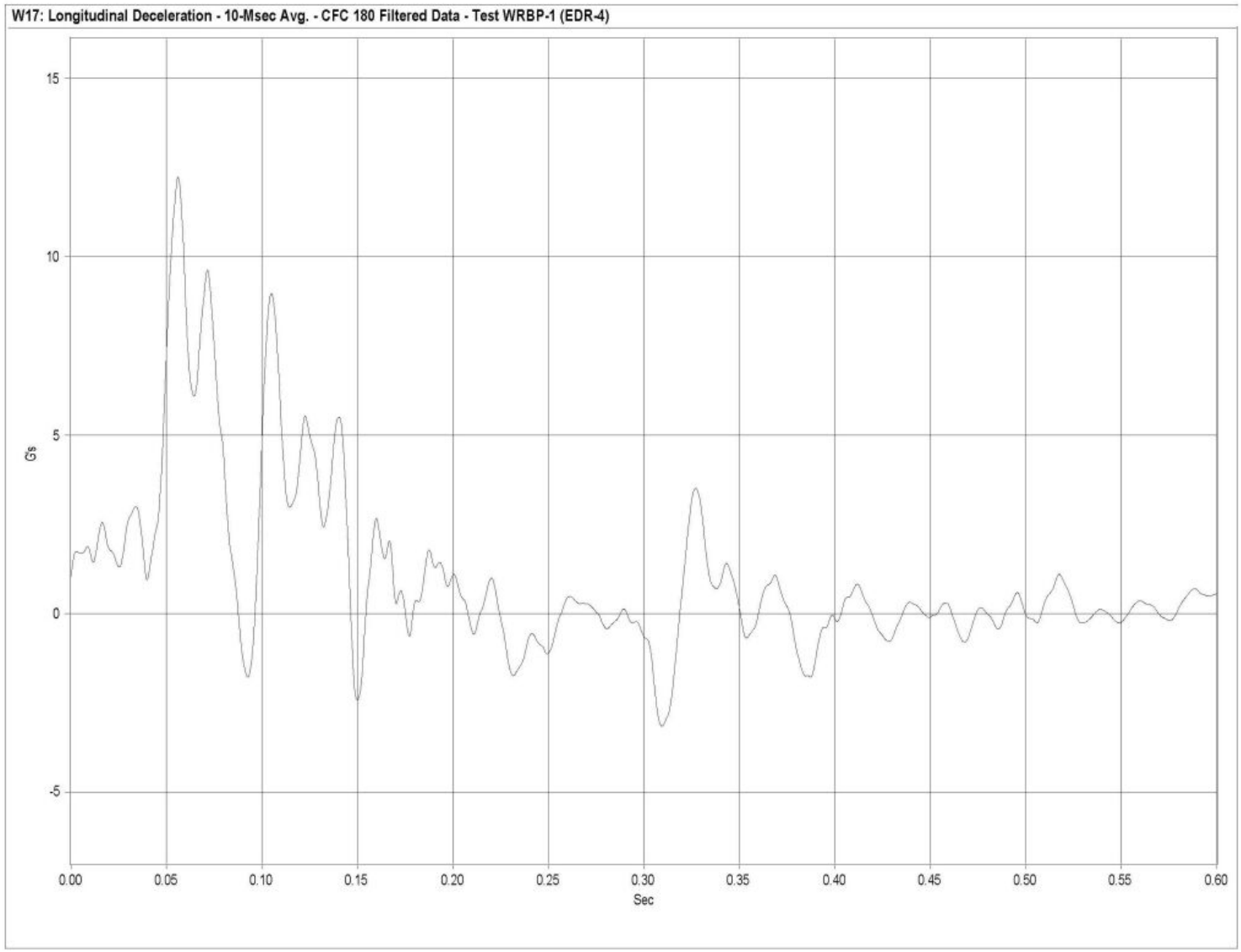

Figure L-1. Graph of Longitudinal Deceleration, Test WRBP-1

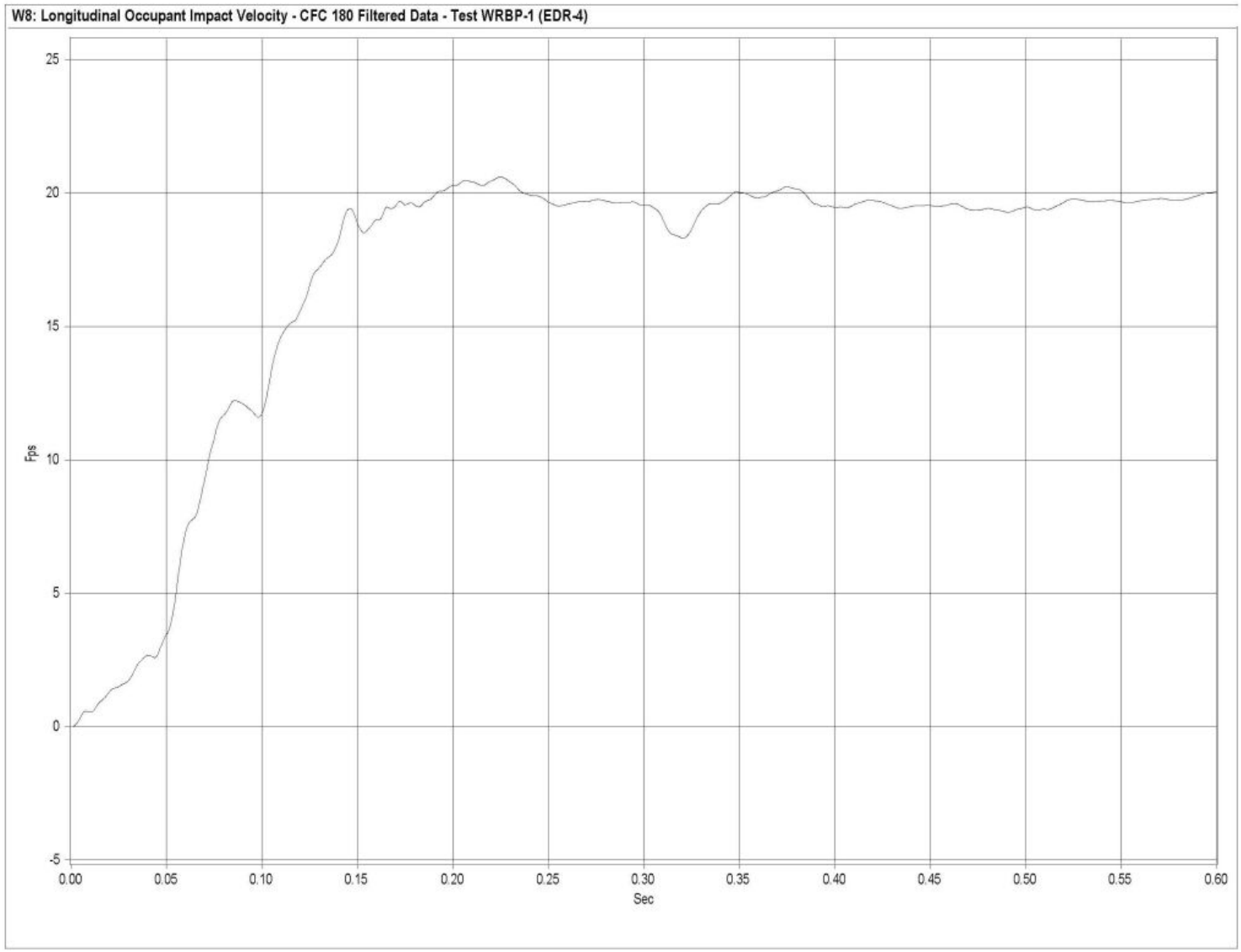

Figure L-2. Graph of Longitudinal Occupant Impact Velocity, Test WRBP-1

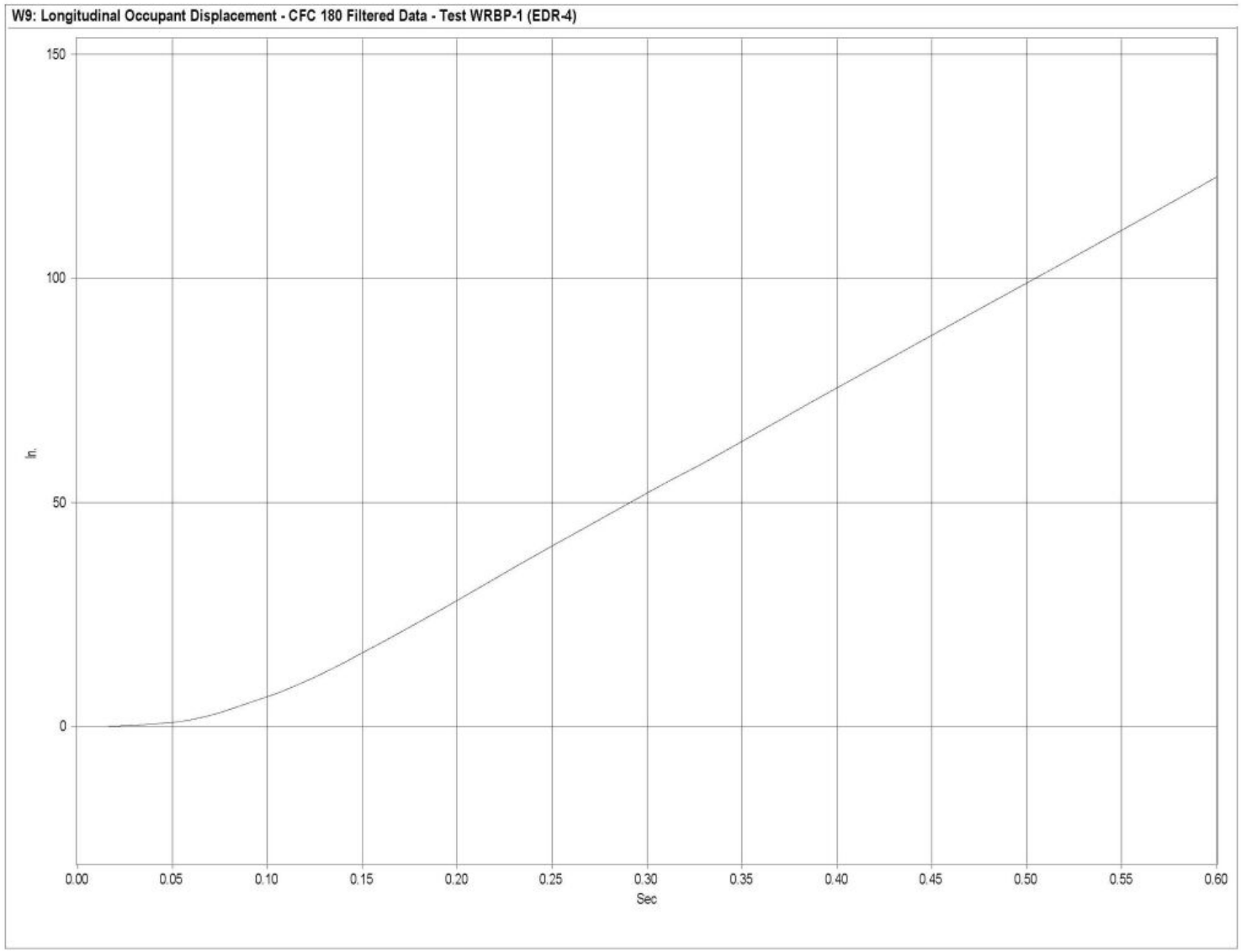

Figure L-3. Graph of Longitudinal Occupant Displacement, Test WRBP-1

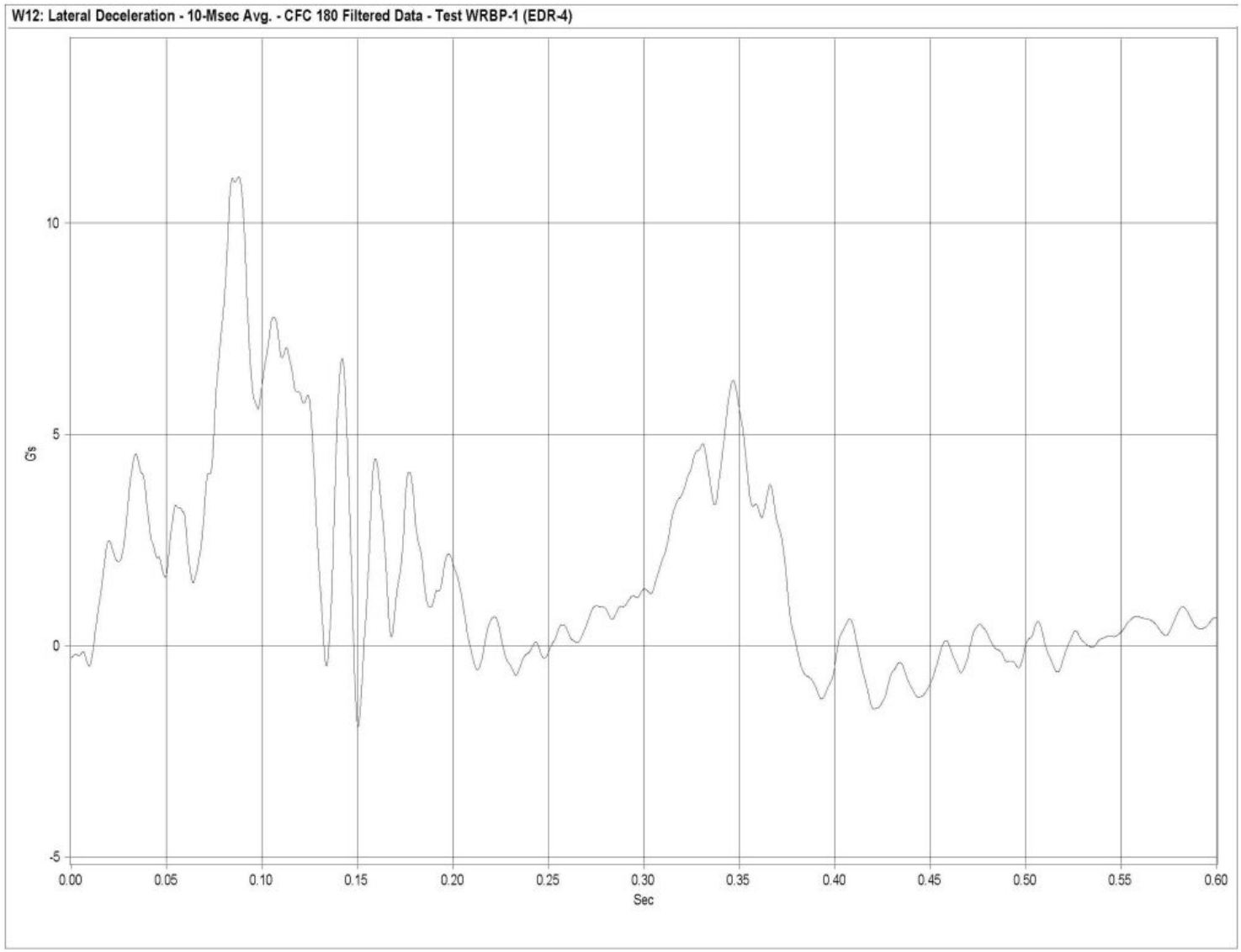

Figure L-4. Graph of Lateral Deceleration, Test WRBP-1

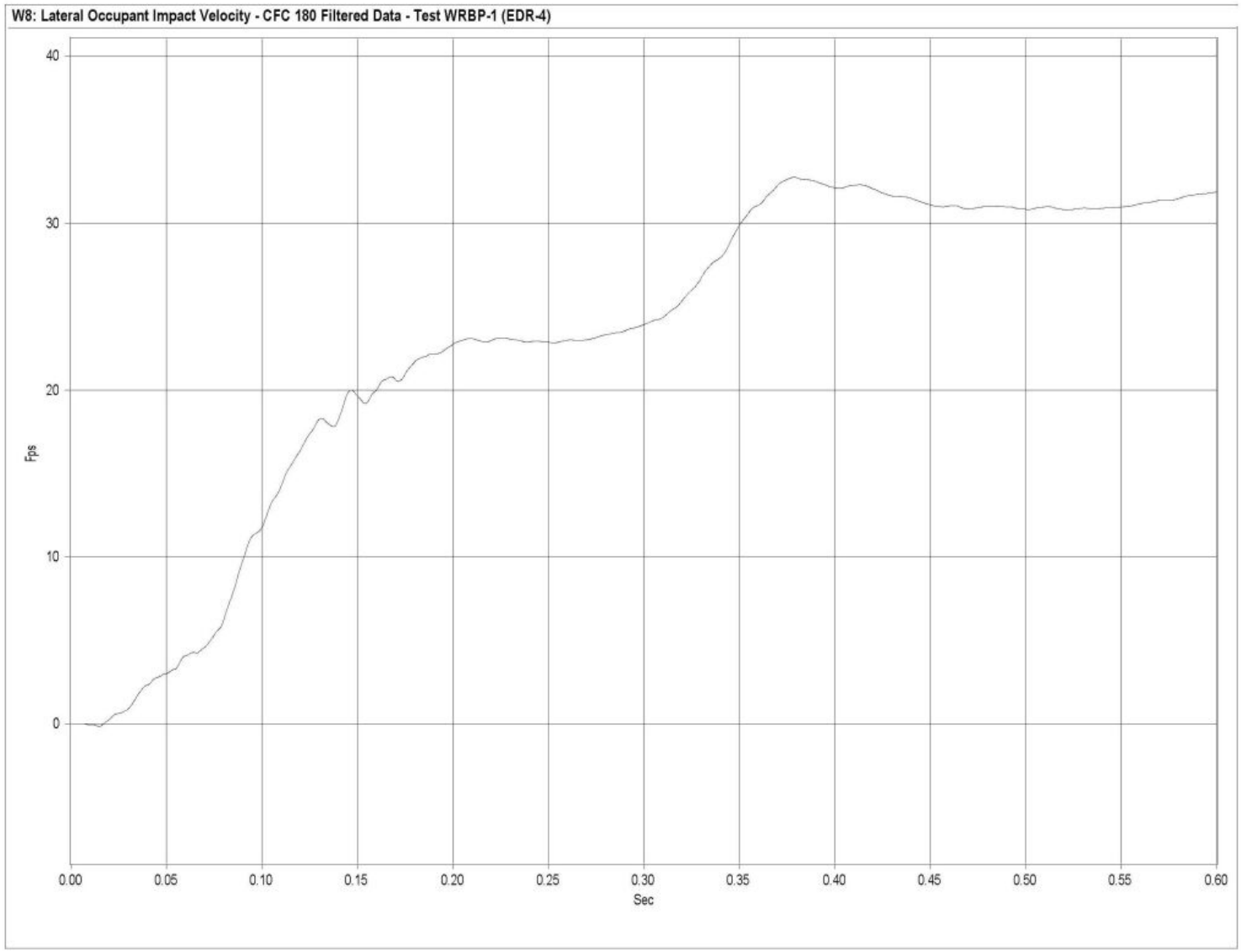

Figure L-5. Graph of Lateral Occupant Impact Velocity, Test WRBP-1

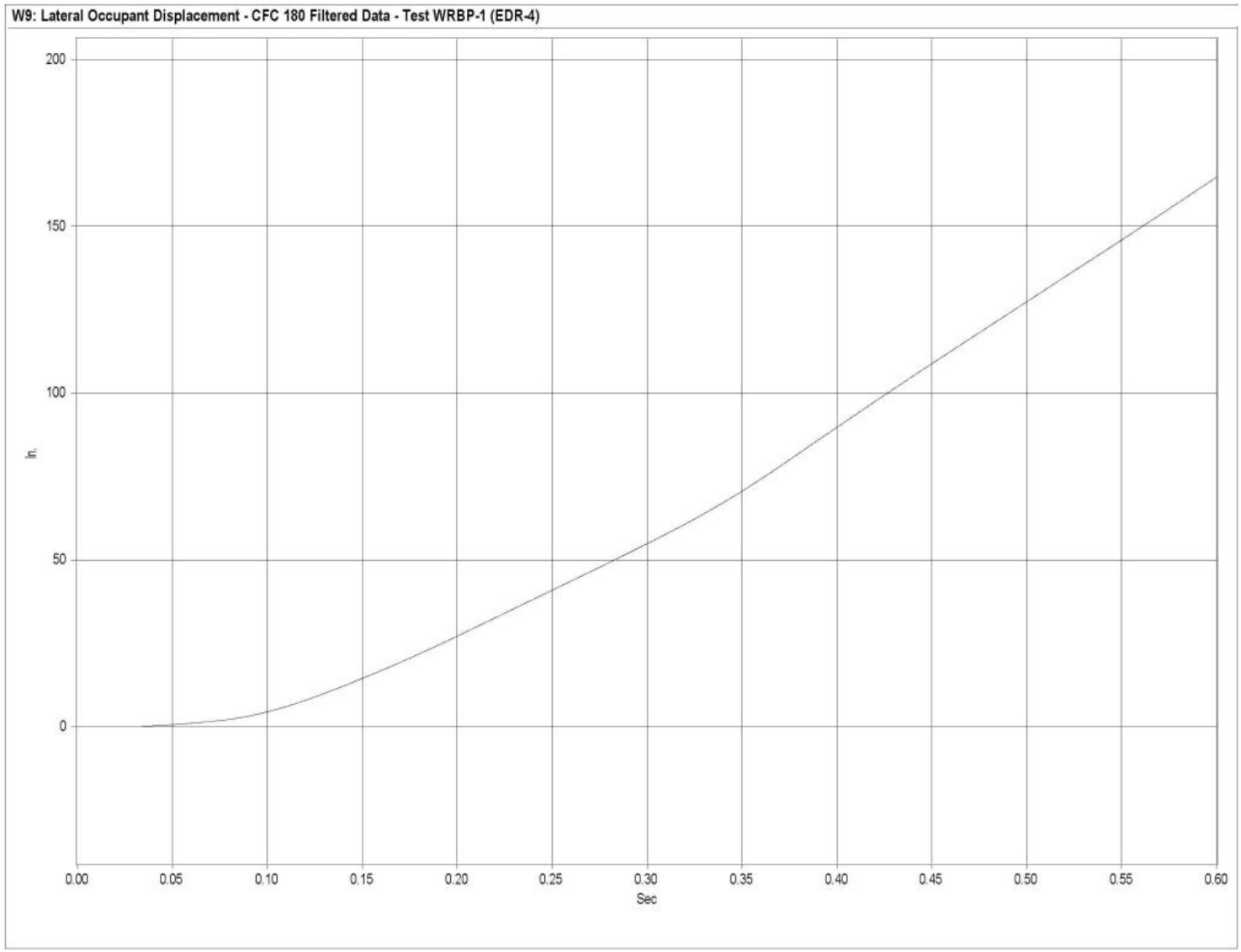

Figure L-6. Graph of Lateral Occupant Displacement, Test WRBP-1

APPENDIX M

Roll, Pitch, and Yaw Data Analysis - Test WRBP-1

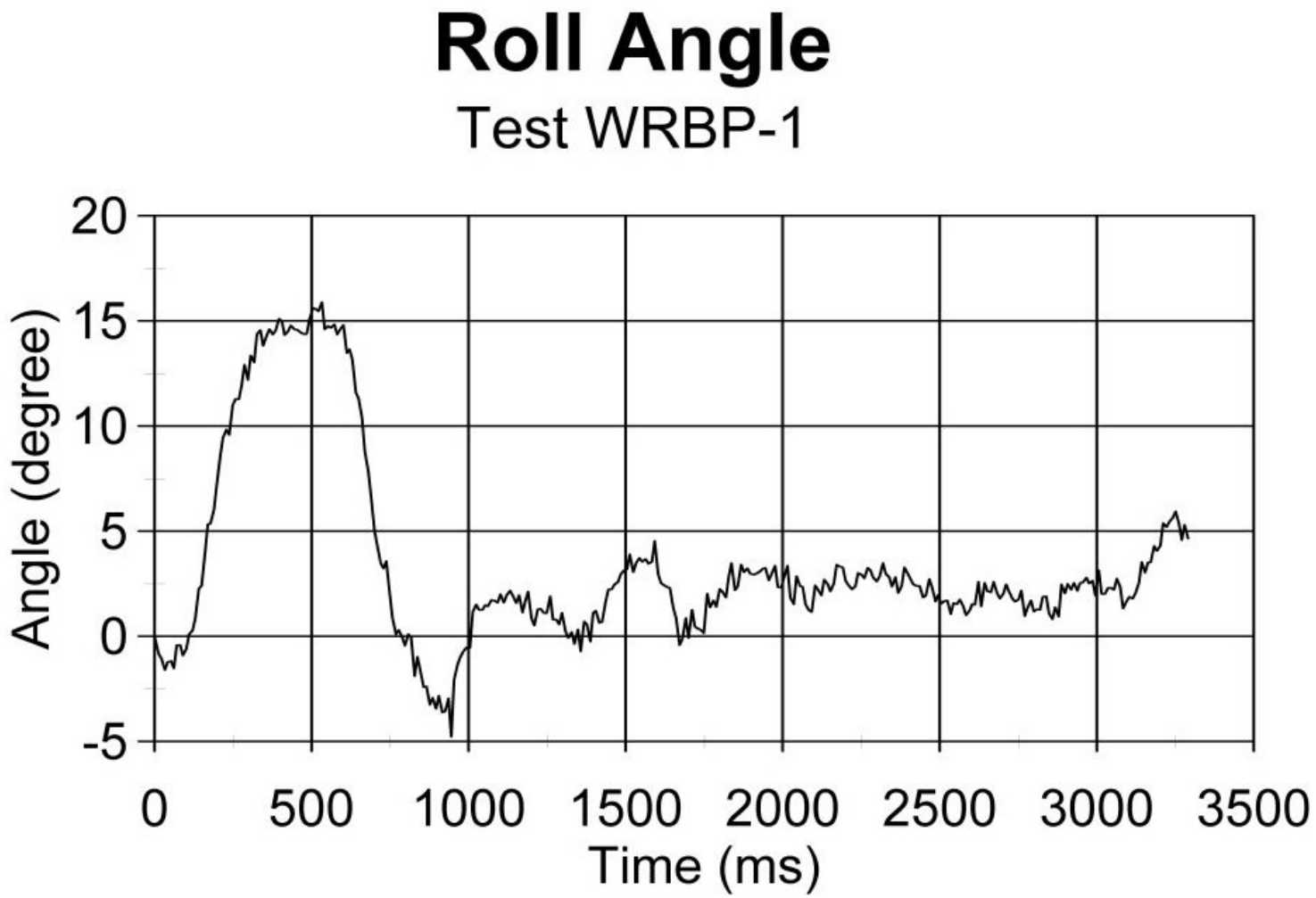

Figure M-1. Graph of Roll Angular Displacements, Test WRBP-1

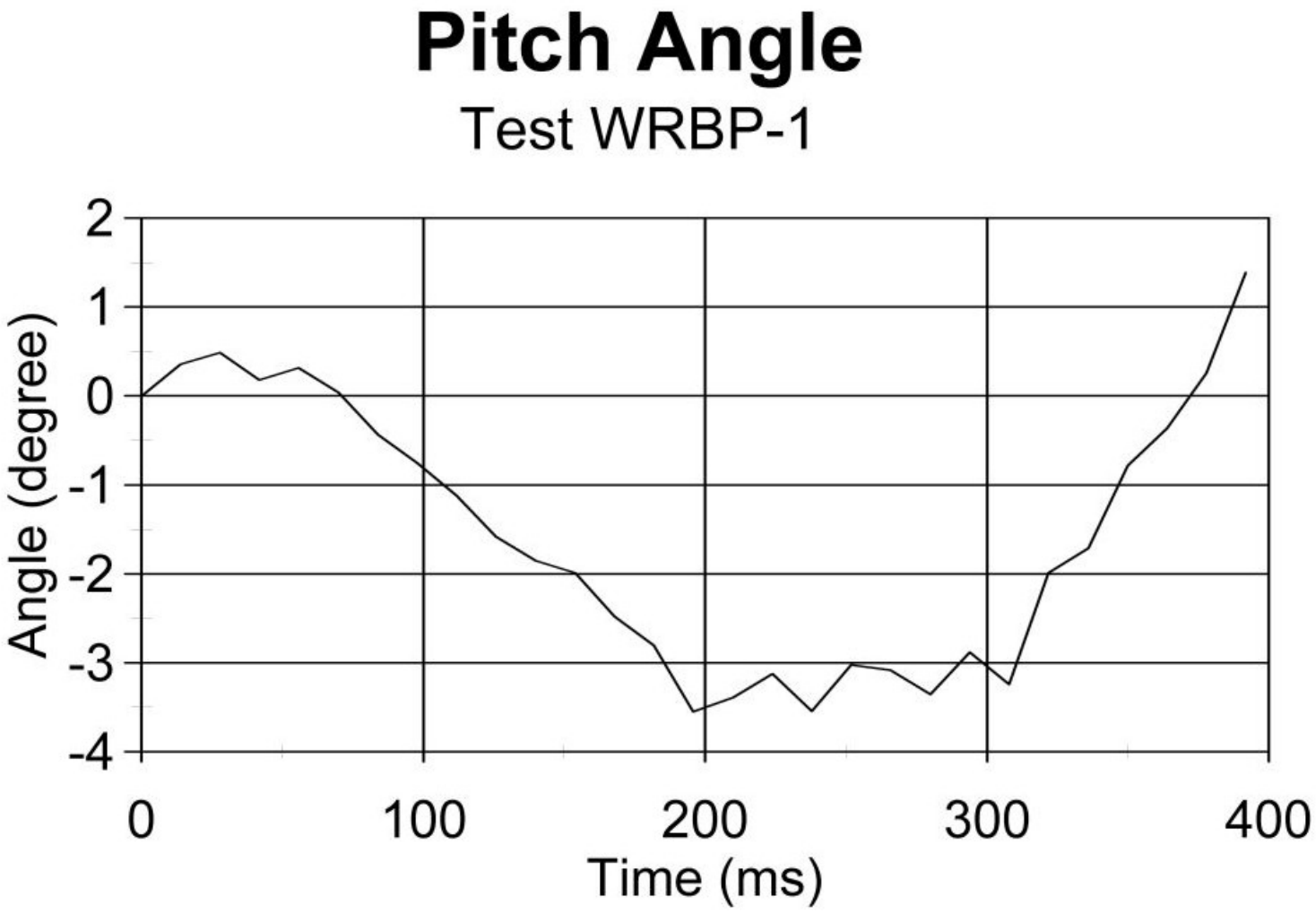

Figure M-2. Graph of Pitch Angular Displacements, Test WRBP-1

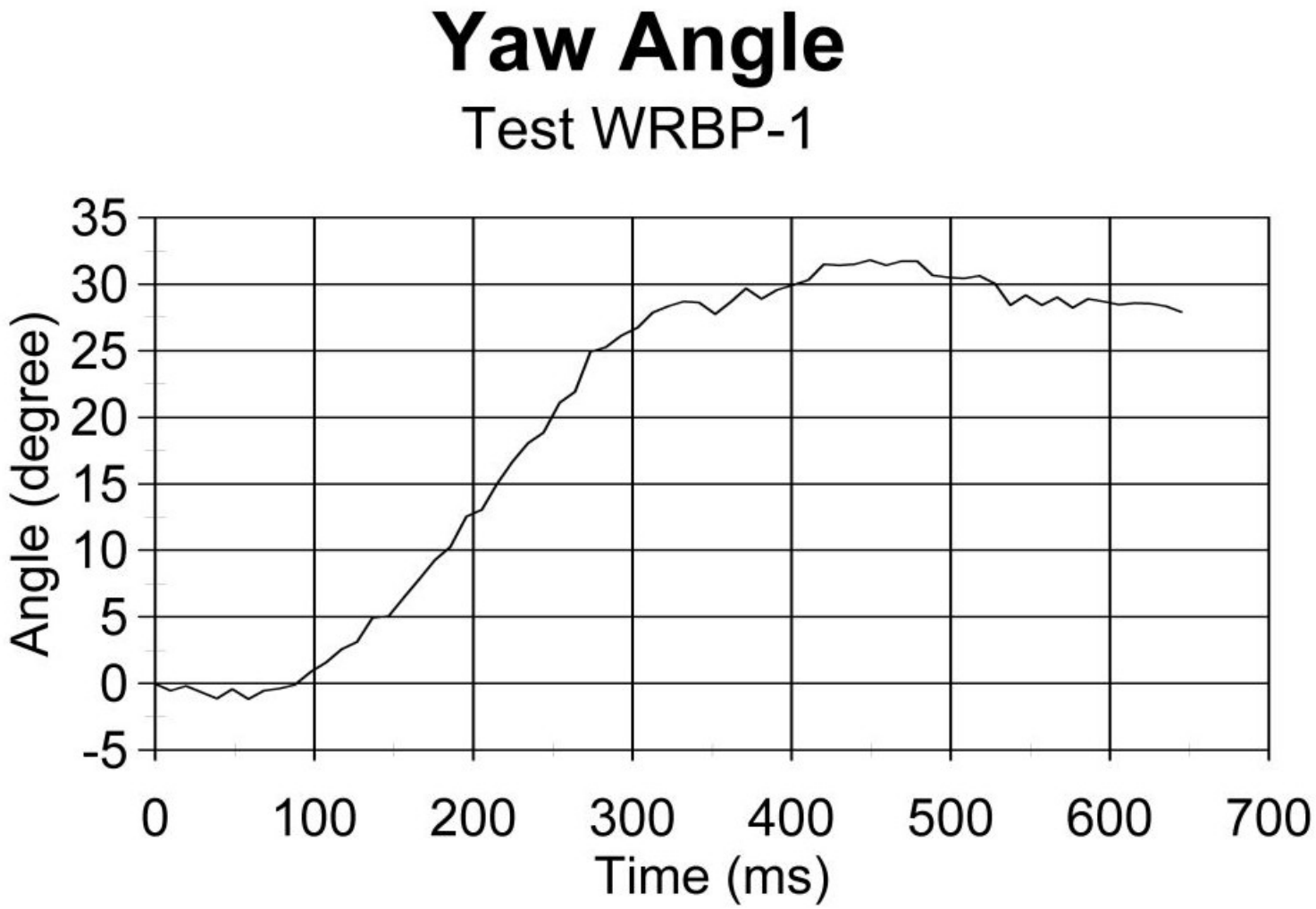

Figure M-3. Graph of Yaw Angular Displacements, Test WRBP-1

APPENDIX N

Strain Gauge Data Analysis - Test WRBP-1

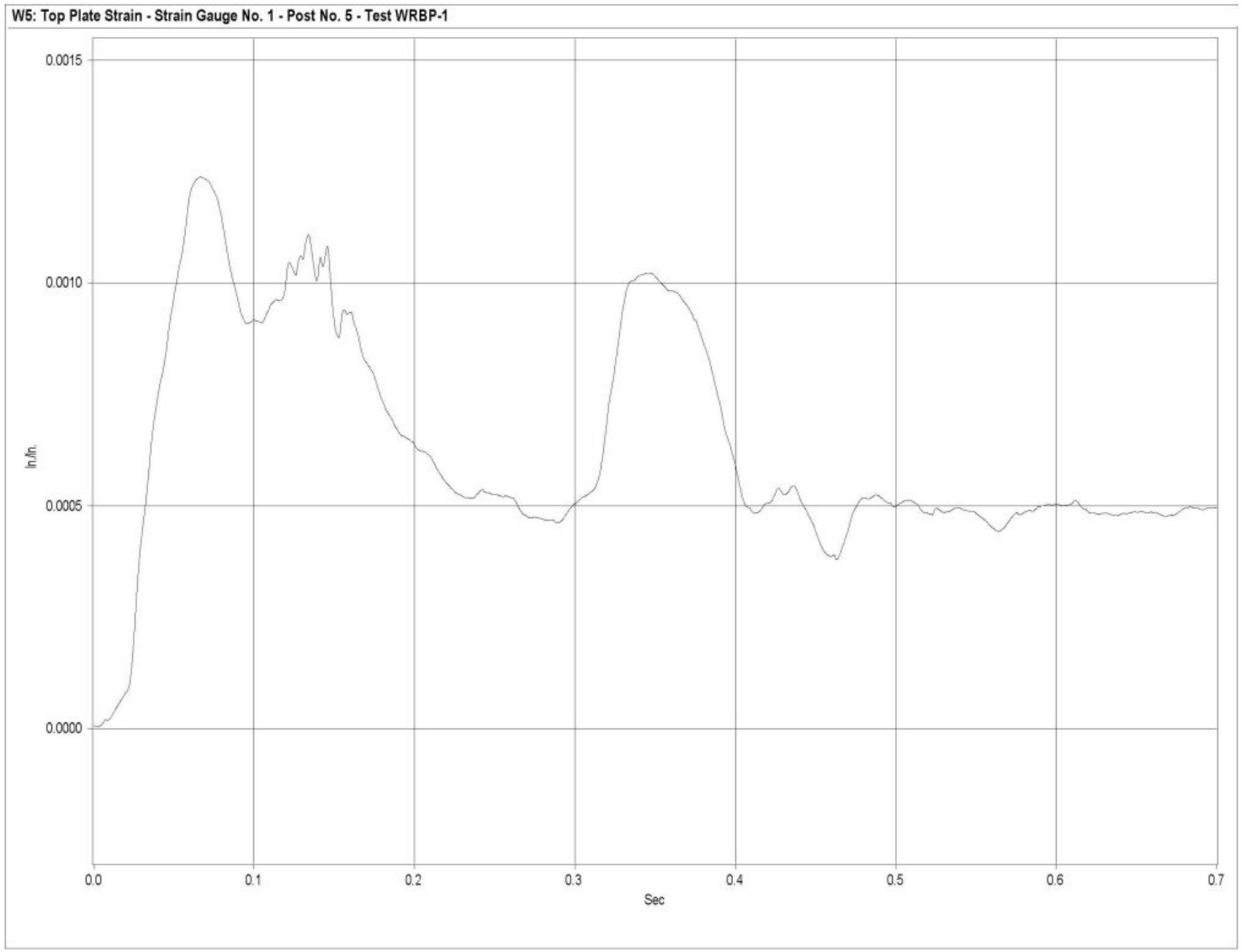

Figure N-1. Graph of Top Plate Post No. 5 - Strain Gauge No. 1 Perpendicular to Rail - Strain, Test WRBP-1

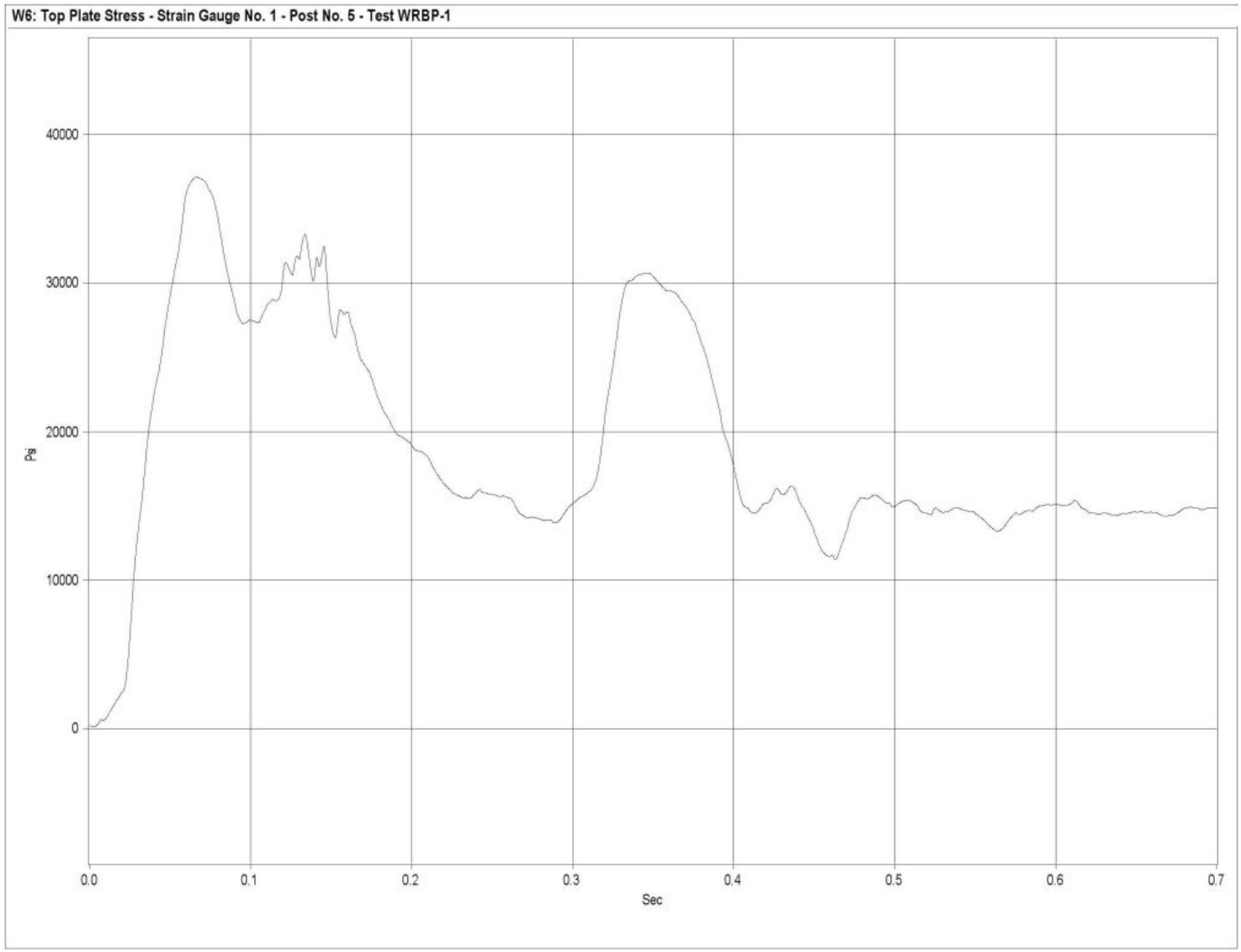

Figure N-2. Graph of Top Plate Post No. 5 - Strain Gauge No. 1 Perpendicular to Rail - Stress, Test WRBP-1

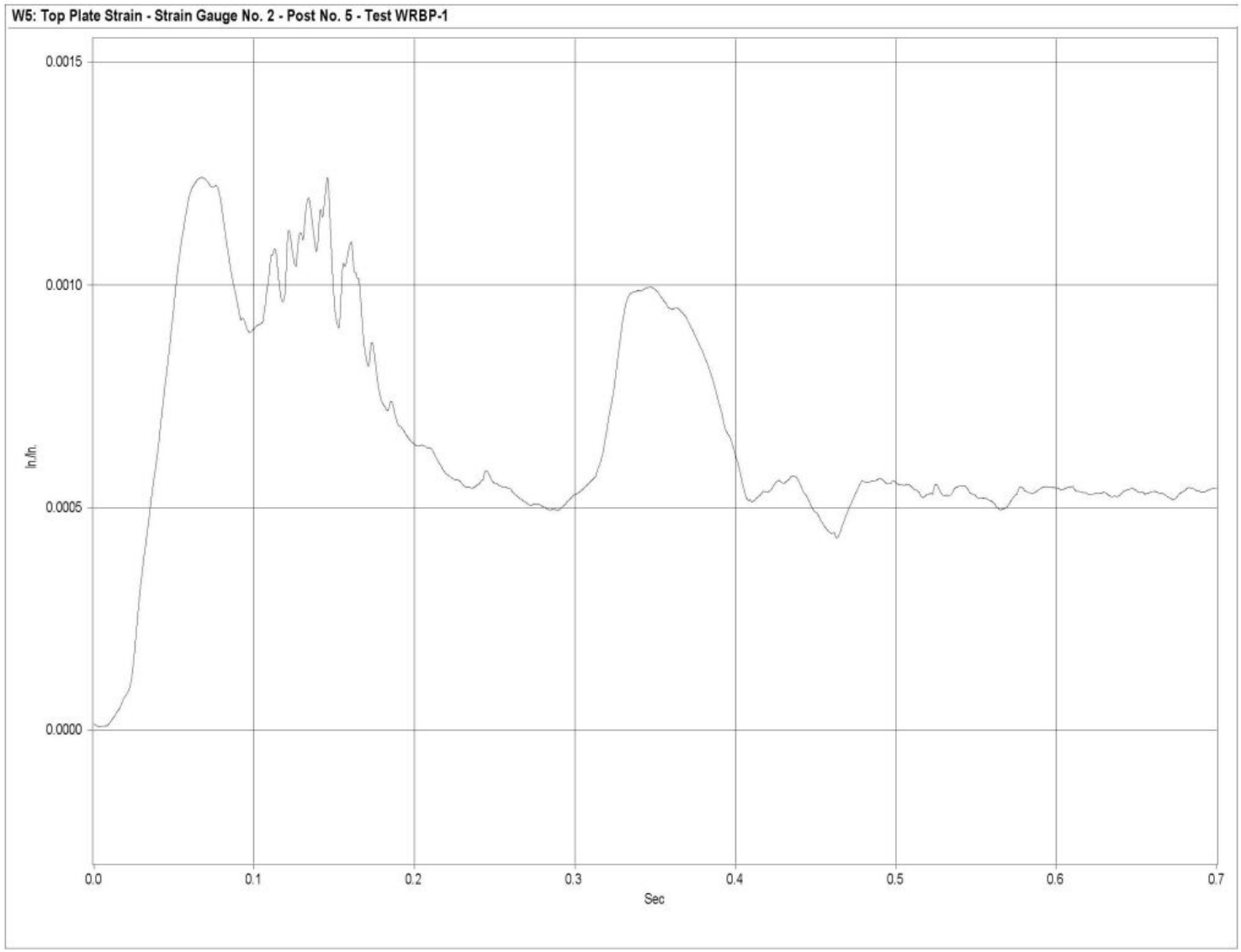

Figure N-3. Graph of Top Plate Post No. 5 - Strain Gauge No. 2 Perpendicular to Rail - Strain, Test WRBP-1

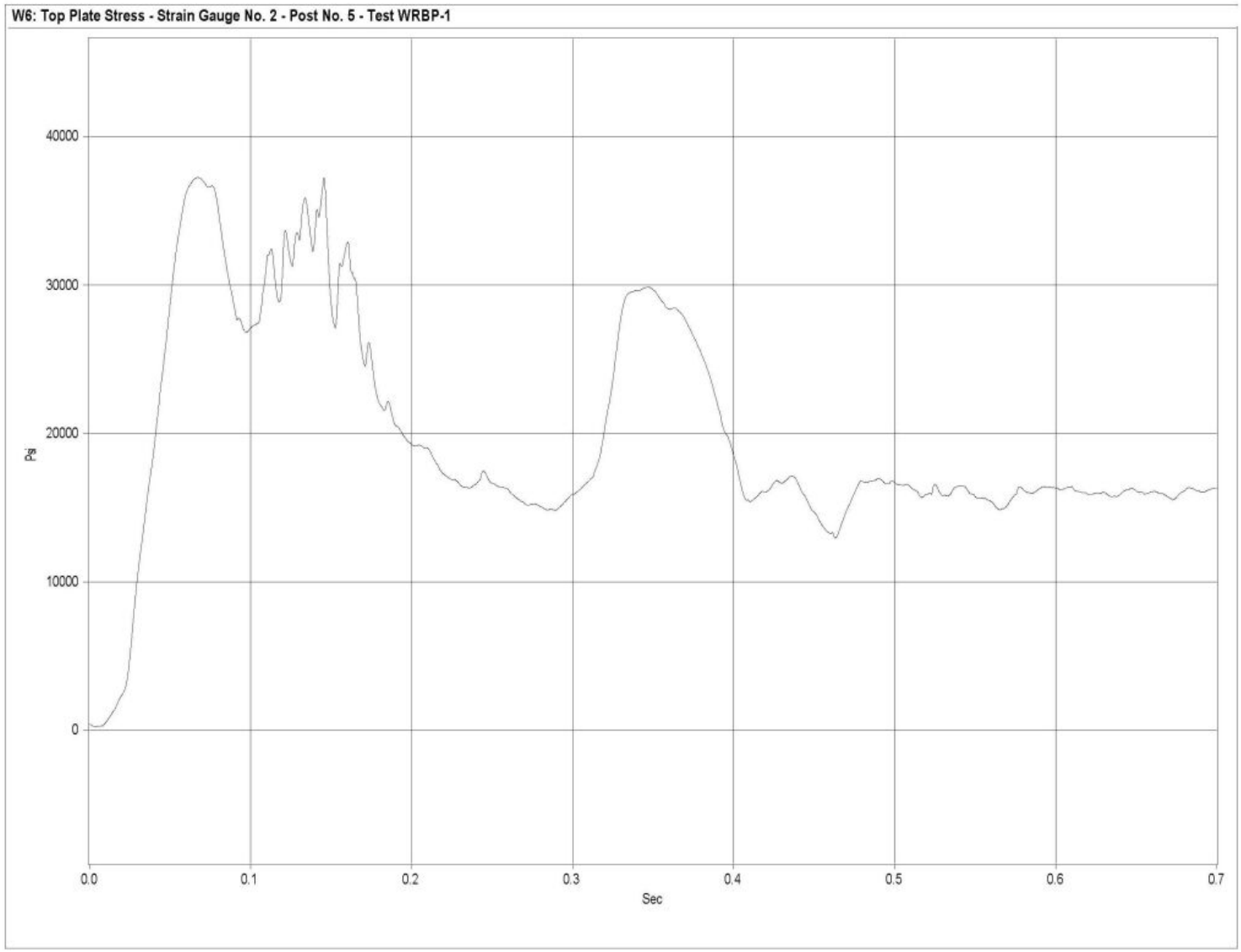

Figure N-4. Graph of Top Plate Post No. 5 - Strain Gauge No. 2 Perpendicular to Rail - Stress, Test WRBP-1

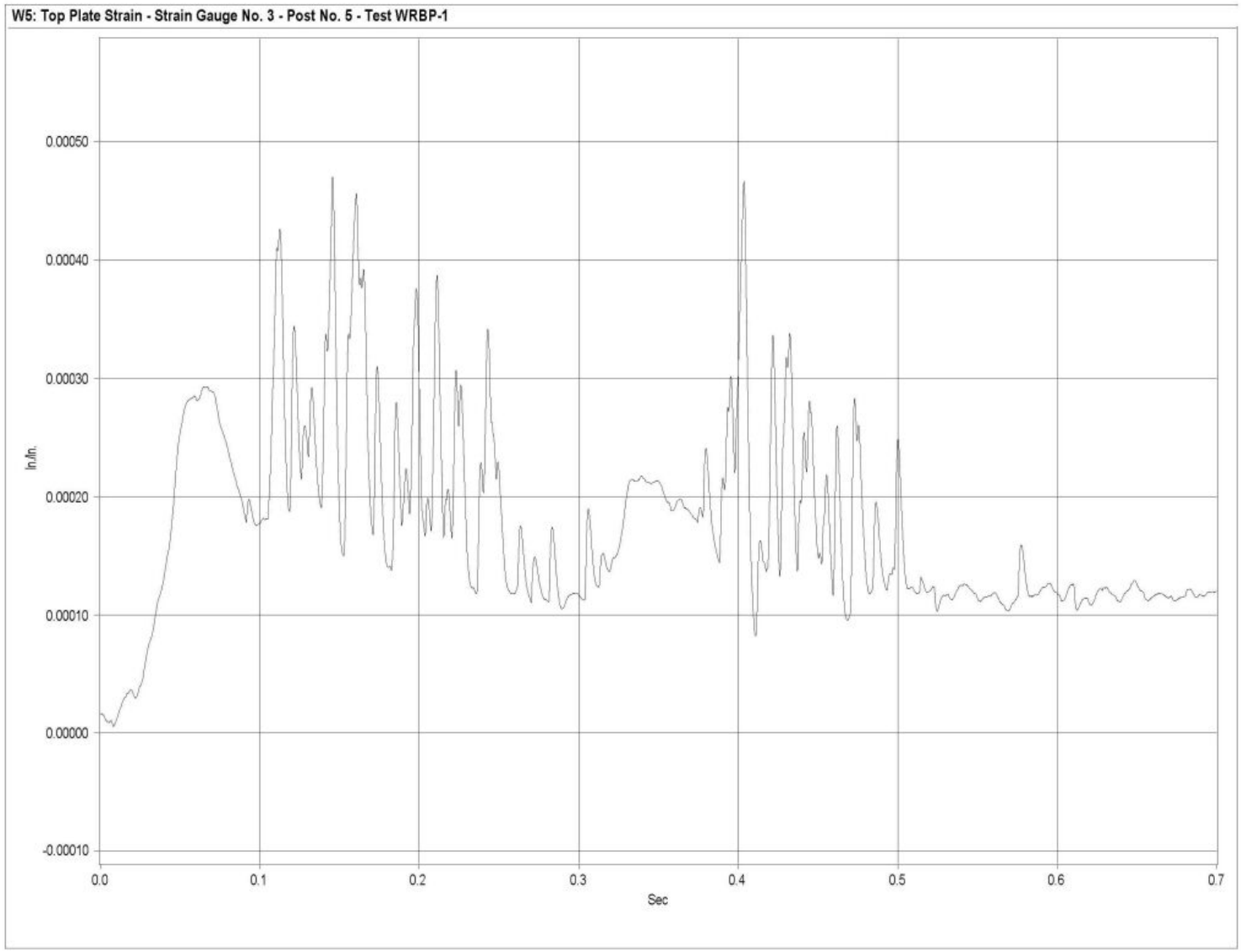

Figure N-5. Graph of Top Plate Post No. 5 - Strain Gauge No. 3 Perpendicular to Rail - Strain, Test WRBP-1

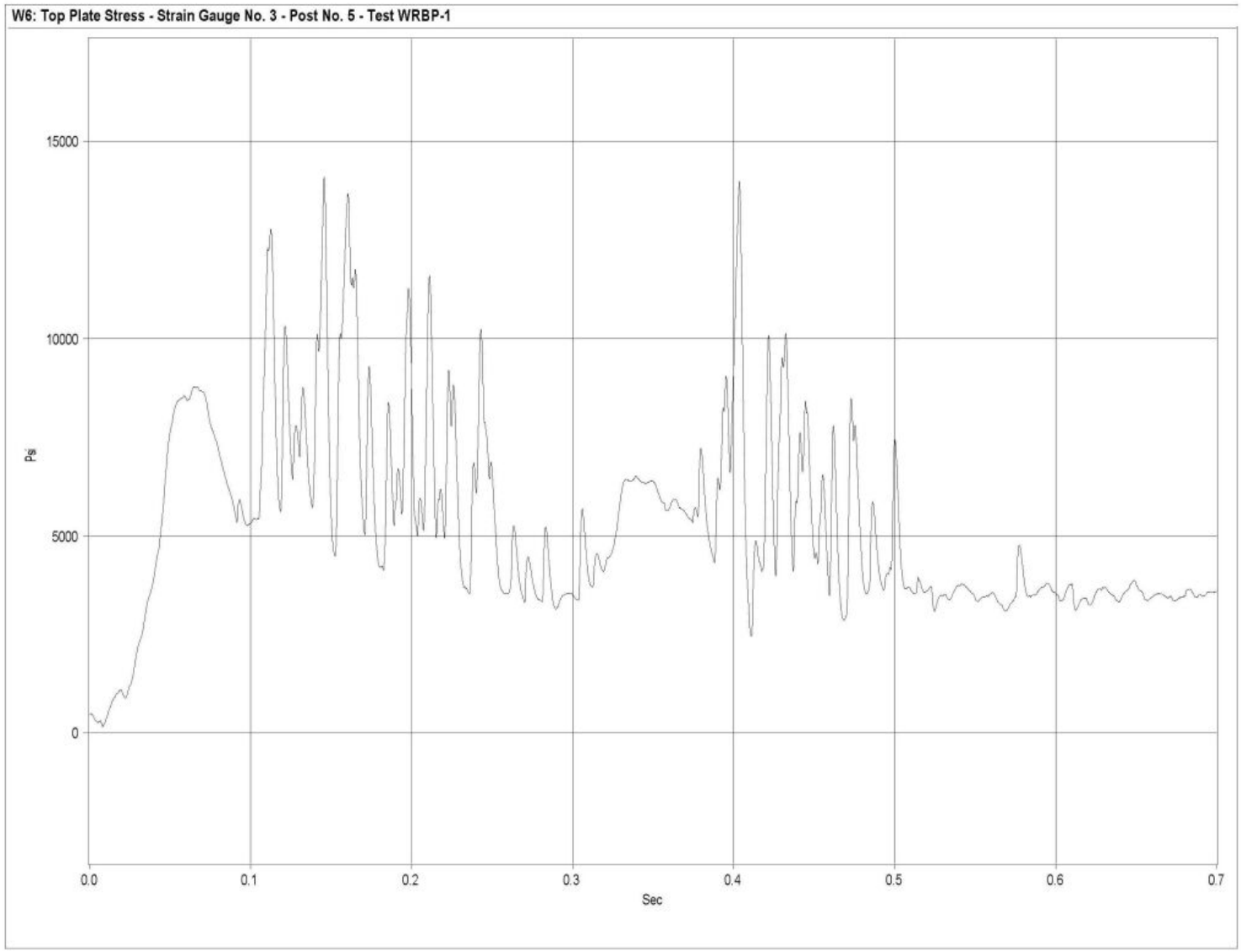

Figure N-6. Graph of Top Plate Post No. 5 - Strain Gauge No. 3 Perpendicular to Rail - Stress, Test WRBP-1

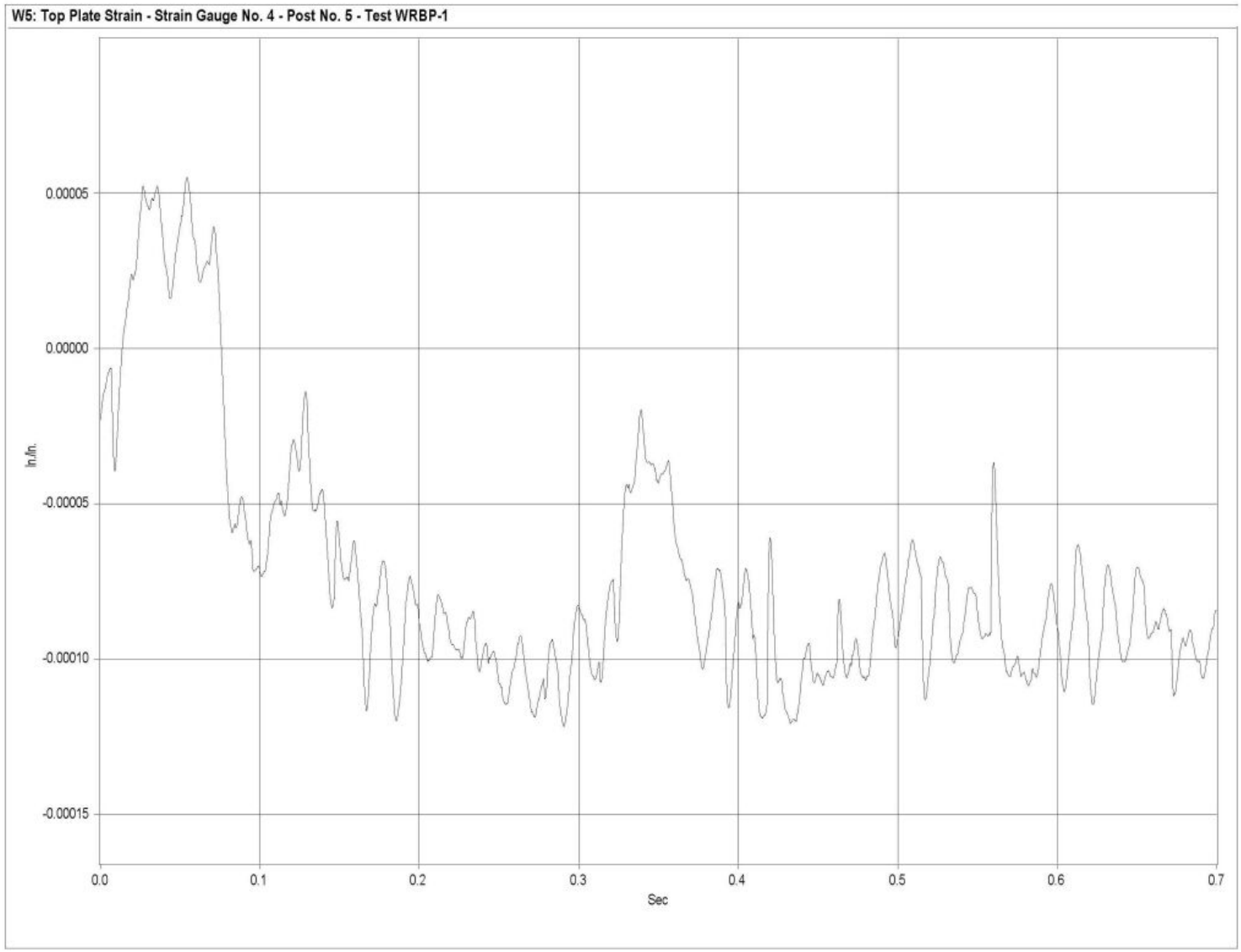

Figure N-7. Graph of Top Plate Post No. 5 - Strain Gauge No. 4 Perpendicular to Rail - Strain, Test WRBP-1

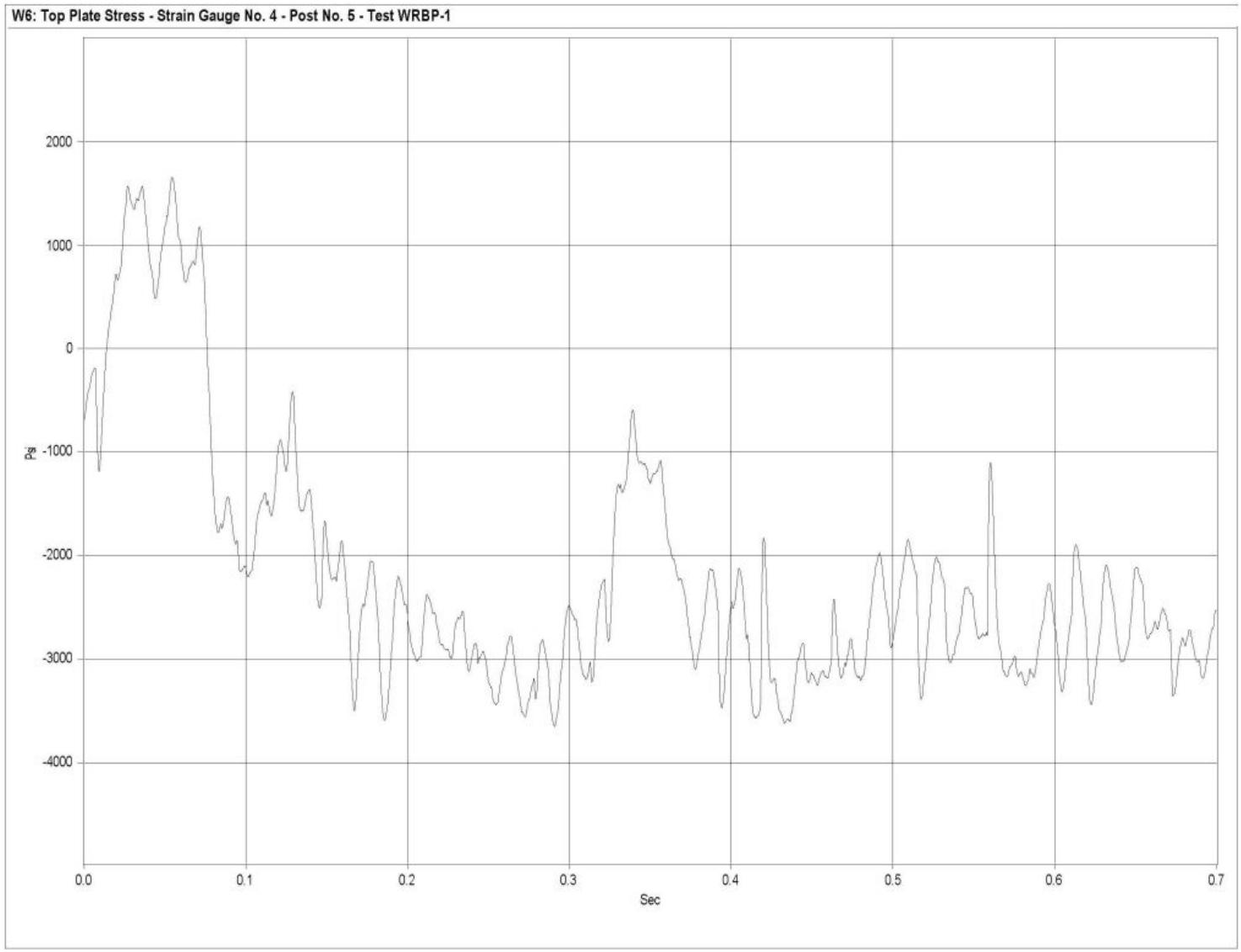

Figure N-8. Graph of Top Plate Post No. 5 - Strain Gauge No. 4 Perpendicular to Rail - Stress, Test WRBP-1

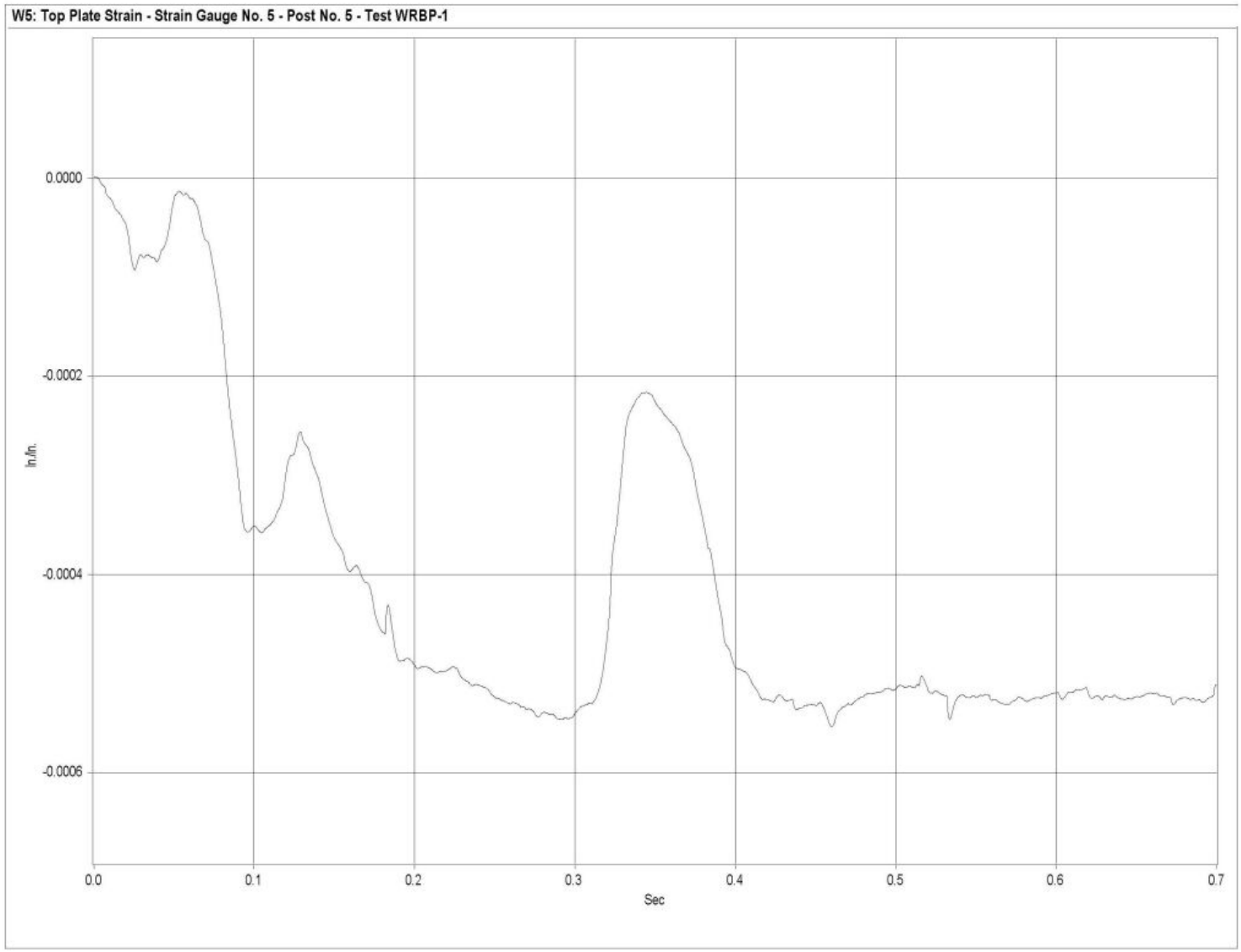

Figure N-9. Graph of Top Plate Post No. 5 - Strain Gauge No. 5 Perpendicular to Rail - Strain, Test WRBP-1

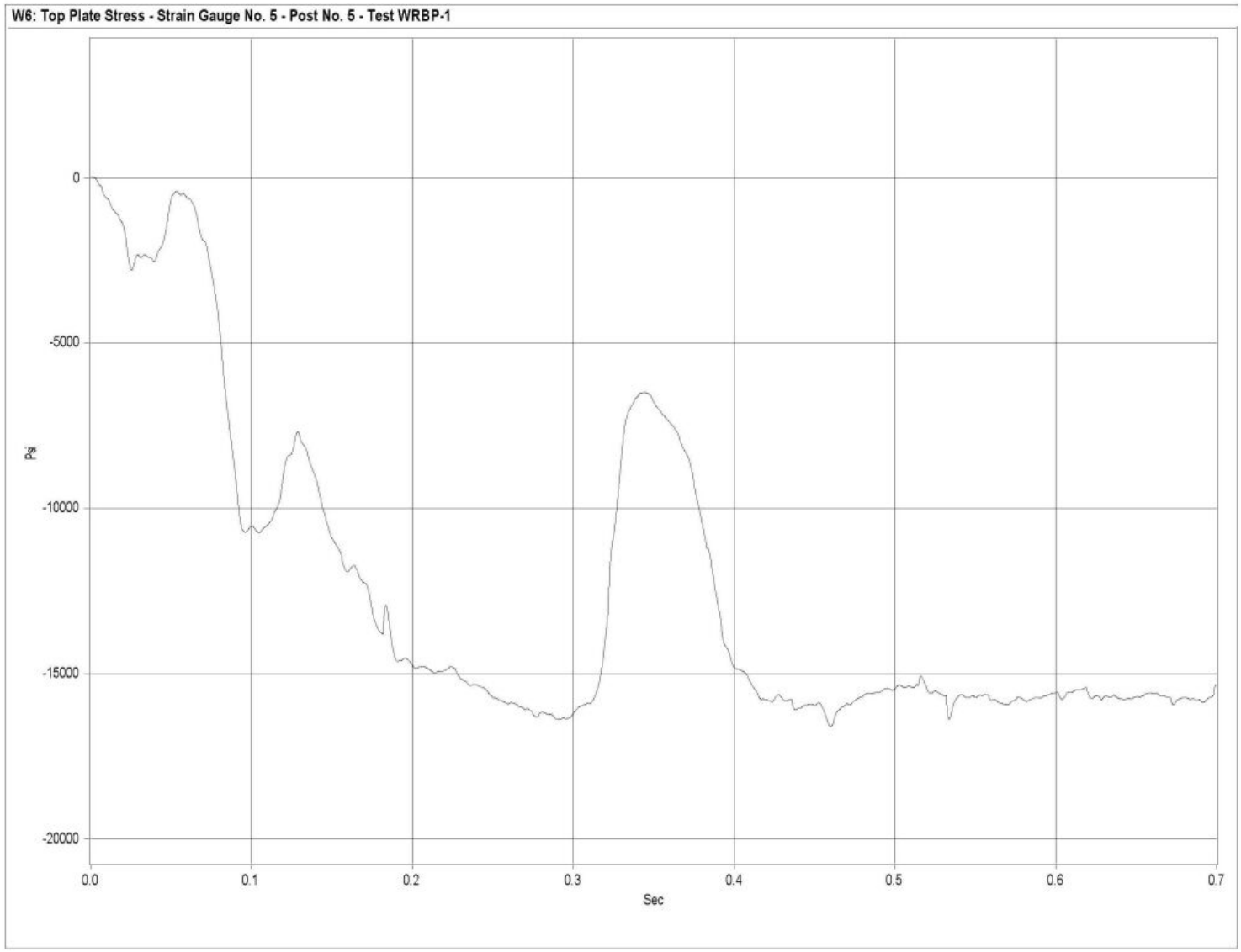

Figure N-10. Graph of Top Plate Post No. 5 - Strain Gauge No. 5 Perpendicular to Rail - Stress, Test WRBP-1

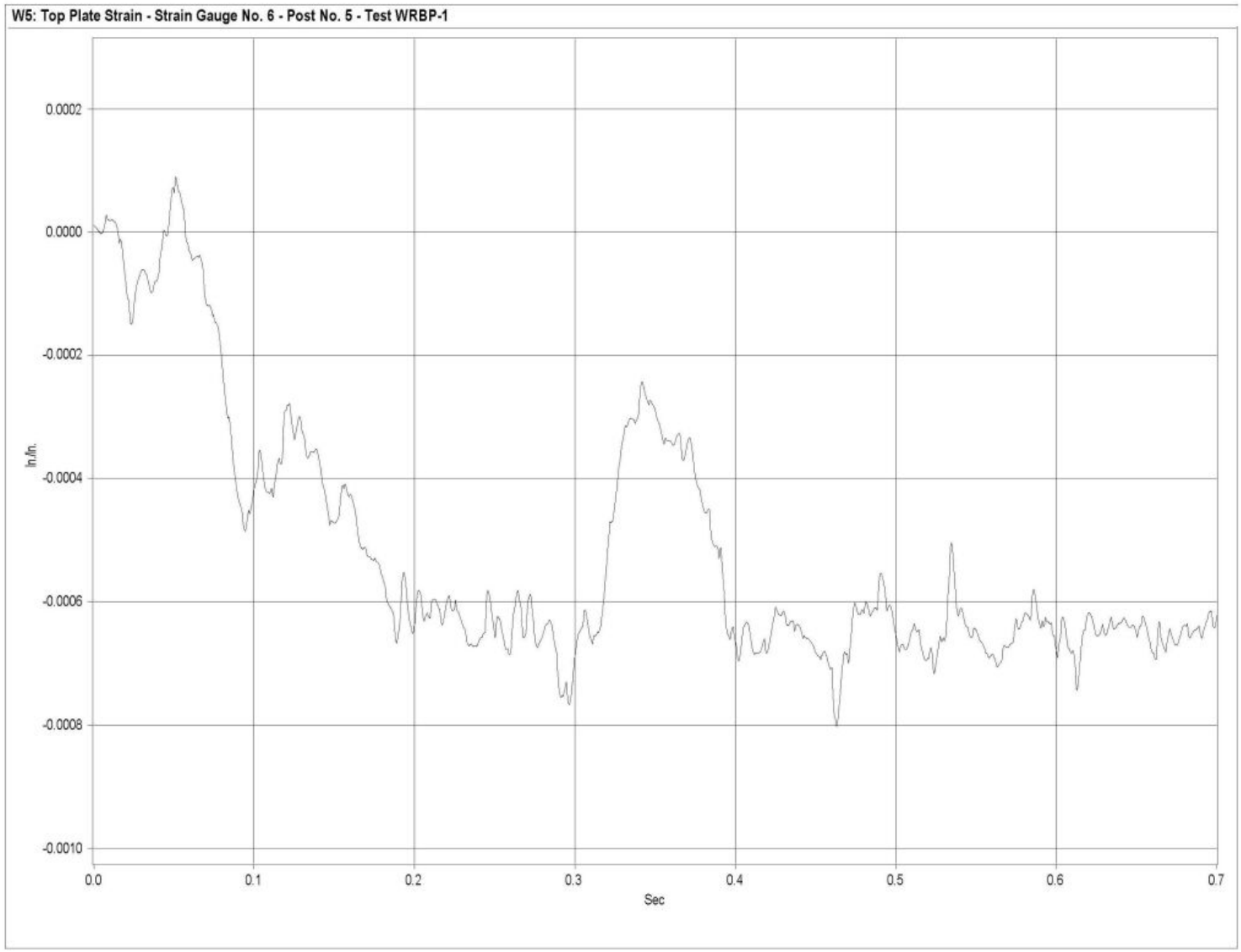

Figure N-11. Graph of Top Plate Post No. 5 - Strain Gauge No. 6 Perpendicular to Rail - Strain, Test WRBP-1

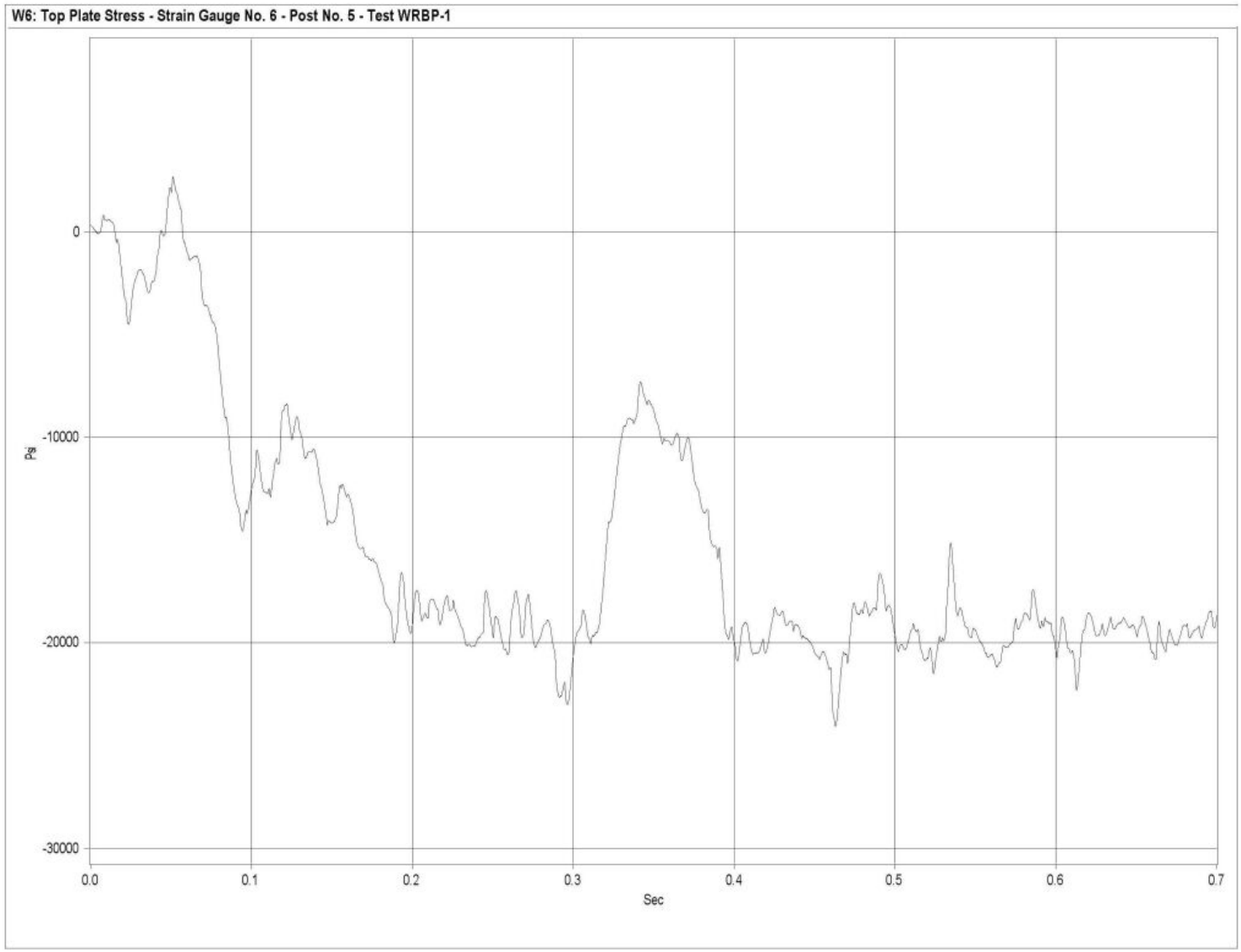

Figure N-12. Graph of Top Plate Post No. 5 - Strain Gauge No. 6 Perpendicular to Rail - Stress, Test WRBP-1

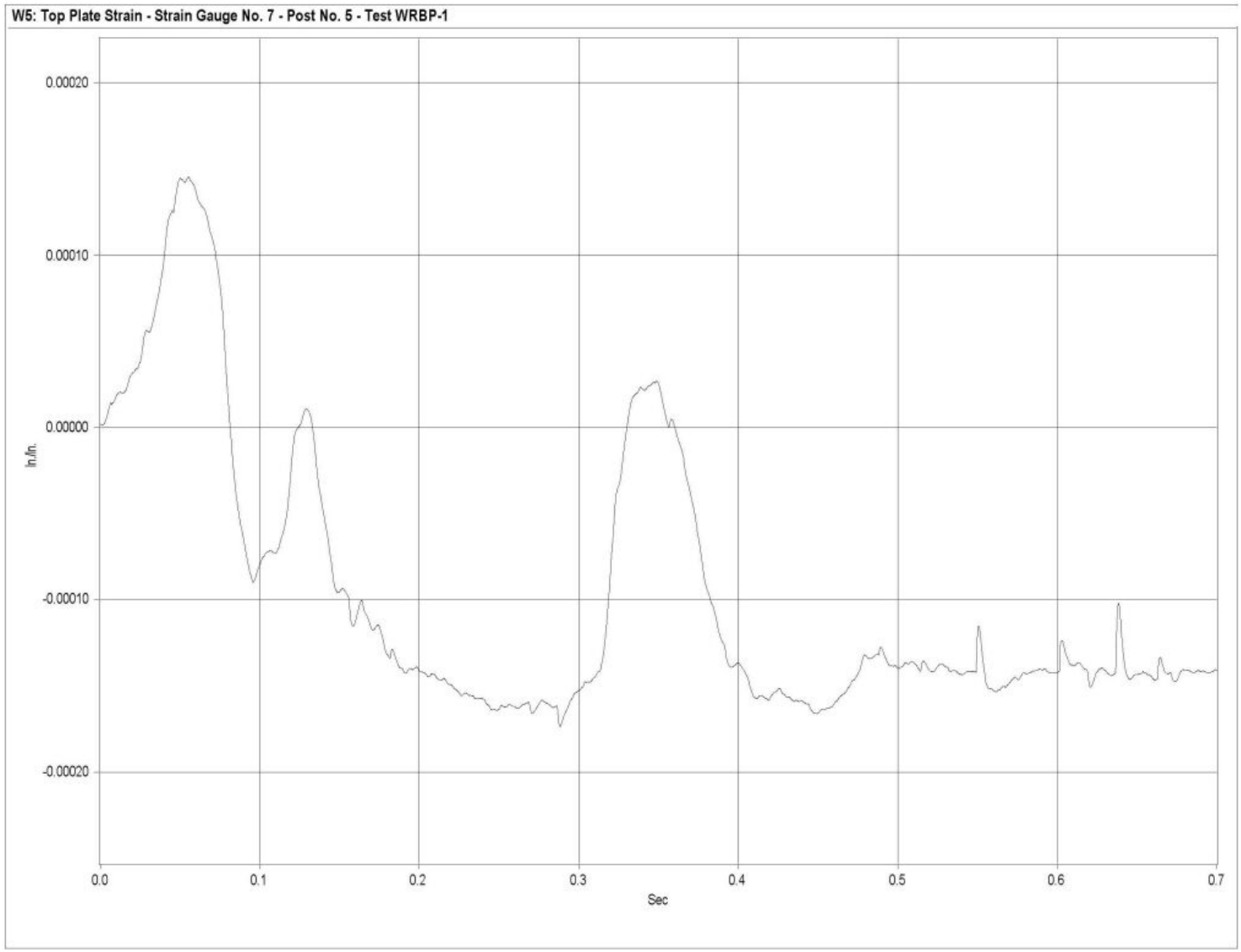

Figure N-13. Graph of Top Plate Post No. 5 - Strain Gauge No. 7 Perpendicular to Rail - Strain, Test WRBP-1

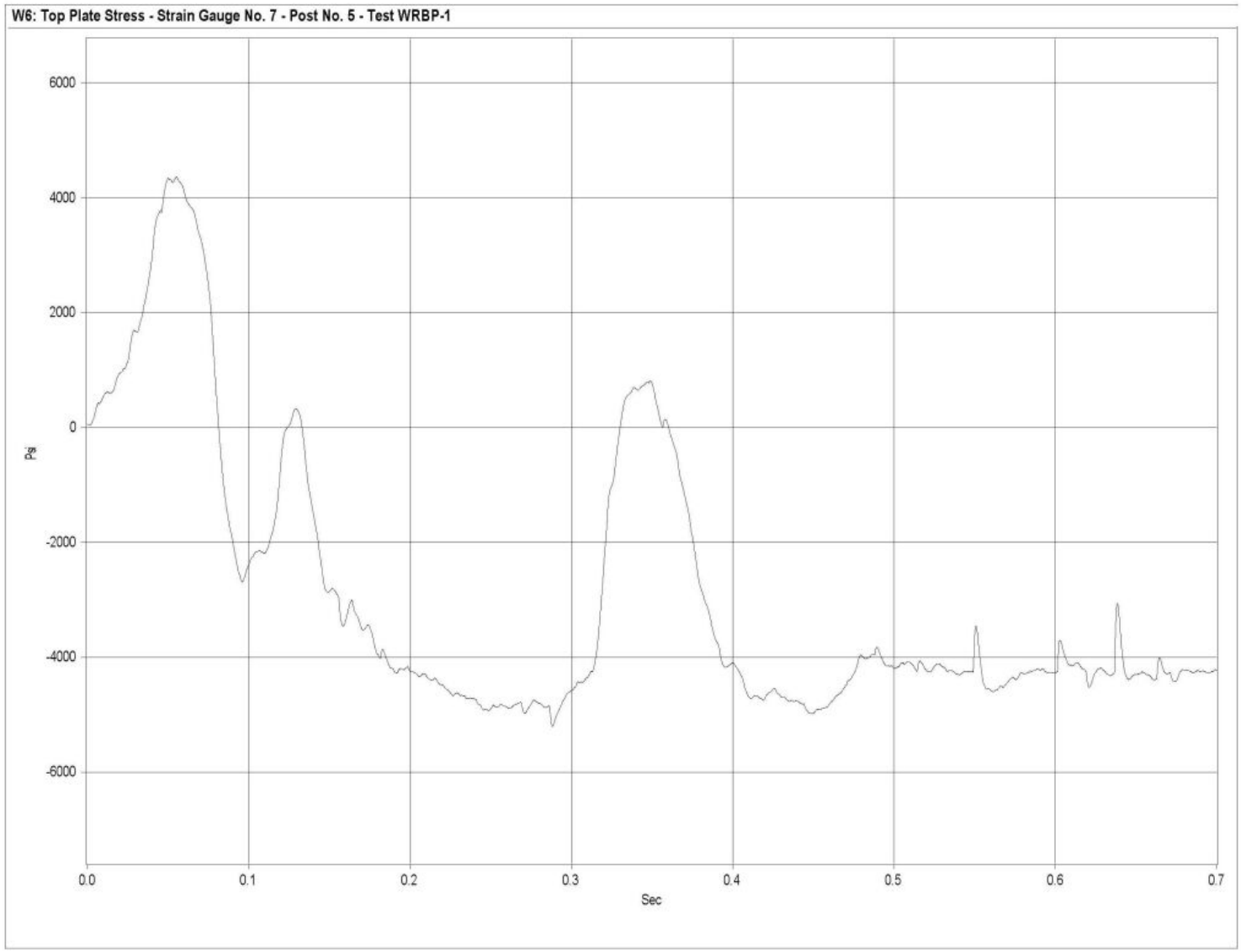

Figure N-14. Graph of Top Plate Post No. 5 - Strain Gauge No. 7 Perpendicular to Rail - Stress, Test WRBP-1

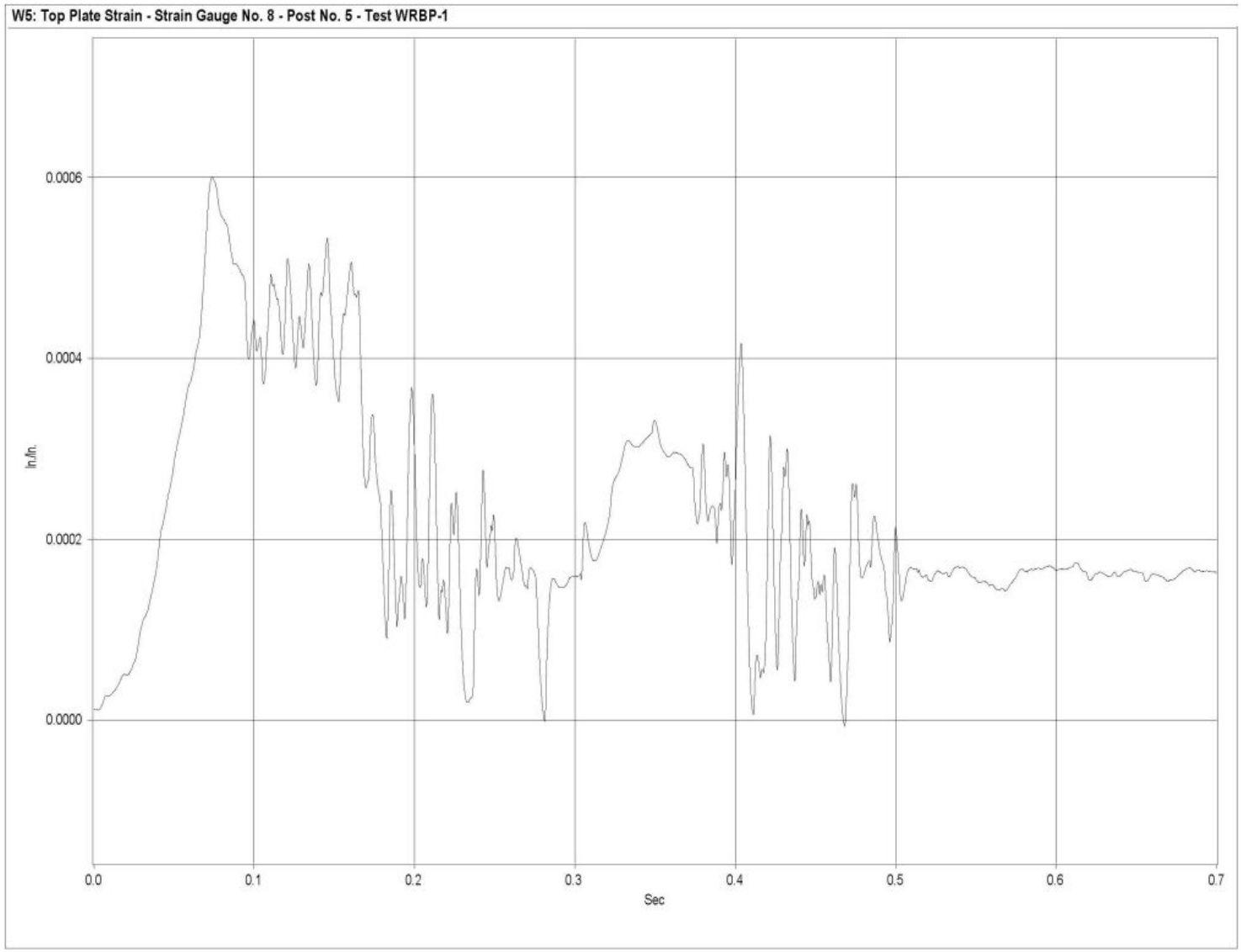

Figure N-15. Graph of Top Plate Post No. 5 - Strain Gauge No. 8 Perpendicular to Rail - Strain, Test WRBP-1

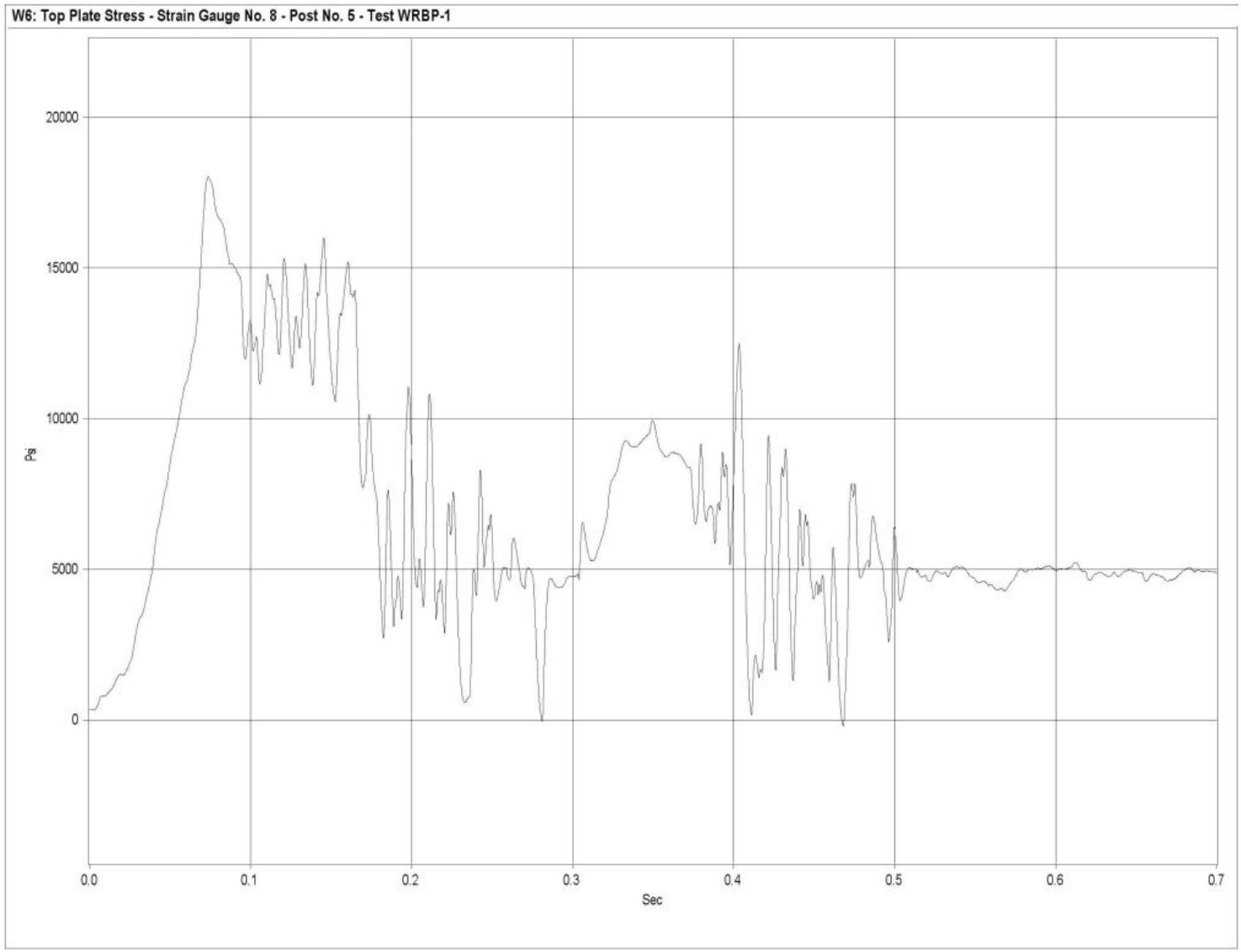

Figure N-16. Graph of Top Plate Post No. 5 - Strain Gauge No. 8 Perpendicular to Rail - Stress, Test WRBP-1

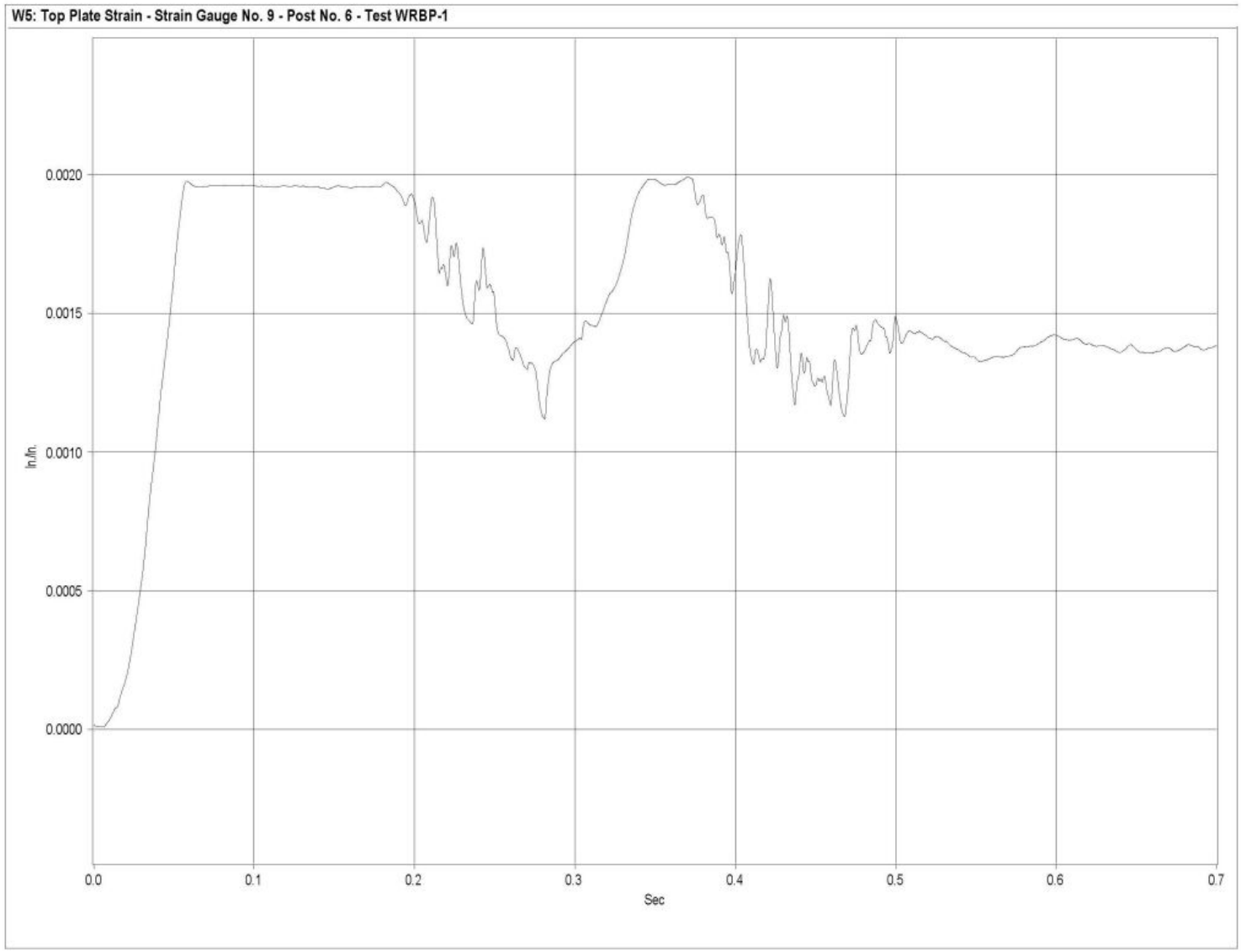

Figure N-17. Graph of Top Plate Post No. 6 - Strain Gauge No. 9 Perpendicular to Rail - Strain, Test WRBP-1

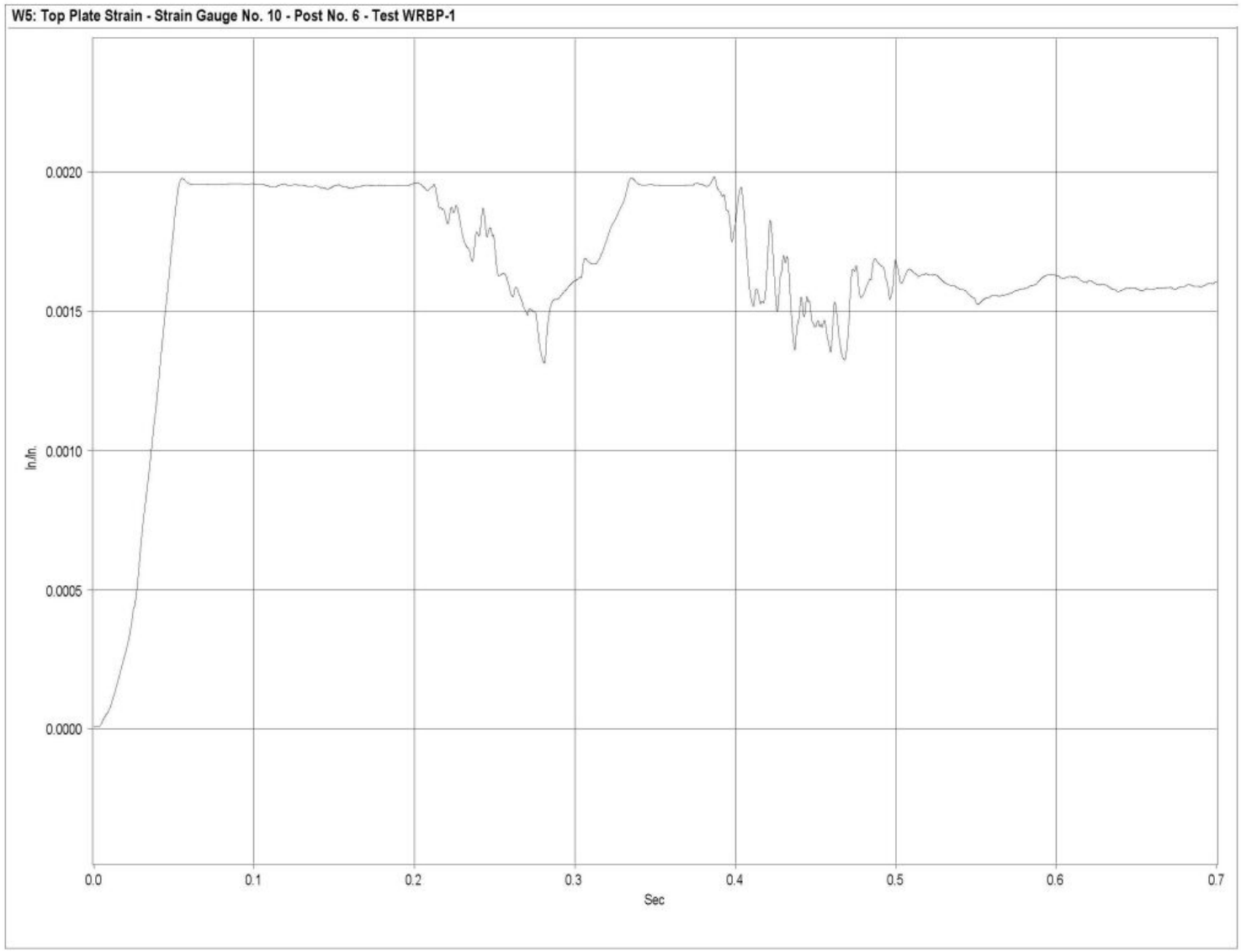

Figure N-18. Graph of Top Plate Post No. 6 - Strain Gauge No. 10 Perpendicular to Rail - Strain, Test WRBP-1

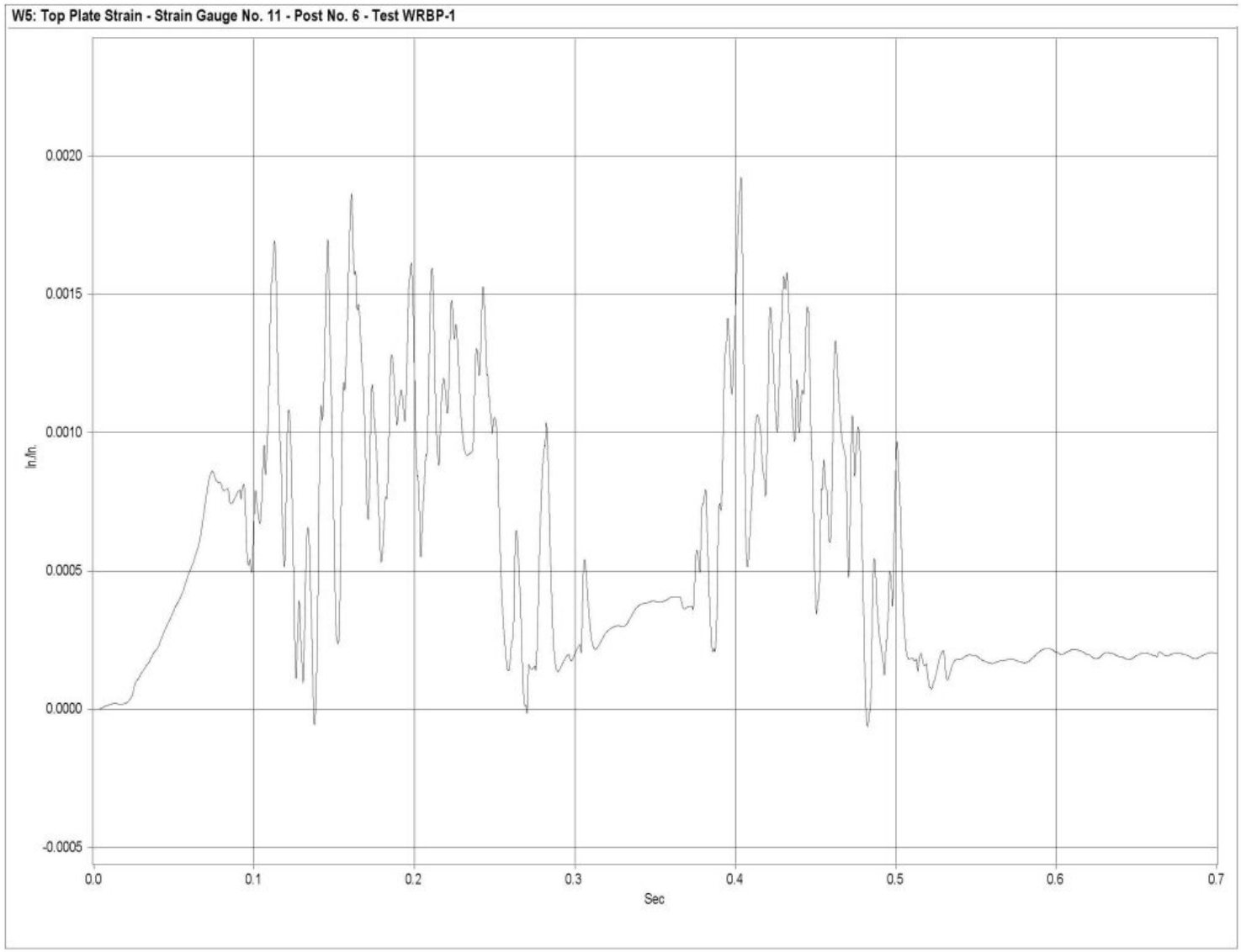

Figure N-19. Graph of Top Plate Post No. 6 - Strain Gauge No. 11 Perpendicular to Rail - Strain, Test WRBP-1

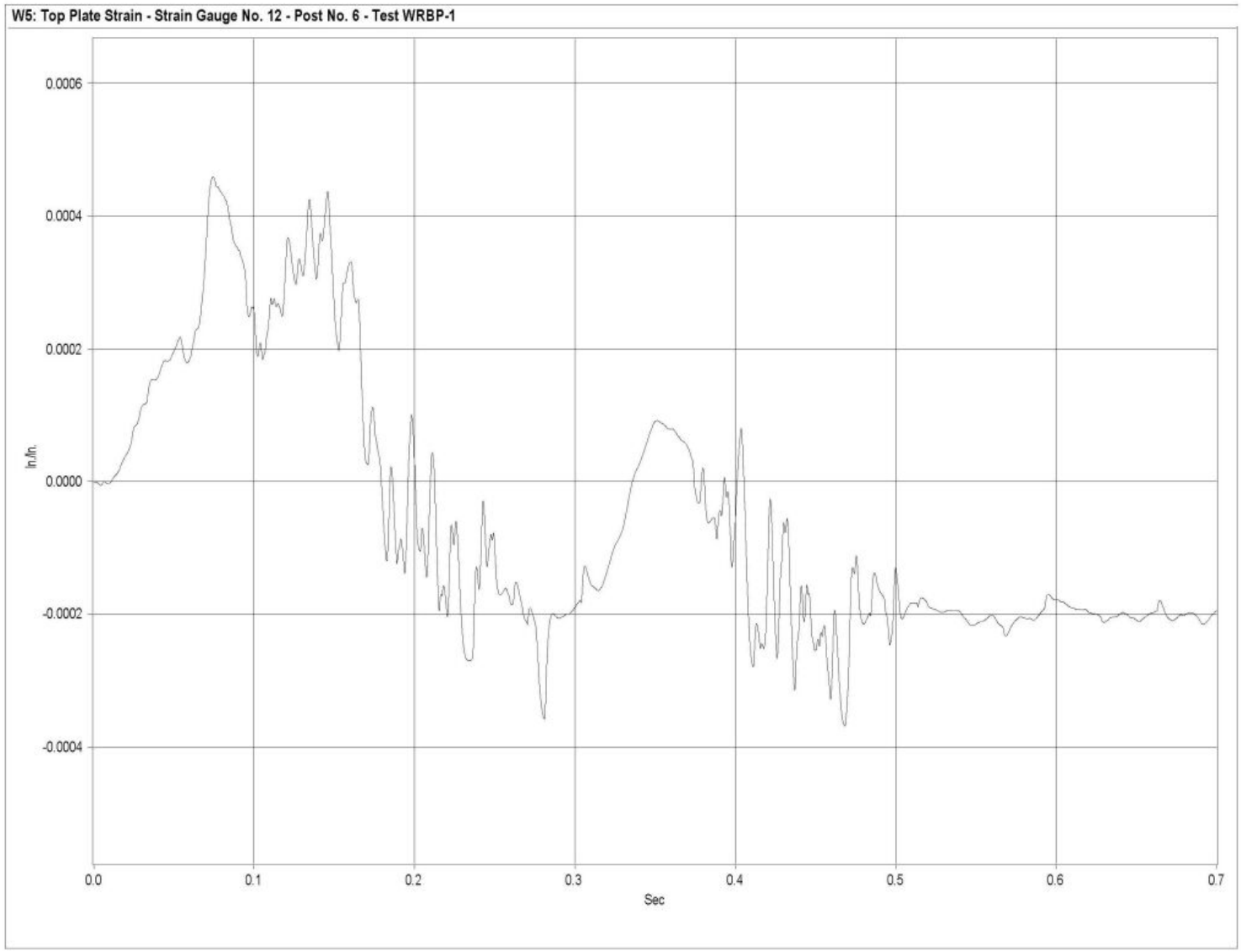

Figure N-20. Graph of Top Plate Post No. 6 - Strain Gauge No. 12 Perpendicular to Rail - Strain, Test WRBP-1

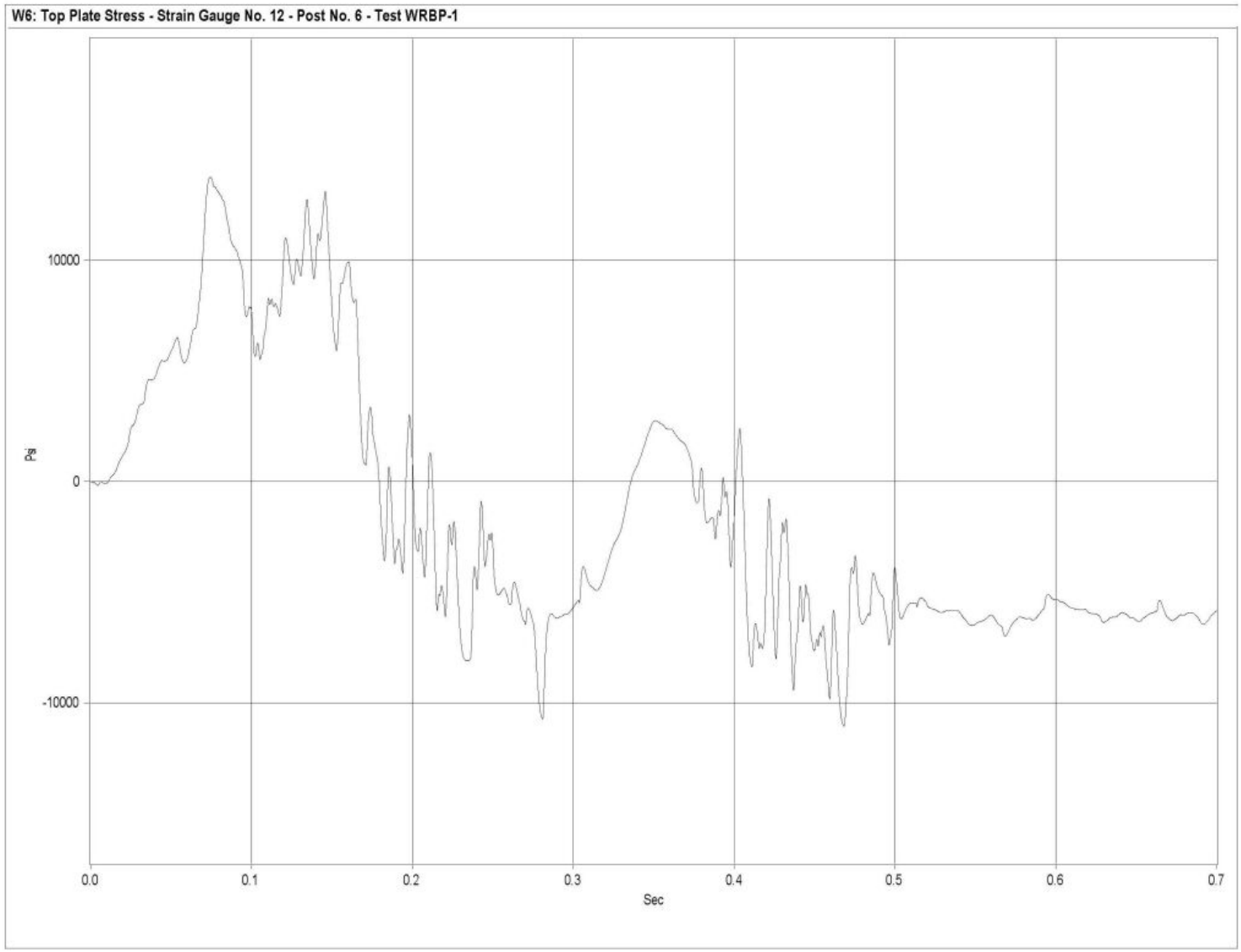

Figure N-21. Graph of Top Plate Post No. 6 - Strain Gauge No. 12 Perpendicular to Rail - Stress, Test WRBP-1

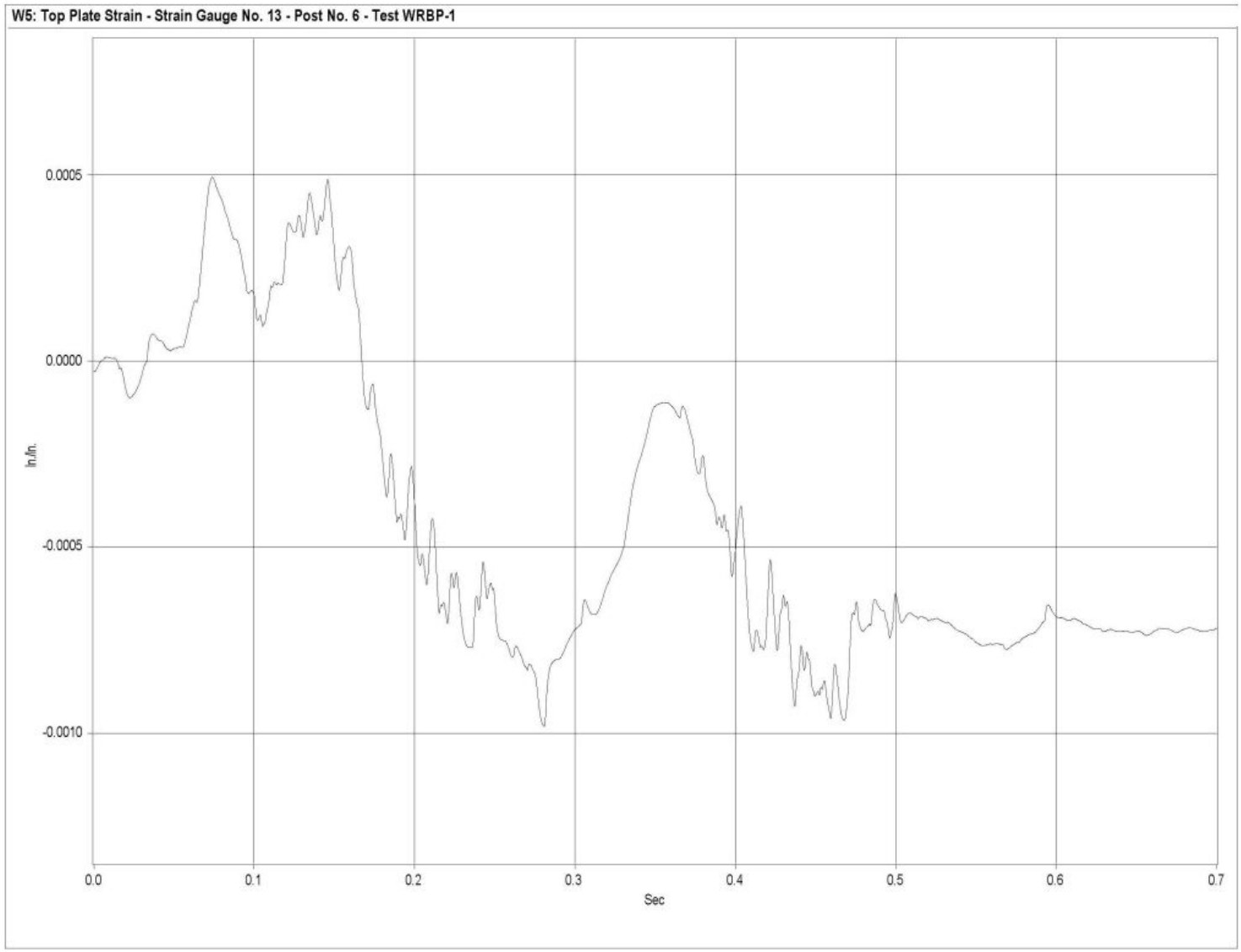

Figure N-22. Graph of Top Plate Post No. 6 - Strain Gauge No. 13 Perpendicular to Rail - Strain, Test WRBP-1

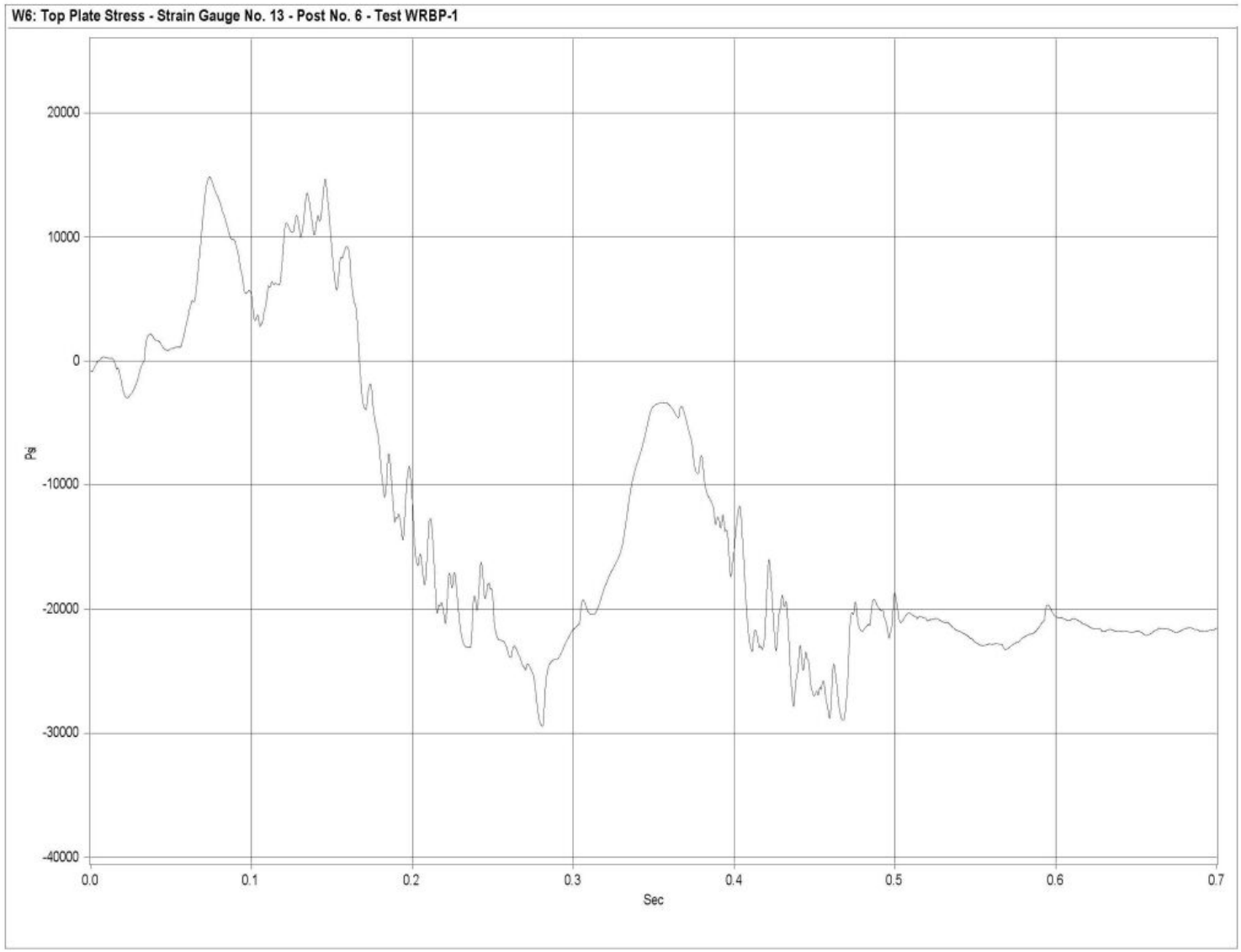

Figure N-23. Graph of Top Plate Post No. 6 - Strain Gauge No. 13 Perpendicular to Rail - Stress, Test WRBP-1

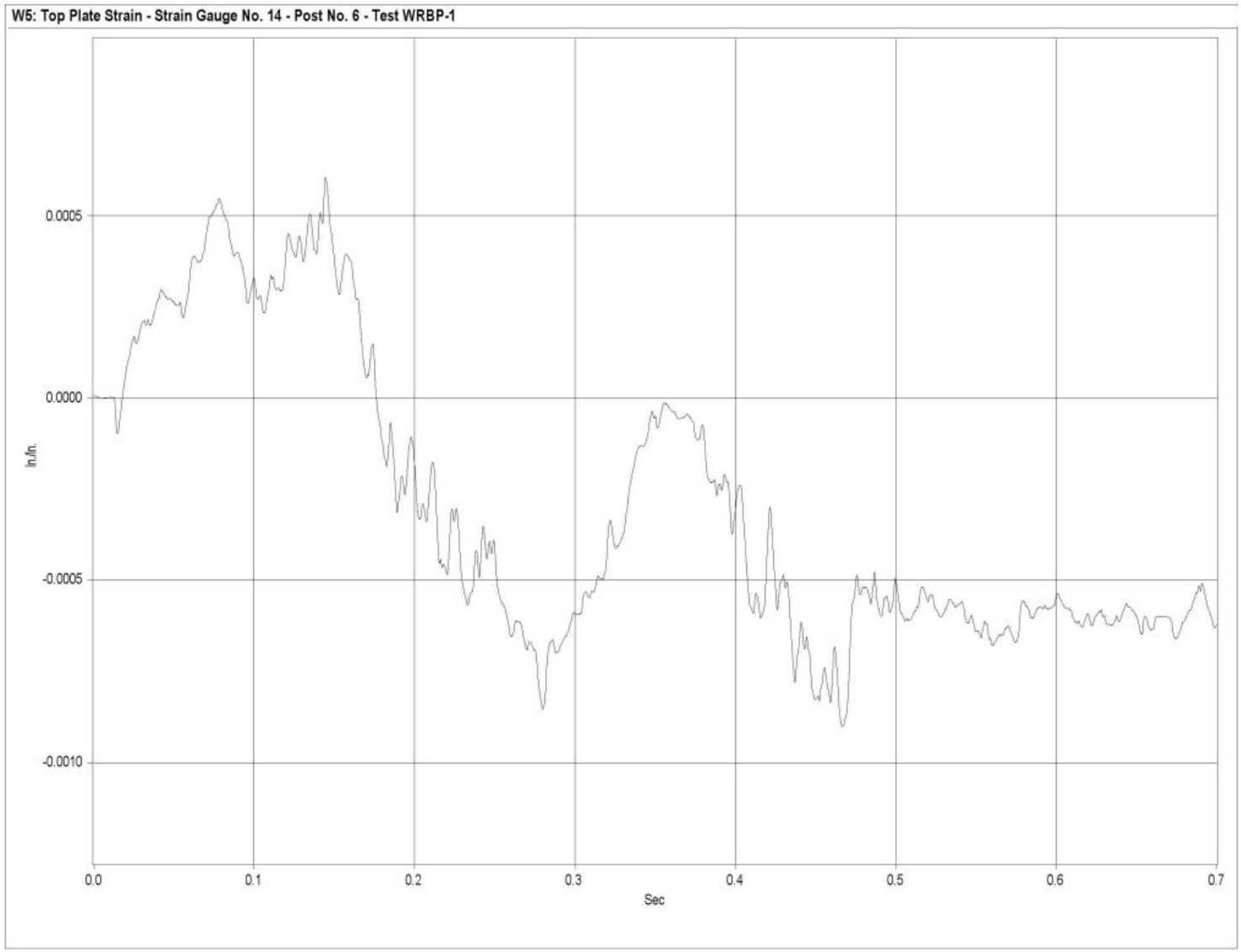

Figure N-24. Graph of Top Plate Post No. 6 - Strain Gauge No. 14 Perpendicular to Rail - Strain, Test WRBP-1

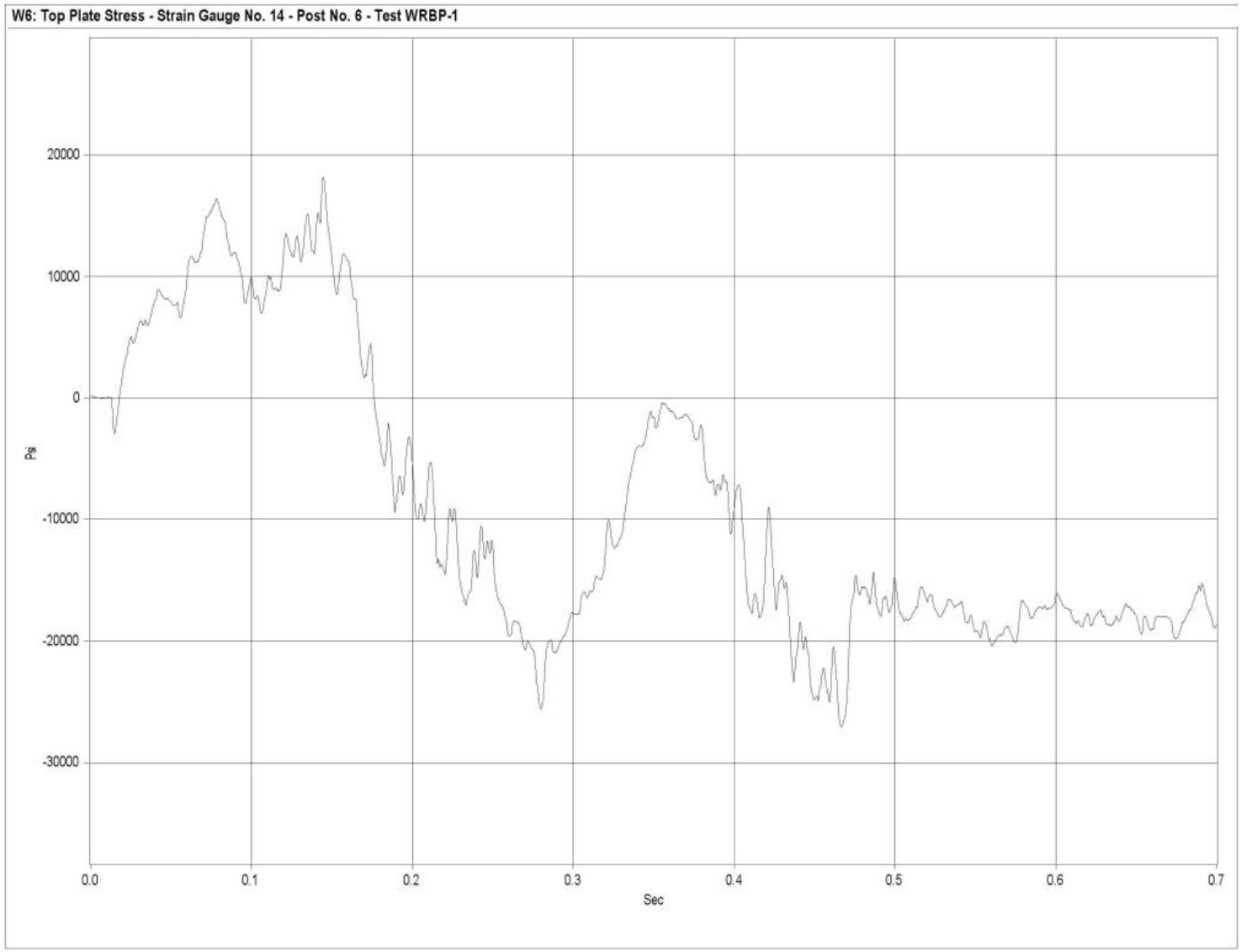

Figure N-25. Graph of Top Plate Post No. 6 - Strain Gauge No. 14 Perpendicular to Rail - Stress, Test WRBP-1

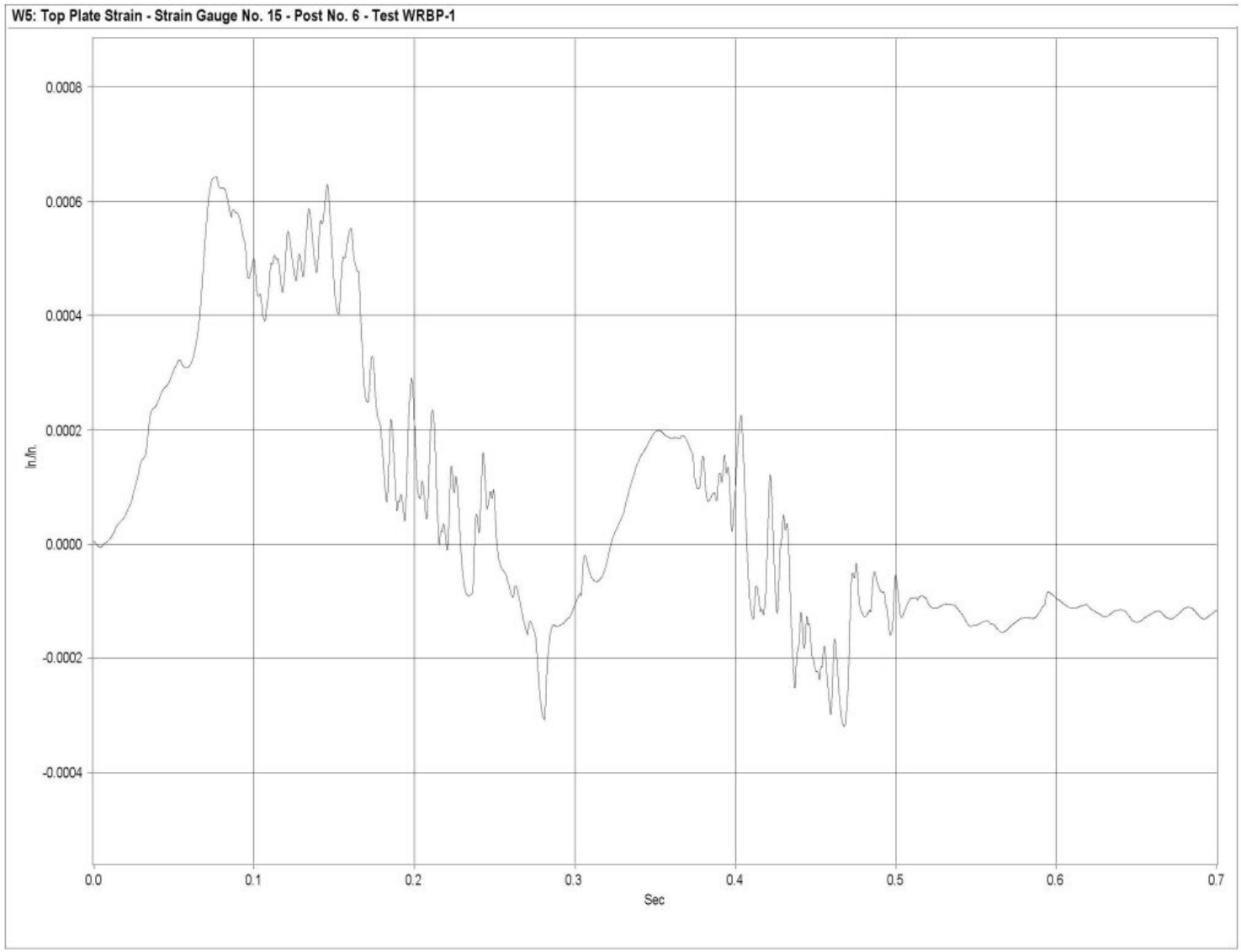

Figure N-26. Graph of Top Plate Post No. 6 - Strain Gauge No. 15 Perpendicular to Rail - Strain, Test WRBP-1

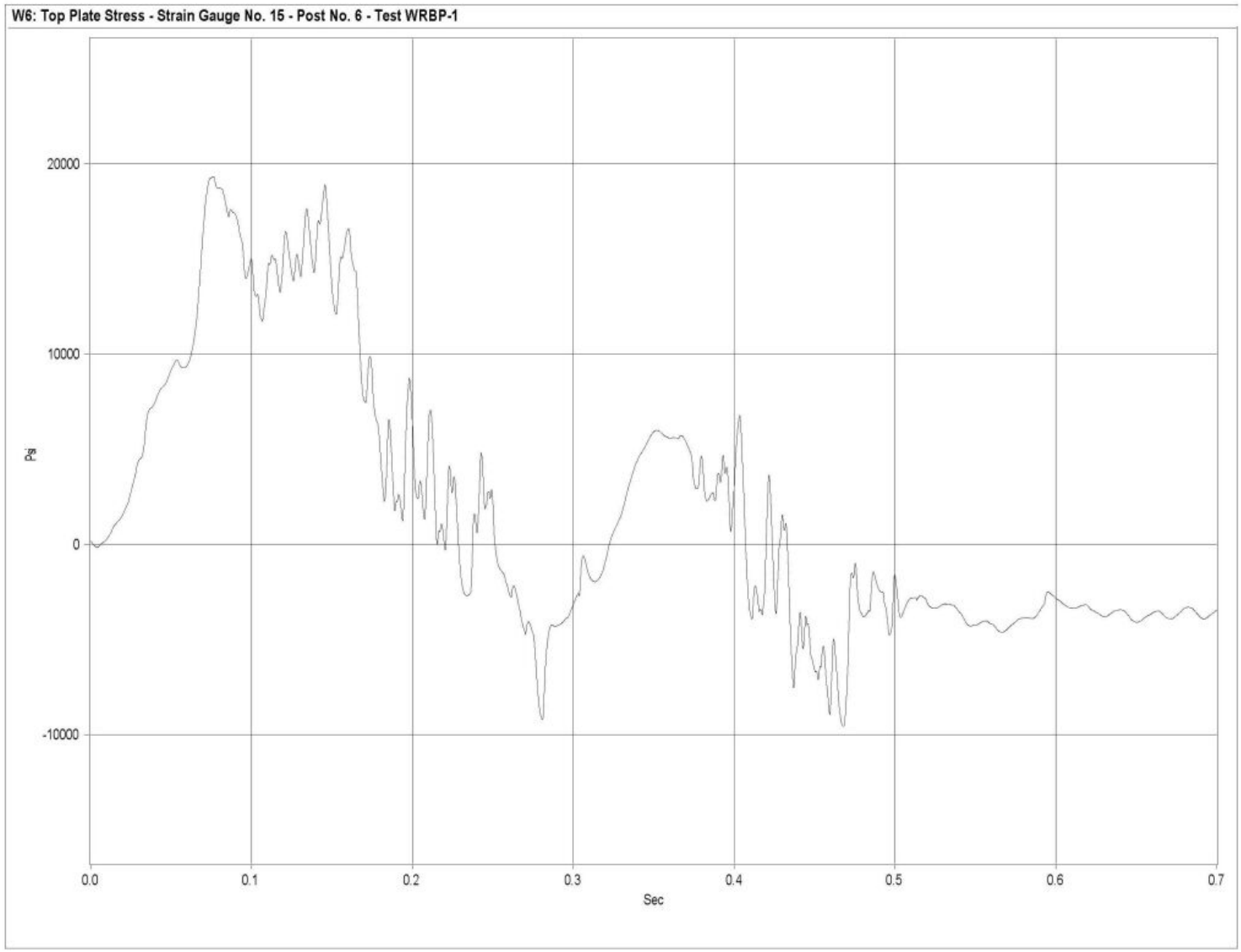

Figure N-27. Graph of Top Plate Post No. 6 - Strain Gauge No. 15 Perpendicular to Rail - Stress, Test WRBP-1

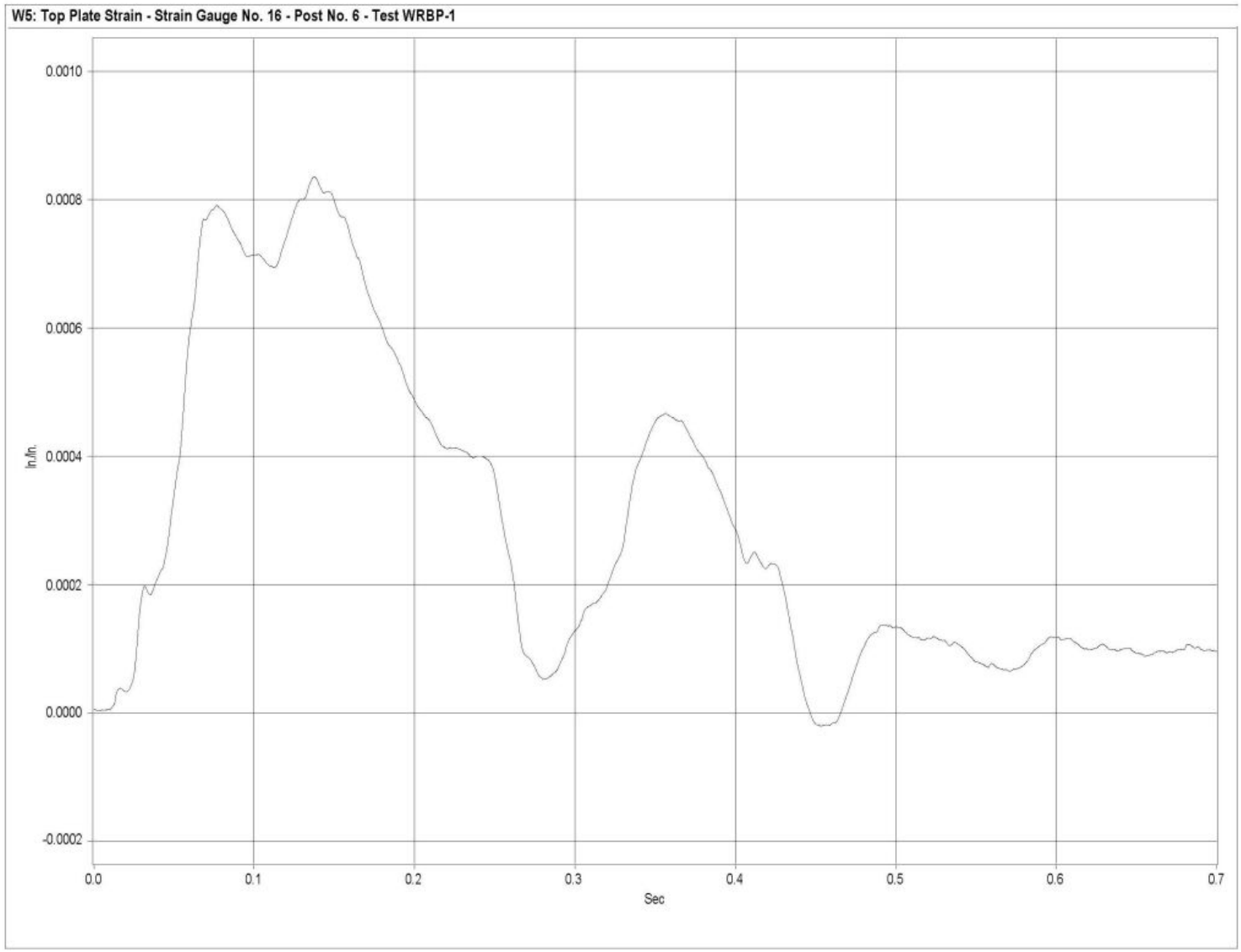

Figure N-28. Graph of Top Plate Post No. 6 - Strain Gauge No. 16 Perpendicular to Rail - Strain, Test WRBP-1

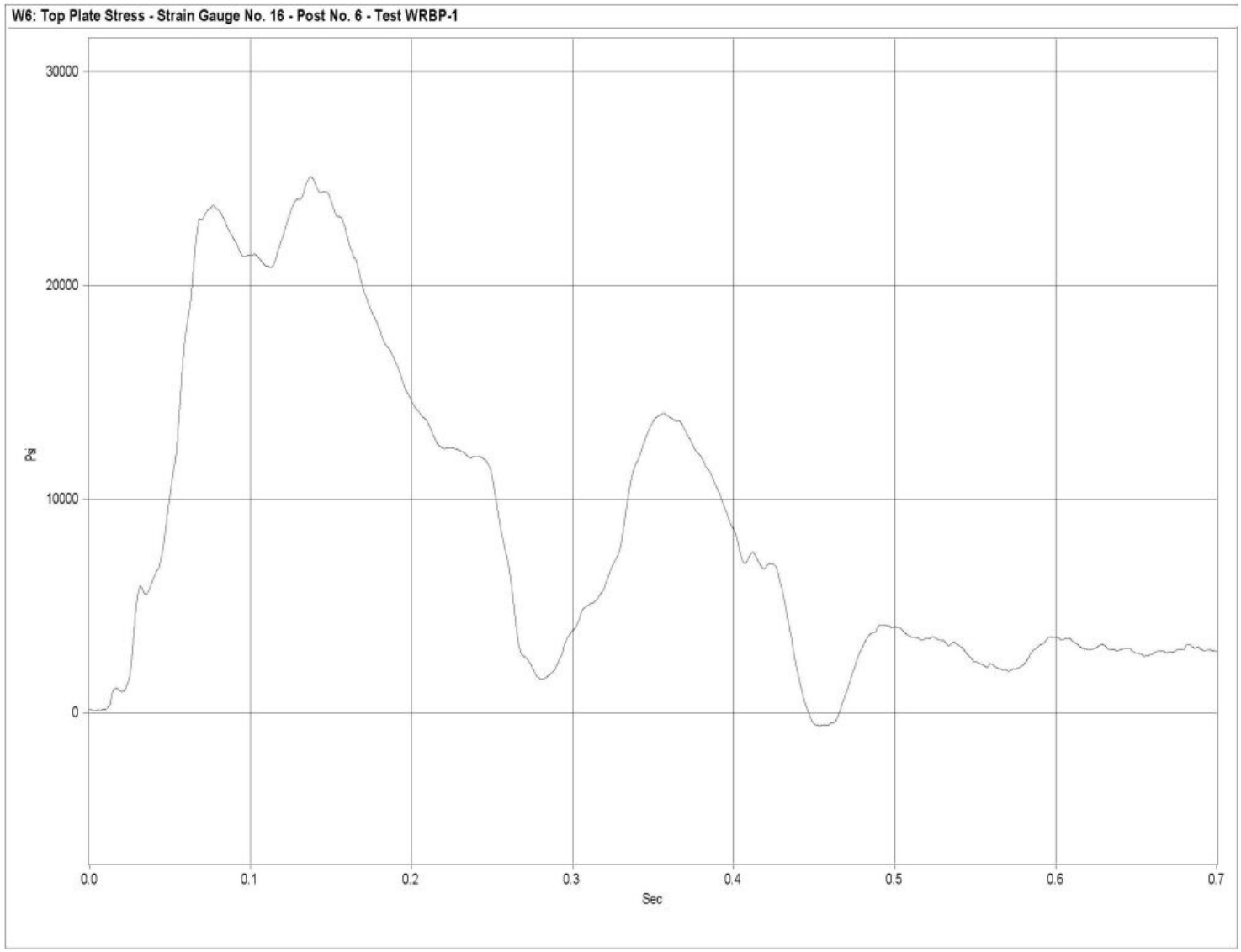

Figure N-29. Graph of Top Plate Post No. 6 - Strain Gauge No. 16 Perpendicular to Rail - Stress, Test WRBP-1

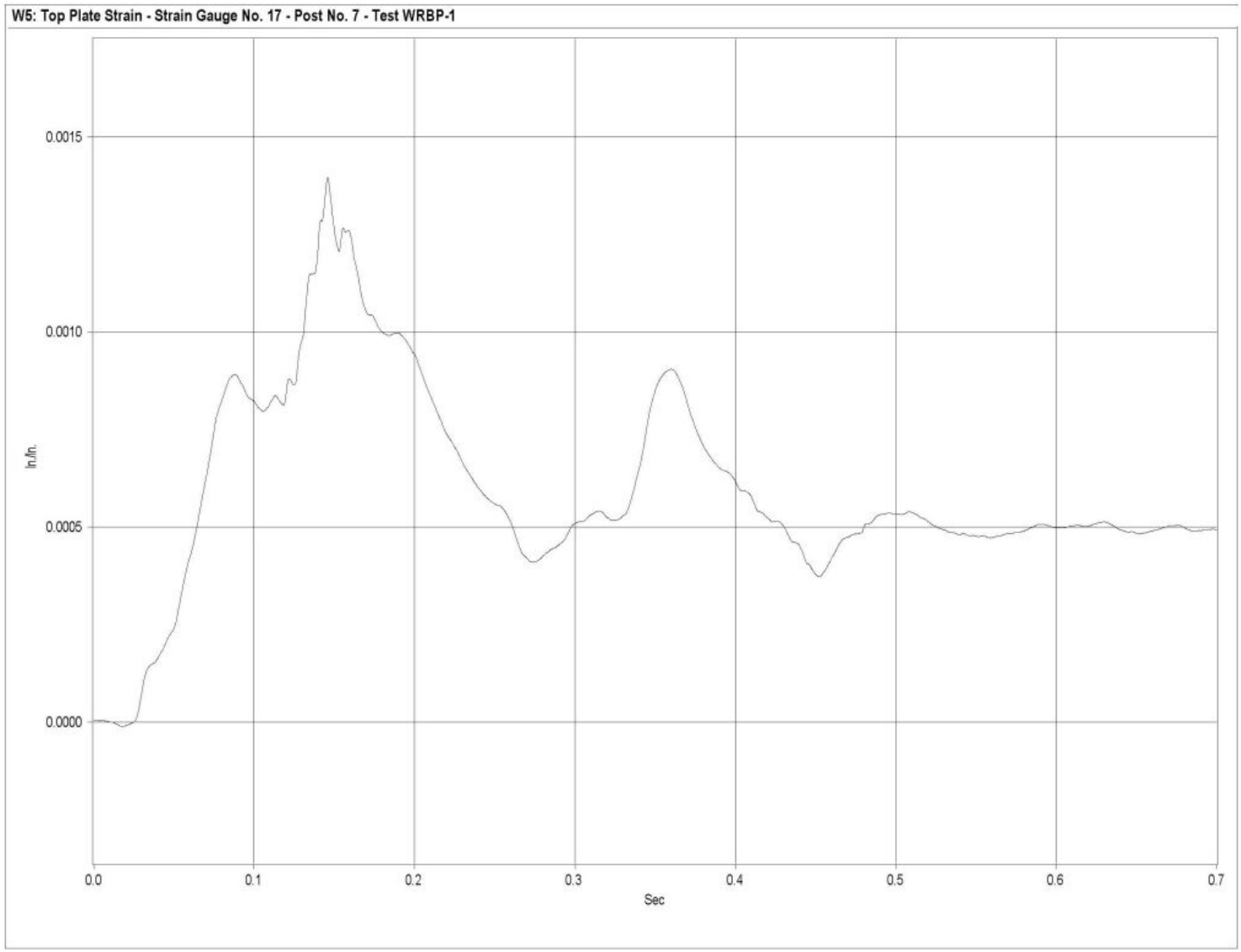

Figure N-30. Graph of Top Plate Post No. 7 - Strain Gauge No. 17 Perpendicular to Rail - Strain, Test WRBP-1

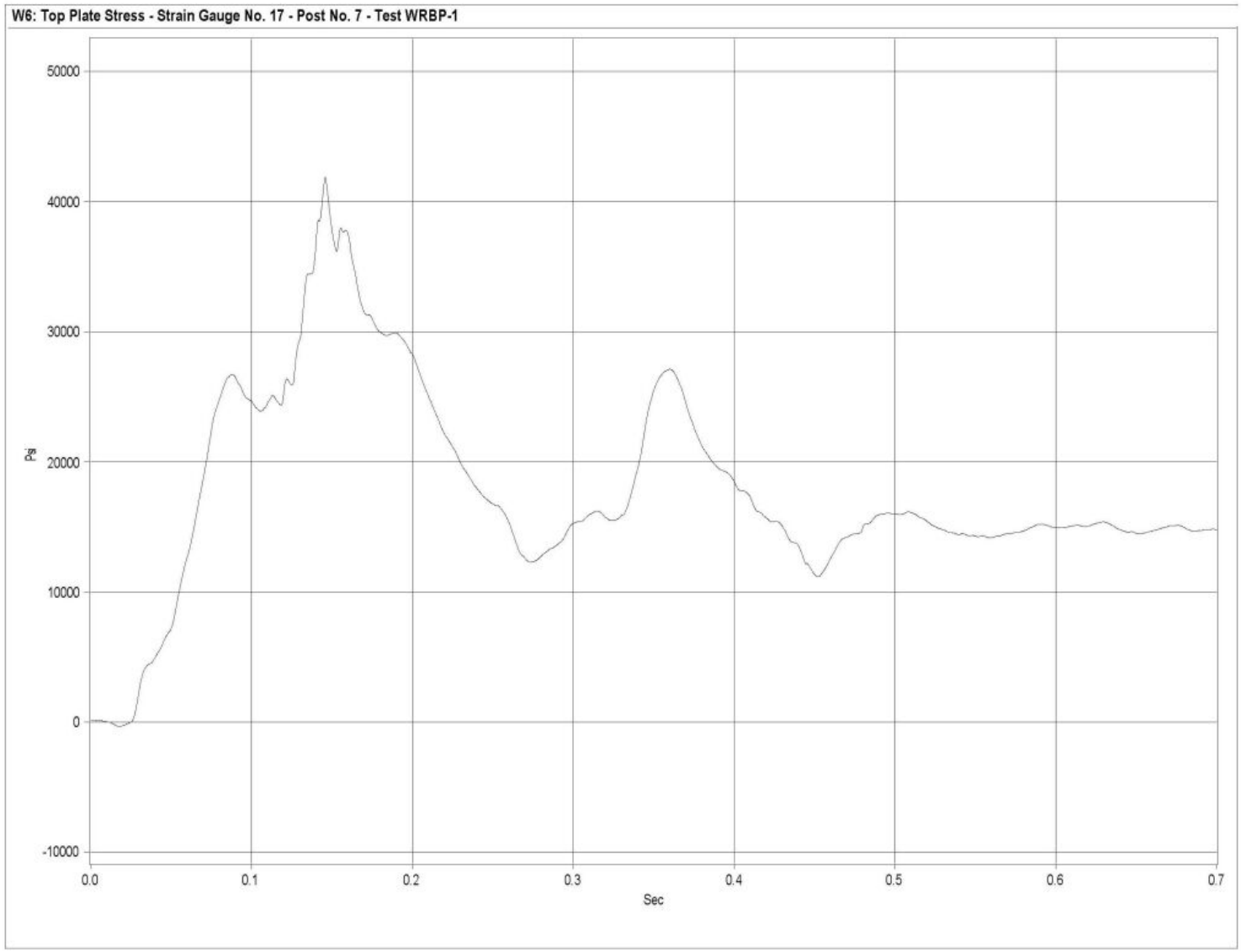

Figure N-31. Graph of Top Plate Post No. 7 - Strain Gauge No. 17 Perpendicular to Rail - Stress, Test WRBP-1

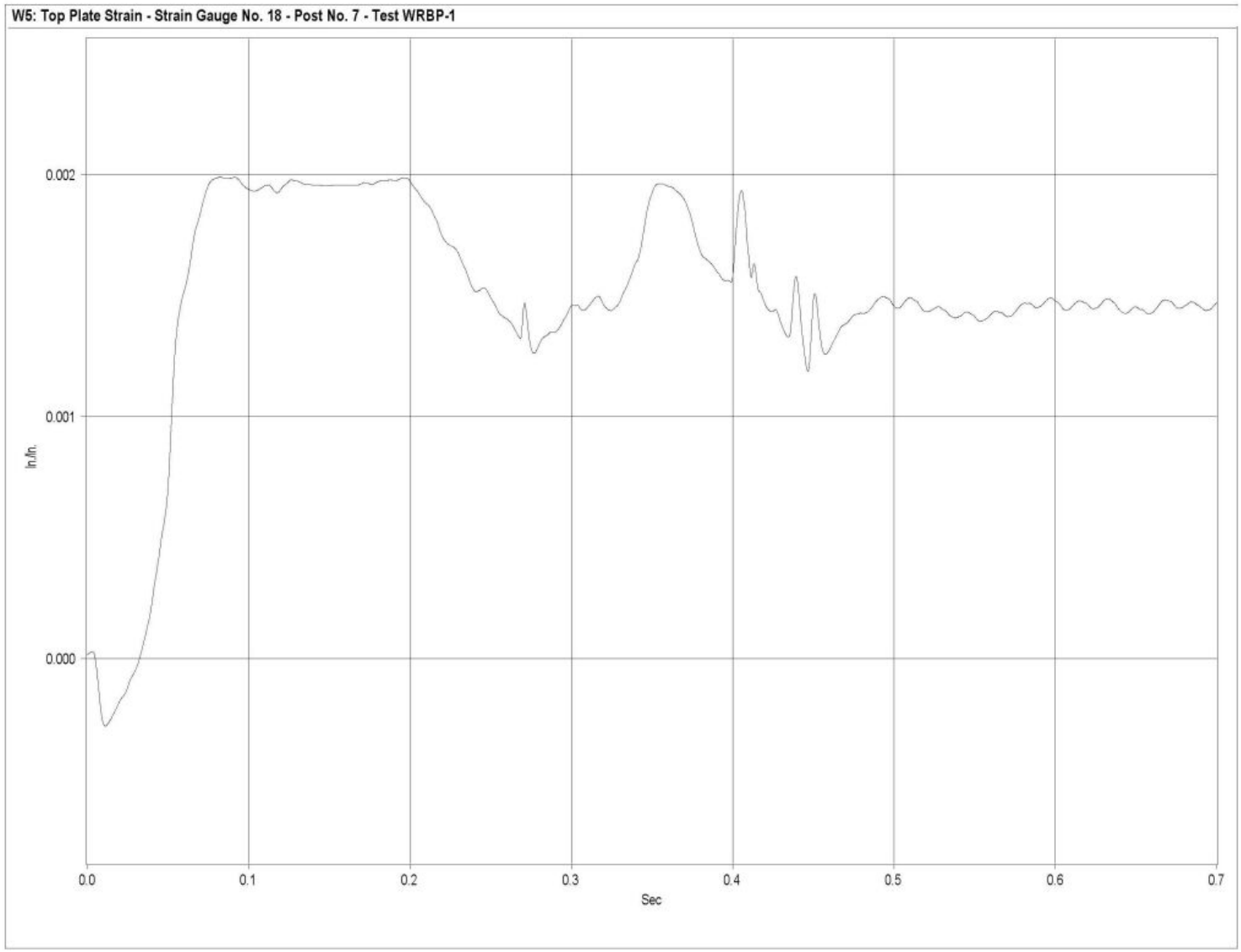

Figure N-32. Graph of Top Plate Post No. 7 - Strain Gauge No. 18 Perpendicular to Rail - Strain, Test WRBP-1

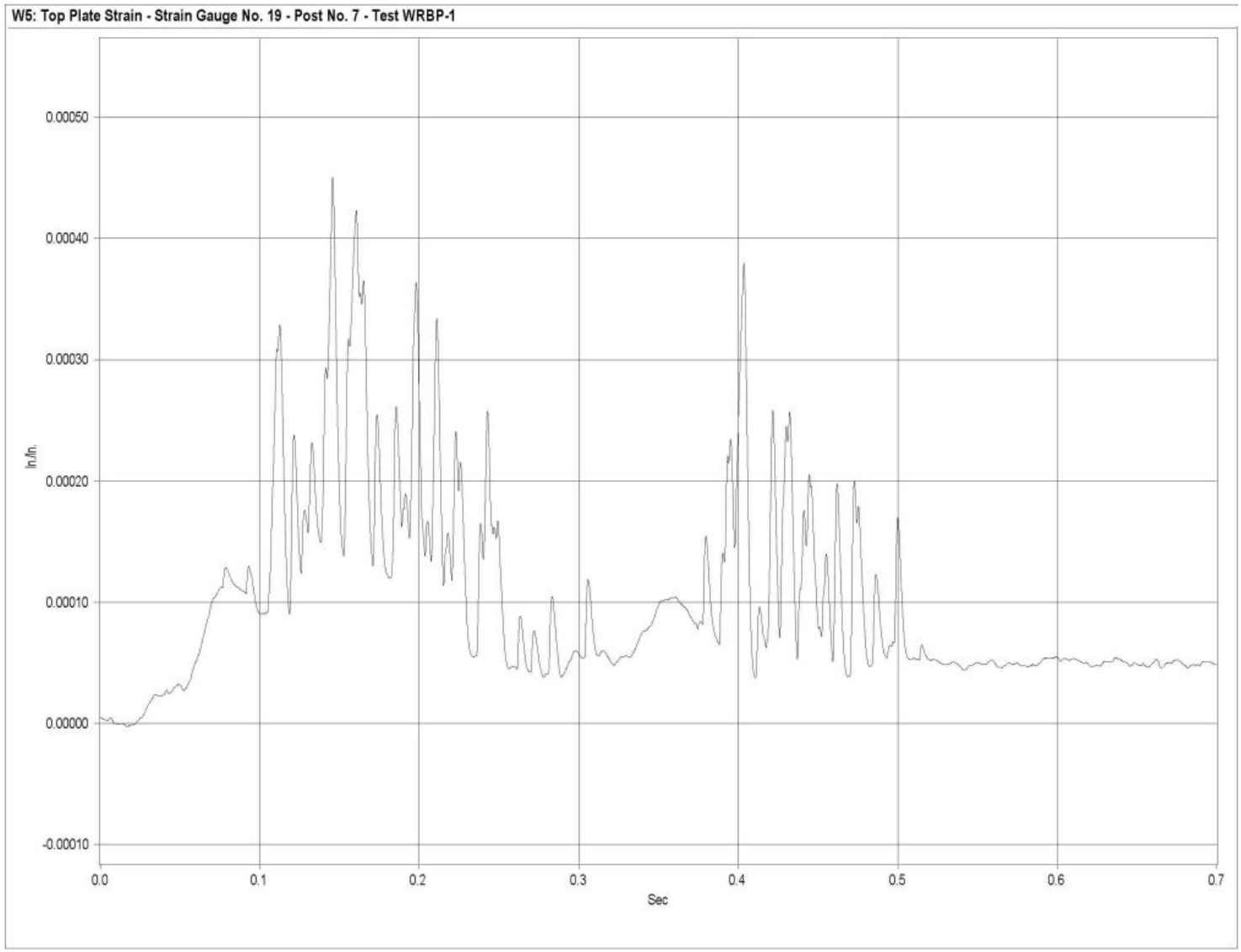

Figure N-33. Graph of Top Plate Post No. 7 - Strain Gauge No. 19 Perpendicular to Rail - Strain, Test WRBP-1

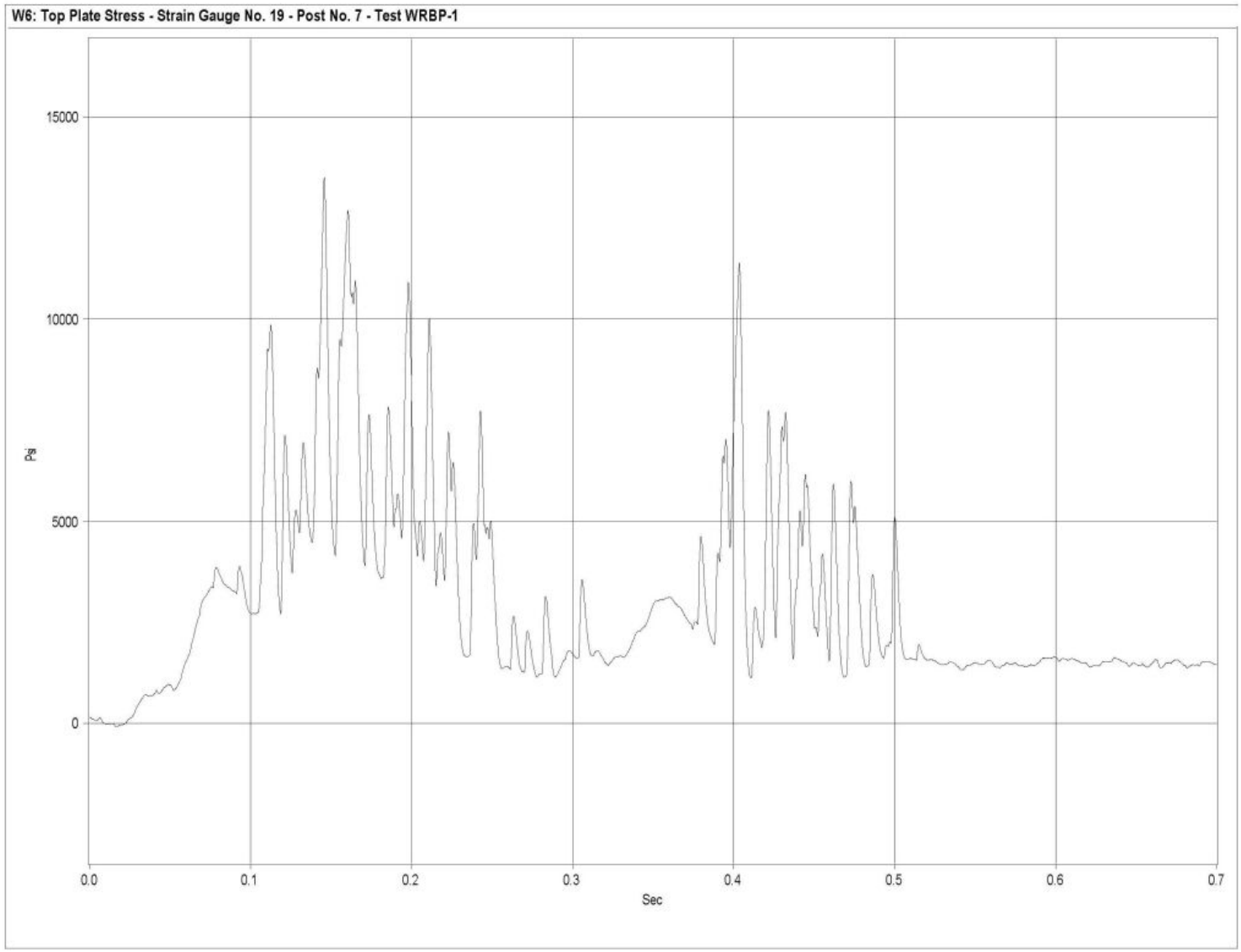

Figure N-34. Graph of Top Plate Post No. 7 - Strain Gauge No. 19 Perpendicular to Rail - Stress, Test WRBP-1

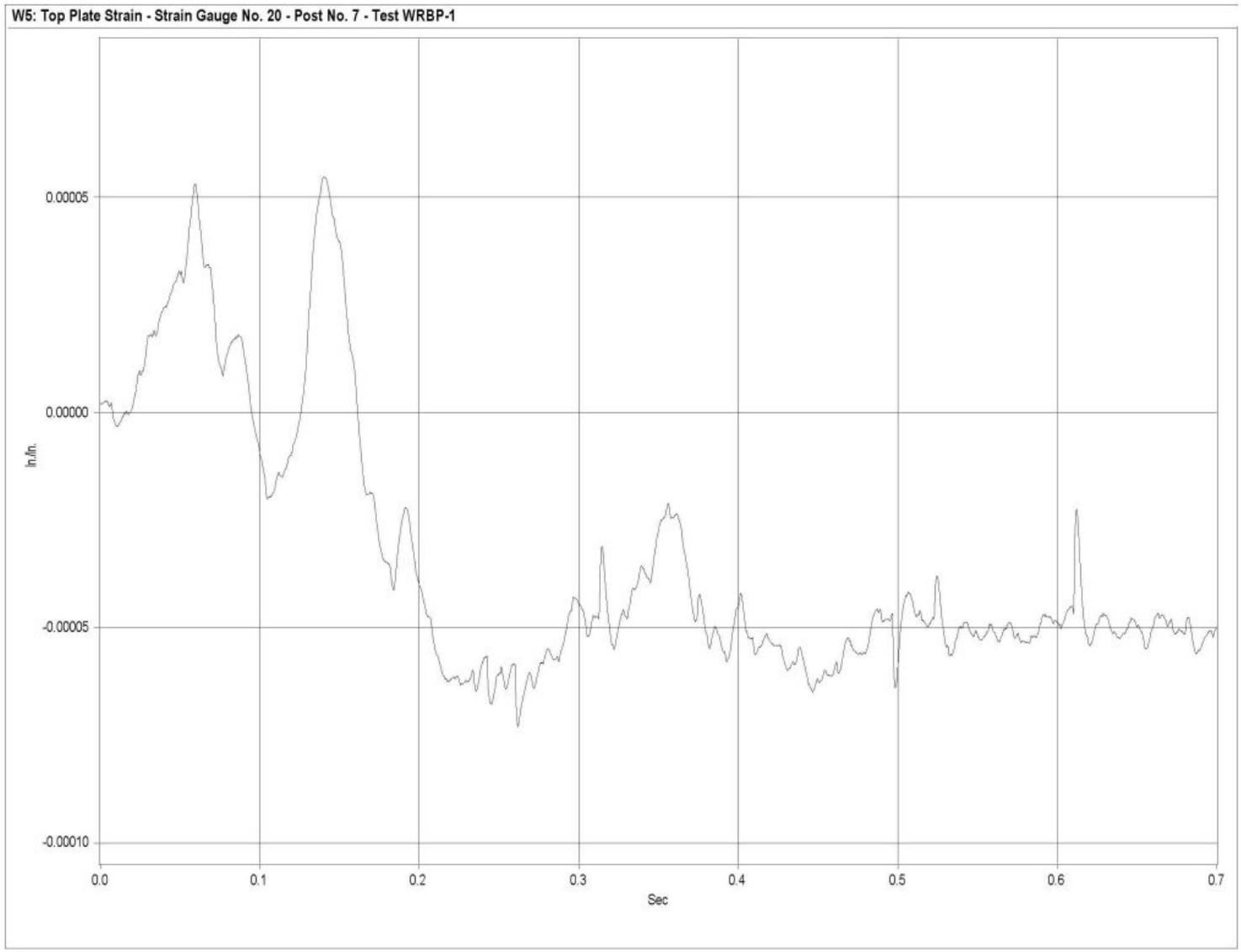

Figure N-35. Graph of Top Plate Post No. 7 - Strain Gauge No. 20 Perpendicular to Rail - Strain, Test WRBP-1

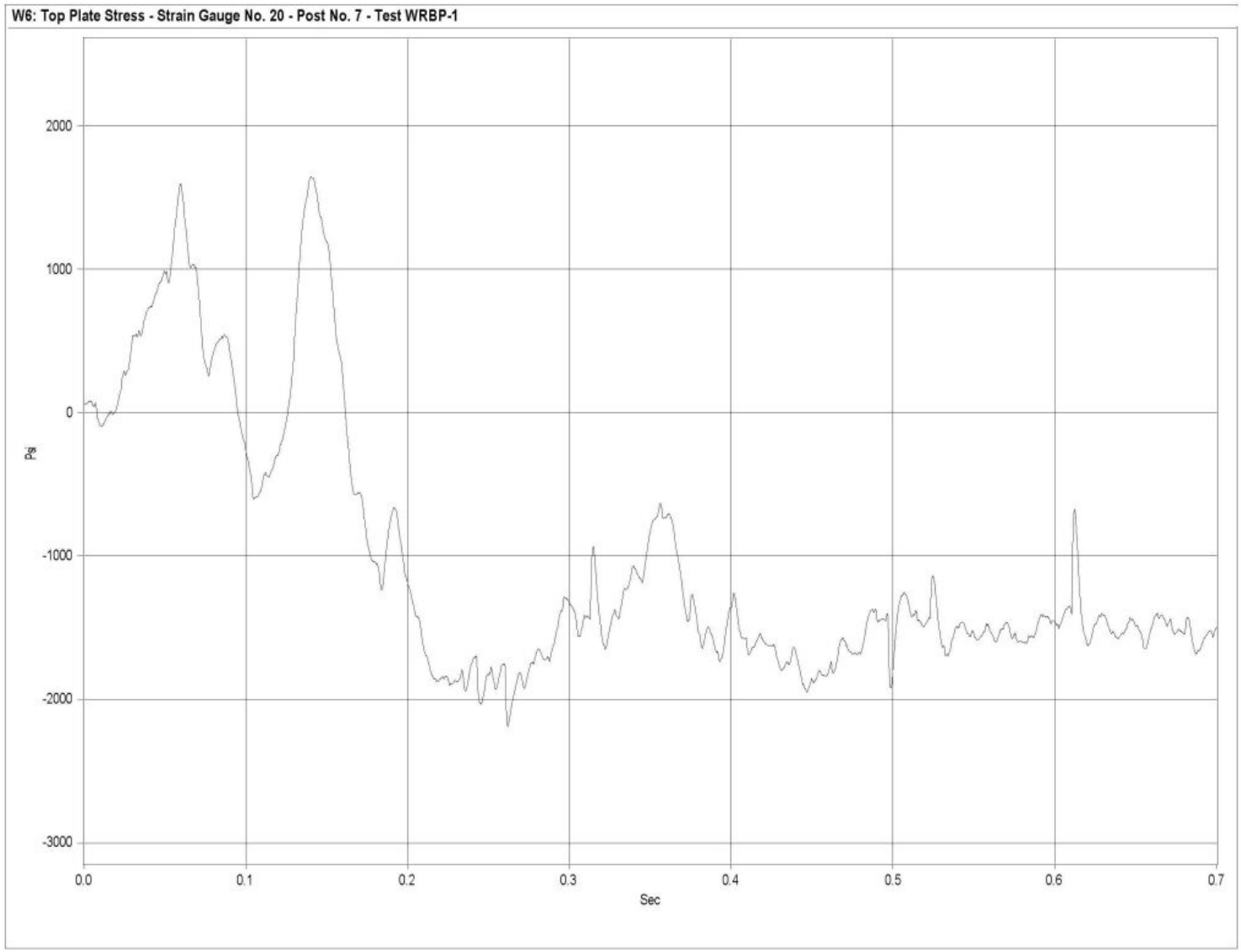

Figure N-36. Graph of Top Plate Post No. 7 - Strain Gauge No. 20 Perpendicular to Rail - Stress, Test WRBP-1

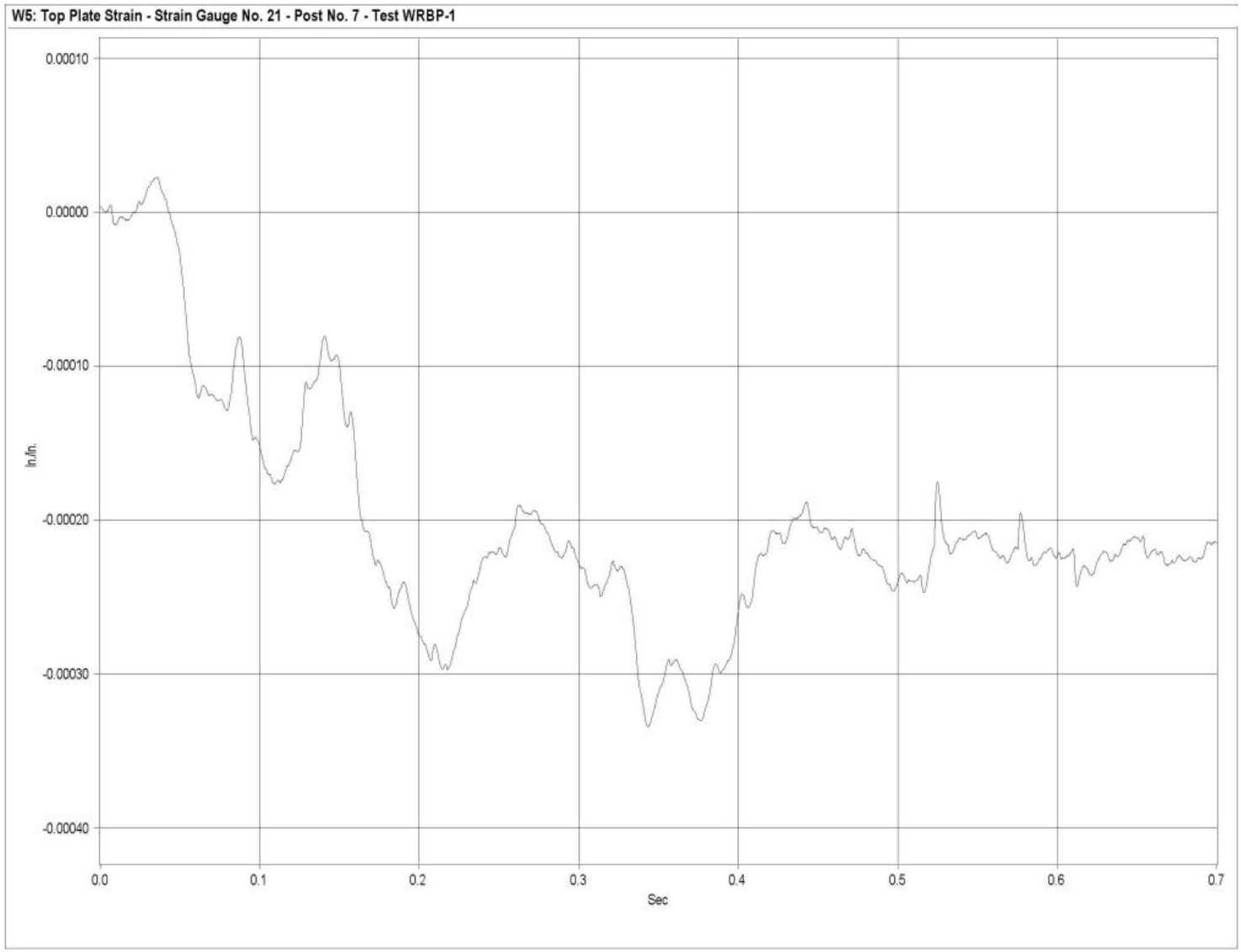

Figure N-37. Graph of Top Plate Post No. 7 - Strain Gauge No. 21 Perpendicular to Rail - Strain, Test WRBP-1

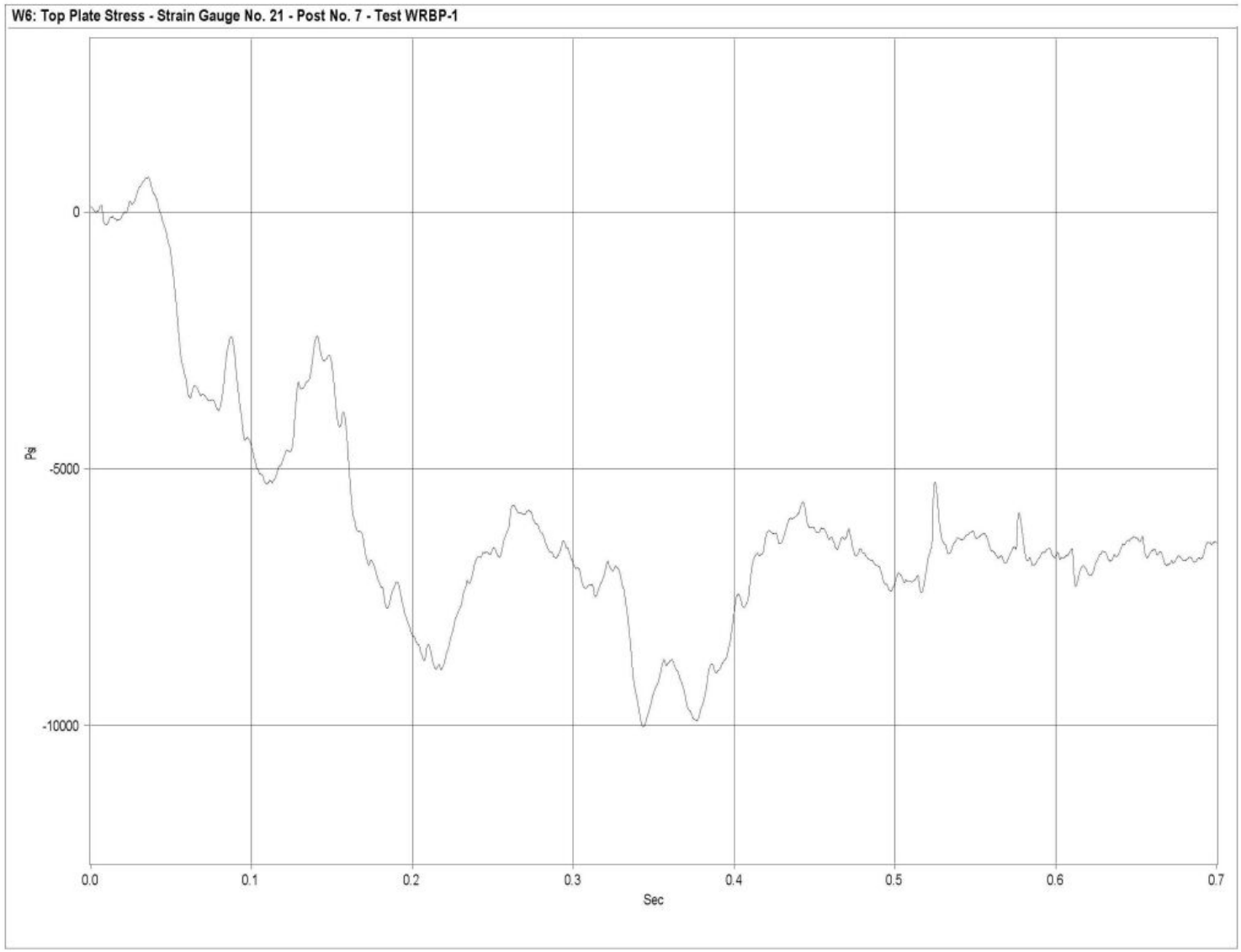

Figure N-38. Graph of Top Plate Post No. 7 - Strain Gauge No. 21 Perpendicular to Rail - Stress, Test WRBP-1

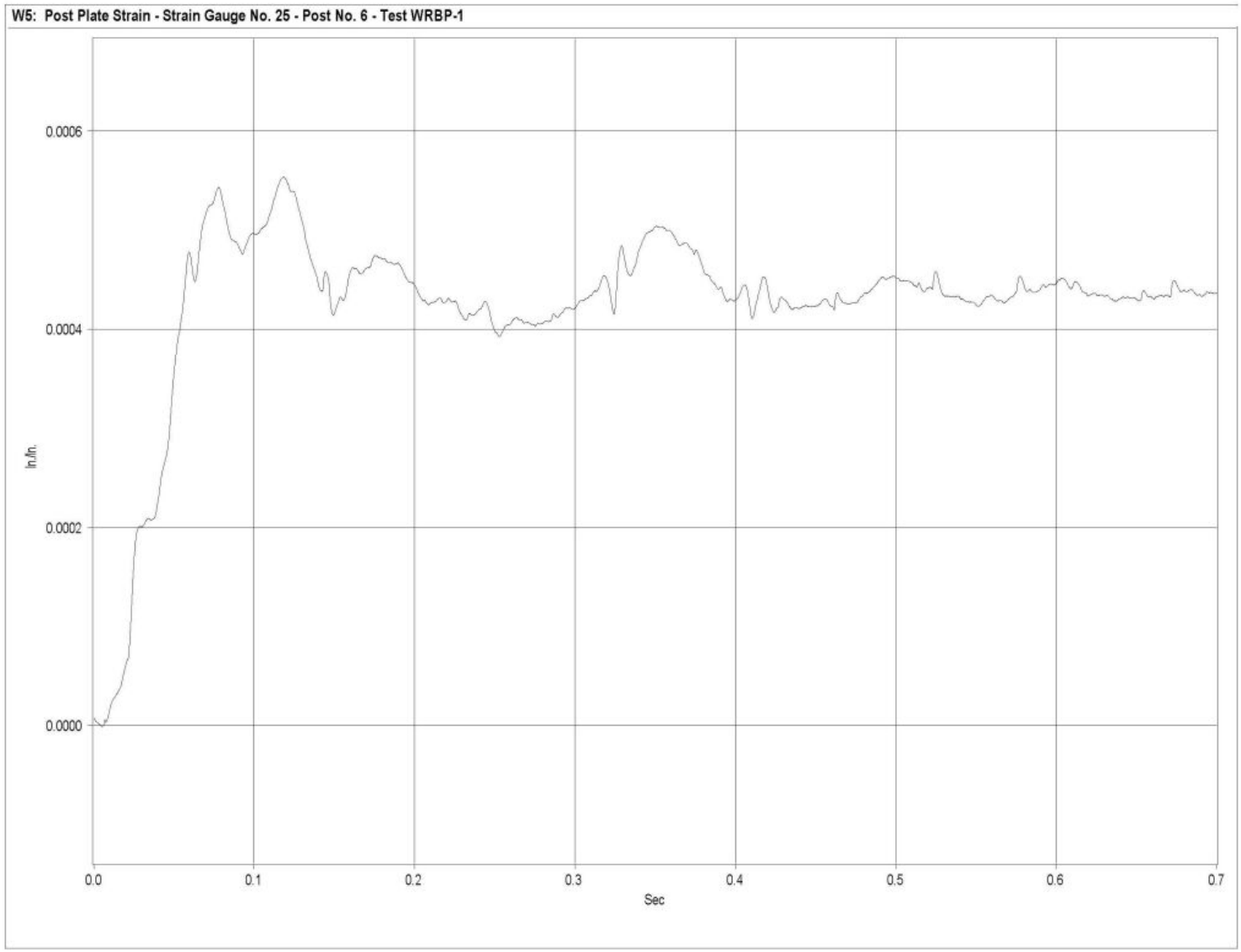

Figure N-39. Graph of Upstream-Side Bent Post Plate Post No. 6 - Strain Gauge No. 25 - Strain, Test WRBP-1

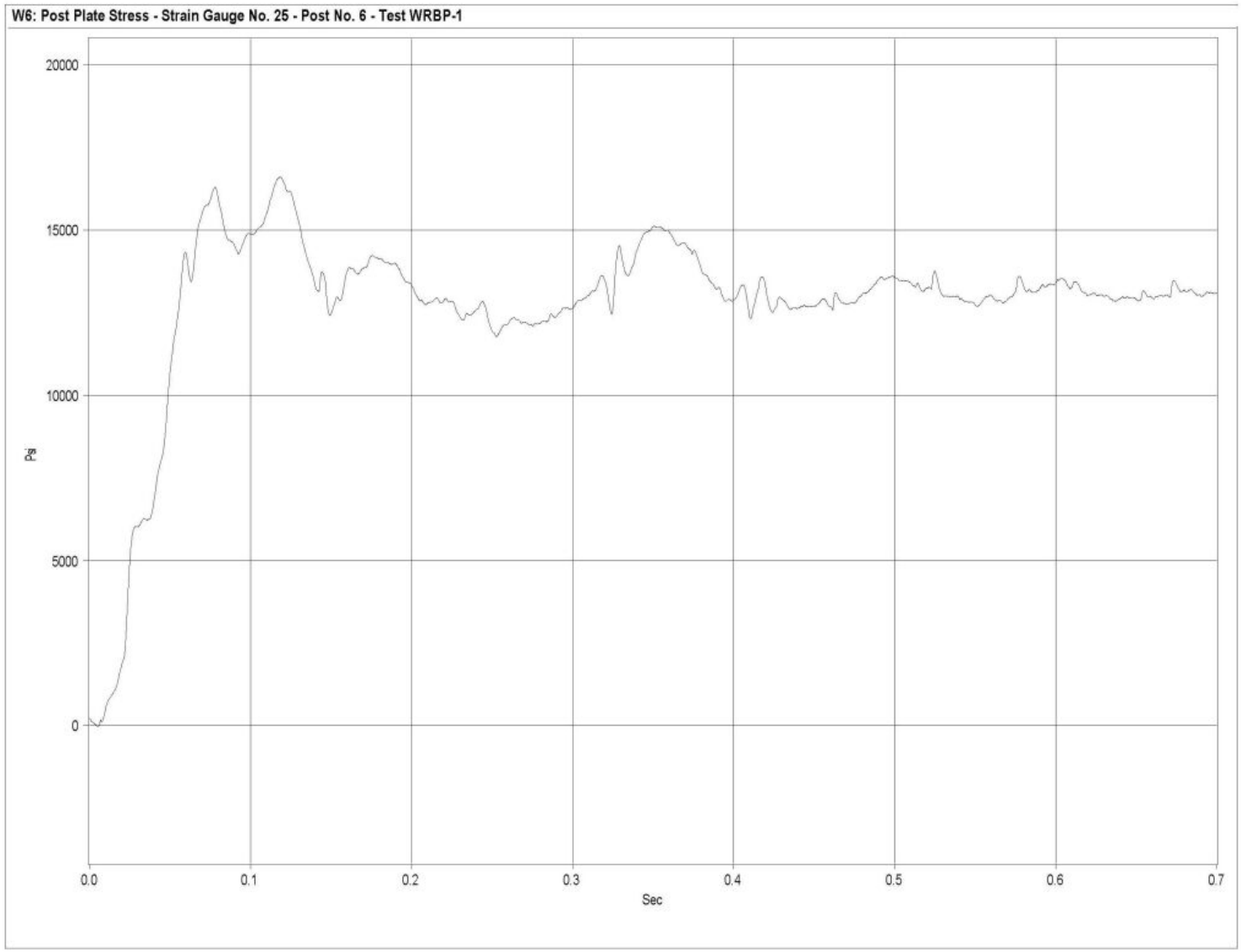

Figure N-40. Graph of Upstream-Side Bent Post Plate Post No. 6 - Strain Gauge No. 25 - Stress, Test WRBP-1

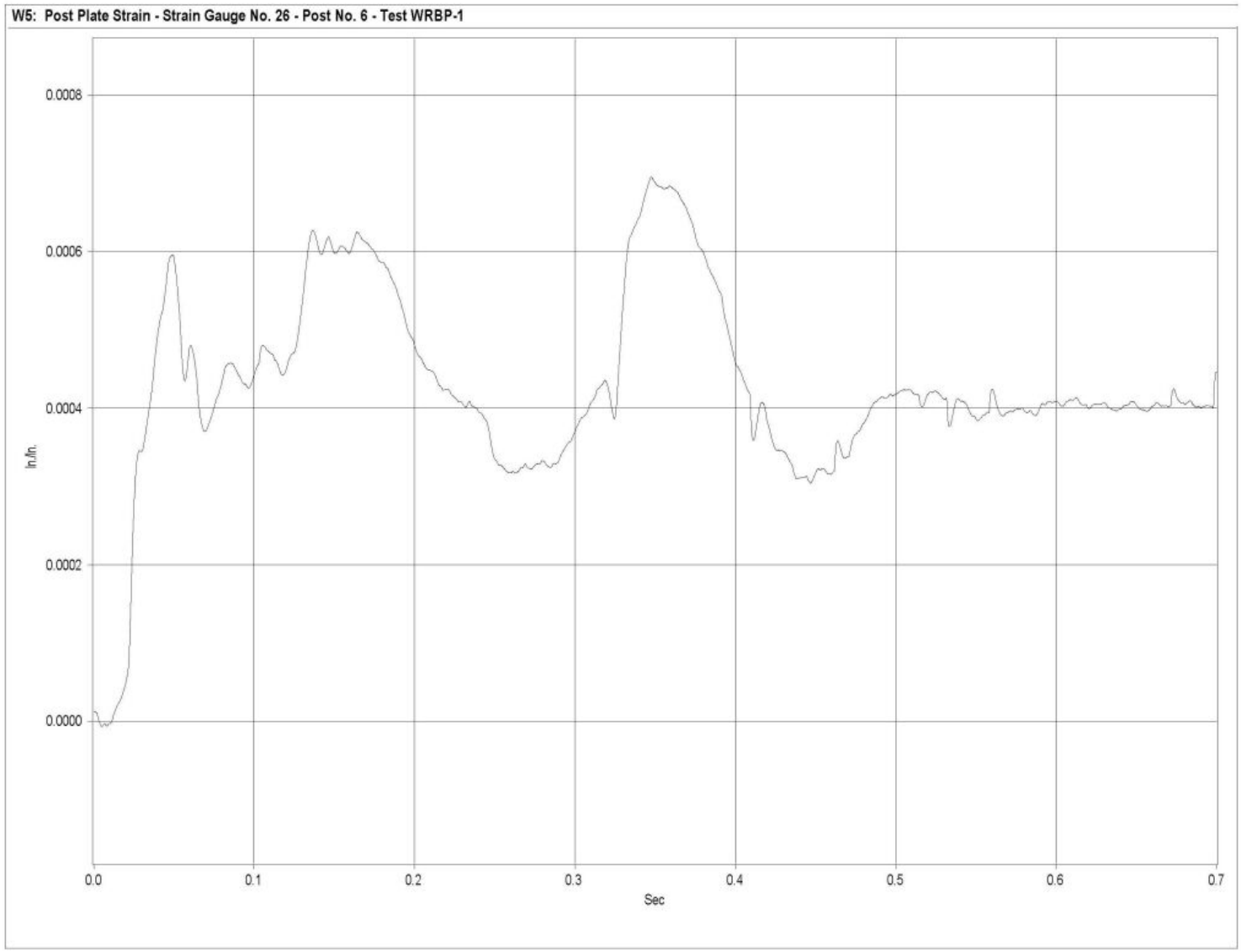

Figure N-41. Graph of Downstream-Side Bent Post Plate Post No. 6 - Strain Gauge No. 26 - Strain, Test WRBP-1

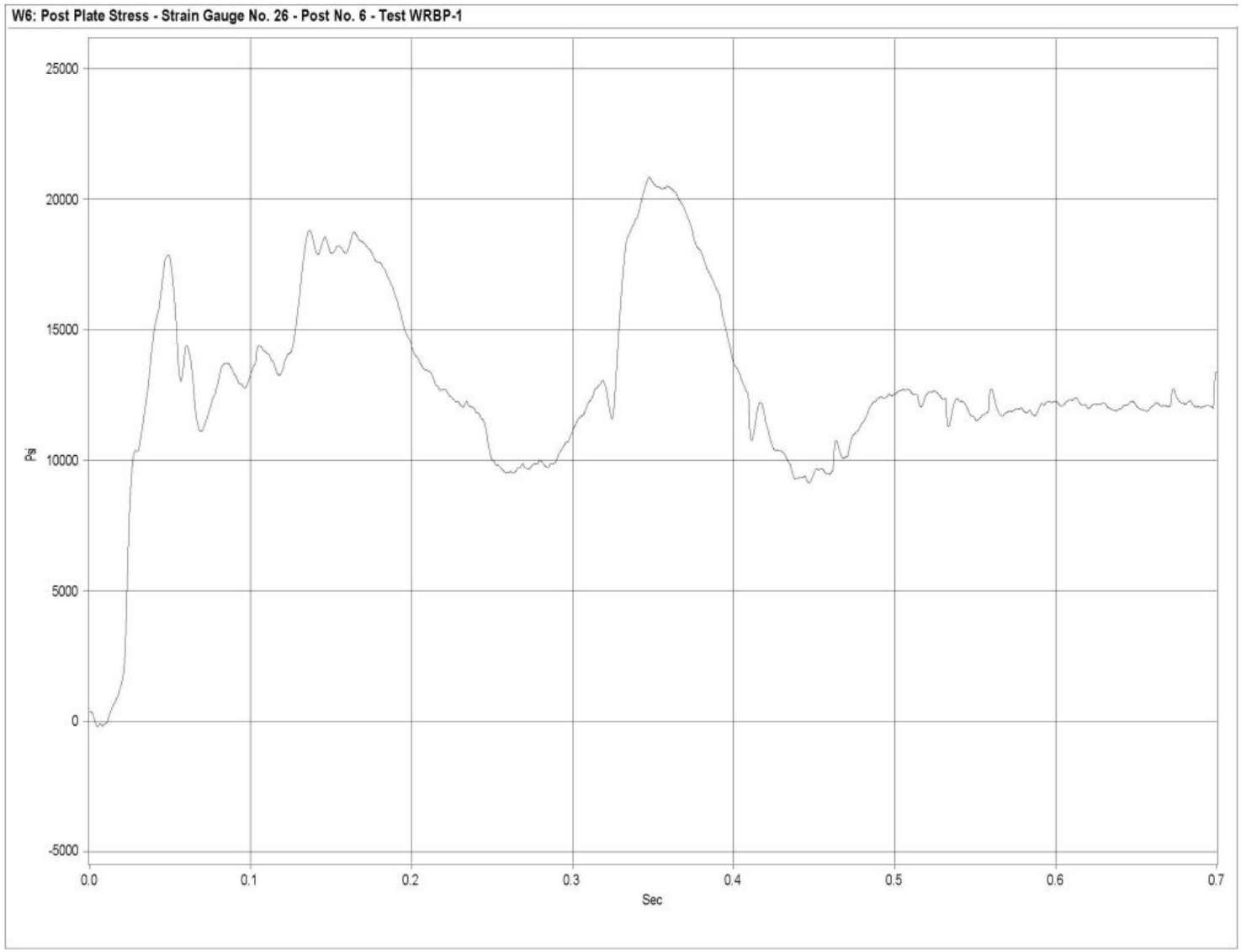

Figure N-42. Graph of Downstream-Side Bent Post Plate Post No. 6 - Strain Gauge No. 26 - Stress, Test WRBP-1

APPENDIX O

Accelerometer Data Analysis - Test WRBP-2

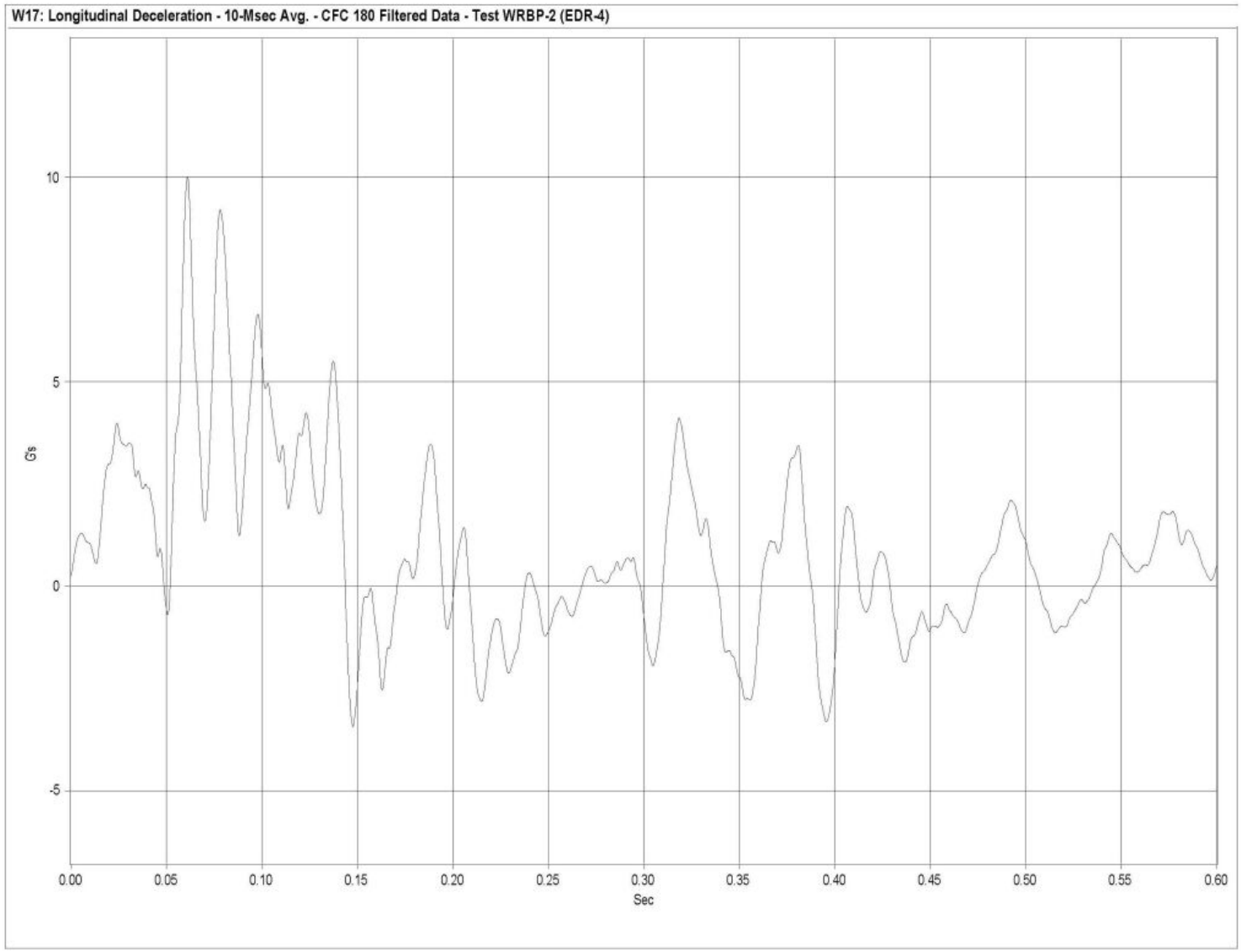

Figure O-1. Graph of Longitudinal Deceleration, Test WRBP-2

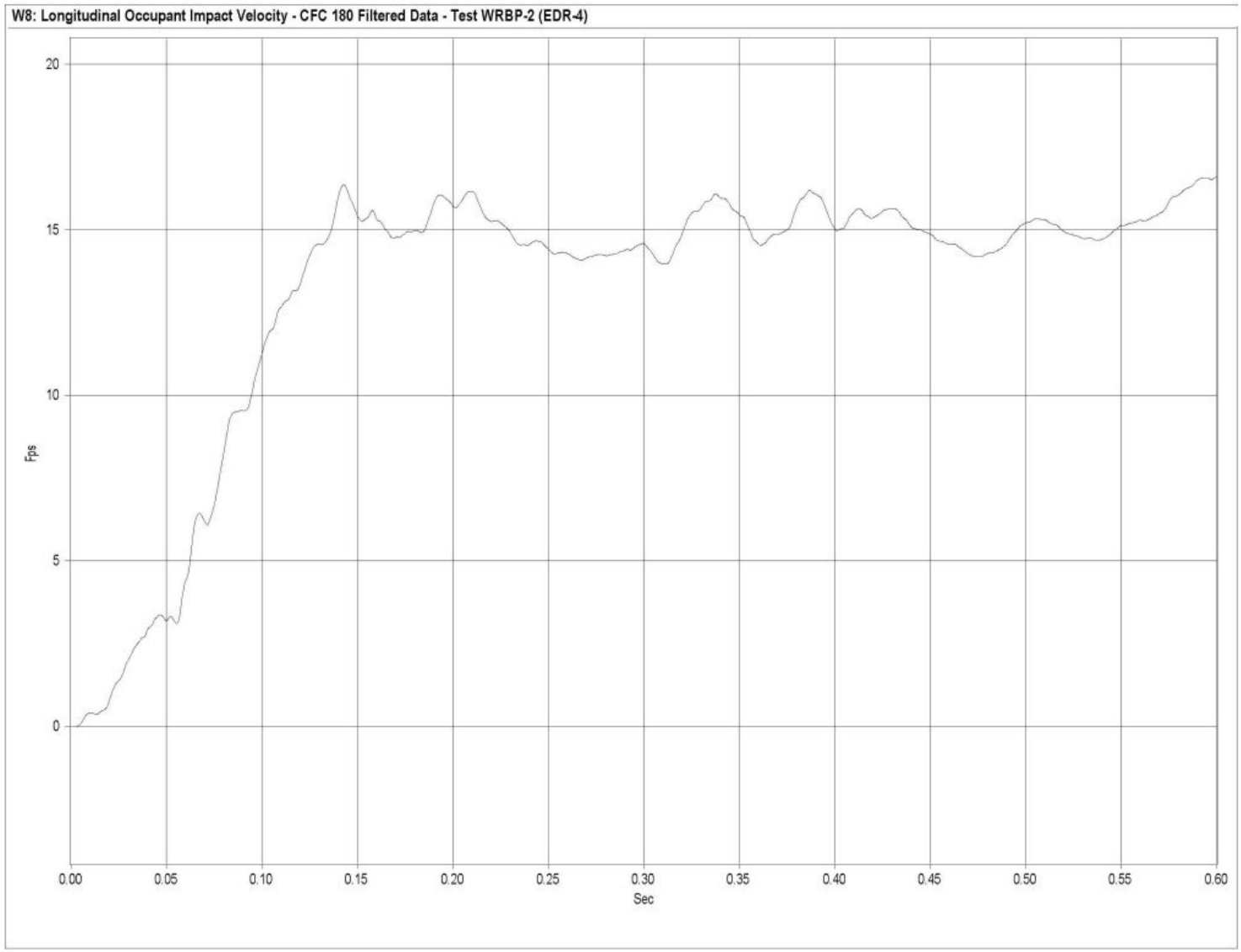

Figure O-2. Graph of Longitudinal Occupant Impact Velocity, Test WRBP-2

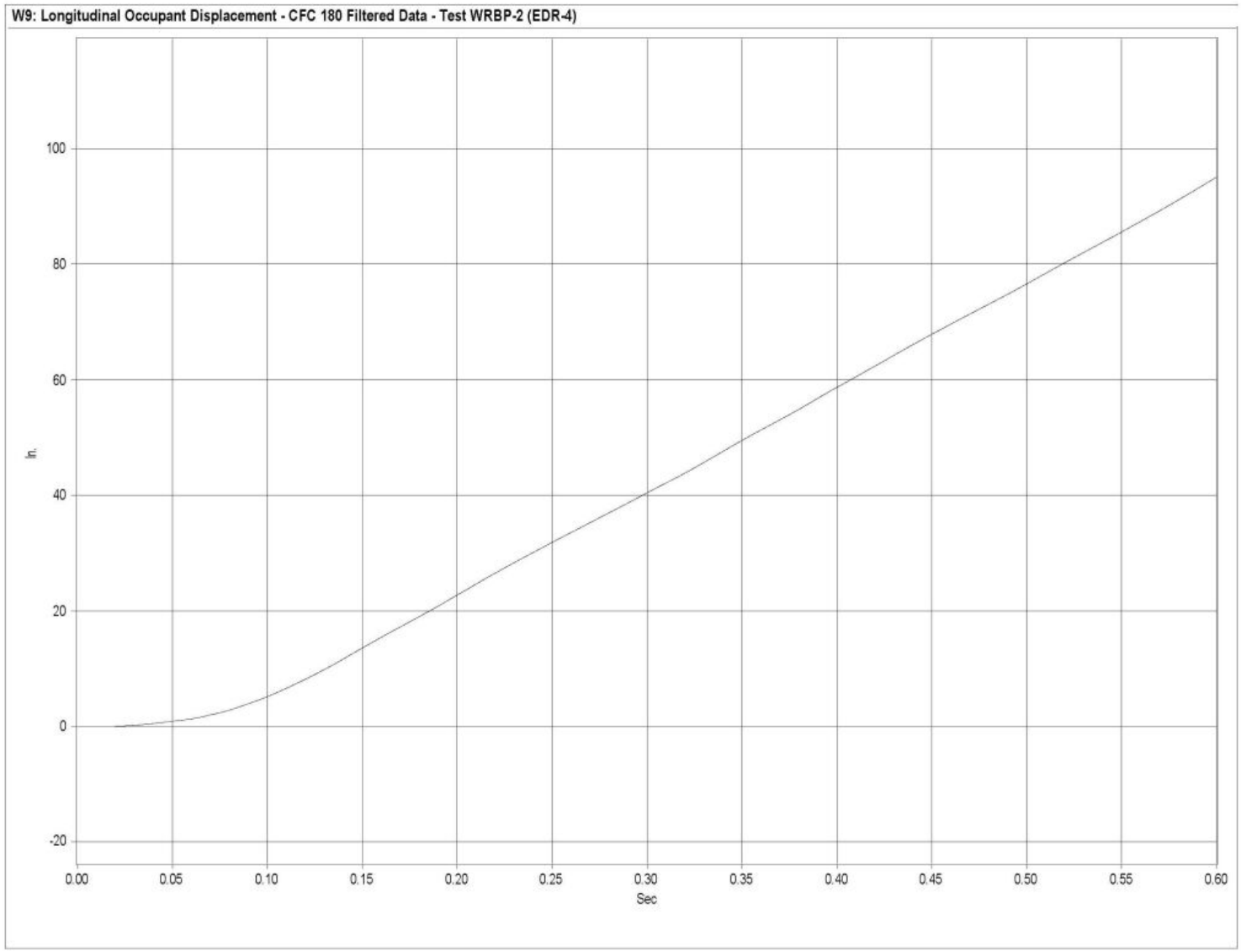

Figure O-3. Graph of Longitudinal Occupant Displacement, Test WRBP-2

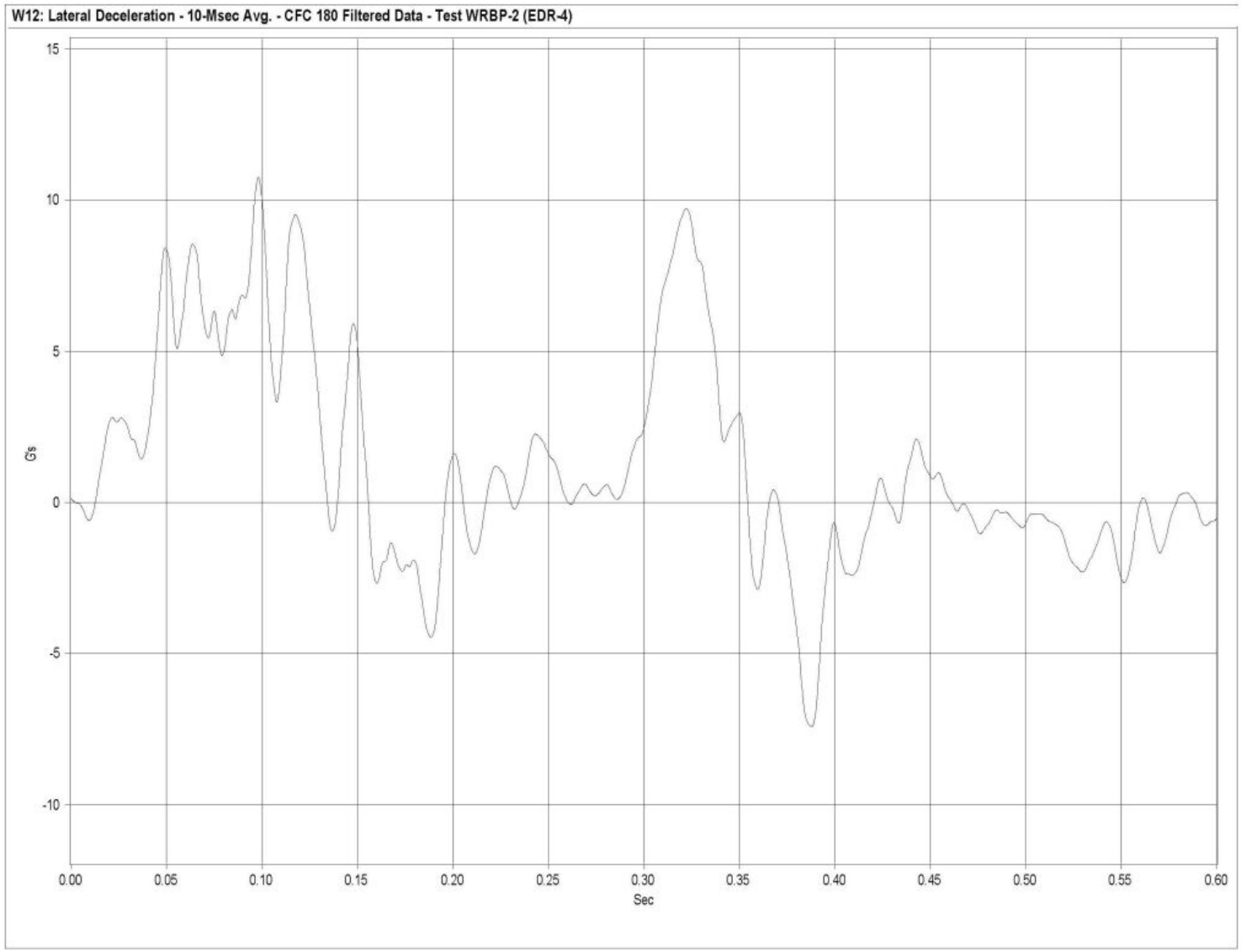

Figure O-4. Graph of Lateral Deceleration, Test WRBP-2

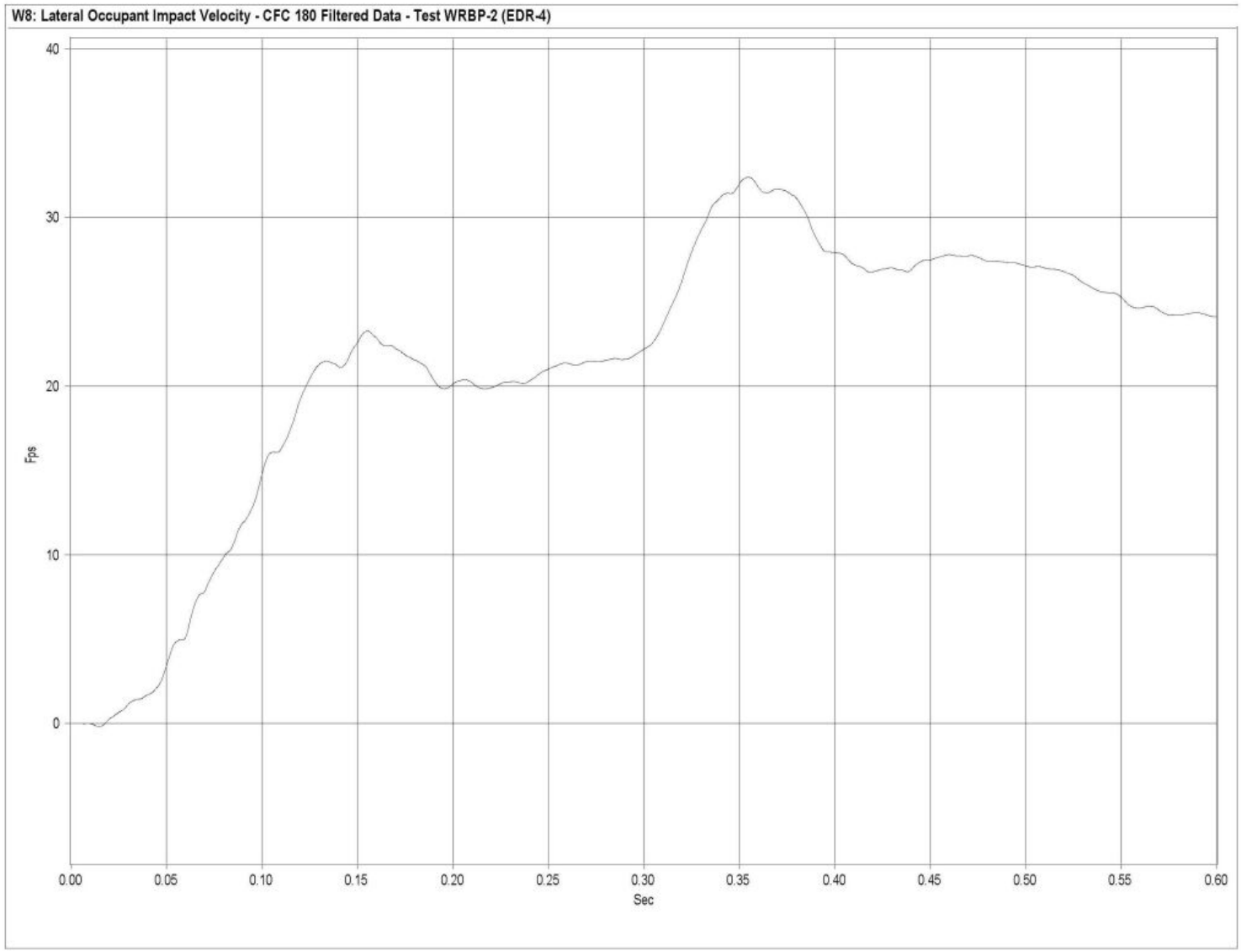

Figure O-5. Graph of Lateral Occupant Impact Velocity, Test WRBP-2

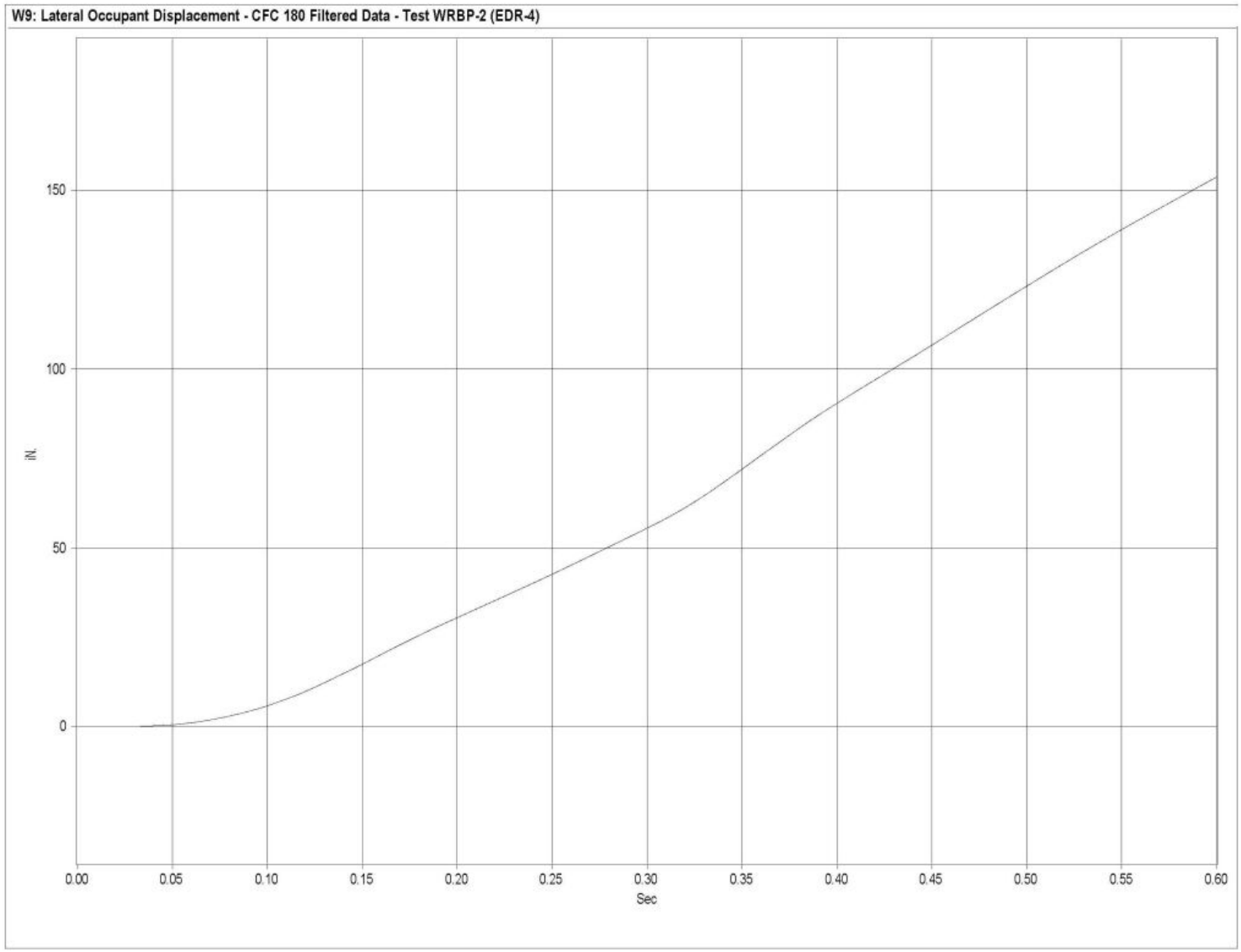

Figure O-6. Graph of Lateral Occupant Displacement, Test WRBP-2

APPENDIX P

Roll, Pitch, and Yaw Data Analysis - Test WRBP-2

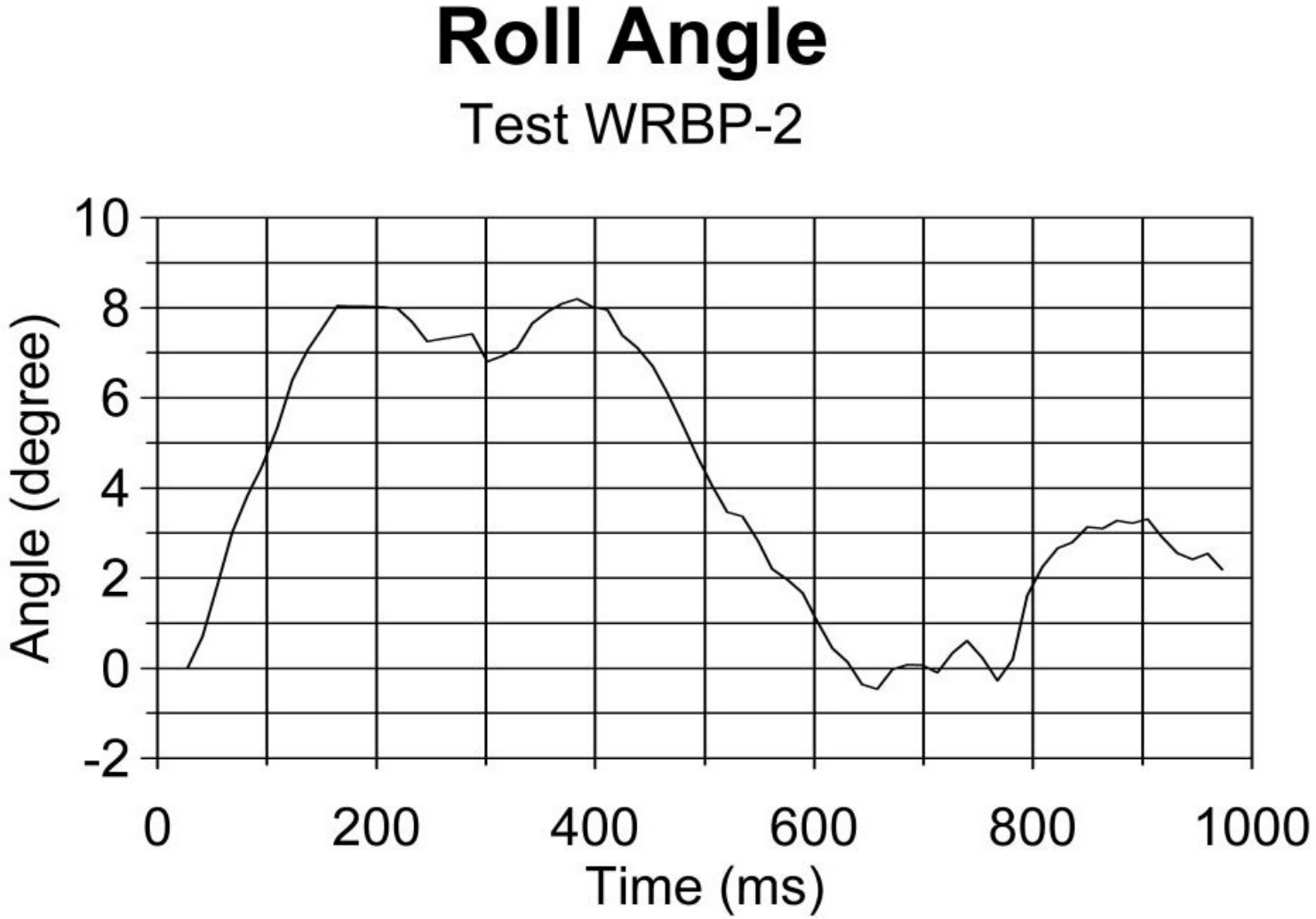

Figure P-1. Graph of Roll Angular Displacements, Test WRBP-2

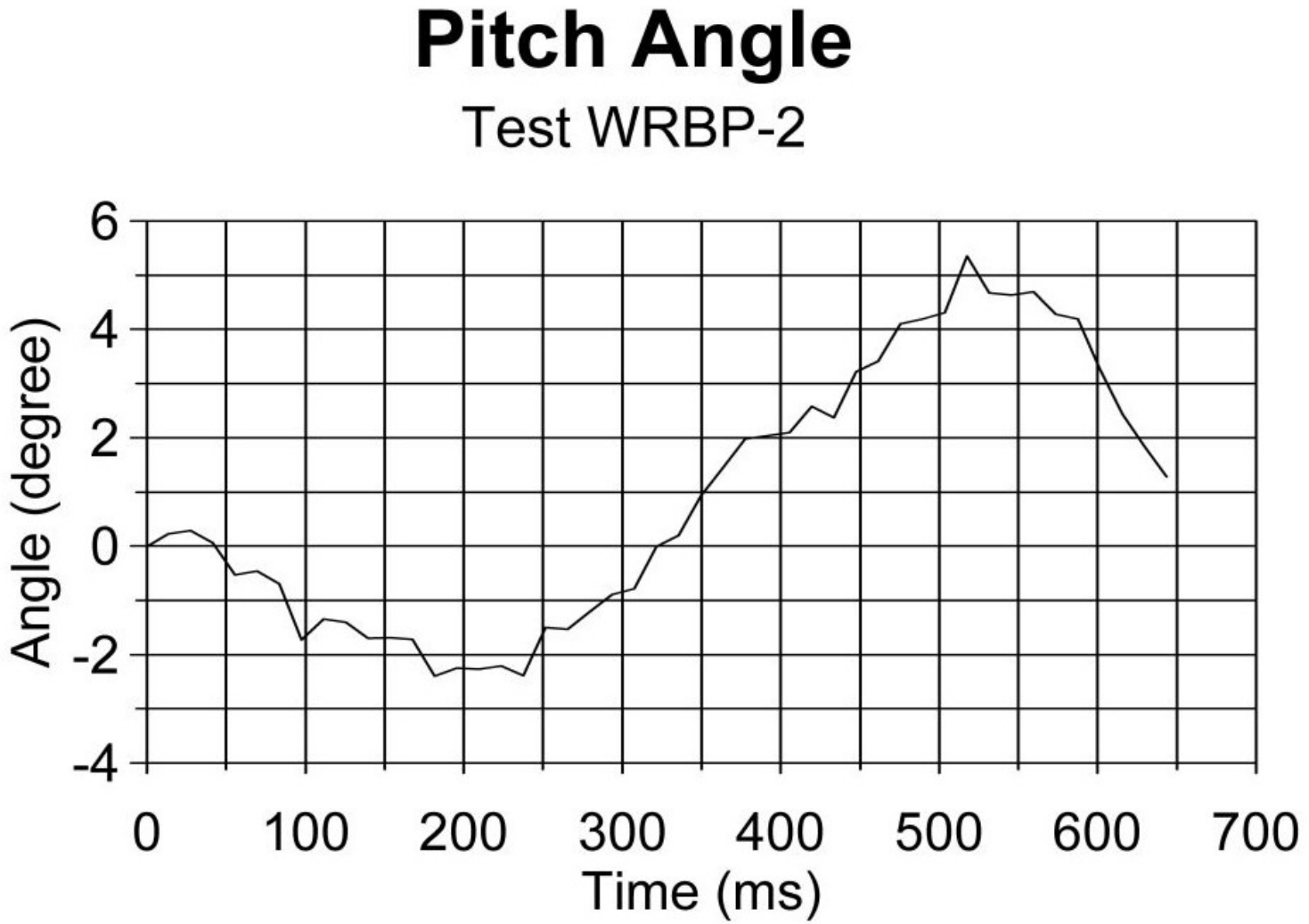

Figure P-2. Graph of Pitch Angular Displacements, Test WRBP-2

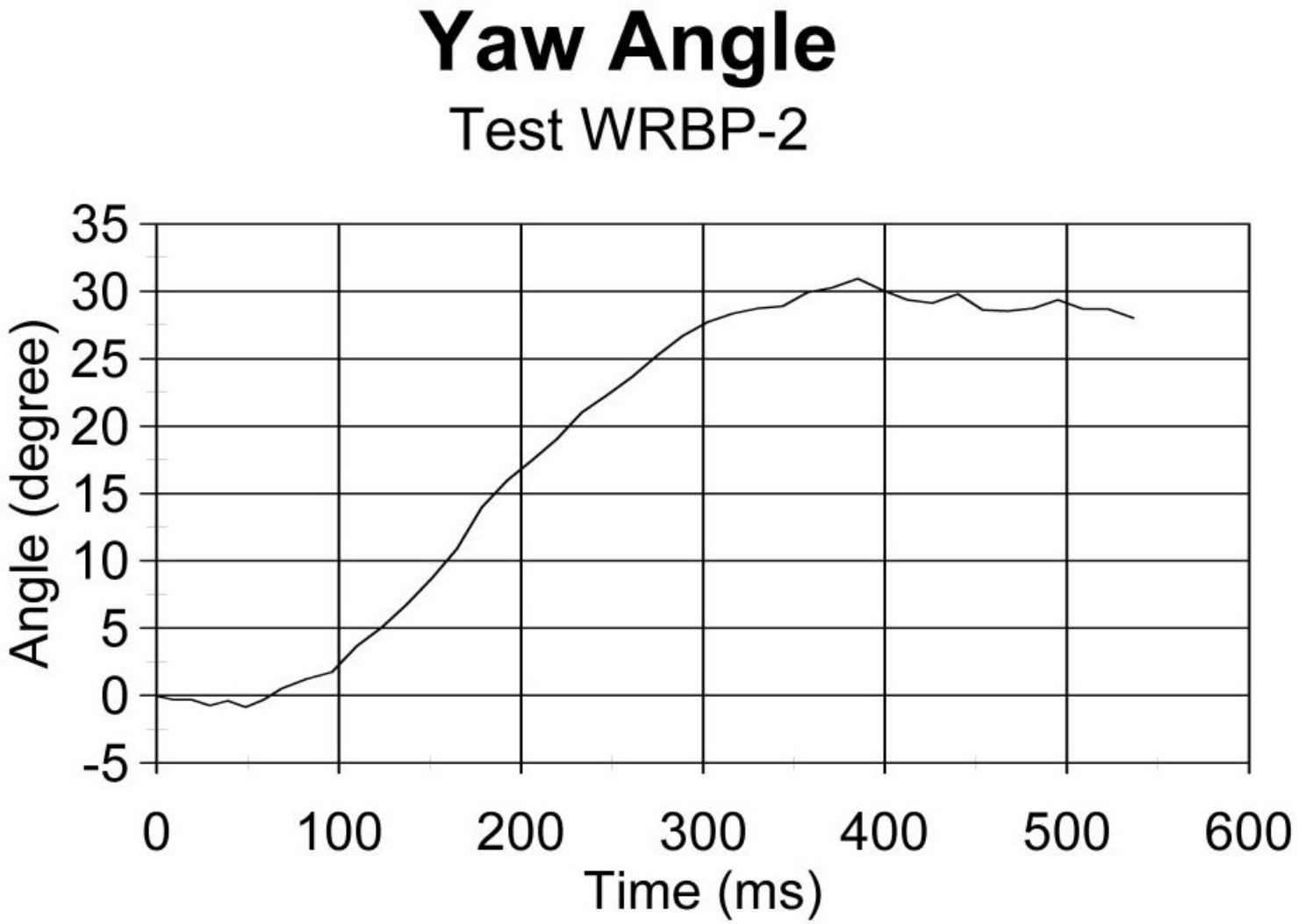

Figure P-3. Graph of Yaw Angular Displacements, Test WRBP-2